Synthesis of Nitrogen-Containing Bicyclic Sesquiterpenes as Potential Transition State Inhibitors of Aristolochene Synthase

by

Naeemah Jabbar Owaid Al-lami

A thesis submitted to

Cardiff University

for the degree of

DOCTOR OF PHILOSOPHY

School of Chemistry

Cardiff University

September 2013

DECLARATION

This work has not previously been accepted in substance for any degree and is not concurrently submitted in candidature for any degree.

Signed ……………………………………… Date ………………………

STATEMENT 1

This thesis is being submitted in partial fulfilment of the requirements for the degree of PhD.

Signed ……………………………………… Date …………………………..

STATEMENT 2

This thesis is the result of my own independent work/investigation, except where otherwise stated. Other sources are acknowledged by explicit references.

Signed ……………………………………… Date …………………………..

STATEMENT 3

I hereby give consent for my thesis, if accepted, to be available for photocopying and for inter-libraey loan, and for the title and summary to be made available to outside organisations.

Signed ……………………………………….. Date ……………………………

ACKNOWLEDGEMENTS

Abstract

Aristolochene synthase from *Penicillium roqueforti* (PR-AS) is sesquiterpene synthase that catalyses the Mg^{2+}-dependent conversion of farnesyl diphosphate FDP to (+)-aristolochene. Through the use of site directed mutagenesis, fluorinated FDPs and an aza-analogue of the eudesmane cation, the reaction was previously shown to involve germacrene A and eudesmane cation as intermediates. The subsequent series of rearrangements that transform the eudesmane cation to (+)-aristolochene have not been investigated previously. To probe the carbocationic nature of these 1,2-hydride and methyl shifts, new aza-analogues were designed to mimic the geometric and electrostatic properties of postulated carbocation intermediates in the catalytic mechanism of PR-AS. Here is described the synthesis of both enantiomers of 10-aza-eremophilane in enantiomerically pure from the common precursor (4S)-limonene oxide and their analysis as inhibitors of PR-AS.

The synthesis of *(7R,4S,5S)*-10-aza-eremophilane cation was accomplished in 8 steps, starting from a known keto ester that in turn was obtained by degradation of (-)-limonene oxide. An identical synthetic protocol was repeated from (4R)-limonene oxide to give the enantiomer of 10-aza-eremophilane cation. Inhibition studies with compound *(7R,4S,5S)*-10-aza-eremophilane indicated that this ammonium salt acted as a moderate competitive inhibitor of PR-AS (K_i = 38 μM), and showed that eremophilane cation is likely a true intermediate on the pathway from FDP to aristolochene during PR-AS catalysis. The inhibition potency of 10-aza-eremophilane was increased by the addition of diphosphate PPi (K_i = 2.9 μM). This synergetic kinetic effect suggests that the possible involvement of PPi as a stabilizing anion for the eremophilane carbocation in PR-AS biosynthesis. Inhibition studies of the enantiomer of *(7R,4S,5S)*-10-aza-eremophilane cation, *(7S,4R,5R)*-10-aza-eremophilane cation, which has incorrect stereocenteres, with PR-AS indicated that this ammonium salt was a poor inhibitor of PR-AS (K_i = 1.03 mM). The data obtained for this compound highlight the chiral environment of the active site of PR-AS, and more importantly supports the postulate that terpene synthases form a product-like contour at their active site that steers the carbocationic cascade catalyzed by PR-AS toward the production of a single enantiomer.

In the second part of the present work, progress was made towards the stereoselective synthesis of 5-aza-eudesmane cation. This teriary amine is a structural mimic of the 5-eudesmane carbocation, another putative intermediate in the reaction cascade catalysed by PR-AS. However, this tertiary amine was not obtained with desired stereochemistry, nevertheless, two diastereoisomers of the desired compound were obtained.

TABLE OF CONTENTS

LIST OF FIGURES

LIST OF SCHEMES

LIST OF TABLES

LIST OF ABBREVIATIONS

[α]	Specific rotation
Aq	Aqueous
Amp	Ampicillin
Ar	Unspecified aryl substituent
AS	Aristolochene synthase
AT-AS	Aristolochene synthase from *Aspergillus terreus*
BuLi	Butyl lithium
c	Concentrated
CoA	Coenzyme A
*m*CPBA	*meta* chloroperoxybenzoicacid
DBU	1, 8-diazabicyclo[5.4.0]undec-7-ene

DCM	Dichloromethane
DEPT	Distortionless Enhancement by Polarisation Transfer
DIBAL	Diisobutylaluminium hydride
DMAPP	Dimethylallyl diphosphate
DPPA	Diphenylphosphoryl azide
DMF	Dimethylformamide
DMSO	Dimethyl sulfoxide
EI	Electron impact
FDP	Farnesyl diphosphate
HMBC	Heteronuclear multiple-bond correlation spectroscopy
HRMS	High resolution mass spectrometry
HSQC	Heteronuclear single-quantum correlation
HOAc	Acetic acid
h	Hours
i	iso
IR	Infra Red
IDP	Isopentenyl diphosphate
J	Coupling constant (in Hz)
K_M	Michaelis constant
LDA	Lithium diisopropyl amide
LTA	Lead tetraacetate
M	Molar
Me	Methyl
MeLi	Methyl lithium
MEP	Methylerythritol phosphate
min	Minutes
m.p.	Melting point
MS	Mass spectrometry

MVA	Mevalonic acid
MTO	Methyltrioxorhenium
MW	Molecular weight
n	*normal*
NADPH	Reduced nicotinamide adenine dinuleotide phosphate
NMR	Nuclear Magnetic Resonance
nOe	Nuclear Overhauser effect
NOESY	Nuclear Overhauser effect spectroscopy
OD	Optical density
p	*para*
PCC	Pyridinium chlorochromate
Ph	Phenyl
PPi	Inorganic diphosphate
PR-AS	Aristolochene synthase from *Penicillium roqueforti*
PTSA	*para*-Toluenesulfonic acid
R	Unspecified substituent
TFA	Trifluoroacetic acid
TFAA	Trifluoroacetic anhydride
THF	Tetrahydrofuran
TLC	Thin layer chromatography
TsCl	*para*-Toluene sulfonyl chloride
TMSCl	Trimethylsilyl chloride
TEAS	5-*epi*-Aristolochene synthase from *Nicotiana tabacum*
UHP	Urea hydrogen peroxide

CHAPTER ONE

INTRODUCTION

1.1 General introduction to terpenes

Terpenes are a group of small molecule natural products that are widespread in nature. They are produced in all forms of life but are particularly prevalent in the plant kingdom, that generates more than half their number which currently exceeds 30,000 identified compounds.[1] The term terpene originates from "turpentine", a fluid obtained through steam distillation of resin obtained from pine trees. Terpenes are a large and varied class of hydrocarbons, when they are modified biochemically, such as through oxidation or rearrangement of the carbon skeleton, the resulting compounds are generally referred to as terpenoids.

The majority of these compounds are secondary metabolites and in most cases the actual role they play in the organism that produces them are unidentified. They are often not essential for viability of the organism. Instead, they play important roles, for example, in communication or defence.[2] There is also a small group of terpenoids which are used in primary metabolism, such as the phytol side chain of chlorophyll.[3]

The terpenoids form a large and structurally diverse family of natural products derived formally from C_5 isoprene units[4] (**1**) joined in a head-to-tail fashion. Dimethylallyl diphosphate (DMADP, **2**) and isopentenyl diphosphate (IDP, **3**) are biological equivalents of isoprene and are universal precursors of the isoprenoids in all living organisms (Scheme 1.1).[5] Typical structures contain carbon skeletons represented by $(C_5)_n$, and are classified as hemiterpenes (C_5) (Scheme 1.1), monoterpenes (C_{10}), sesquiterpenes (C_{15}), diterpenes (C_{20}), sesterterpenes (C_{25}), triterpenes (C_{30}) and tetraterpenes (C_{40}). All these acyclic precursors can then be modified to generate acyclic, monocyclic or multicyclic products.[6,7]

The head to tail condensation of IDP (**3**) and DMADP (**2**) catalysed by geranyl diphosphate synthase yields geranyl diphosphate (GDP, **4**) the universal precursor of all monoterpenes. This process involves ionization of the DMADP to give an allylic carbocation that adds to the double bond of IDP, to form a new carbocation that is quenched by selective proton elimination (Scheme 1.2).[8] With the specific prenyl transferase, this model electrophilic reaction can be further extended to produce further linear isoprenoid diphosphates by sequential addition of IDP units. Farnesyl diphosphate (FDP, **5**), and geranylgeranyl

diphosphate (GGDP, **6**) arise by the addition of one molecule of IDP to either geranyl or farnesyl diphosphate or the loss of one molecule of diphosphate ion. They are, the universal precursors of all sesqui- and diterpenes found in nature. All the double bonds in these linear precursors display *E*-stereochemistry.[9] These linear diphosphates are further processed by terpene synthases to give rise to cyclic and acyclic terpenoids.
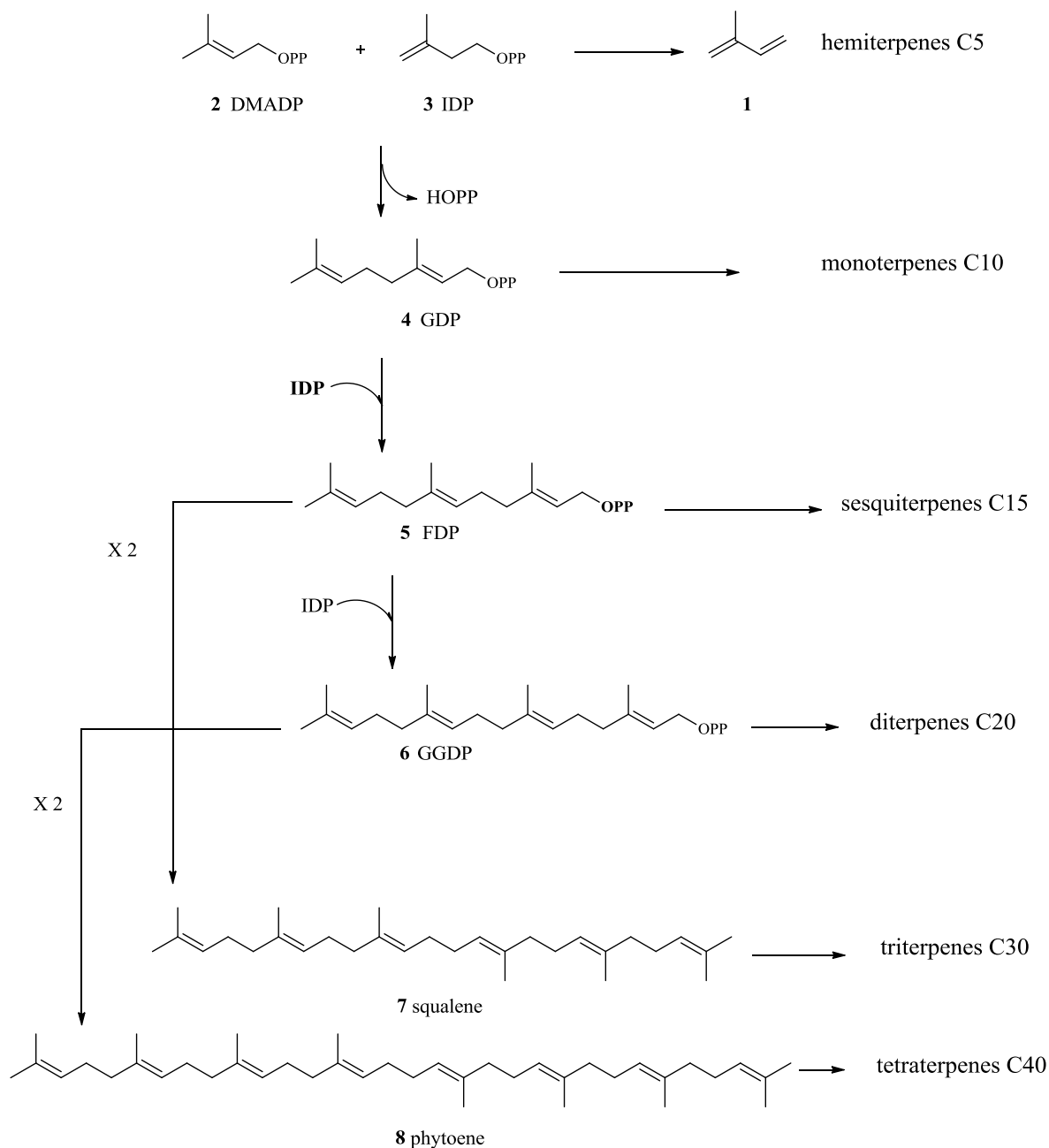
Scheme 1.1: *Biosynthesis of the prenyl diphosphates*
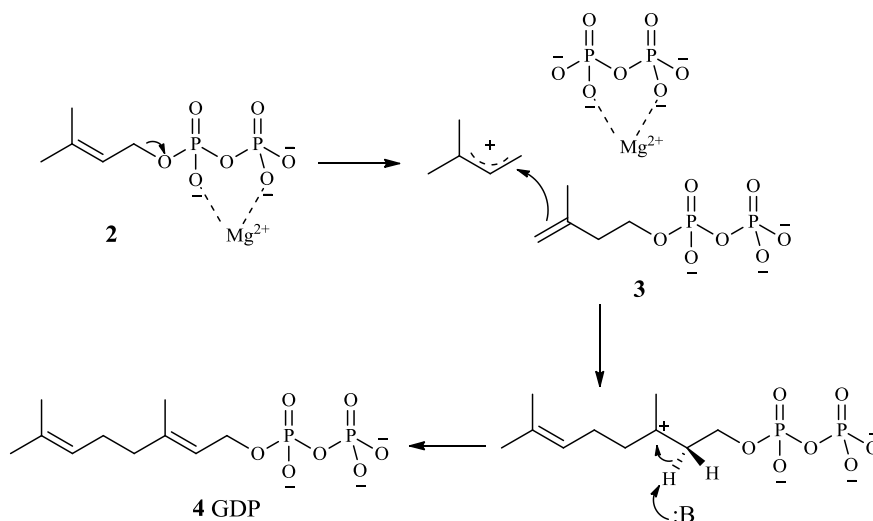
Scheme 1.2: *Head to tail condensation between IDP (3) and DMADP (2) to produce geranyl diphosphate (4).*

Triterpenes (C30) are not formed by an extension of the process of adding IDP to the growing chain. Instead, two molecules of FDP (**5**) are joined head to head to yield the hydrocarbon squalene (**7**). Squalene synthase (SS) catalyses the 1`-1 condensation between two molecules of farnesyl diphosphate (**5**) via a tertiary cyclopropyl carbinyl intermediate, presequalene diphosphate PSDP (**9**) (Scheme 1.3) to yield squalene (**7**). While the formation of the tetraterpenes skeleton, for example phytoene (**8**) (Scheme 1.1), involves coupling of two molecules of geranylgeranyl diphosphate GGDP (**6**).[10]
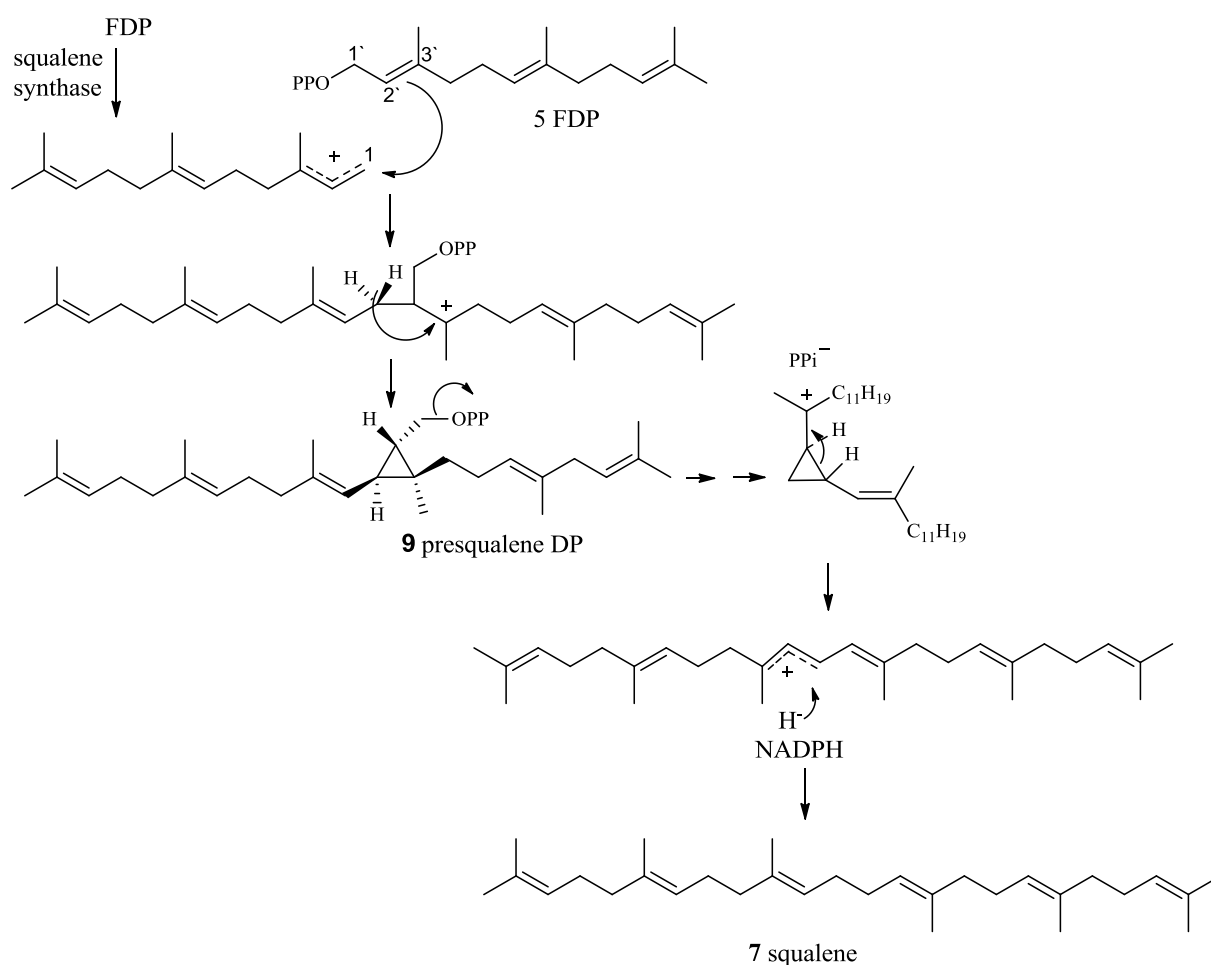
Scheme 1.3: *Biosynthesis of squalene (7)*

1.2 Importance and ecological role of terpenes

Apart of their huge array of structural diversity, terpenoids also have varied biological activity in nature. For example, plants produce a wide range of this family of molecules for very different purposes, such as for attraction of insects, for the inhibition of the growth of competitor plants in resource-limited areas or for antimicrobial and antifungal properties.[11]

Monoterpenoids are usually found in the essential oils of citrus and other plants.[12] They have a high economic value as flavours and fragrances. However, recently, more medical and ecological functions have been allocated to this group of terpenoid compounds. α-Pinene (**10**) (Figure 1.1) has been discovered as sex pheromone attracting the female cotton boll weevil.[13] The primary oxidation product of α-pinene is verbenone (**11**), which

has an important role in the control of the southern pine bark beetle. Recent publications have revealed that verbenone also has antimicrobial properties.[14] δ-Limonene (**12**) has been used as a medicinal compound, it is extracted from orange peel oil and has chemopreventative activity against some cancer cell lines.[13]

10   **11**   **12**
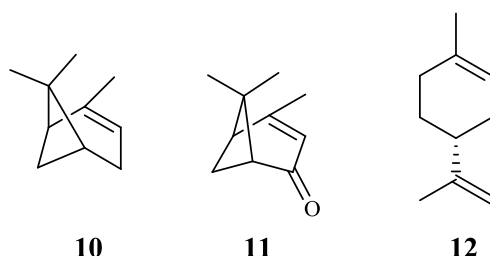
Figure 1.1: *Structures of α-pinene (**10**), verbenone (**11**) and δ-limonene (**12**)*

All terpenoids derive from a small number of linear isoprenoid diphosphate precursors. The 15-carbon compound farnesyl diphosphate FDP (**5**) is the universal precursor to all sesquiterpenes in plants, bacteria and fungi.[15-18] Sesquiterpenoids have been used as traditional medicines for thousands of years and more recently modified sesquiterpenoids as therapeutic agents.[19] For example artemisinin (**13**), an endoperoxide-containing sesquiterpene lactone from the Chinese-Vietnamese plant-*Artimisia annua L.* (sweet wormwood) has been used in China as a traditional anti-malaria and antipyretic drug.[20] The biosynthesis of artemisinin is believed to involve the cyclization of farnesyl diphosphate FDP (**5**) to amorpha-4,11-diene (**14**), which is further oxidized to an dihydroartemisinic acid (**16**), an advance precursor of artemisinin (Scheme 1.4).[21]
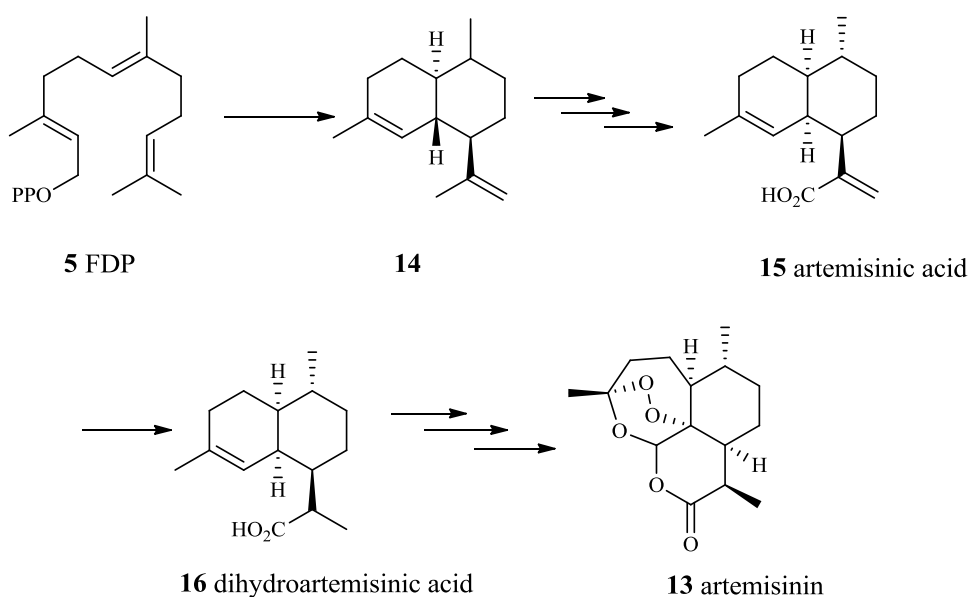
Scheme 1.4: *Biosynthesis of artemisinin (13)*

Parthenolide (**17**) (Scheme 1.5) is another sesquiterpene lactone present in several medicinal plants that has been used in folk medicine for its anti-inflammatory or analgesic properties. It is also used as the antimigraine agent in Feverfew and as a traditional herbal remedy for the relief of arthritis, toothache and menstrual difficulties.[10] Germacryl cation (**18**), which results from a 1,10-cyclisation of FDP (**5**), is the precursor of germacrene A-derived sesquiterpenes such as parthenolide. Compound **17** is actually classified as germacranolide, the suffix "olide" referring to the lactone group. Whilst the details of the pathway are not known, a series of simple oxidative transformations can produce the α,β-unsaturated lactone and epoxide groupings (Scheme 1.5).[10]
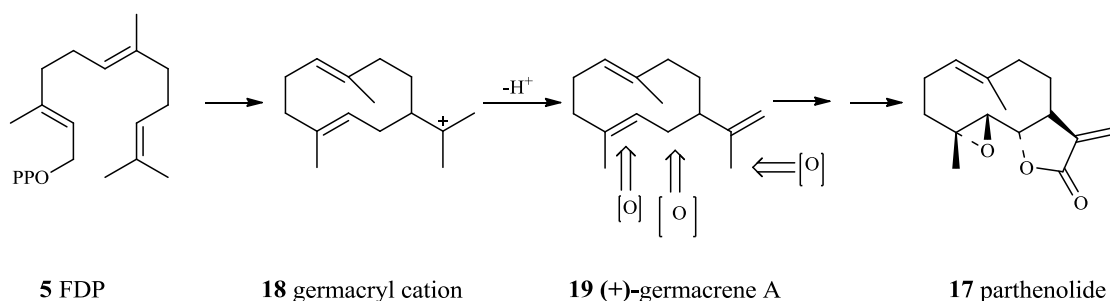
Scheme 1.5: *Presumed biosynthesis of parthenolide (17)*

While some sesquiterpenoids (e.g. **13** and **17**) have medicinal properties useful for humans, the vast majority of these secondary metabolites are efficiently exploited by the organism that produce them. Aphids, for example, when attacked or irritated produce defensive secretions from their cornicles, known as volatile alarm pheromones, that cause other aphids in the area to disperse. While the most common alarm pheromone identified for aphids is the acylic *E*-β-farnesene (**20**) (Figure 1.2),[22] termites use the macrocycle (-)-germacrene A (**21**) as their preferred semiochemical.[23]

20 **21**
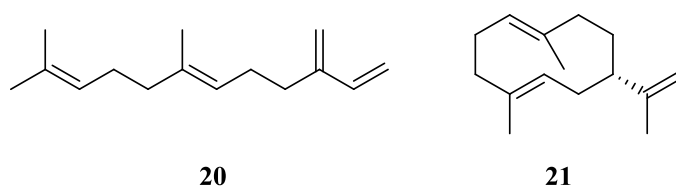
Figure 1.2*: Structures of E-β-farnesene (20) and (-)-germacrene A (21)*

Plants and microorganisms also produce sesquiterpenes to their advantage. Gossypol (**22**), a sesquiterpene dimer derived from δ-cadinene (**23**) is used by cotton plants as a defensive phytoalexin.[24] similarly, fungi, when under stress, produce a blend of defensive sesquiterpenoid mycotoxins, used as deterrents against competing organisms. Aristolochene (**24**) (Figure 1.3) is the biochemical precursor of several fungal toxins including the potentially lethal PR- toxin (**25**).[25]

23 δ-cadinene

24 (+)-aristolochene

22 gossypol
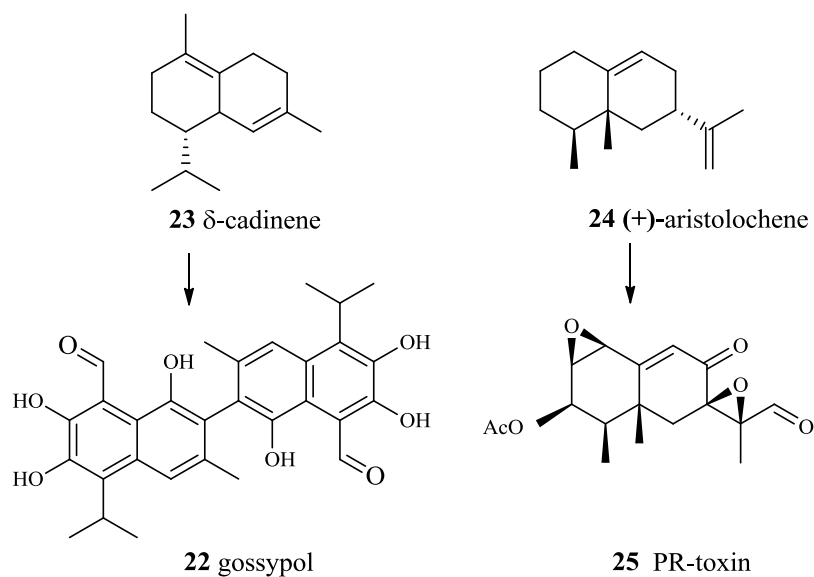
25 PR-toxin

Figure 1.3: *Structures of gossypol (**22**), (+)-δ-cadinene (**23**), (+)-aristolochene (**24**) and PR toxin (**25**)*

As with other groups of terpenes, diterpenes have quite a few different uses both in nature and in medicine. Casbene (**26**) (Figure 1.4),[26] a macrocyclic hydrocarbon, has been reported to appear at much higher levels in castor bean seedlings when the plant is under fungal attack than in sterile conditions. With both antibacterial and antifungal properties, this diterpene is considered to be a phytoalexin.[26]

Of particular interest in therapeutic terms is the diterpene-derivative paclitaxel (Taxol[TM]) (**27**) (Figure 1.4),[27] which is extracted from the pacific yew tree and has remarkable antitumour activity and antileukemic activity. One common characteristic of cancer cells is their rapid rate of cell division. In order to accommodate this, the cytoskeleton of a cell undergoes extensive restructuring. Paclitaxel is an effective treatment for aggressive cancers, due to its adverse affect on the process of cell division by preventing this restructuring by binding to tubulin. It is most commonly used to treat ovarian, breast and non-small cell lung cancer.[27]
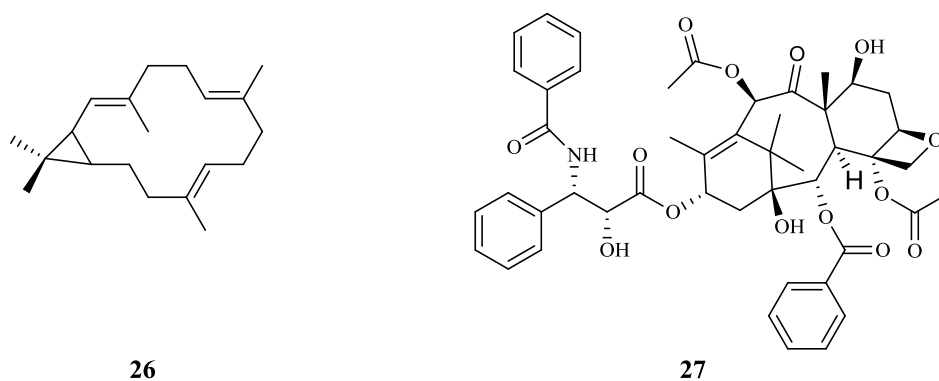
Figure 1.4: *Structures of casbene (26) and paclitaxel (27)*

Cholesterol (**28**) and other steroids are considered as triterpenes even though they possess (C27-C30) skeletons. This is because they are derived from the C30 linear precursor, squalene (**7**), which is derived from two molecules of FDP (**5**) (Scheme 1.3). Oxidation by squalene monooxygenase of one of the terminal double bonds of squalene gives 2,3-squalene oxide (**29**), which undergoes enzyme-catalyzed cyclisation to afford lanosterol (**30**), and is then elaborated into cholesterol (**28**) and other steroids (Scheme 1.6).[28] Cholesterol is the source of sexual hormones, bile acid and vitamin D in animals. It is also involved in controlling calcium and phosphorus metabolism. Another important function is the maintenance of membrane fluidity and permeability.[28]

Carotenoids comprise the family of naturally occurring pigments derived from the C40 linear precursor phytoene (**8**) (Scheme 1.1).[29] Carotenoids are central for the absorption of light in photosynthetic organisms due to their highly conjugated structures. They are also the precursors of the essential growth factor retinol also known as vitamin A (**31**) (Figure 1.5), which has important functions for example in the vision process, for resistance to infectious disease and bone remodelling.[30,31]
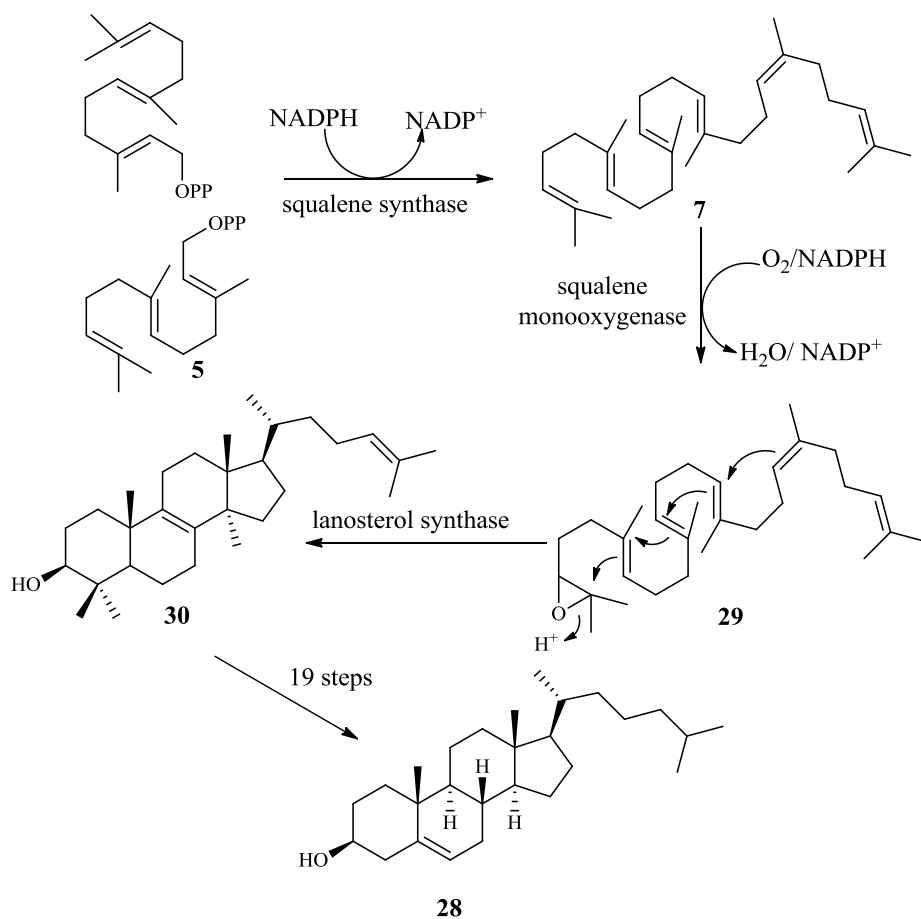
Scheme 1.6: *Generation of cholesterol (**28**) from FDP (**5**).*
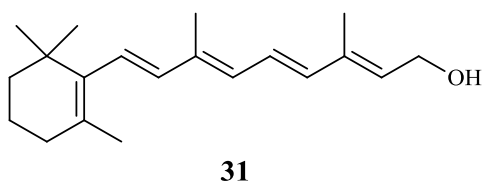
Figure 1.5: *Structure of vitamin A (**31**).*

1.3 Biosynthesis of terpenes

Isoprene, namely 2-methyl-1,3-butadiene (**1**) was first discovered during distillation of natural rubber in a low-boiling fraction, and identified during the degradation of terpentine oil and cyclic monoterpenes. The initially postulated "isoprene rule" by Wallach stated that most terpenoids could be hypothetically constructed by repetitive joining of isoprene (**1**) units.[32] In 1953 Leopold Ruzicka postulated the "biogenetic isoprene rule" stating that the carbon skeleton of terpenes is composed of isoprene units linked either in a regular (head to tail) or irregular arrangement.[33] For example, a number of natural monoterpene structures contain carbon skeletons which, although obviously derived from isoprene C5 units, do not seem to fit the regular head-to-tail coupling mechanism (Figure 1.6).[10]

regular monoterpene skeleton   irregular monoterpene skeleton
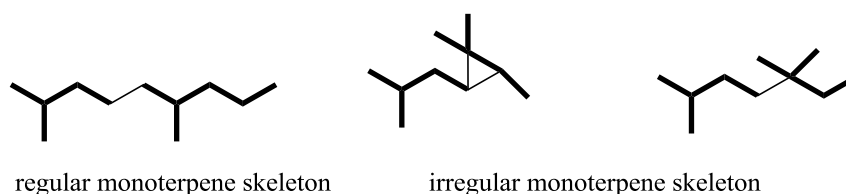
Figure 1.6: *Examples of regular and irregular monoterpene skeletons*

Even though the isoprene unit is the structural feature characteristic of all terpenes nature utilizes two C5 diphosphates, dimethylallyl diphosphate (DMADP, **2**) and isopentenyl diphosphate (IDP, **3**) (Scheme 1.1),[34] as the actual biological building blocks from which terpenes are derived. Isopentenyl diphosphate (IDP, **3**) and dimethylallyl diphosphate (DMADP, **2**) are the substrates of isoprenyl diphosphate synthases, a family of terpenes enzymes that mediate their condensation giving rise, to geranyl diphosphate (GDP, C_{10}), farnesyl diphosphate (FDP, C_{15}), and geranyl geranyl diphosphate (GGDP, C_{20}) (Scheme 1.1) by the iterative addition of IDP. There are two pathways leading to IDP and DMADP, the mevalonate pathway and a recently discovered mevalonate-independent pathway via deoxyxylulose phosphate.[35]

1.3.1 Mevalonic acid (MVA) pathway

The mevalonic acid pathway is usually used by mammals, higher plants, fungi and even some bacteria.[36] This pathway starts with three molecules of acetyl-CoA (**32**). The first two units of acetyl-CoA react in a Claisen condensation reaction catalysed by acetoacetyl-CoA synthase which release coenzyme A to afford acetoacetyl-CoA (**33**) (Scheme 1.7). A third molecule of acetyl-CoA is subsequently added in an aldol-like manner with the help of β-hydroxy-β-methylglutaryl-CoA (HMG-CoA) synthase yielding HMG-CoA (**34**).[36] Next, HMG-CoA reductase catalyses the reduction of the thioester group of **34** to give the primary alcohol functionality of mevalonic acid (**36**). Two equivalents of NADPH cofactor are required in this transformation. The first NADPH reduces HMG-CoA to its corresponding aldehyde (mevaldic acid, **35**), and the second further reduces the newly formed carbonyl group to (3*R*)-mevalonic acid (MVA, **36**).[37] The two hydroxyl groups of (3*R*)-mevalonic acid are then diphosphorylated by three molecules of ATP to yield mevalonic acid triphosphate (**38**). The final product IDP (**3**) arises from the decarboxylation of mevalonic acid triphosphate. IDP (**3**) and DMADP (**2**) are interconvertible by stereospecific isomerisation. It has been shown by tritium-labelling experiment that only the pro-*R* hydrogen of **3** at C2 is involved in the isomerisation process.[38]

1.3.2 Non-mevalonate (non-MVA) pathway

The non-MVA pathway was discovered at the end of the last century by Rohmer and co-workers.[39,40] This pathway takes place in plastids and has also been named as the pyruvate/glyceraldehyde-3-phosphate pathway or MEP pathway. Pyruvate (**39**) and D-glyceraldehyde-3-phosphate (**40**) (Scheme 1.8) are the starting compounds and 2-C-methyl-D-erythritol-4-phosphate (MEP, **43**) is an important intermediate of this alternative metabolic pathway leading to the formation of isopentenyl diphosphate (IDP) and dimethylallyl diphosphate (DMADP).
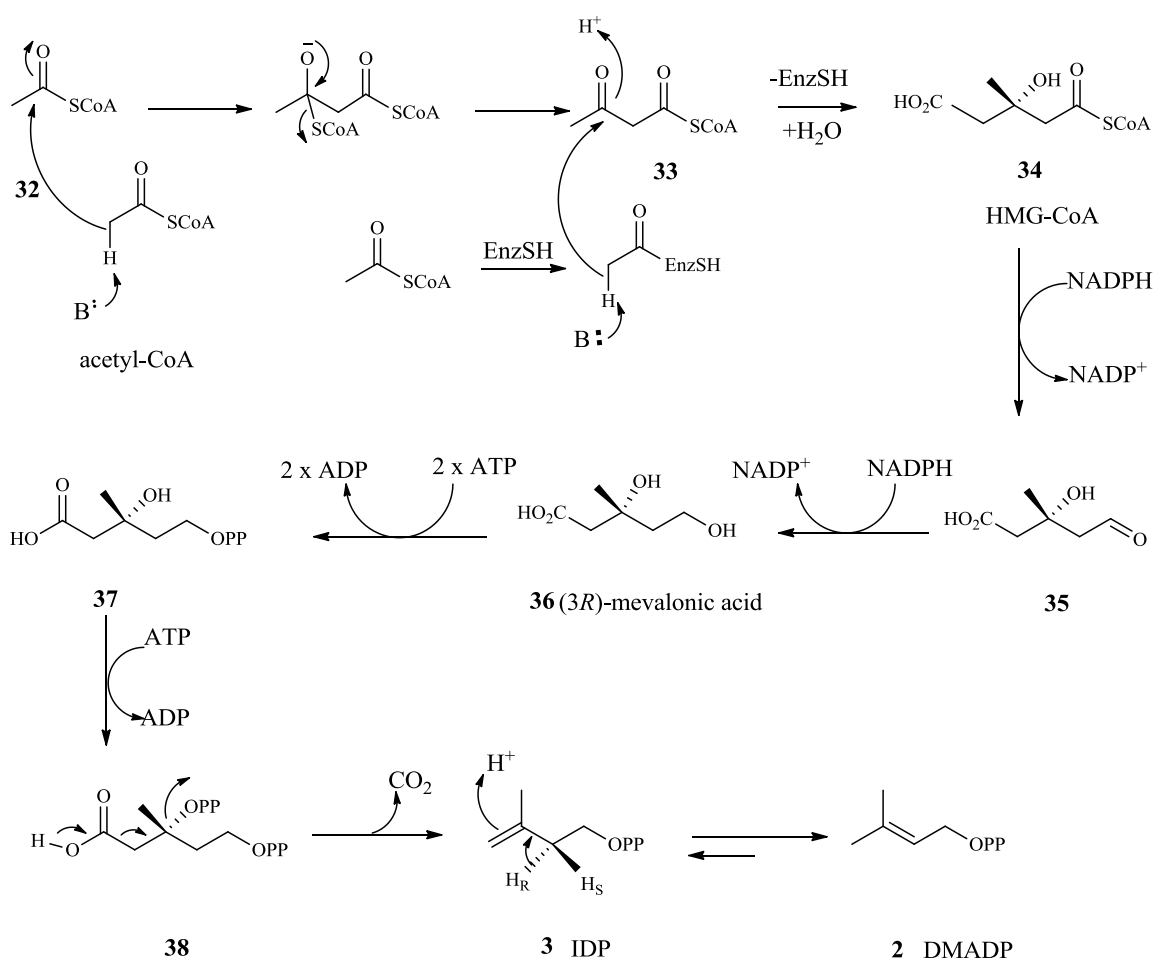
Scheme 1.7: *Mevalonic acid pathway to IDP (3) and DMADP (2).*

This route starts by a thiamine diphosphate (TPP) mediated decarboxylation of pyruvate (**39**) that affords an enamine that further reacts with glyceraldehydes-3-phosphate (**40**) to give 1-deoxy-D-xylulose-5-phosphate (DXP, **41**). After a pinacol-like rearrangement of DXP,

the resulting intermediate is reduced with NADPH by DXP-reductoisomerase affording 2-C-methyl-D-erythritol-4-phosphate (MEP, **43**).[40] MEP reacts with cytidine triphosphate CTP and is then phosphorylated with one equivalent of ATP to yield 2-phospho-4-cytidinediphosphate-2-C-methylerythritol (**45**), which is converted to 2-C-methyl-D-erythritol-2,4-cyclodiphosphate (**46**).[40] Afterwards, IDP (**3**) and DMADP (**2**) are synthesized following a reduction-dehydration step that an electron transport chain.[41]
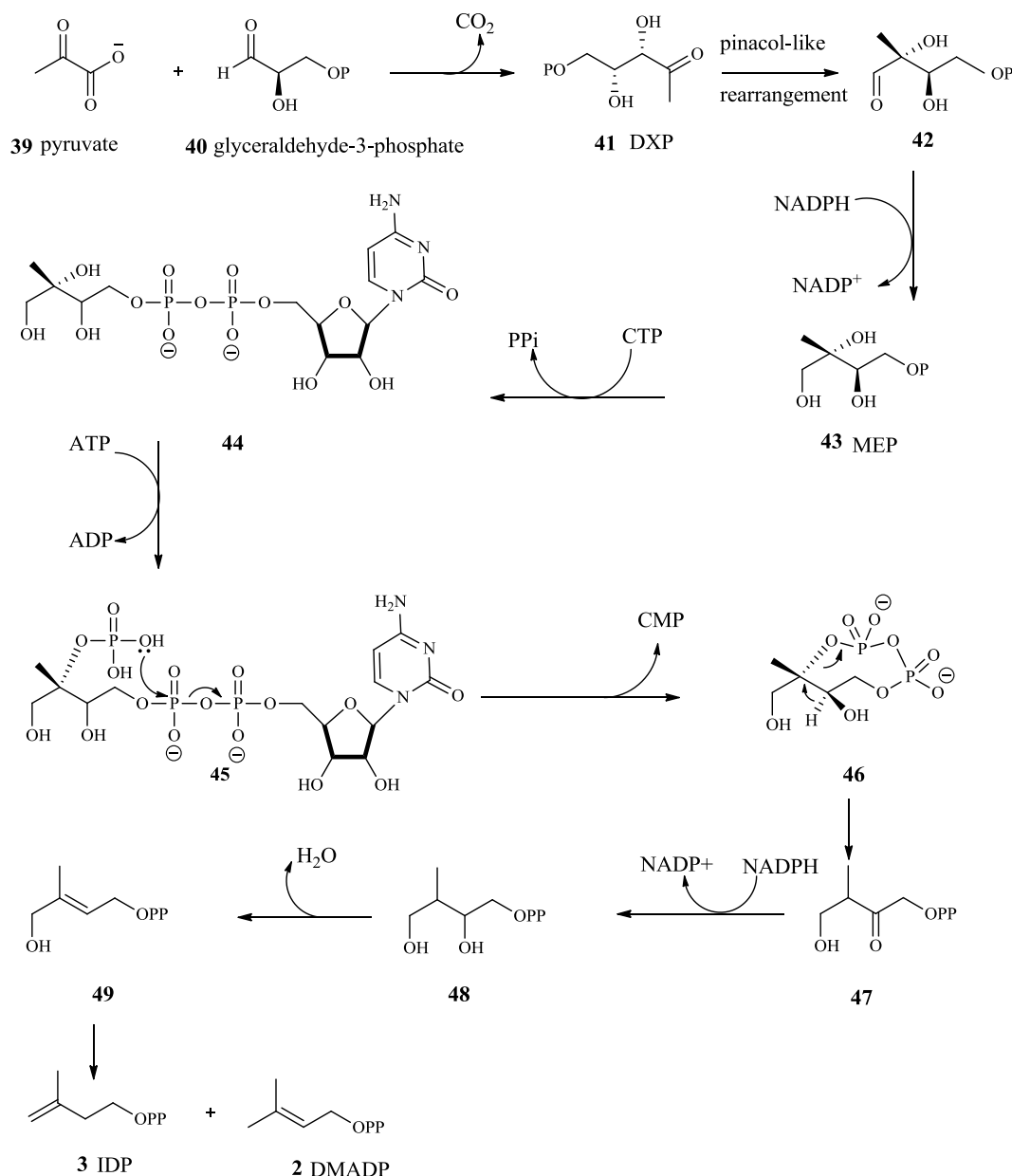
Scheme 1.8: *The non-mevalonate pathway to IDP (3) and DMADP (2)*

1.4 Sesquiterpenes (C15)

Addition of a further molecule of IDP to geranyl diphosphate in an extension of the isoprenyl diphosphate synthase reaction leads to the sesquiterpene precursor, farnesyl diphosphate FDP (**5**). FDP can then be further transformed to linear and cyclic sesquiterpenes.[41] The first step for the majority of enzymatic formation of sesquiterpenes is belived to involve the ionization of FDP (**5**) to the transoid farnesyl cation (**50**) (Scheme 1.9).[7] The cyclisation of farnesyl cation may occur from the distal double bond to generate either the ten-(*E,E*-germacradienyl cation) (**18**) or eleven-membered ring (*trans*-humulyl cation) (**51**). However, due to the *E*-geometry of the C2-C3 double bond of FDP, a 1,6-cyclisation is prevented by steric constraints.[18] To achieve 1,6-cyclisation, sesquiterpene synthases generate nerolidy cation (**52**) by isomerisation of the C2-C3 double bond to generate the cisoid isomer (**53**) of the nerolidyl cation, thereby permitting the cyclisation from either the central or distal double bond to form the six-(bisabolyl cation) (**54**) or seven-(cycloheptanyl cation) (**56**), as well as ten and eleven membered rings; -*Z,E*-germacradienyl cation (**55**) and -*cis*-humulyl cation (**57**) respectively (Scheme 1.9).[10]

Further cyclisations, hydride shifts, methyl migrations (Wagner-Meerwein rearrangements) may occur following the generation of initial cyclic carbocation prior to termination of the reaction by deprotonation or nucleophilic capture.[42,43]
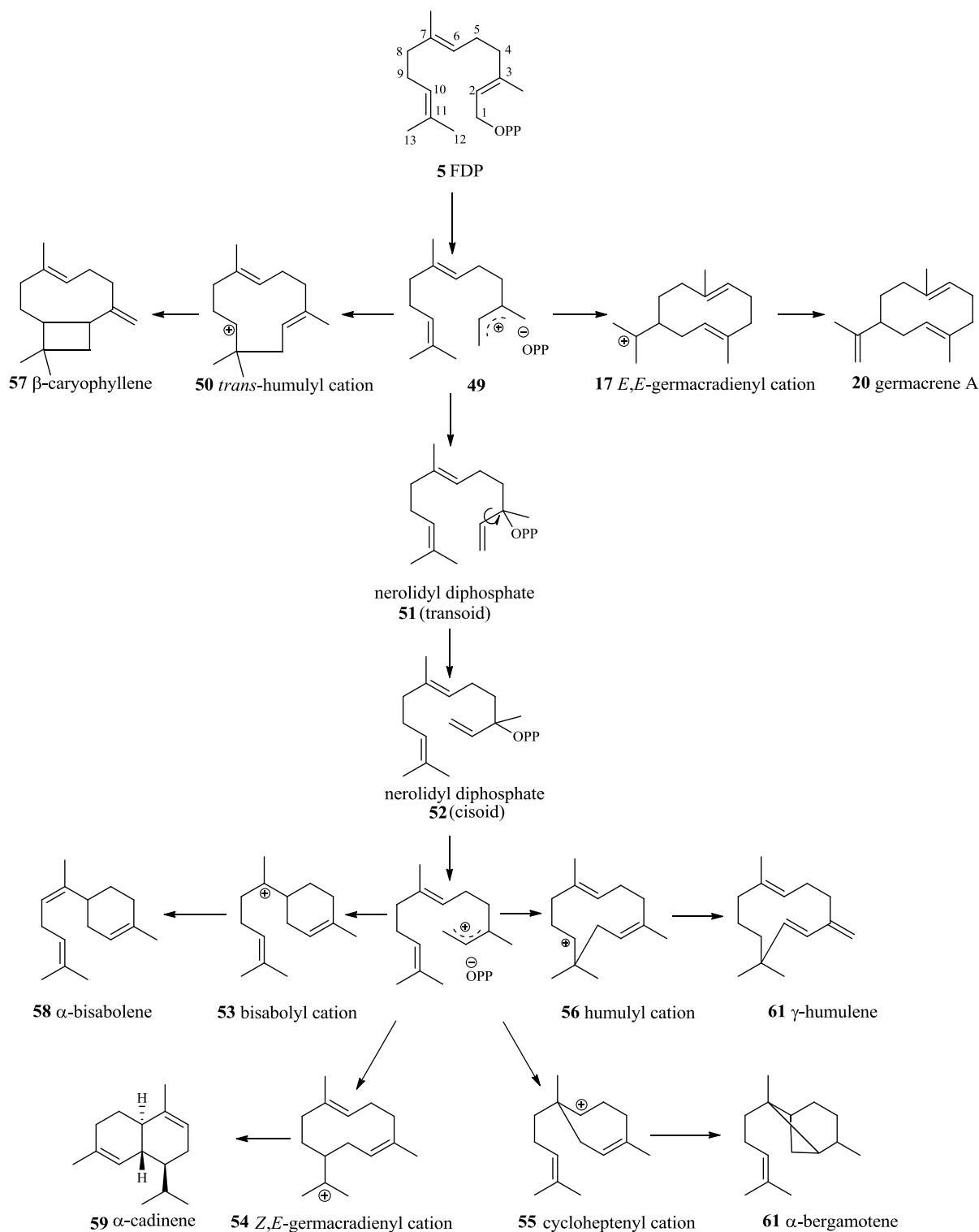
Scheme 1.9: *Biosynthesis of selected sesquiterpenes from FDP[10]*

1.5 Terpene Synthases

Terpene synthases (often also called terpene cyclases) are metal ion-dependent enzymes that catalyse the conversion of a given universal polyisoprenoid precursor (eg. GDP, FDP or GGDP) to one (or more) cyclic terpene products. Structural biology work has shown that class I terpene synthases posses two specific binding motifs that anchor the metal ions essential for catalysis.[44] These metal ions coordinate to the diphosphate leaving group and trigger the heterocyclic cleavage of the C-O diphosphate ester bond that leads to the formation on an allylic carbocation.[44] Often, a series of intramolecular cyclisations, methyl and hydride shifts and other rearrangements occur to produce the final products after proton loss or water capture. The divalent metals are mostly Mg^{2+} or Mn^{2+}, with Mg^{2+} being used most often.[45,46]

Terpene synthases, especially those from different kingdoms of life forms, share little amino acid sequence similarity among them (in many instances below 25-35%).[47] For example, despite producing almost identical hydrocarbons, the fungal aristolochene synthase from *Penicillium roqueforti* (PR-AS) and the plant *epi*-aristolochene synthase from *Nicotiana tabacum* (TEAS) only share 16% sequence similarity.[48] Interestingly, the crystal structures of all sesquiterpene synthase solved up to date have shown that these proteins all share a common fold, which has been named the class I terpene fold, usually containing ten to twelve α-helices arranged in an anti-parallel fashion.[49] The shape of catalytic active site varies between the different synthases but is always nested deep within this α-helical barrel.[49]

Usually, the catalytic cavity of terpene synthases is surrounded by about 5 helices, which are connected by loops.[50] The loops are relatively short at the bottom of the active site but long at the top, making the shape of the active site somewhat conical.[51] The active site of terpene synthases provides a chiral molecular environment (or template) that enforces the unique conformation of the substrate that leads to the often exclusive enzymatic product.[47] Indeed, terpene synthases display striking accuracy regarding stereo- and regio-specificity as exemplified by lanosterol synthase, an enzyme that produces only one isomer of lanosterol (**30**) (Figure 1.7) among the 128 possible steroisomers.[51]
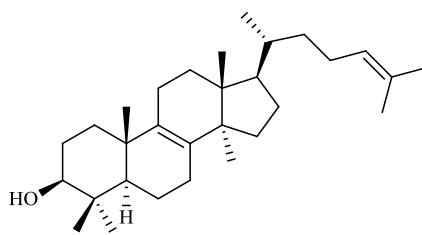
30

Figure 1.7: *Structure of lanosterol (**30**)*

Terpene synthase can be classified into two groups according to their general reaction mechanism.[17] While class I terpene synthases such as mono- and sesquiterpene synthases initiate their reaction cascades by diphosphate ionisation, class II terpene synthases feature a protoned-initiated cyclisation mechanism involving a double bond or an epoxide.[52] As mention earlier, class I terpene synthases contain two specific metal binding sites, namely the DDXX(D/E), found at the entrance of the active site. [44, 53] In contrast, class II terpene synthase contain only one DXDD metal binding motif.[52] Some terpene synthases contain structural features of both class I and II types. For example, the C-terminal catalytic domain of tobacco 5-*epi*-aristolochene synthase belongs to the class I terpenoid fold , whereas *N*-terminal domain belongs to class II terpenoid fold but has unknown function.[50,54]

1.6 Aristolochene Synthase from *Penicillium roqueforti*

Aristolochene synthase is a class I sesquiterpene synthase that produces aristolochene from FDP (**5**). Aristolochene, the C15 bicyclic eremophilane-type sesquiterpene[55] produced by aristolochene synthase has been isolated from several sources. While plants and animals prefer the (-)-enantiomer,[56] fungal sources such as *Penicillium roqueforti* and *Aspergillus terreus* produce (+)-aristolochene.[55,57] The formation of aristolochene catalyzed by aristolochene synthase in *Penicillium roqueforti* is thought to represent the first step in the biosynthesis of a large group of sesquiterpenoid fungal toxins, the most poisonous of which is the bis-epoxide PR-toxin (**25**)[58] (Figure 1.8).
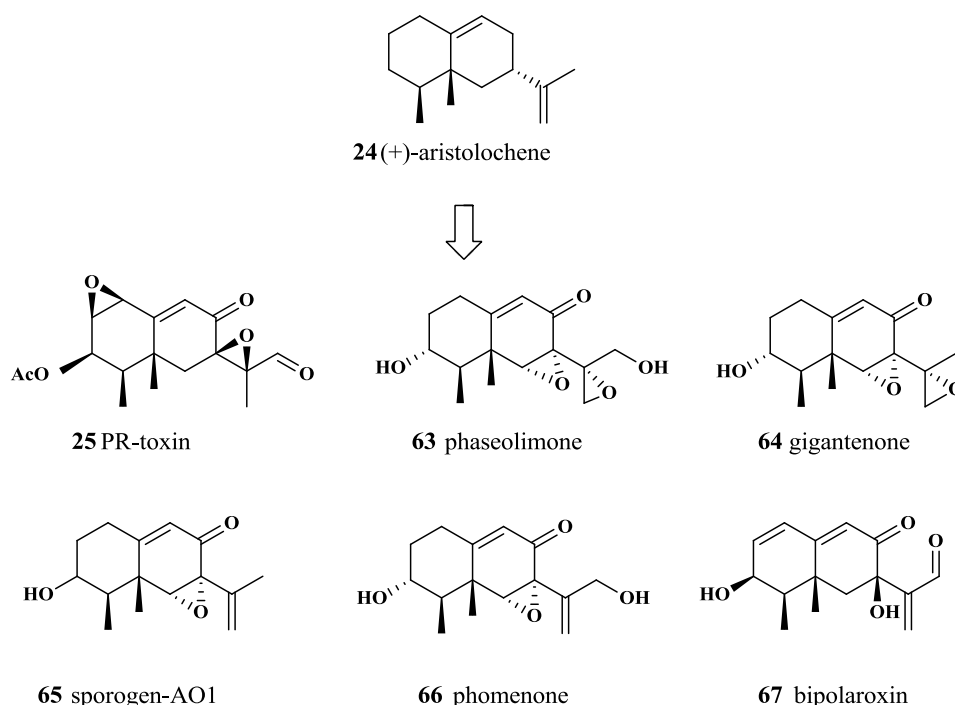
Figure 1.8: *Structures of fungal toxins thought to be derived from aristolochene (**24**)* [58]

Aristolochene synthase was first isolated and purified from the fungus *Penicillium roqueforti* in 1989.[59] The X-ray crystal structure of the apo-enzyme at 2.5 Å resolution was solved in 2000.[48] The crystal structure of recombinant PR-AS showed the typical α-helical class I terpene synthase fold with two Mg^{2+} binding mofits (Figure 1.9).[17,48] Aristolochene synthase (PR-AS) is a monomeric sesquiterpene cyclase with 342 amino acid residues and a molecular weight of 38000.[48] Like other sequiterpene synthases, both Mg^{2+} and Mn^{2+} can

be used as cofactors of the reaction, although Mn^{2+} can act as an inhibitor at high concentration.[59] The enzyme's structure consists of 11 α-helices, six of which form the hydrophobic active site cavity. Based on the X-ray crystallographic analyses, it was identified that some of amino acid residues (Phe-178, Phe-112, Trp-334) in the active site were involved in stabilising various carbocation intermediates.[60-63] The fungal aristolochene synthase from *Aspergillus terreus* (AT-AS) also catalyses the conversion of farnesyl diphosphate to (+)-aristolochene as a single sesquiterpene product.[25] Its molecular weight is 36000, which is less than PR-AS. Apart from this, the amino acid sequence of AT-AS is 61% identical with that of PR-AS.[48] Recent work on X-ray crystal structures of AT-AS by Christianson *et al.* demonstrated that it has a tetrameric quaternary structure, in which each subunit adopts the α-helical class I terpene synthase fold with the active site in a solvent-exposed conformation.[49] However, solution of the X-ray crystal structure of its complex with inorganic diphosphate and Mg^{2+} ions (resolved to 2.15 Å) revealed that one subunit was bound to three Mg^{2+} ions and PPi and was stabilised in the "closed" conformation required for catalysis.[49] There are two metal binding motifs in AT-AS, the DDLLE motif beginning with D90 and the NSE motif beginning with N219.[49]

Figure 1.9: *Ribbon diagram representation of the crystal structure of aristolochene synthase from Penicillium roqueforti (1DGP.pdb). The red colour indicates the location of the two Mg-binding motifs.*

1.7 Description of the reactions catalysed by aristolochene synthase

The first step in the reaction cascade (Scheme 1.10) catalysed by aristolochene synthase is the loss of the diphosphate group from farnesyl diphosphate (**5**). Upon binding of three magnesium ions, diphosphate expulsion from the C1 position of FDP is triggered by the intramolecular attack of the distal C10,C11 π-bond on C1 in a concerted reaction that occurs with inversion of configuration at C1.[55,64] Deprotonation of the resulting germacryl cation (**18**) leads to the germacrene A (**21**).[65,66,67,68] Protonation of germacrene A by an unidentified active site acid[48,49,66,67] and electron flow from the C2-C3 π-bond to C6 leads to the formation bicyclic eudesmane cation (**68**).[48] Residue Y92 was initially suggested to act as an acid in the formation of the eudesmane cation (**68**).[48,63,66,67] However, after Felicetti and Cane removed the hydroxyl group of tyrosine, generating a Y92F mutant, this still produced aristolochene, but in low amount.[25] The positive charge on the eudesmane cation is thought to be stabilised by the π-system of W334.[60] Successive 1,2-hydride shift and methyl migration followed by loss of H_S on C8 complete biosynthesis of (+)-aristolochene (**24**).[55,65]
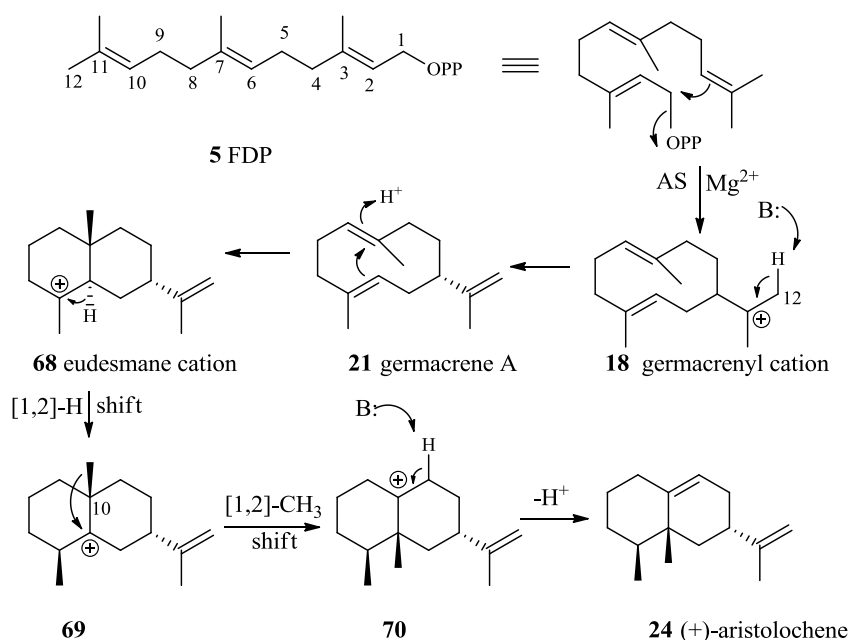
Scheme 1.10: *Proposed reaction catalysed by aristolochene synthase PR-AS*

Based on the X-ray crystal structure of isoprene synthase bound to a substrate analogue (dimethylallyl-S-thiolodiphosphate),[69] and due to the nearly physiological pKa of $H_2P_2O_7^{2-}$/ $HP_2O_7^{3-}$ pair, it was suggested that the enzyme bound diphosphate leaving group could serve as the general base in a *syn*-periplanar elimination (Scheme 1.11).[69]

2 DMADP   **1** isoprene
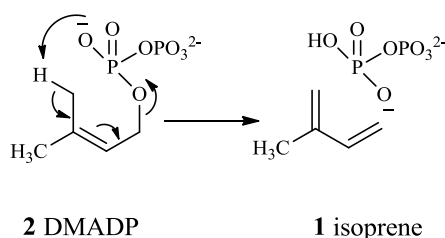
Scheme 1.11: *Conversion of DMADP (2) to isoprene (1) through a concerted reaction pathway*

Several aromatic residues are usually found in the active site of terpene synthases, and cation-π interactions involving the quadrupole moment of the aromatic ring are thought to stabilize cationic intermediates along the biosynthetic pathway.[70,71] The electrostatic component arises from interactions of the quadrupole moments of the aromatic rings, which are produced by the uneven distribution of charge. Greater electron density concentrates on the face of the ring, resulting in reduced electron density on the edge of the ring.[70,71]

FDP analogues have been used to study the complex reaction mechanism of PR-AS, Cane and co-workers synthesised four ^2H labelled FDP analogues at position C12, C13 and C8, which enable them to locate the site of the final deprotonation at C12.[65] In addition Cane *et al* found good evidence for the intermediacy of germacrene A during catalysis.[72] The incubation of the 6,7-dihydro-analogue of FDP (**71**) with AS generates the abortive cyclisation product, dihydrogermacrene A (**72**). This was confirmed by a direct GC/MS comparison with a synthetic sample.[72] According to the proposed mechanism of AS, the cyclisation step to form eudesmane cation would be prevented because of the loss of the C6-C7 double bond in this 6,7-dihydro-analogue of FDP causing dihydro-germacrene A (**72**) to accumulate (Figure 1.10).[72]
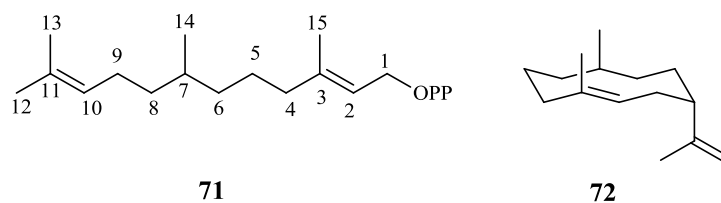
Figure 1.10: *Structures of 6,7-dihydro-analogue of FDP (**71**) and dihydro-germacrene A (**72**)*

At Cardiff University, the cationic reaction mechanism of the PR-AS, the route to aristolochene was probed with fluorinated farnesyl diphosphate. 2-Fluorofarnesyl diphosphate (**73**) was synthesised and incubation with aristolochene synthase resulted in the formation to 2-fluorogermacrene A (**74**). These results have shown that 2-F-FDP (**73**) was a poor substrate, and also suggest the absence of farnesyl cation (**50**) during the cyclisation pathway (Figure 1.11).[73]

Incubation of 6- and 14-fluoro farnesyl diphosphate **75** and **76** with PR-AS produced the corresponding fluorinated germacrene A analogues **77** and **78**. These results provided compelling evidence of intermediacy of germacrene A (**21**) during PR-AS catalysis (Figure 1.11).[68]

Incubation of the 12, 13-difluorofarnesyl diphosphate (**79**) (Figure 1.11) with PR-AS did not give any products as judged by GC-MS analysis.[64] The steady-state kinetic parameters of purified AS were measured in the presence of different amounts of 12,13-difluorofarnsyl diphosphate and radiolabelled [1-^{3}H]-FDP showing that **79** was a reversible competitive inhibitor of AS, with an inhibition constant (K_i = 0.8 ± 0.2 μM) comparable to the Michaelis constant of FDP (K_M = 2.3 μM),[64] suggesting that the initial cyclisation during AS catalysis generates germacryl cation (**18**) in a concerted process and also ruling out the possible existence of the farnesyl cation (**50**) in the enzymatic reaction catalysed by PR-AS, due to the electronic effects of fluoro substituents. The electrophilic attack of C1 by the C10, C11 π-bond would be inhibited if farnesyl cation **80** was generated in the first place. Thus, the accumulation of the 12,13-difluorofarnesyl cation would go through an elimination, forming 12,13-difluoro-(E,E)-α-farnesene (**81**) and 12,13-difluoro-(E)-β-farnesene (**82**)[64] (Scheme 1.12).

The formation of eudesmane cation (**68**) has been inferred by site-directed mutagenesis experiments. X-ray crystallographic analysis reveals that this cation **68** could be established by W334 through cation-π interaction. Tryptophan 334 was mutated with the aliphatic amino acids valine and leucine, which led to accumulate of germacrene A, therefore suppressing the native aristolochene activity of this enzyme.[60]

A recent mutagenesis study with non-canonical residues has shown the importance of cation π- interactions as the means of carbocation stabilisation during PR-AS catalysis. In particular, when Trp334 was replaced with unnatural phenylalanines [W334*p*-(Cl)Phe, W334*p*-(CF$_3$)Phe and W334*p*-(NO$_2$)Phe] harbouring para-substituents with increasing electron-withdrawing properties, accumulation of germacrene A (**21**) was observed. The amount of **21** generated as a proportion of the hydrocarbon products proved to be directly proportional to the electron withdrawing power of the *para* substituent. These results provided strong evidence for the stabilising role played by Trp334 during AS-catalysis since they demonstrate that reduction in the cation-π stabilising ability of the aromatic amino acid side chains leads to a reduced propensity, in this case, to form the eudesmane cation.[74] Taken together, these studies have provided compelling evidence supporting a cyclisation cascade involving at least two discrete intermediates: the neutral hydrocarbon germacrene A (**21**) and the highly reactive eudesmane cation (**68**) (Scheme 1.10). However, little is known about the last three steps (Scheme 1.10) leading to aristolochene from the enzyme-bound eudesmane cation (**68**).
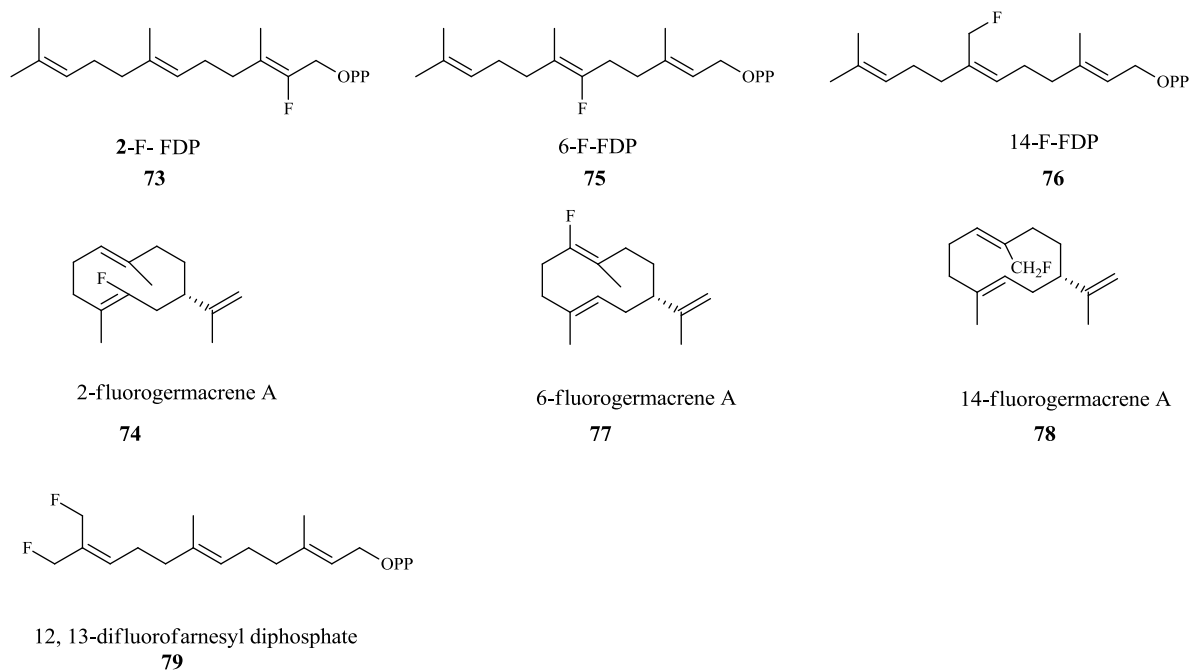
Figure 1.11: *Structures of fluorinated farnesyl diphosphates **73**, **75**, **76** and **79** and the fluorinated germacrene A analogues **74**, **77** and **78***
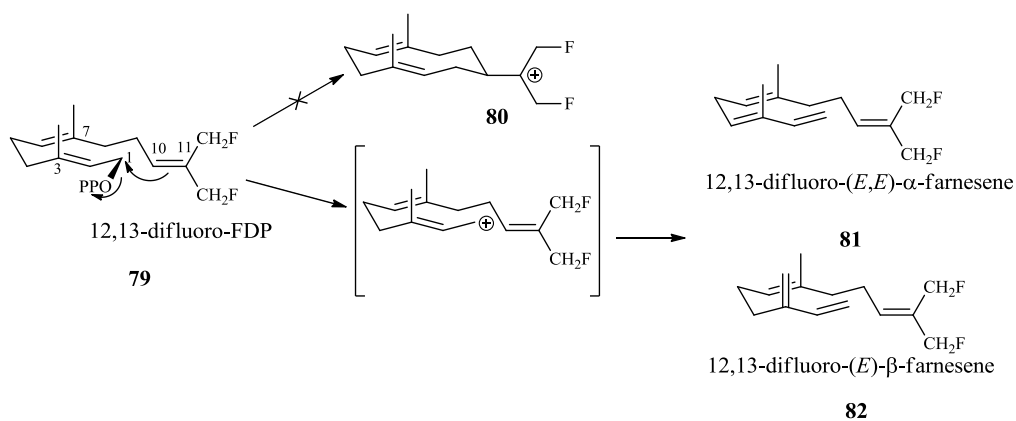
Scheme 1.12: *Proposed mechanism for the conversion of 12,13-difluorofarnesyl diphosphate (**79**) to 12,13-difluoro-(E,E)-α-farnesene (**81**) and 12,13-difluoro-(E)-β-farnesene (**82**)*

1.8 Aza-analogues of highly reactive carbocations

Since the carbocations involved in terpene chemistry are highly unstable intermediates that cannot be isolated, their transient existence within the active sites of terpene synthases can be inferred indirectly through the use of FDP analogues or mutagenesis (as discussed above). A complementary approach to study the complex cationic reactions catalysed by terpene synthases consist of the use of stable aza-analogues of the putative carbocations. To probe the carbocationic nature of the 1,2-hydride and methyl shifts, two novel aza-analogues (**83** and **84**, Figure 1.12) have been designed for synthesis and evaluation of their capacity as inhibitors of PR-AS. These compounds were designed to mimic the geometric and electrostatic properties of postulated carbocation intermediates **69** and **70** in the catalytic mechanism of PR-AS.
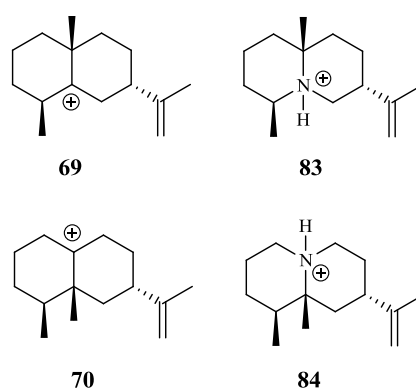
Figure 1.12: *Structures of 5-eudesmyl cation (**69**) and eremophilenyl cation (**70**) and their aza-analogues **83** and **84** respectively*

There are four possible pathways to determine the mechanism of the last transformations in PR-AS biosynthesis (Scheme 1.13): stepwise, concerted/stepwise, stepwise/concerted and concerted processes. In the stepwise mechanism, the enzymatic reaction goes through two carbocations **69** and **70** from eudesmane cation (**68**). While, in the fully concerted pathway, the transformation of eudesmane cation (**68**) to aristolochene (**24**) take place in one step. The other two possible mechanisms are partway between these two extremes. Therefore, the kinetic evaluation of the two analogues **83** and **84** as inhibitors of PR-AS should provide us with evidence about the existence of the putative carbocationic intermediates **69** and **70** on the pathway from FDP (**5**) to aristolochene (**24**) during PR-AS

catalysis. Hence, this study could be enable us to confirm the mechanism of the later steps in the catalytic cascade of PR-AS.
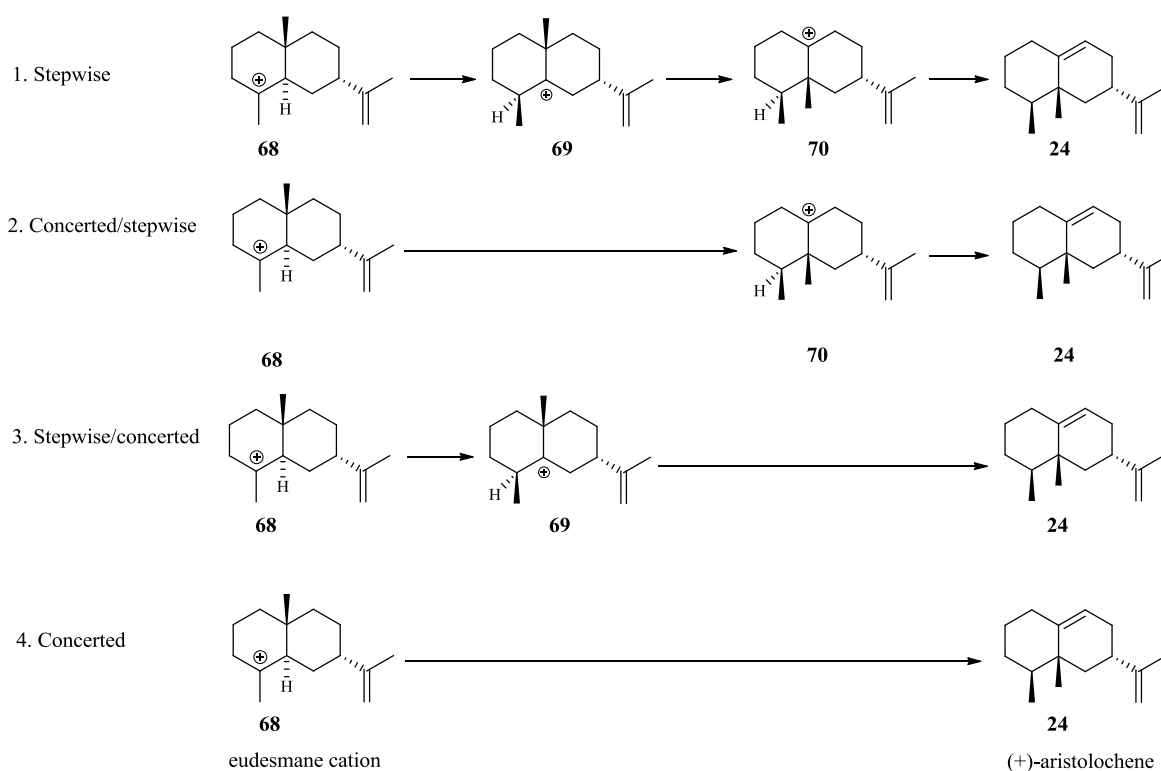
Scheme 1.13: *Stepwise versus concerted processes in aristolochene biosynthesis*

Aza-analogues of terpenes are nitrogen containing terpenoids that resemble postulated carbocationic intermediates in terpene biosynthesis. In particular, they are designed to mimic the geometric and electrostatic properties of presumed carbocationic species, but since they cannot be turned-over by the enzyme, they act as tightly bound inhibitors. The absence of the empty p-orbitals required to undergo the usual transformations of highly reactive carbocations generated by terpene synthases make them useful active site probes of these enzymes and as a consequence they are, for the most part, competitive inhibitors of these enzymes. Indeed aza-analogues have been reported as inhibitors of mono-,[75,76] sesqui-[77] and diterpene synthases,[78,79] as well as inhibitors of squalene and oxidosqualene synthases.[80-83] This concept has proven useful in the design of enzyme inhibitors aimed at suppressing sterol biosynthesis.[84-87] Aza-analogues presenting a positive charge at a position identical to that of the *sp²*-carbon in the carbocationic HEI (high energy intermediate). Hence, the trigonal carbcationic center is replaced by a tetrahedral

positively charged nitrogen.[82] The replacement of the *sp²* hybridised carbon of the proposed intermediate with a *sp³* hybridised nitrogen atom allows for a stable molecule to be synthesised in the laboratory providing a somewhat imperfect geometric model of the carbocation to study the cationic chemistry characteristic of terpene synthases. The positive charge has been shown to be distributed over the hydrogens carried by the α-carbons and the nitrogen atom being negatively charged. Thus, the alkyl ammonium group appears as a large, positively charged surface, with the nitrogen atom buried in the center.[88]

Our group recently provided an approach to identify eudesmane cation (**68**) by employing the aza analogue **85**[89] that effectively mimics the topological and electrostatic properties of eudesmane cation (**68**) (Figure 1.13).

68   **85**
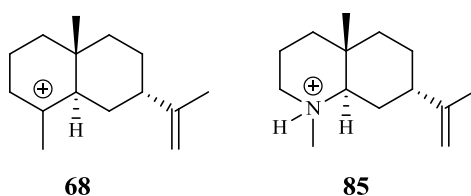
Figure 1.13: *Structures of eudesmane cation (68) and its aza-analogue 85*

Aza analogue **85** was synthesised in seven steps starting from chiral enamine **86** (Scheme 1.14), which was then alkylated with methyl acrylate to produce Michael adduct **87** as the only regioisomer. Protection of the ketone group of **87** as an acetal, and then reaction with NH₄OH afforded primary amide **88**. Reduction of amide **88** was achieved by using LiAlH₄, to the corresponding primary acetal amine and subsequent cyclisation to Schiff base **89** was induced by use of aqueous acid. Reduction of Schiff base **89** was carried out using sodium in ethanol and then reductive *N*-alkylation with formaldehyde in the presence of NaBH₃CN produced *N*-methyl trans-decahydroquinoline (**91**). This was exposed to hydrochloric acid in diethyl ether to yield ammonium salt **85**.[89]
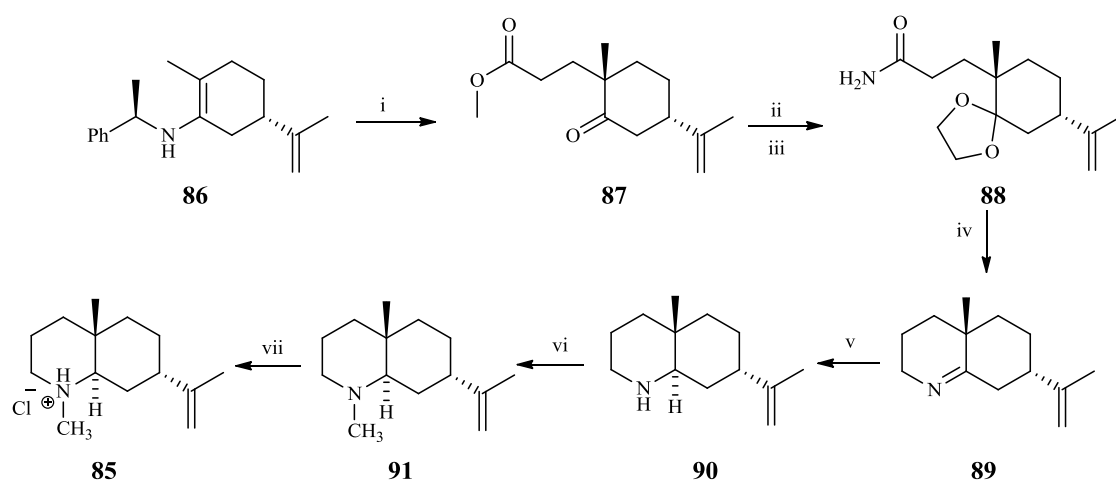
Scheme 1.14: *Stereoselective synthesis of 4-aza-eudesmane cation (85)[89] Reagents: (i)*
1. methyl acrylate, 2. Aq H⁺, (ii) ethylene glycol, cat H⁺, (iii) Aq NH₃, (iv) 1. LiAlH₄, 2. 10%
HCl, (v) Na, anh. EtOH, (vi) H₂CO, NaCNBH₃, (vii) HCl, Et₂O

Inhibition studies of PR-AS with ammonium salt **85**[89] have shown that the compound **85**
was clearly bound in the active site of the enzyme, with binding affinity (K_i = 0.34 μM)
almost identical to that displayed by FDP (K_M = 2.3 μM) in both, the absence and presence
of inorganic diphosphate (PPi). Consequently compound **85** is an excellent mimic of the
postulated eudesmane cation **68**, providing therefore strong evidence for the formation of
this highly reactive intermediate in the active site of the enzyme.[89]

Some aza analogues have been synthesized in both enantiomeric forms. The different
inhibition data for the two enantiomers gives enantioselective information for the
inhibitors in the enzyme active site. For example, Coates and co-workers reported the
synthesis of both enantiomers of aza analogues *R* and *S*-**93** for trichodiene synthase studies
(Scheme 1.15).[77] Although both of the enantiomers are inhibitors of trichodiene synthase,
no significant difference was found in the affinity of the enantiomers for the enzyme (K_i
=2.6 μM for the *R* isomer and 2.9 μM for the *S* isomer). Hence, the ability of trichodiene
synthase to bind both enantiomers of **93** with identical affinity is consistent with notion
that the active site of this synthase is permissive rather than restrictive with respect to
these particular enantiomeric pair of aza-analogues.[77]
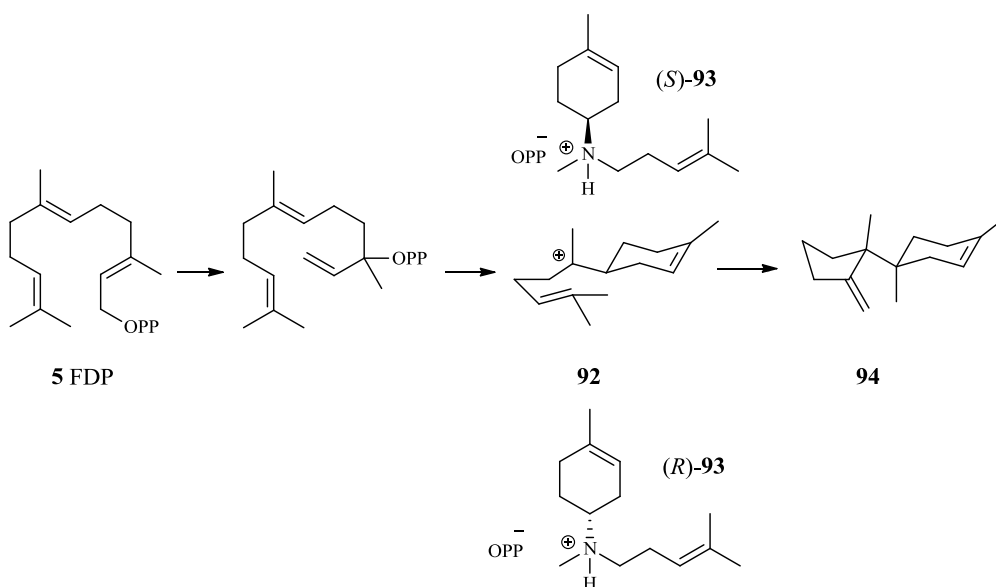
Scheme 1.15: *Aza analogues for studies of trichodiene (**94**) biosynthesis*

Another example, squalene synthase (SS) catalyses the 1`-1 condensation between two molecules of farnesyl diphosphate (**5**) via tertiary cyclopropyl carbinyl intermediate, presequalene diphosphate PSDP (**9**) (Figure 1.14) to yield squalene (**7**).[80] Because of its key position in the cholesterol biosynthetic pathway, squalene synthase is an attractive target for pharmacological intervention to reduce serum cholesterol level. Thus, Coates and co-workers reported the synthesis and characterization of two enantiopure aziridine analogues (-)-(2*R*, 3*S*)-**95**- and (+)-(2*S*, 3*R*)-**95**-diphosphates of PSDP (**9**) (Figure 1.14) and their evaluation as inhibitors of recombinant yeast squalene synthase.[90] These studies revealed that the (-)-(2*R*, 3*S*)-**95**- diphosphate enantiomer matching the configuration of PSDP (**9**) showed better inhibition (IC$_{50}$ 1.17 ± 0.08 μM) than other enantiomer (+)-(2*S*, 3*R*)-**95**-diphosphate in the absence and the presence of inorganic diphosphate (16-fold and 4-fold, respectively).[90]
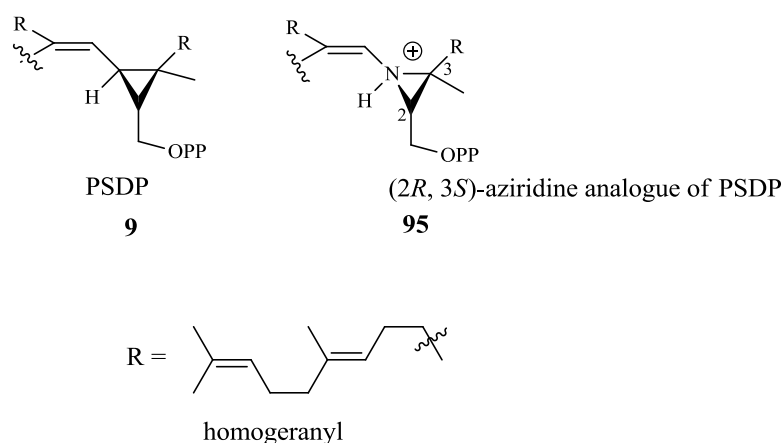
Figure 1.14: *Structures of PSDP (9) and (2R,3S)-aziridine analogue (95) of PSDP* [90]

Due to their kinetic behaviour, aza analogues of cationic intermediates have been used in X-ray crystallographic studies of terpene synthases and useful structural information has been obtained. Christianson, Croteau and Coates reported 2-azabornane (**97**) and 7-aza-7,8-dihydrolimonene (**96**), two inhibitors of bornyl diphosphate synthase (BDPS) as crystallisation aids (Scheme 1.16). The X-ray structures of the enzyme-aza analogue complexes obtained at 2.0 Å resolution,[75] providing key mechanistic interferences regarding the cyclisation sequence of geranyl diphosphate including the position, the orientation of the substrate, and the interaction between the substrate and the key active site amino acid residues.
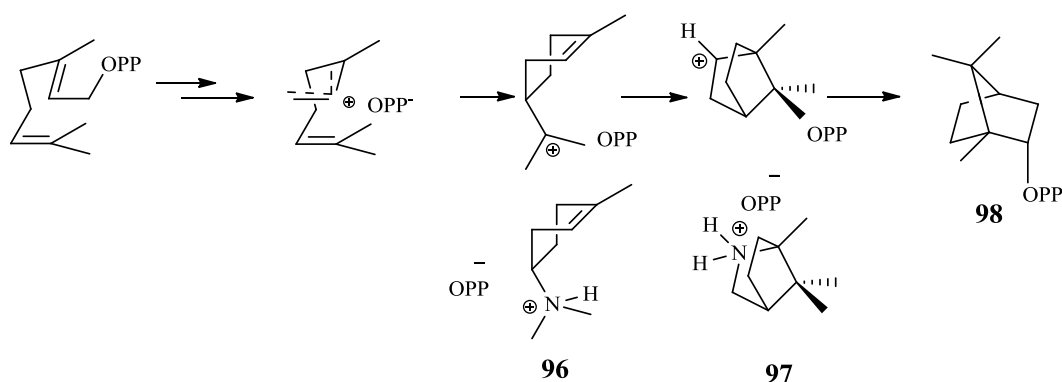
Scheme 1.16: *Aza-analogues for studies of BDPS* [75]

It is worth noting that in practice, the inhibition studies of aza-analogues are performed in both the presence and absence of inorganic diphosphate (PP$_i$), since the effectiveness of some aza-analogues is enhanced by the presence of PP$_i$. The effect of PP$_i$ on the

experiment can provide insight into the role of PP_i as a stabilising counter ion in the enzymatic mechanism. For example, *ent*-kaurene synthase catalyses the conversion of geranylgeranyl diphosphate (GGDP, **6**) through copalyl diphosphate (CDP, **99**) to *ent*-kaurene (**101**) (Scheme 1.17).[91] The secondary carbocation *ent*-beyeran 16-yl cation (**100**) is a key branch intermediate in the proposed mechanistic scheme. In order to evaluate this mechanistic hypothesis, Roy and co-workers synthesised the aza analogues of 16-aza-*ent*-beyerane (**102**) and 16-aza-*ent*-trachylobane (**103**) that mimic the *ent*-beyeran-16-yl ion (**100**) and protonated *ent*-trachylobane (**104**)[91] (Figure 1.15). These aza-analogues **102** and **103** have inhibited *ent*-kaurene synthase with inhibition constants of IC_{50} = 1 x 10^{-7} and 1 x 10^{-6} M similar in value to the binding constant of the *ent*-copalyl diphosphate substrate (K_M = 3 x 10^{-7} M). Indeed, these two analogues showed strong synergism in the presence of 1 mM inorganic PPi (IC_{50} = 4 x 10^{-9} and 2 x 10^{-8} M). The strong synergy displayed by these compounds with PPi suggested a large stabilization of the corresponding carbocationic intermediate, by ion pairing with the (PPi.Mg) released in the first ionization of copalyl diphosphate substrate (**99**).[91]

6 GGDP   **99** copalyl diphosphate   **100** *ent*-beyeran 16-yl cation   **101** *ent*-kaurene
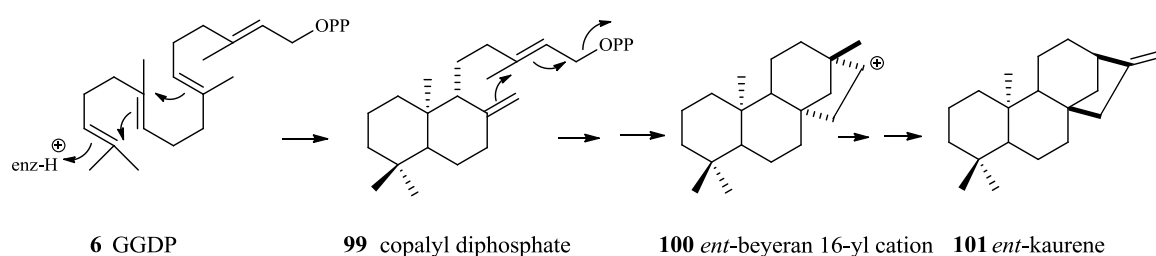
Scheme 1.17: *Biosynthesis of ent-kaurene (101)*

100 *ent*-beyeran-16-yl ion   **102**

104 *ent*-trachylobane   **103**
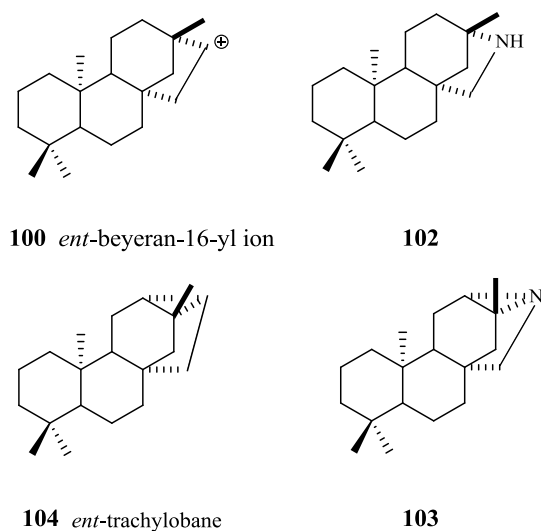
Figure 1.15: *Structures of 16-aza-ent-beyerane (**102**) and 16-aza-ent-trachylobane (**103**), proposed aza analogue mimics for the ent-beyeran-16-yl ion (**100**) and protonated ent-trachylobane (**104**)*[91]

1.9 Quinolizidine alkaloids

The synthetic bicyclic tertiary amines **105**-**111** and iminium ion **112** (Figure 1.16) belong to the quinolizidine family of alkaloids and previous routes for the synthesis of these bicyclic amines are presented below.

105   **106**   **107**   **108**

109   **110**   **111**   **112**
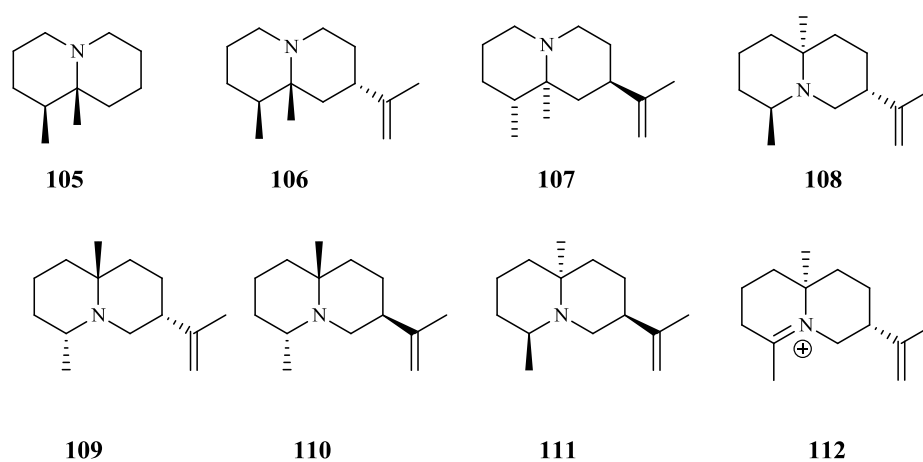
Figure 1.16: *Structures of quinolizidines **105**-**112***

Quinolizidine alkaloids represent about 2% of the 7000 known plant alkaloids. The lupin alkaloids responsible for the toxic properties associated with *Lupinus*, are characterized by

a quinolizidine skeleton. Quinolizidine alkaloids are mainly found in plants of the *Leguminosae* family. They prevent or repel feeding of herbivores, and are toxic to them through a variety of mechanisms. A number of plants (*Laburnum, Cytisus, Lupinus*) contain significant quantities of these alkaloids and are known to be responsible for human poisoning.[10]

Further examples of natural products containing the quinolizidine skeleton are cermizine C (**113**), senepodine G (**114**) and cermizine D (**115**) (Figure 1.17). These compounds are so-called *Lycopodium* alkaloids because this plant produces a number of alkaloids that have unique structures and biological activities, such as acetylcholine esterase (AchE) inhibitory activity. Thus, *Lycopodium* alkaloids have been attractive targets for organic and medicinal chemistry.[92]

cermizine C

113

senepodine G

114

cermizine D

115
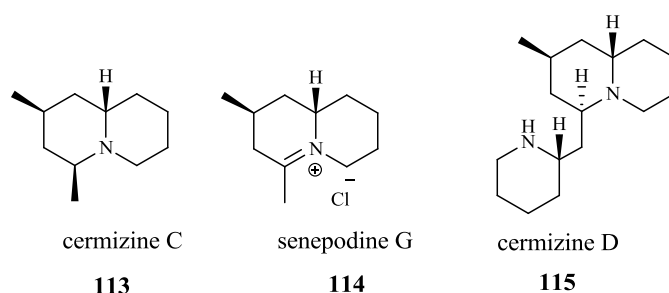
Figure 1.17: *Structures of cermizine C (**113**), senepodine G (**114**) and cermizine (**115**)[92]*

The quinolizidine or octahydroquinolizidine structure (**116**) is a central framework in numerous important natural products, representing the simplest member of the family, with only one substituent at the C1 position, as shown for lupinine alkaloids (**117**) and epilupinine (**118**) (Figure 1.18).[93] Lupinine carries the hydroxymethyl group in an axial position. By comparison with the decalins the preferred conformation of the lupinine structure is expected to be that in which the rings are *trans*-fused because this minimises 1,3-diaxial interactions. [93] Thus, despite the axial opposition between the hydroxymethyl group, axial hydrogen atoms and axial lone-pair in lupinine, the *trans*-conformation must still be important. In this instance the intramolecular hydrogen bonding between the nitrogen atom and the hydroxyl group occurs to favour the *trans*-conformation. While,

epilupinine (**118**) bears the hydroxymethyl group in equatorial position, or this configuration is associated with the preferred *trans*-fused conformation.[93]

Bohlmann has shown that a prominent infrared band at 2800-2700 cm^{-1} occurs in the spectra of *trans*-fused quinolizidines, in which the nitrogen lone-pair is *trans* to at least two axial hydrogen atoms on carbon atoms adjacent to nitrogen.[94] This characteristic absorption is seen at 2750 cm^{-1} in the infrared spectrum of quinolizidine and (-)-lupinine (**117**).

The lower frequency of the *trans*-bands compared with the normal C-H region was due to charge delocalization of the nitrogen lone pair of electrons to the axial C-H bonds. In the *trans*-fused quinolizidine system, all three axial C-H bonds should take part in this delocalization. The axial C-H bonds on both C-1 and C-9 (**116**, Figure 1.18) have the same symmetry and force constants, so vibrational coupling can occur, and two bands appear at 2800 and 2700 cm^{-1} respectively. The first is due to asymmetric, and the second due to symmetric, stretching vibrations.[93,94]

116 quinolizidine   *trans*-**116**   *cis*-**116**

117 (-)-lupinine   *trans*-**117**   **118** epilupinine   *trans*-**118**
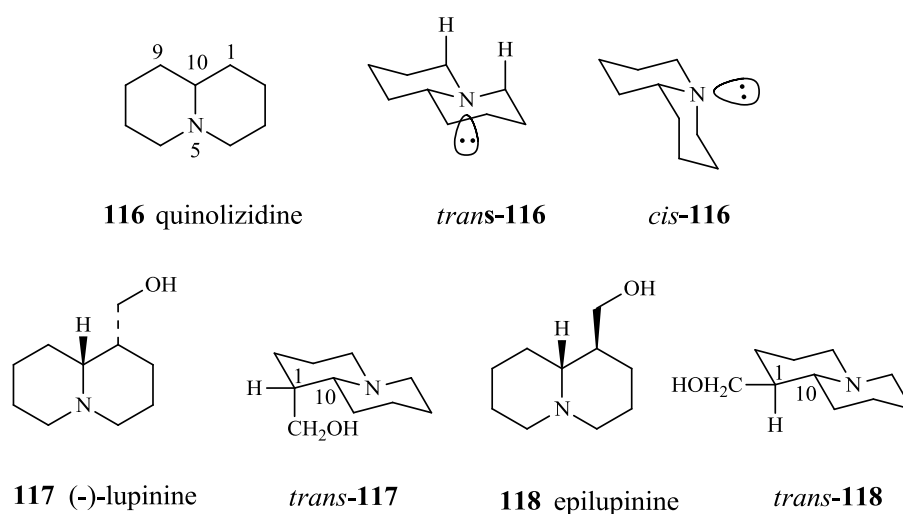
Figure 1.18: *Structures of quinolizidine (**116**), lupinine alkaloid (**117**) and epilupinine (**118**)*

The predominance of the *trans*-fused conformation has also been demonstrated by ^{1}H- and ^{13}CNMR spectroscopy.[93] Quinolizidines having the *cis* ring fusion either show much weaker or no Bohlmann bands at all.[93]

1.9.1 Synthesis of lupinine and related compounds

The azabicyclic skeleton of quinolizidine is an important structural subunit present in numerous alkaloids. The wide range of biological activities found in this family of natural products make them ideal targets for total synthesis. Quinolizidine (**116**) was prepared by Boekelheide and Rothchild.[95] For this synthesis, 1,1-dicarbethoxy-3-(2-pyridyl)-propane (**121**) was prepared by Michael addition of diethyl malonate (**120**) to vinyl pyridine (**119**) (Scheme 1.18). The preparation of 4-quinolizidone (**122**) was carried out by means of Raney nickel hydrogenation of 1,1-dicarbethoxy-3-(2-pyridyl)-propane (**121**) in dioxane solution at 125-150 °C under hydrogen pressure according to the procedure reported by Bohlman and co-workers.[96] The lactam **122** was then converted in high yield to quinolizidine (**116**) by the action of lithium aluminium hydride (Scheme 1.18).
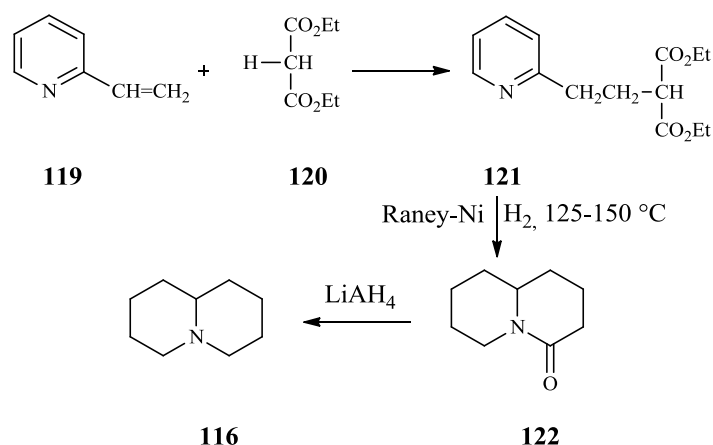
Scheme 1.18: *General procedure for synthesis of quinolizidine (**116**)*[95,96]

The absolute configuration of (-)-lupinine (**117**) was established by X-ray diffraction[97] as (1*R*,10*R*)-1-hydroxymethyquinolizidine.[93,97] Synthesis of (-)-lupinine has been carried out directly, without a separate resolution step. Reductions of (-)-and (+)-1-menthoxycarbonyl-1-(10)-dehydroquinolizidines-**123** with NaBH$_4$ yielded (-) and (+)-menthoxycarbonyl quinolizines-**124** (Scheme 1.19). Subsequent treatment with lithium aluminium hydride afforded (+)-and (-)-lupinines-**117** in 10% yield.[98] The enantiomeric 1-menthoxycarbonyl-1-(10)-dehydroquinolizidines (-)-**123**-**a** and (+)-**123**-**b** were prepared separately (Scheme 1.20) by reaction of 1(10)-dehydroquinolizidine (**125**) with enantiomerically pure menthyl chloroformates (-)-**126**-**a** and **126**-**b**. The later compound was obtained via reaction of

enantiomeric menthol **127**-**a** and **127**-**b** with phosgene (Scheme 1.20).[98] The dehydroquinolizidine **125** was prepared by dehydrogenation of quinolizidine (**116**) with mercuric acetate as reported by Leonard and co-workers.[99]
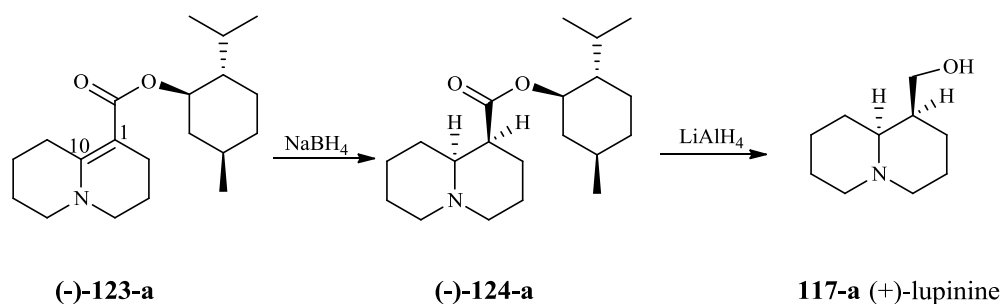
Scheme 1.19: *Asymmetric synthesis of (+)-lupinine by Goldberg[98]*
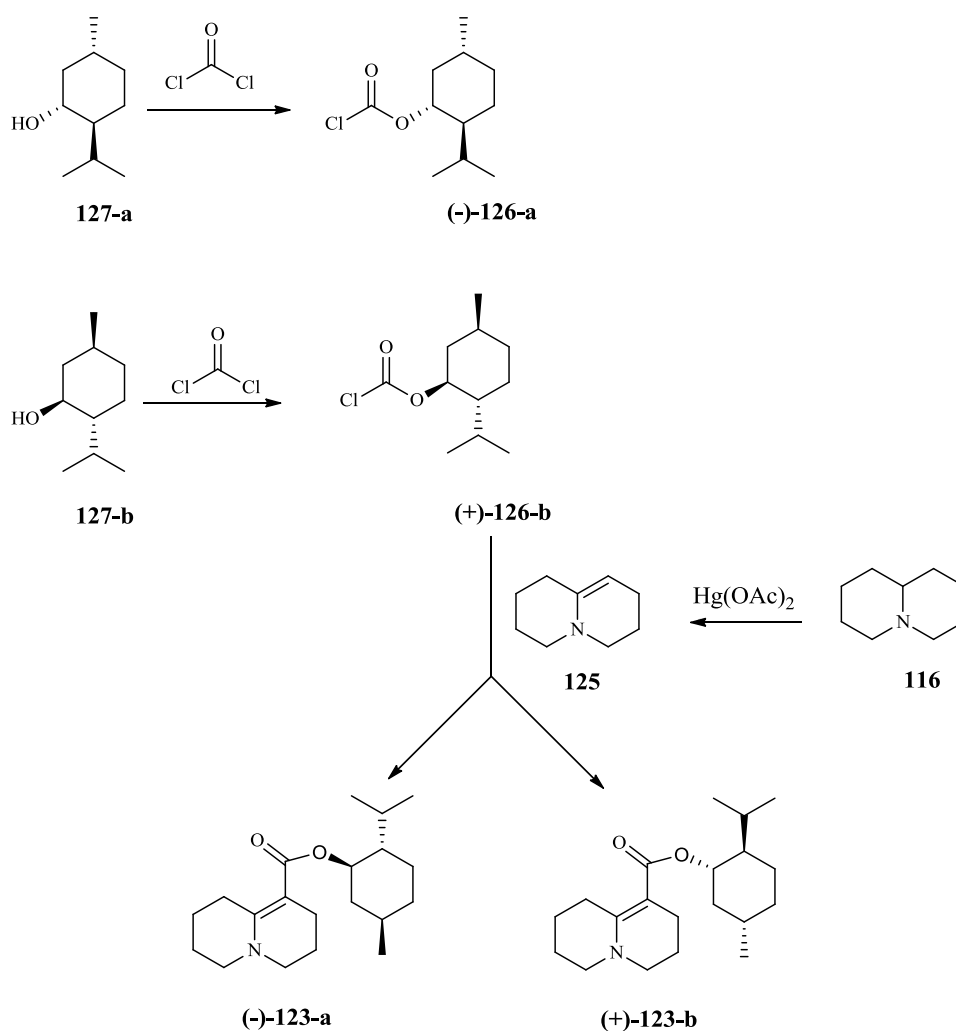
Scheme 1.20: *Synthesis of both enantiomers of 1-menthoxycarbonyl-1-(10)-dehydroquinolizidines (-)-**123-a** and (+)-**123-b**[98]*

Another synthesis of lupin alkaloids was described by Boekelheide and co-workers.[100] It was shown that ɣ-(2-pyridyl)-butyronitriles (**129**) (Scheme 1.20) upon mild hydrogenation over platinum in the presence of acid, underwent cyclisation to afford quinolizidine derivatives (**130-132**, Scheme 1.21). Since the requisite ɣ-(2-pyridyl)-butyronitriles (**129**) was synthesised from either 2-vinylpyridine (**128**) or ethyl 2-pyridyl acetate, these two steps were useful for preparing 1- and 3-substituted quinolizidines, compounds which are of interest because of their relationship to the lupin alkaloids.[100]

128 **129** **130** R = CO$_2$Et
131 R = C$_6$H$_5$
132 R = CH$_2$OH
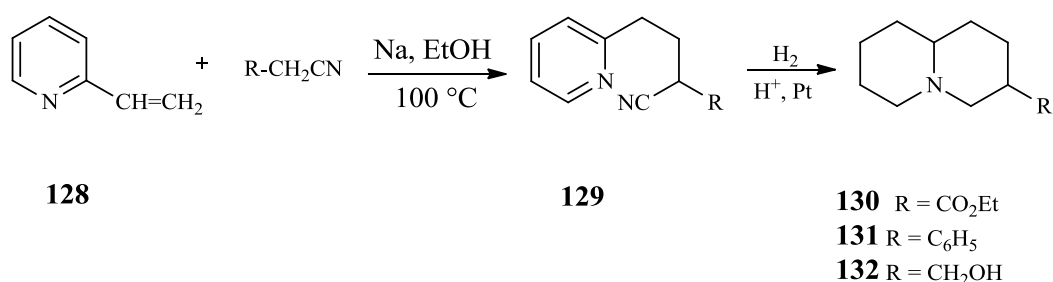
Scheme 1.21: *Boekelheide's method for the synthesis of 1- and 3-substituted quinolizidines.*[100]

Gerrans reported another approach to the synthesis of various substituted pyrrolizidine, indolizidine and quinolizidine ring systems.[101] The key steps of this approach involved the selective use of the ambident nucleophilicity of the vinylic urethane group at the α- and ɣ-C atoms **135** (Scheme 1.22). 2-Thiopiperidone (**133**) was treated with ethyl acrylate in the presence of catalytic amount of NaH to give the N-alkyl derivative **134**, which was then treated with ethyl bromoacetate and Et$_3$N/Ph$_3$P to give the vinylic urethane **135**. The saturated ester group of **135** was selectively reduced with LiAlH$_3$OEt to give the alcohol **136**, which on treatment with NaH/*p*-TsCl followed by warming in CH$_3$CN, afforded directly the bicyclic vinylogous urethane **137**. Conversion of compound **137** to *rac*-lupinine (**117**) was achieved by using NaBH$_4$ followed by LiAlH$_4$.[101]
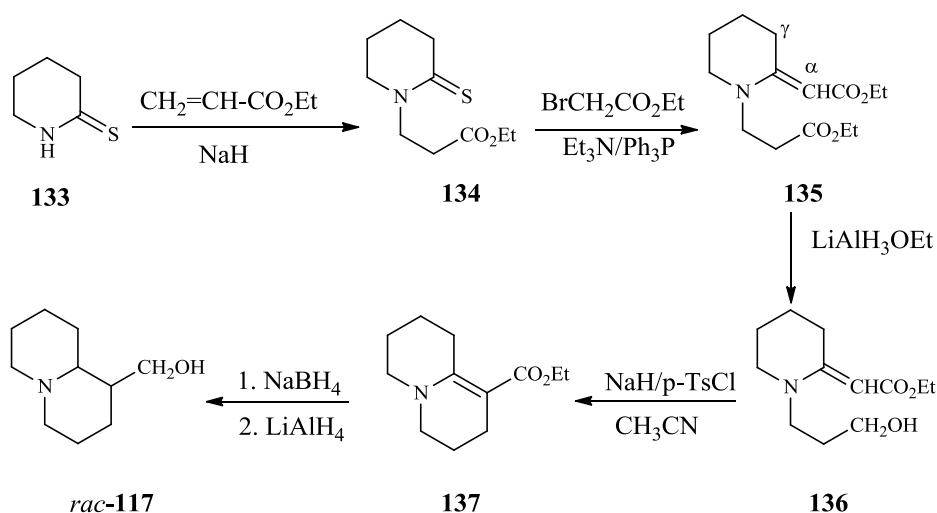
Scheme1.22: *Conversion of 2-thiopiperidone to lupinine as reported by Gerrans.*[101]

In a different approach, epilupinine (**118**) was synthesized starting from cyclic thioimidate (**138**) that underwent Robinson annulation using methyl 3-oxo-4-pentenoate (Nazarov's reagent).[102,103] Reaction of cyclic thioimidate (**138**) with Nazarov's reagent (**139**) in the presence of $HgCl_2$ to give quinolizidine **140** (Scheme 1.23). Stereospecific reduction of **140** with diisobutylaluminum hydride (DIBAL) gave saturated β-ketoester **141** and then complete reduction of the ketone by using Mozingo's methodology[104] followed by reduction of the ester group with $LiAlH_4$ afforded (±)-epilupinine (**120**).
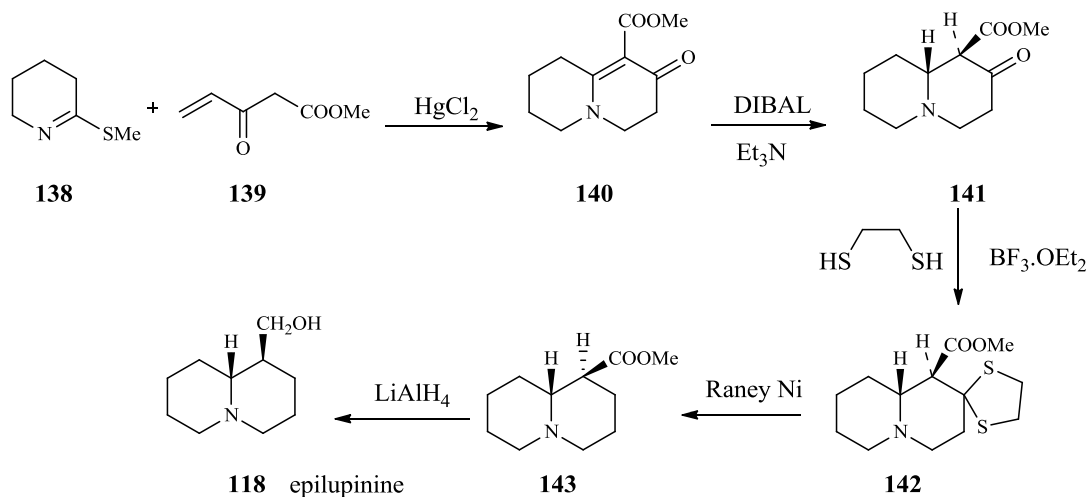
Scheme 1.23: *Robinson annulations using Nazarov's reagent to synthesis (±)-epilupinine (118) reported by Hiroki et al* [102]

The conversion of the quinolizidine product **140** to lupinine (**117**) was also described (Scheme 1.24).[102] Thianation of the ketone group with Lawesson's reagent produced enaminothioketone **144** which was then desulfurised with Raney Ni to give enaminoester **145**. Stereospecific reduction of **145** was achieved with sodium borohydride to afford methyl lupinate **146** and subsequent conversion to (±)-lupinine (**117**) was completed by reduction with LiAlH$_4$.[102]
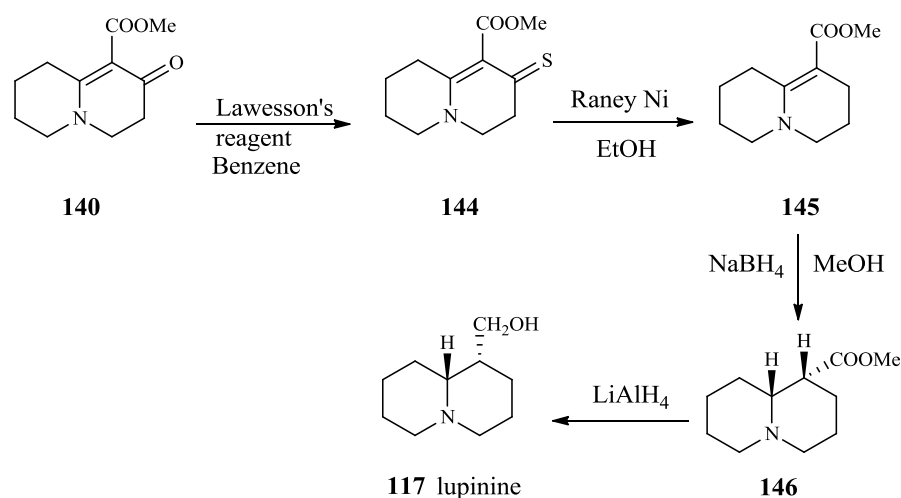
Scheme 1.24: *Synthesis of (±)-lupinine (**117**) reported by Hiroki et al.* [102]

Oxidation of quinolizidine (**116**) with mercuric acetate yielded $\Delta^{1(10)}$-dehydroquinolizidine (**125**, Scheme 1.25) that yielded upon treatment with perchloric acid the $\Delta^{5(10)}$-dehydroquinolizidinium salt (**147**). Subsequently introduction of a bridgehead methyl group at the C10 position was performed. The formation of 10-methylquinolizidine (**148**) was achieved by treatment of dehydroquinolizidinium salt (**147**) with methyl magnesium iodide (Scheme 1.25).[99]

Enamines and iminium salts can be distinguished using IR spectroscopy. The IR spectrum of enamine **125** showed an absorption at 1625 cm^{-1}, while the perchlorate salt **147** absorbed intensively and sharply at 1696 cm^{-1}. The shift of infrared absorption frequency to higher value from enamine to its iminium salt has been shown to be characteristic of α, β-unsaturated amines (enamines).[105]
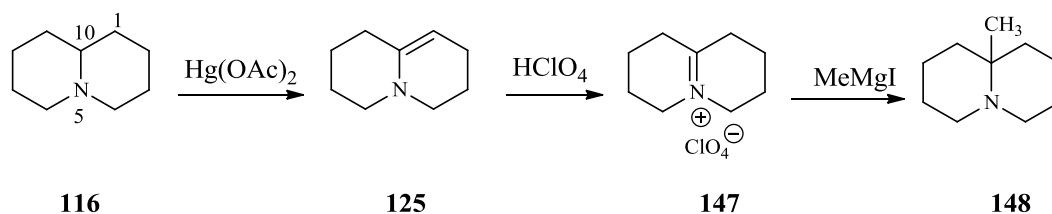
Scheme 1.25: *Synthetic sequence for conversion of quinolizidine (**116**) to 10-methylquinolizidine (**148**)*[99]

In order to synthesise disubstituted quinolizidine, recent efforts have established a procedure for the conjugate addition of lithiated methyl pyridines **149** to enone **150** (Scheme 1.26).[106] The utility of this reaction was demonstrated by the concise synthesis of (±)-cermizine C (**113**) and (±)-*epi*-cermizine C (**151**). To carry the synthesis forward, the 1,4-addition product **152** was protected as the acetal **153** (Scheme 1.26). Catalytic hydrogenation of compound **153** gave a 1: 1 ratio of the diastereomers **154** and **155** that it was possible to separate by chromatography. Separately, exposure of each diastereomer to acid yielded the unstable alkaloids (±)-senepodine G (**114**) and (±)-*epi*-senepodine G (**156**). Reduction of each with NaBH$_4$ afforded the alkaloids (±)-cermizine C (**113**) and (±)-*epi*-cermizine C (**151**).[106]

Methiodide salts (**158**, **160**, Scheme 1.27) of quinolizidines have been prepared in two ways, firstly by direct quaternisation of quinolizidine with methyl iodide and secondly by cyclisation of 2-4`-iodobutyl-1-methylpiperidine (**157**).[93] The ^{1}H-NMR spectra of these compounds indicated that the compound formed by direct quaternisation has the trans-fused ring structure. However, the free bases, quinolizidine, 1-, 2- and 3-methylquinolizidine, all exist predominantly in the trans-fused ring conformation with an equatorial methyl group except 4-methylquinolizidine[93] (Figure 1.19), which would not be expected to hinder the approach of a quaternising reagent, so, the resulting methiodide salts would all be expected to preserve the *trans*-ring fusion and the equatorial C-methyl group. In general, quaternisation of methylquinolizidnes that contain the *trans*-fused

conformation with an axial methyl group on the same side of the molecule as the nitrogen lone pair lead to products with the cis-ring configuration.[93]

1. *n*-BuLi, 0 °C, 1h
2. CuBr.SMe$_2$, -30 °C, 2h
3. [O structure] -78 °C, 2h

149

150

152

Ethylene glycol, PTSA, Benzene

153

PtO$_2$, H$_2$, CH$_2$Cl$_2$

154   1:1   **155**

HCl, MeOH/H$_2$O   HCl, MeOH/H$_2$O

114 (±)-senepodine G   **156** (±)-*epi*-senepodine G

NaBH$_4$ NaBH$_4$

113 (±)-cermizine C   **151** (±)-*epi*-cermizine C
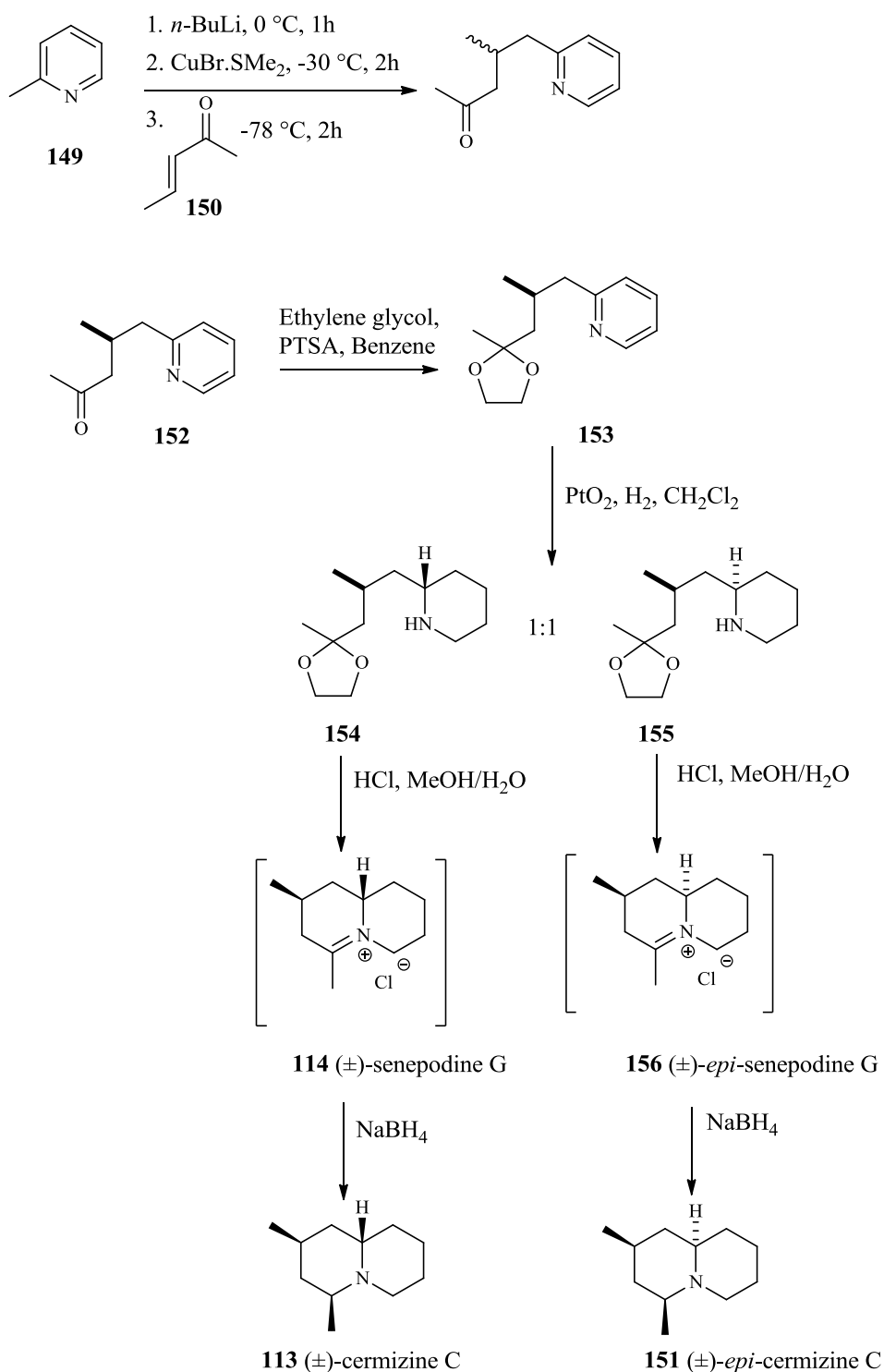
Scheme 1.26: *Stereoselective synthesis of (±)-cermizine C (113) and (±)-epi-cermizine C (151).[106]*
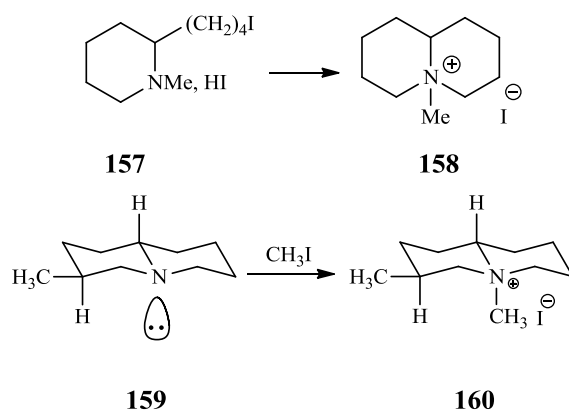
Scheme 1.27: *Routes to quinolizidines methiodide salts **158** and **160**.*

1-methylquinolizidine   2-methylquinolizidine   3-methylquinolizidne   4-methylquinolizidne

161   **162**   **163**   **164**
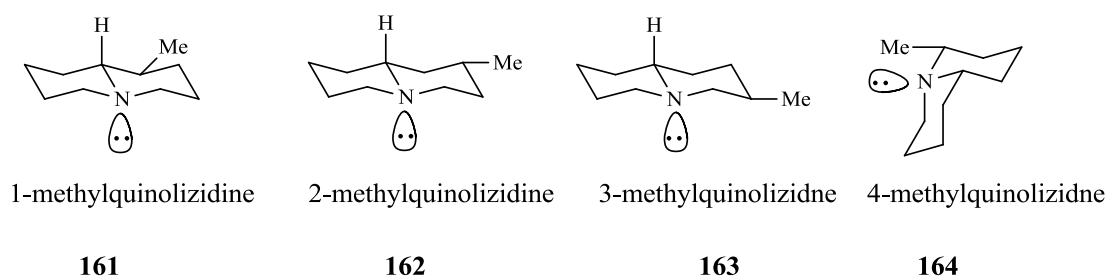
Figure 1.19: *Conformations of 1-, 2-, 3- and 4-methylquinolizidines*

1.10 2, 3, 4, 5-Tetrahydropyridine and its derivatives

2,3,4,5-Tetrahydropyridine and its derivatives have also attracted attention as key precursors for the synthesis of some alkaloids.[107] 2-Methyl-3,4,5,6-tetrahydropyridine **165** exist as two tautomers (Scheme 1.28). Compounds such as 2-methyl-3,4,5,6-tetrahydropyridine (**165**) are readily converted to a lithium derivative **166** with LDA that could react with an electrophile to further functionalise this ring (Scheme 1.28).[107]

165-a   **165-b**

165   **166**
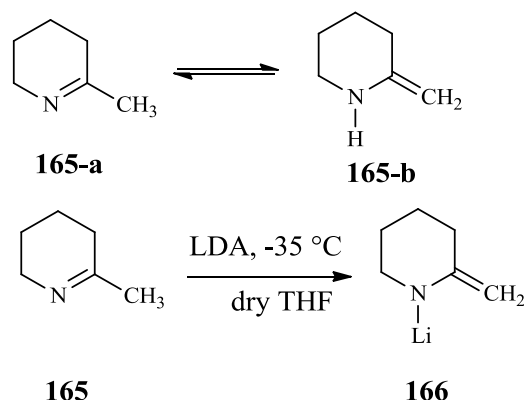
Scheme 1.28: *Structure and deprotonation of 2-methyl-2,3,4,5-tetrahydropyridine (**165**)[107]*

Indeed, the cyclic enamines as versatile synthetic intermediates have played an important role in the design of numerous alkaloid syntheses. For example, Evans and co-workers[108] have developed a general method for the synthesis of cyclic enamines from structurally varied imine anions. This method is generally applicable to the synthesis of Δ^2-tetrahydropyridine derivatives. Deprotonation at the α-position of imines **167** using LDA at low temperature in anhydrous conditions afforded an imine anion that was then alkylated with alkyl dihalides to produce cylic enamines **168** and **169** (Scheme 1.29).[108]
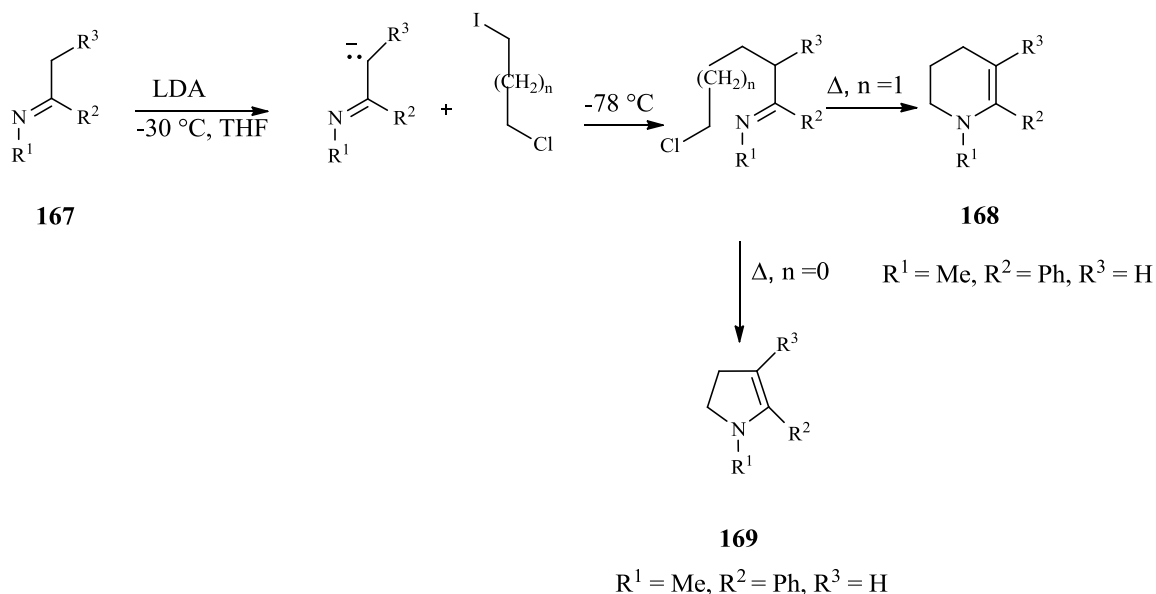
Scheme 1.29: *Synthesis of cyclic enamines **168** and **169***[108]

The above annulation sequence was then applied to the synthesis of 2-methyl-Δ^1-tetrahydropyridine (**165**) and $\Delta^{1(9)}$-octahydroquinoline (**170**), which were further transformed into bicyclic quinolizidines **171** and **172** respectively (Scheme 1.30).[108]
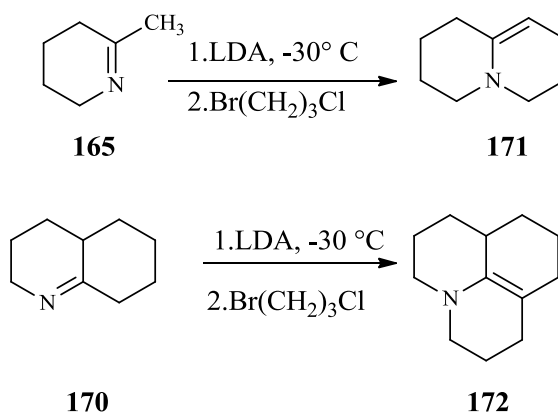
Scheme 1.30: *Evans' procedure for the synthesis of bicyclic enamines alkaloids **171** and*

172[108]

This methodology was later applied to the synthesis of 1,2,3,4,5,6,7,8-octahydro-1,6-naphthyridines (**175-177**) (Scheme 1.31),[109] another type of important nitrogen-containing bicyclic structures with potential biological activity, as predicted by the PASS

programme.[110] The computer software package PASS (prediction of activity spectra for substances) is used to rapidly predict various biological activities for selected compounds. These are pharmacological effects, mechanisms of action, mutagenicity and carcinogenicity.[110] PASS prediction is based on the analysis of structure-activity relationships of the training set including a great number of non-congeneric compounds with different biological activities. PASS once trained is able to predict many types of activity for a new substance. Compounds (**175-177**) may possess psychotropic, neuroleptic, spasmolytic and analgesic activities. Kinetic deprotonation of imine **173** with LDA in anhydrous conditions (Scheme 1.31), followed by consecutive alkylation with 1-bromo-3-chloro propane afforded **174**. The reaction mixture was then heated under reflux to effect final ring closure to (**175-177**).[109]
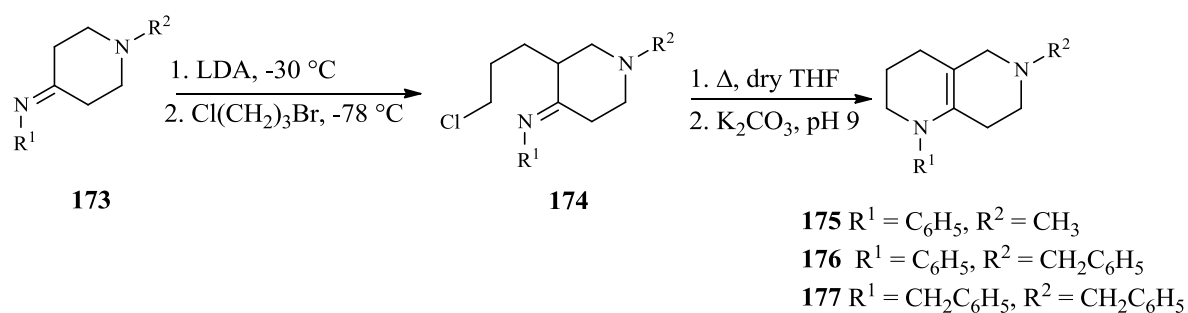
Scheme 1.31: *One pot syntheses of **175-177** using Evans' procedure.*[109]

1.11 Aim of this project

To further explore the reaction mechanism of PR-AS, the aim of this project was to synthesise of two novel aza-analogues, 5-aza-eudesmane cation (**83**) and 10-aza-eremophilene (**84**), designed to mimic the geometric and electrostatic properties of the carbcationic intermediates **69** and **70**, postulated to be involved in the last steps of Aristolochene biosynthesis. The kinetic evaluation of these two analogues **83** and **84** with PR-AS should provide us with evidence about the existence of the putative carbocationic intermediates **69** and **70** on the pathway from FDP (**5**) to aristolochene (**24**) catalysed by PR-AS. Moreover, the study of the binding affinity of these aza analogues with PR-AS should further our understanding of the mechanism of action of this class of enzyme and be applicable to other system.
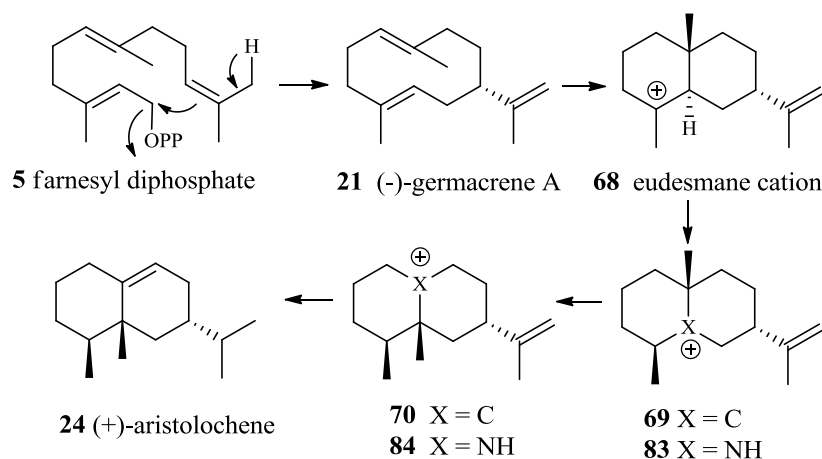
Scheme 1.32: *Carbocations proposed to be involved in aristolochene biosynthesis and the aza-analogues **83** and **84** targeted for synthesis*

CHAPTER TWO

STEREOSELECTIVE SYNTHESIS OF 10-AZA EREMOPHILANES

2.1 Target molecules

In this chapter, the synthesis of three analogues **178**, (7*R*,4*S*,5*S*)-**84** and (7*S*,4*R*,5*R*)-**84** (Figure 2.1) and their kinetic evaluation with PR-AS are described. These quinolizidine analogues possess the typical eremophilane skeleton of sesquiterpenes such as aristolochene and *epi*-aristolochene, with two vicinal methyl groups. These salts mimic the putative carbocations such as **70** (Figure 2.1) involved in sesquiterpene biosynthesis.
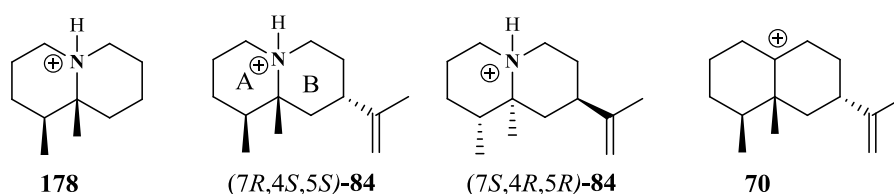
Figure 2.1: *Structures of target molecules **178**, (7R,4S,5S)-**84** and (7S,4R,5R)-**84** and eremophilanyl cation (**70**)*

2.2 Eremophilane skeleton

The biogenetically interesting eremophilane class of sesquiterpenes possess the basic carbon skeleton **179** showed in Figure 2.2. Eremophilone **180**, a sesquiterpene ketone isolated by Simonsen and co-workers in 1932 represented the first eremophilane-type sesquiterpene. [111] The most characteristic feature of these compounds are the *cis*-vicinal methyl groups at C4 and C5 in ring A, and the C7-isopropyl side chain in ring B. The numbering system normally employed for this class of compounds is shown in Figure 2.2.

179 eremophilane   **180** eremophil-11-en-3-one   **181** (4,5)-dimethyl-7-(prop-2-yl) decahydroquinolizidine
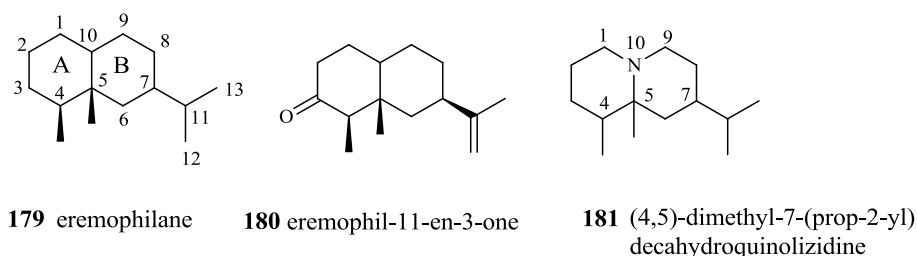
Figure 2.2: *Structure and numbering system of the eremophilane skeleton **179**, eremophilone (**180**) and quinolizidine (**181**)*

Eremophilane compounds are historically interesting in that they pose a disagreement with the original isoprene rule, which stated that, in case of sesquiterpenes, three isoprene units must be joined by head-to-tail linkages.[32] In this case however, the methyl group on C5 breaks this rule – it would be on on C-10 in eremophilane **179**, but it has migrated to C-5 during PR-AS catalysis.

2.3 Retrosynthetic analysis

Retrosynthetic analysis is the process of disconnecting a target molecule through a sequence of gradually simpler structures which leads to simple or commercially available starting materials. The transformation of a molecule to a synthetic precursor is accomplished by the application of a "*transform*", the theoretical reverse of a synthetic reaction to a target structure. The precursor species from which the target may be assembled are called *synthons*.[112]

Since the aza analogues **83** and **84** are structural mimics of the 5-eudesmane (**69**) and eremophilane (**70**) cations respectively, two proposed intermediates in the biosynthesis of PR-AS, the former would be potential inhibitors of PR-AS (Figure 2.3). The target molecules **83** and **84** were subjected to the disconnection process, giving the simpler precursors **182** and **183**. Each of the precursors so generated was then examined in the same way, and the process was repeated until simple or commercially available structure resulted. (4*S*)-limonene oxide (**187**) was chosen as the starting material for both aza analogues **83** and **84** as it is commercially available in both enantiomeric forms and possesses the required 4*S*-isopropylidene group.

The Robinson annulation consists of an initial Michael alkylation followed by an aldol condensation. The product of a Robinson annulation is a six-membered ring containing an α, β-unsaturated ketone. For example, compound **190** (Figure 2.4) may be formed by a combination of a Michael addition and an aldol reaction. The C=C bond in the ring is derived from the aldol reaction, while another new bond is created by the Michael reaction. Thus, the synthetic precursors of this transformation are compounds **191** and **192**.[113]
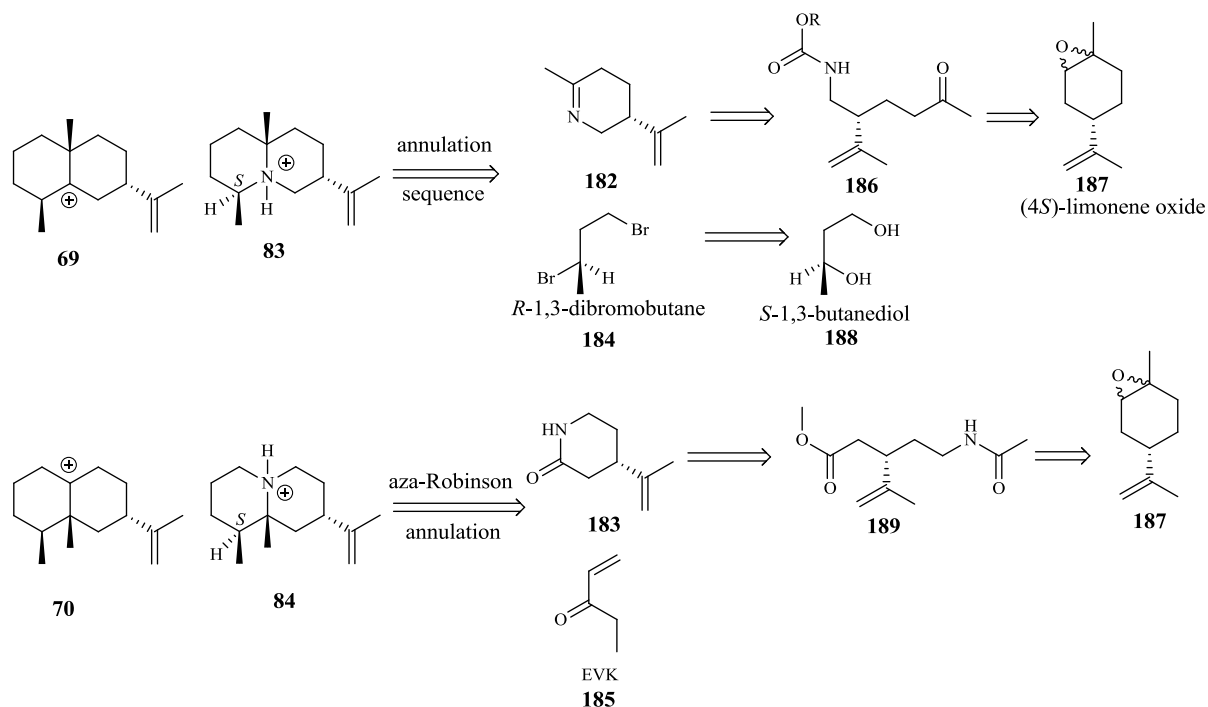
Figure 2.3: *Retrosynthetic analysis of aza analogues 83 and 84*
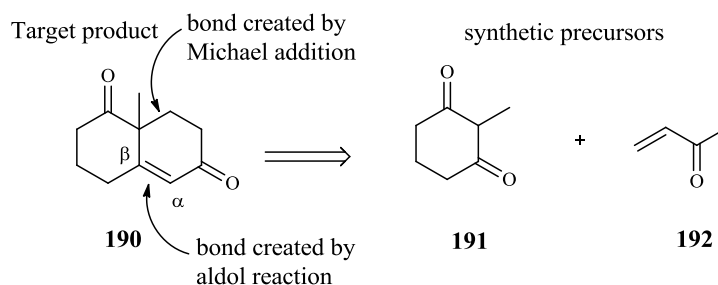
Figure 2.4: *Retrosynthetic analysis of compound 190*

The aza-Robinson annulation was decided upon for the synthesise enaminones **193** and **194** (Figure 2.5), one of the key intermediates *en route* to the tertiary amines **105** and **106**. Enaminone **193** was used in pilot experiments and synthesised by aza-Robinson annulation aimed at the construction of the ring A of aza analogue **84** (Figure 2.1). Retrosynthetic analysis of enaminone **193** led to the synthetic precursors, piperidone-2-thione (**195**) and ethyl vinyl ketone (**185**), while the retrosynthetic analysis of enaminone **194** involved (4*S*)-(prop-1-ene-2yl) piperidine-2-thione (**196**) and ethyl vinyl ketone (**185**).
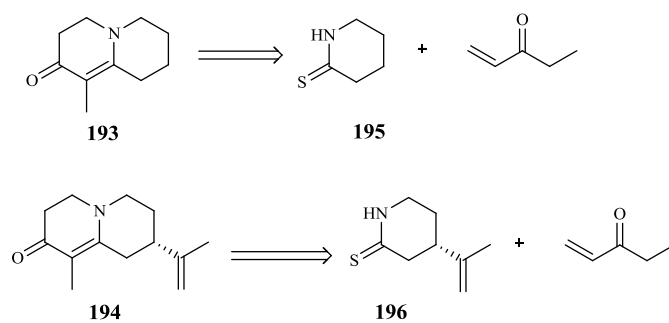
Figure 2.5: *Retrosynthetic analysis of enaminones **193** and **194** involving aza-Robinson annulations*

For the synthesis of the quinolizidine **84**, enaminone **194** could be synthesised by aza-Robinson annulation between thiolactam **196** and ethyl vinyl ketone (EVK) **185** via tandem Michael alkylation and aldol condensation (Figure 2.6). Lactam **183** could be obtained via cyclisation of acetamide **189**, which would be obtained via keto ester **198** through degradation of limonene oxide (**187**) and subsequent Beckmann rearrangement of **198**.
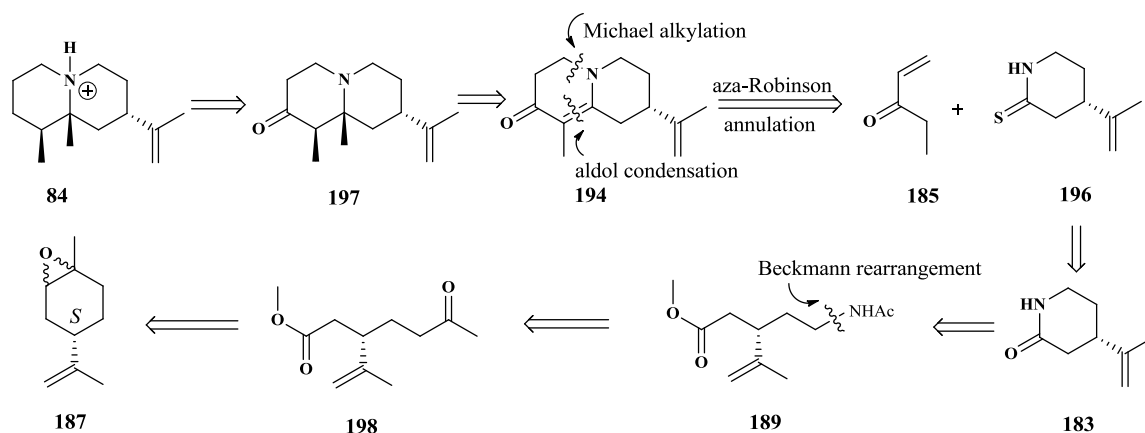
Figure 2.6: *Retrosynthetic analysis of 10-aza-eremophilane salt **84***

2.4 Preparation of monocyclic lactam 183

The first stage of this synthesis is the preparation of lactam **183**. Among the synthetic intermediates, the acyclic keto ester **198** is a very important one, since it allows the regioselective introduction of nitrogen at the keto position via a Beckmann rearrangement. The preparation of keto ester **198** has been reported before by Kido and co-workers[114] and the same procedures were followed. Reaction of (-)-limonene oxide (**187**) with KOH (5 equivalents), H_2O and DMSO for 24 h afforded a distereomeric mixture of diols **199** in 70% yield (Scheme 2.1). The mixture of epimers was carried forward to the next reaction without purification. In accordance with a standard S_N2 reaction (Scheme 2.1), the hydrolysis of limonene oxide under basic conditions took place through the nucleophilic attack at the least substituted position of the epoxide. Interestingly, Wolinsky and Chane [115] reported epoxide ring opening procedure with the structurally similar limonene 1,2-epoxide **200** under acid-catalysis with 1% H_2SO_4 in acetone which afforded a single anti diol **201-a**, that was different from the diols **201-b** and **201-c** obtained by Mori *et al*. using a similar procedure (Scheme 2.2).[116] The main difference between these two methods is the concentration of the acid catalyst. When concentrated $HClO_4$ was used, the reaction proceeded through a carbocation intermediate (S_N1 reaction), and subsequent attack by H_2O gave *cis* and *trans* diol isomers **201-b** and **201-c**. On the other hand, when diluted sulfuric acid was used at rt, nucleophilic epoxide ring opening is favoured via a S_N2 –like reaction, and a different diol isomer **201-a** was then formed. So, the hydrolysis of (-)-limonene oxide (**187**) in this study was most likely following the mechanism of the Wolinsky procedure.
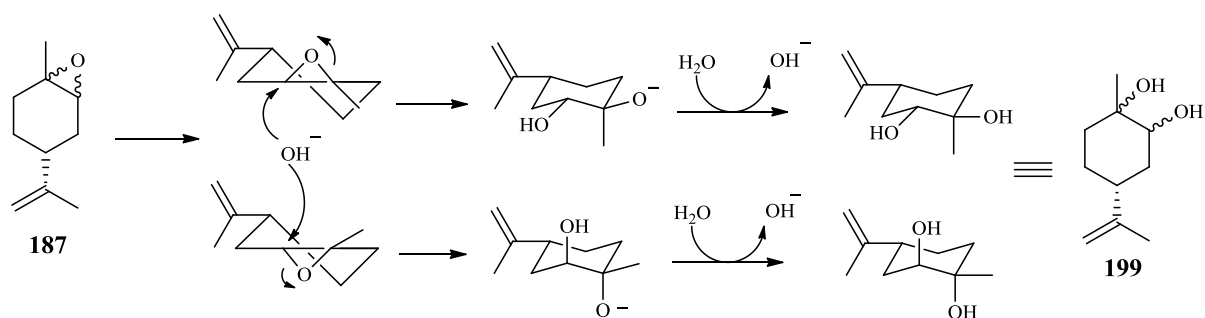
Scheme 2.1: *Base-catalysed hydrolysis of (-)-limonene oxide (**187**) to diastereomeric diol*

199
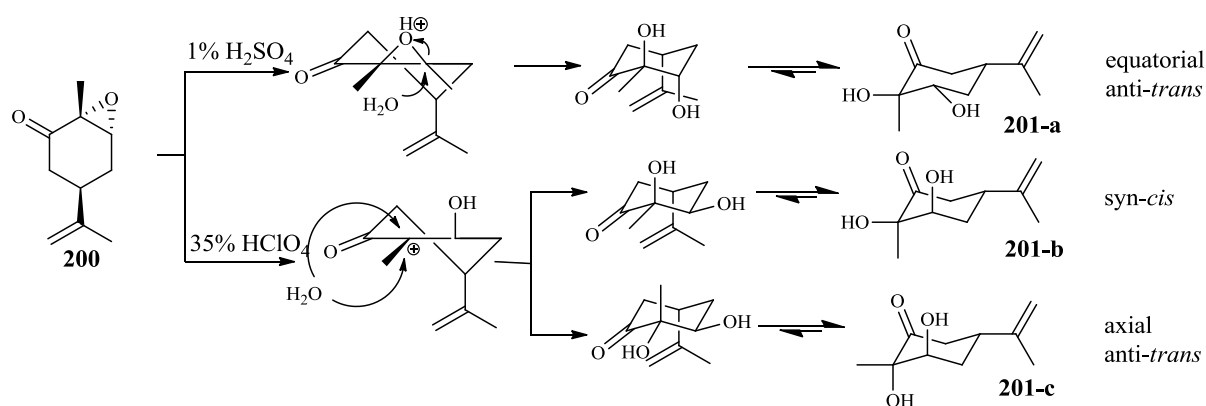
Scheme 2.2: *Acid-catalysed hydrolysis of epoxide **200***

The ^{1}H-NMR spectrum of the diol **199** was consistent with that reported in the literature.[114] Compared to epoxide **187**, the chemical shift for the C-3 methine proton was shifted down field from 3.45 to 3.75 ppm, due to the greater deshielding effect of the newly formed hydroxyl group. The IR spectrum of diol **199** showed two bands, one sharp at 3600 cm^{-1} owing to O-H stretching, and another one as a broad band at 3400 cm^{-1} owing to the intramolecular hydrogen bonded O-H. The ^{13}C-NMR spectrum of diol **199** showed the expected two signals at 71.3 and 73.9 ppm assignable to carbons directly attached to oxygen.

The second step *en route* to the target was the stereoselective oxidation of diol **199** to hydroxy ketone **202.** This transformation was achieved using 5 equivalents of pyridinium chlorochromate (PCC), in DCM.[114] TLC analysis of the reaction mixture showed the

presence of two compounds in 1:3 ratio, due to the presence of two disteroisomers of hydroxy ketone **202** (Scheme 2.3). After purification by flash chromatography on silica gel, hydroxy ketone **202** was isolated in 75% yield.
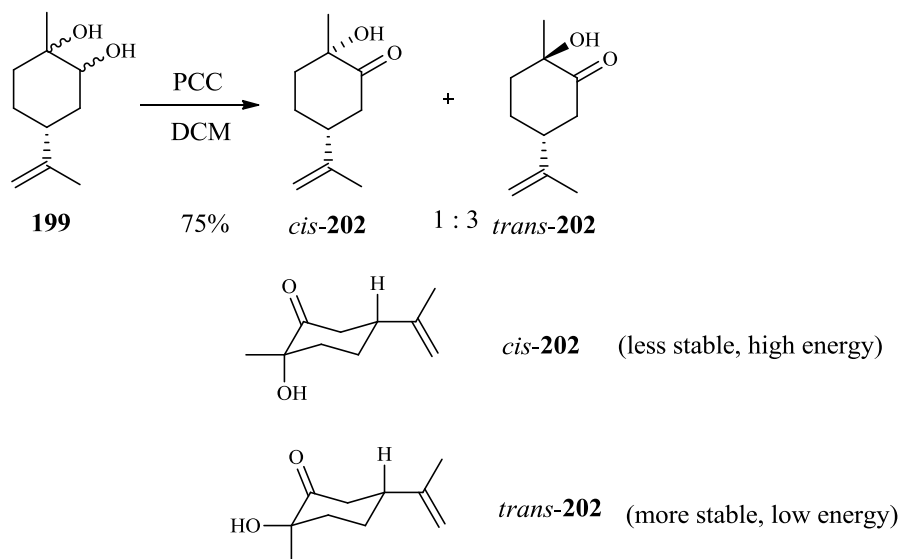
Scheme 2.3: *Stereoselective oxidation of diol **199** to cis-**202** and trans-**202***

Although PCC is commercially available, it could be made by mixing chromium trioxide with pyridine and hydrochloric acid as shown in Scheme 2.4. The oxidizing component of PCC **203** is the chlorochromate anion, $CrClO_3^-$. Oxidation of the secondary alcohol of diol **199** is a two step process. The first step involves the formation of chromate ester, which later undergoes an elimination reaction to generate hydroxy ketone **202** (Scheme 2.4).
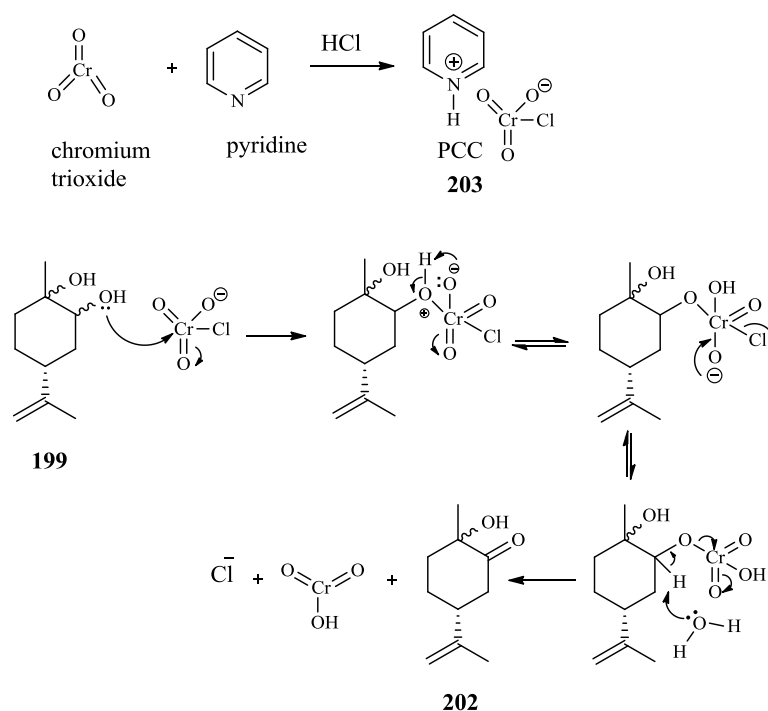
Scheme 2.4: *Mechanism of oxidation diol **199** to hydroxy ketone **202** by chlorochromate anion*

The ^{1}H-NMR spectrum of the hydroxy ketone **202** is consistent with that in the literature.[114] The IR spectrum displayed a broad band at 3350 cm^{-1} for the O-H stretch and a sharp band at 1710 cm^{-1} assignable to carbonyl group.

The third step involved further oxidation of hydroxy ketone **202** *en route* to **198**. Reaction of hydroxy ketone **202** with lead tetraacetate (LTA) [114] in methanol at 0 °C afforded keto ester as a less polar compound than the starting material as judged by TLC. The crude mixture contained Pb(OAc)$_2$ salt, therefore, this mixture was filtered through a bed of alumina before extraction, thus ensuring the proper removal of toxic Pb(OAc)$_2$. The residue was purified by flash chromatography on silica-gel to give **198** in 74% yield. Mechanistically, the first step of this reaction starts with the nucleophilic attack of the alcohol group at Pb(IV) to form an unstable Pb(OAc)$_3$ ester (Scheme 2.5) and a molecule of acetic acid (AcOH). Next the nucleophilic attack of the carbonyl group by methanol is accompanied by the cleavage of a carbon-carbon bond with the elimination of a second molecule of acetic acid and Pb(OAc)$_2$.
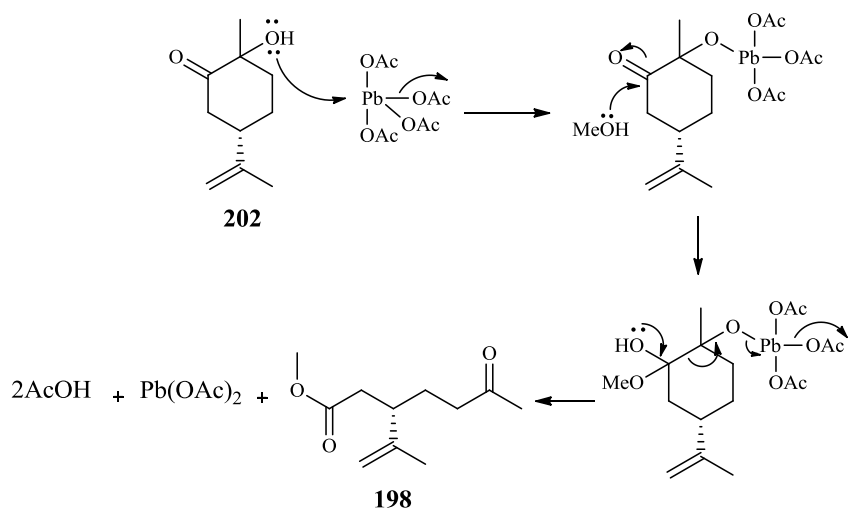
Scheme 2.5: *LTA-oxidative cleavage mechanism of α-hydroxy ketone 202 to form keto ester 198*

The ^{1}H-NMR spectrum of compound **202** displayed characteristic absorbances for the methyl ketone (CH_3C=O) at 2.15 ppm and the methoxy group at 3.65 ppm, both as sharp singlets. The ^{13}C-NMR spectrum of **202** showed two signals at 209.9 and 173.6 ppm arising from the carbonyl groups of the ketone and ester respectively. In addition, in agreement with structure **202**, the IR spectrum of **202** displayed two bands at 1710 and 1725 cm^{-1} owing to the carbonyl stretches of the ketone and ester respectively.

2.4.1 Beckmann rearrangement and lactamization

Following the retrosynthetic scheme, the next objective was to regioselectively introduce the amine functionality at the keto site of **198** and induce cyclization to form lactam **183**. For this purpose, **198** was converted to oxime **204** by treatment with hydroxyl amine hydrochloride and pyridine.[117] Flash chromatography on silica gel afforded the pure oxime **204** in 80% yield (Scheme 2.6).
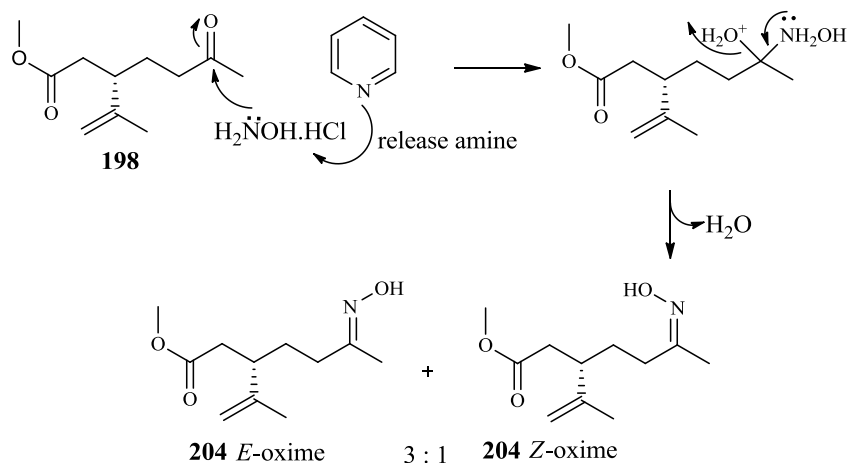
Scheme 2.6: *Formation of oxime 204*

^{1}H-NMR spectroscopic analysis revealed the presence of the oxime as an *E/Z* mixture of isomers in a 3:1 ratio. The major isomer displayed three singlets at δ_H 1.69, 1.79 and 3.59 owing to the *E*-(CH_3C=CH$_2$), *E*-(N=CCH_3) and *E*-(CH_3COO) respectively. Similarly, the corresponding protons of the minor isomer resonated at δ_H 1.62, 1.78 and 3.58 ppm.

Formally, the Beckmann rearrangement is an acid-catalysed rearrangement of an oxime to an amide, in which the OH group of the ketoxime $R^1R^2C=NOH$ (eg. **205**) activated as tosylate to make it good leaving group (Scheme 2.7).[118] The OH group of an oxime can also become a leaving group either by protonation or coordination to a Lewis acid. Thus, oximes activated in this fashion undergo [1,2]-rearrangement of the group that is attached to the C=N bond in the *trans* position with regard to the O atom in the oxime and simultaneous N-O heterolysis. The reactive nitrilium cation **207** formed in this manner is then captured by water to form an imidocarboxylic acid **208**, which tautomerizes immediately to the observed amide **209**.[118]
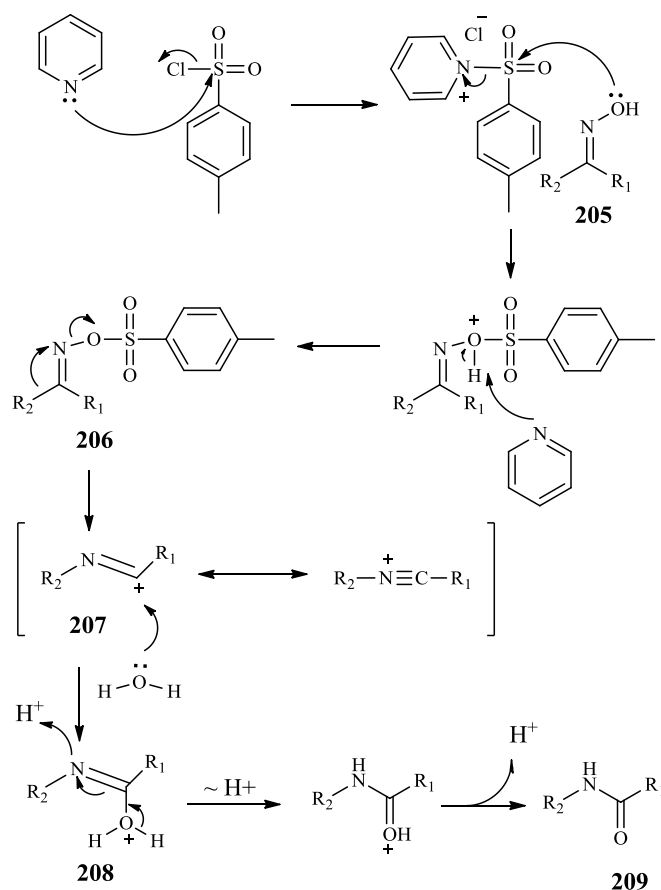
Scheme 2.7: *Mechanism of the Beckmann rearrangement of oxime **205** to acetamide **209**.*

In an attempt to synthesise acetamide **189** in one step, keto ester **198** was treated with hydroxyl-O-sulfonic acid (NH$_2$OSO$_3$H) in the presence of acetic acid under reflux.[119] However, instead of the expected acetamide **189**, an unwanted product **210** was generated (Scheme 2.8).[115] Hence, keto ester **198** underwent an extremely facile intramolecular ester-olefin cyclization reaction with involving a carboxylic acid group generated *in situ* from **198**. This result indicates that the condensation of hydroxyl-O-sulfonic acid with keto group of **198** in a slow process compared to the observed intramolecular cyclisation.

To demonstrate the intermediacy of acid **211** in the process, keto ester **198** was hydrolysed to keto acid **211** using 6N LiOH, and then the above experiment was repeated with keto acid **211** to give the same bicyclic product **210** (Scheme 2.8). The two signals of the vinylic group assignable to the starting material **198** at 4.6 and 4.7 ppm in the ^{1}H-NMR spectrum

were replaced by one olefinic signal at 5.4 ppm (C*H*=C in cyclic lactone), and a new signal at 1.4 ppm was assignable to the angular methyl group of lactone **210**.
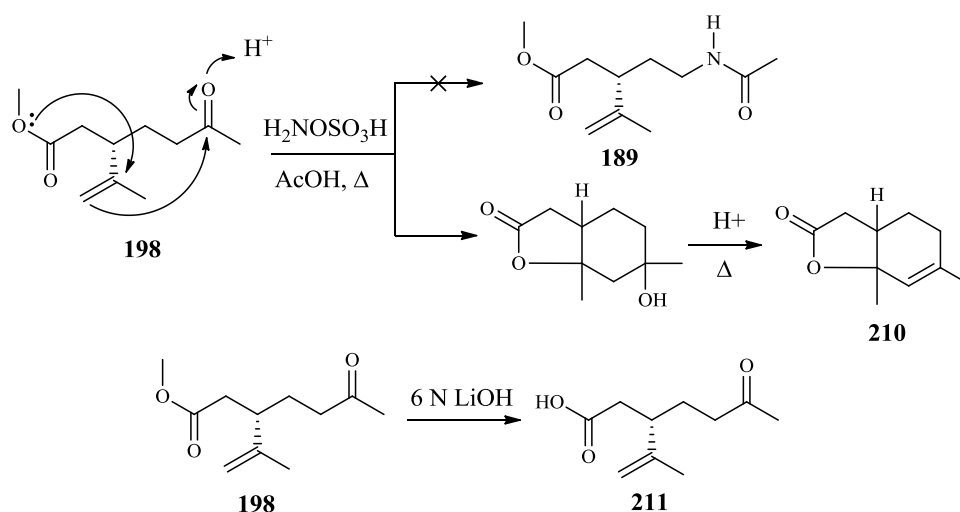
Scheme 2.8: *Intramolecular cyclization reaction of keto acid **211** to bicyclic γ-lactone **210***

Using a compound similar to keto ester **198**, Mehta and co-workers reported that treatment of oxime **212** with *para*-toluenesulfonyl chloride in pyridine led to the smooth formation of the rearranged compound **213** in 57% yield after 24 h at room temperature (Scheme 2.9).[117] In our case, the same procedure with oxime **204** produced only the oxime-tosylate (3: 1) **214** in 86% yield, no rearrangement was obtained even when DMAP was added as a catalyst (Scheme 2.10).
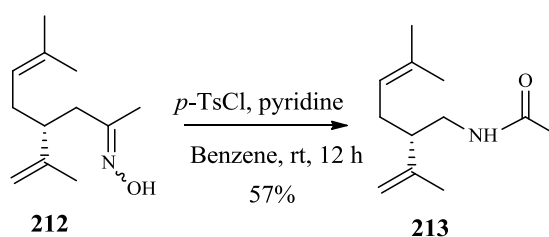
Scheme 2.9: *Beckmann rearrangement of oxime **212** to **213** by the Mehta's procedure[117]*

Furthermore, when oxime tosylate **214** was heated under reflux with triethyl amine in 80% of aqueous ethanol, two rearranged compounds **189** and **215** were obtained. Unfortunately, the undesired amide **215** was obtained in 70% yield although a small amount of the desired amide **189** in 25% yield was isolated (Sheme 2.10). The alkyl group

that migrates is generally *anti-* to the tosylate leaving group, so, it was inferred that oxime tosylate **214** was *syn-* rather than *anti-*configured, thus explaining the formation of compound **215**.[120]
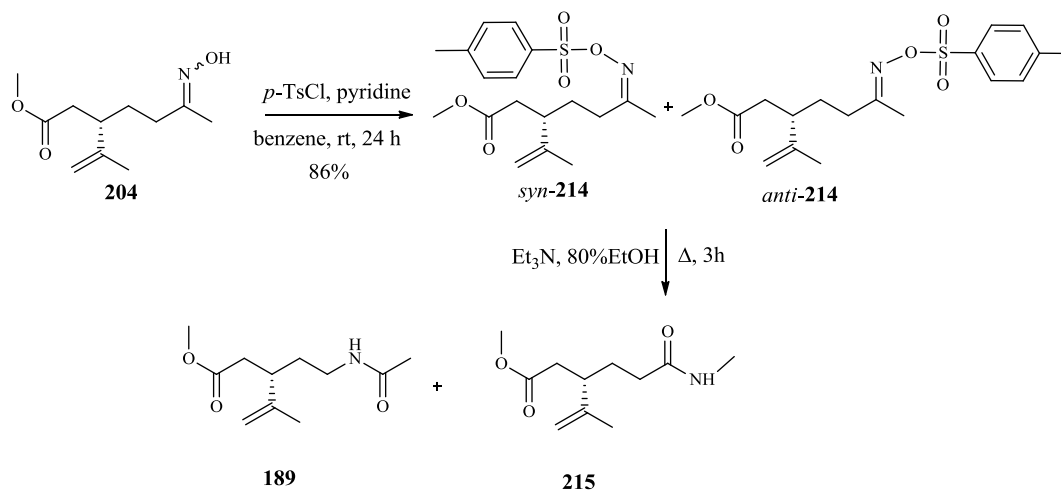
Scheme 2.10: *Rearrangement of oxime tosylate 214 under basic condition to 189 and 215*

Gratifyingly, when oxime **204** was heated at reflux with *p*-TsCl in pyridine for 6 h, acetamide **189** was obtained in 53% yield albeit contaminated with a small amount (20%) of **215**, which was separated from the desired compound by flash chromatography on silica-gel. This procedure was optimised by changing the temperature and time. Indeed, when oxime **204** was treated with *p*-TsCl in pyridine at room temperature for 7 days in the dark under an N_2 atmosphere, acetamide **189** was obtained in 90% yield (Scheme 2.11).
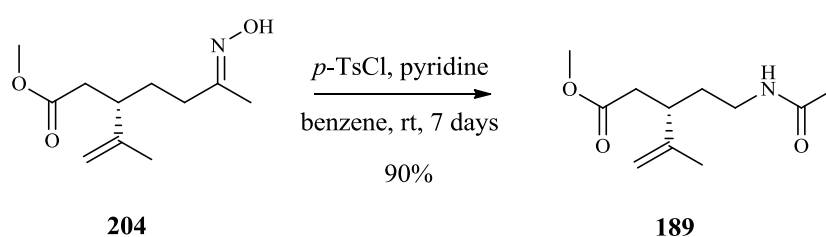
Scheme 2.11: *Beckmann rearrangement of oxime 204 to acetamide 189*

Hydrolysis of acetamide **189** under basic conditions (30% NaOH) produced a ω-aminoaliphatic carboxylic acid, followed by adjustment of reaction to pH 6, and heating to 130 °C drove the equilibrium toward the formation of γ-lactam **183** as white crystals in 77% yield after purification (Scheme 2.12).[121a]
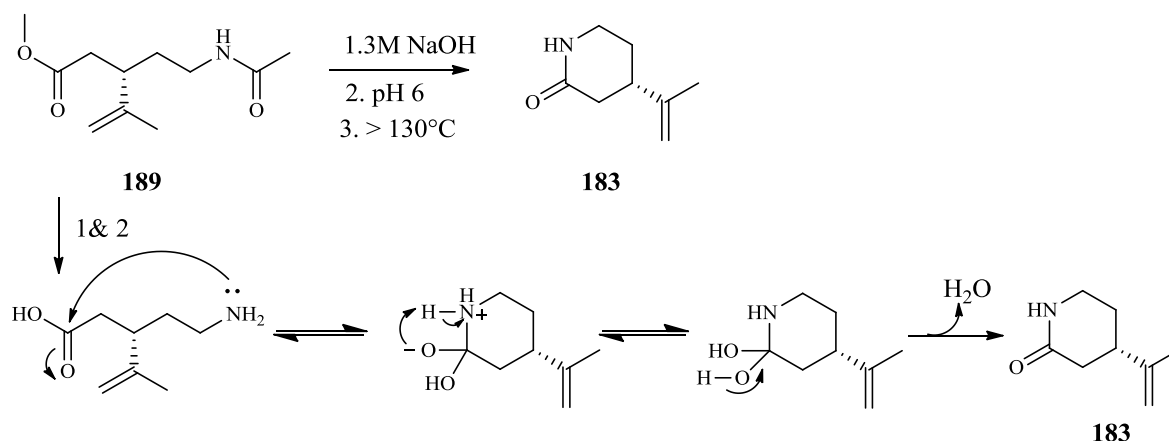
Scheme 2.12: *Cyclisation reaction of acetamide 189 to lactam 183*

^{1}H-NMR and ^{13}C-NMR spectroscopic analysis of lactam **183** revealed signals of this compound at δ_H 6.3-6.4 (a broad singlet, N*H*), 3.27-3.28 (m, C*H$_2$*N), 2.37-2.46 (m, C*H$_2$*CO). These values are in good agreement with those previously reported for γ-valerolactam **216** at δ_H 6.7, 3.28-3.33 and 2.31-2.44 (Figure 2.7).[121b]

216	183
γ-valerolactam (2-piperidone)	4*S*-(prop-1-ene-2yl) -2-piperidone
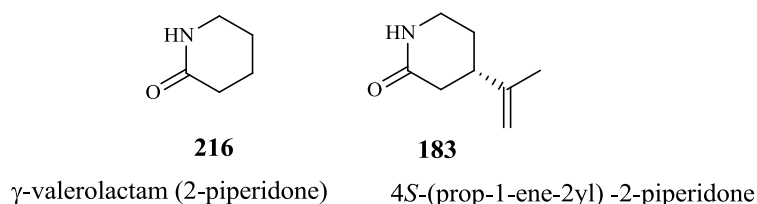
Figure 2.7: *Structures of 2-piperidone (216) and lactam 183*

The γ-valerolactam **216** was used in pilot experiments via aza-Robinson annulation aimed at the construction of the ring A of aza analogue **84** (Figure 2.1).

2.5 Aza-Robinson annulation

The Robinson annulation was introduced in 1935 by Robert Robinson and William Sage during their landmark synthesis of sterol.[113] They demonstrated a unique and unprecedented condensation between enolates and α,β-unsaturated ketones (Figure 2.8). The findings have not only proven an important method for the synthesis of steroidal frameworks; but, since their discovery, have been used in the synthesis of other complex, diverse and important compounds.[113]
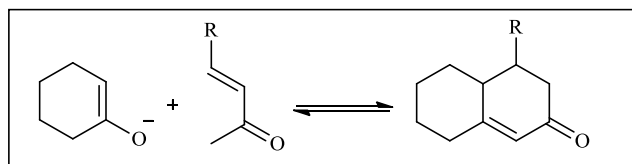
Figure 2.8: *General scheme for the Robinson annulation reaction*

Bicyclic indolizinones and quinolizinones have been prepared previously by Danishefsky, who used a Rh(II) catalyzed reaction between α-diazoketones and thiolactams to bring about the key ring closure reaction[122,123] (Scheme 2.13, 1). However, the use of diazomethane for the preparation of the α-diazoketone could restrict the scope of this methodology to small scale synthesis. Recently, to solve this problem, a novel synthetic strategy towards the development of aza-Robinson annulations–type reaction on a large scale has been reported. This variant involves the conversion of a thiolactam into an iminium ion, which then undergoes intramolecular attack by the internal enolate on the side chain (Scheme 2.13, 2). This methodology was first described by Heathcock[124] and then applied by others.[123,125]
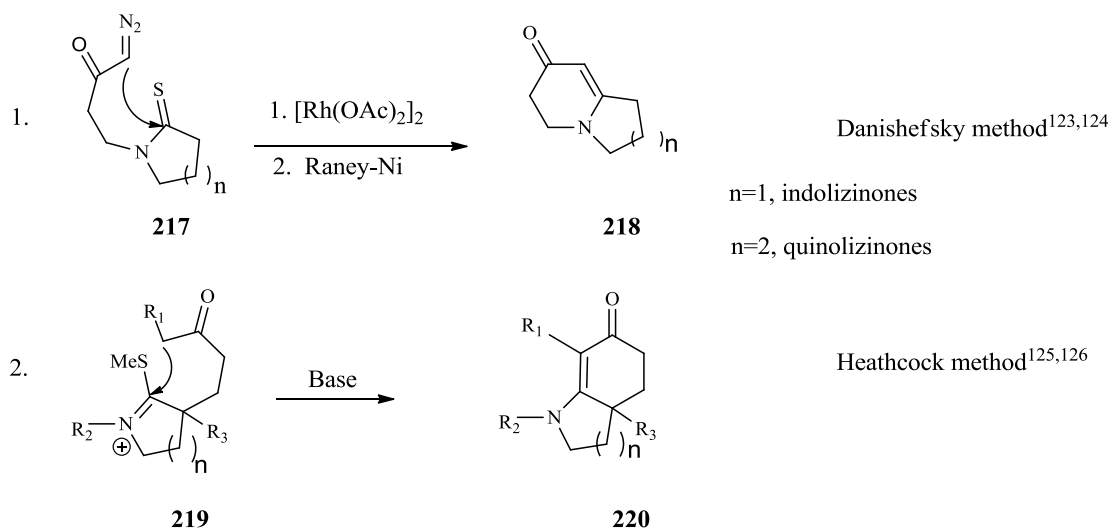
Scheme 2.13: *Danishefsky and Heathcock methods for the preparation of indolizinones and quinolizinones via distinct aza-Robinson annulations reactions.*

2.6 Synthesis of 1-methyl-3,4,6,7,8,9-hexahydroquinolizin-2-one (193)

As mentioned above, the formation of the ring A of compound **84** was first assessed using γ-valerolactam **216** following a modification of the protocol described by Heathcock.[124] Since the lactam **216** itself is not active enough to undergo a cyclisation reaction, activation of the carbonyl group was needed. Some approaches to activate this amide functionality involved its transformation into imino ethers, thiolactams, or thiolactam ethers. On the other hand, another approach consists of the use of a more active α, β-unsaturated ketone such as the Nazarov reagent. Lawesson's reagent was used to obtain the more reactive thiolactam **195** in 85% yield.[126] Mechanistically, the conversion of γ-valerolactam **216** to the corresponding thiolactam **195** is depicted in Scheme 2.14. Lawesson's reagent **221** upon heating decomposes via breakdown of the central phosphorus/sulphur four-membered ring to yield two reactive dithiophosphine ylides R-PS$_2$ (Scheme 2.14). The reaction of this ylide with carbonyl of lactam **216** gives rise to the thiaoxaphosphetane intermediate. The driving force of this reaction is the formation of a stable P-O bond. The ^{1}H-NMR and ^{13}C-NMR data of thiolactam (**195**) were consistent with those found in the literature.[126]

Michael reaction between the deprotonated thiolactam and ethyl vinyl ketone (EVK) in the presence of anhydrous potassium carbonate and 18-crown-6 gave the Michael adduct **222** in 87% yield (Scheme 2.15).[123] Crown ethers are useful as phase transfer catalysts (PTC), that facilitate the migration of a reactant from one phase to another where reaction actually occurs. In this case, the use of 18-crown-6 allows the use of K$_2$CO$_3$ as the base necessary for the alkylation.
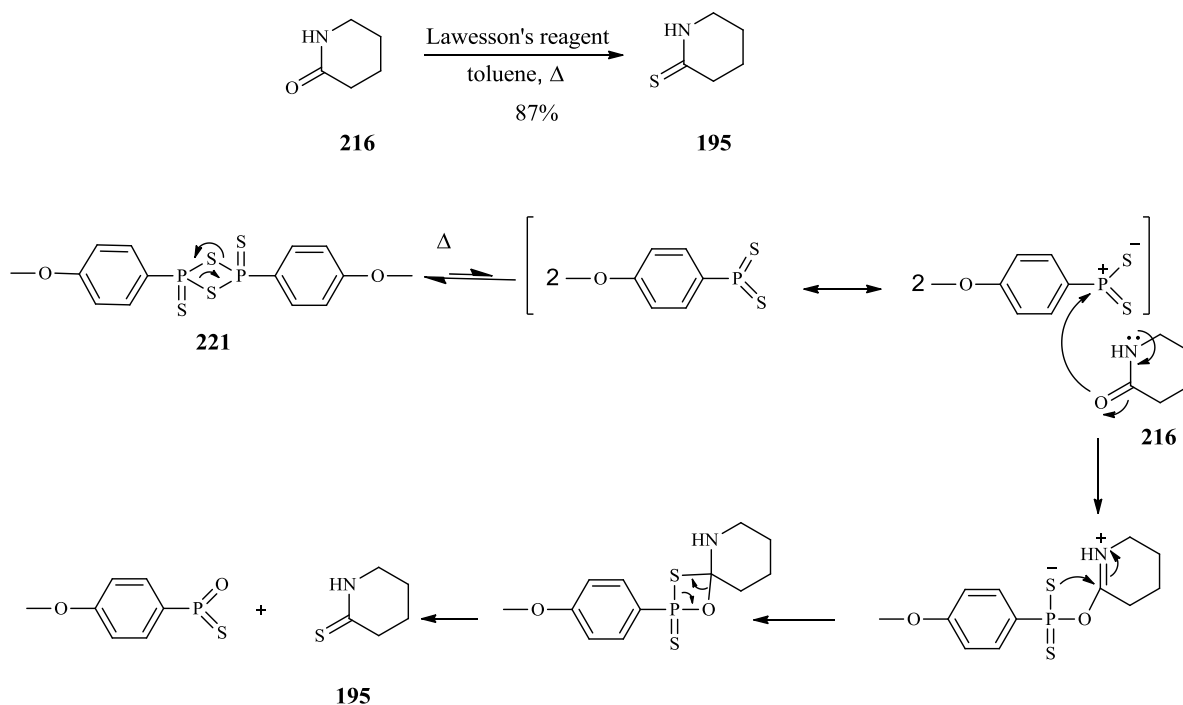
Scheme 2.14: *Mechanism of thiation of γ-valerolactam **216** with Lawesson's reagent*
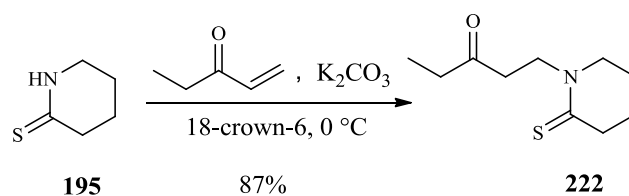
Scheme 2.15: *Michael alkylation of thiolactam **195** with EVK (**185**)*

Cyclisation of the Michael adduct **222** to the bicyclic enaminone **193** was achieved in an aldol condensation, through the generation of the thioiminium ion by treatment with Me$_2$SO$_4$ via an S$_N$2 reaction. DBU was used as a sterically hindered and non nucleophilic base in the second step of the aldol condensation to give enaminone **193** in 78% (Scheme 2.16).[123,127]
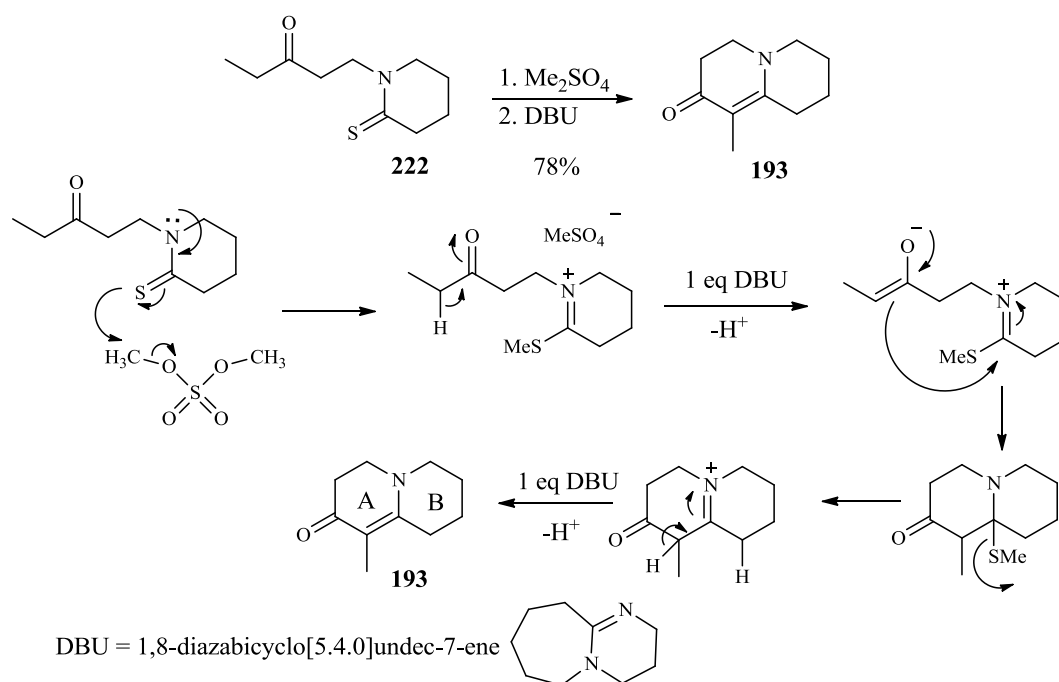
Scheme 2.16: *Mechanism of aza-Robinson annulation to give quinolizinone 193*

The ^{1}H-NMR spectroscopic data of bicyclic enaminone obtained was in good agreement with those reported by Guarna and co-workers.[124] Enaminone **193** displayed signals at δ 3.36 (t, 2H, CH$_2$N) in ring A, 3.22 (t, 2H, CH$_2$N) in ring B, 2.51 (dd, 2H, CH$_2$C=C), 1.73 (s, 3H, CH$_3$C=C). The IR spectrum showed a band at 1715 cm^{-1} for the C=O stretch with a conjugated alkene C=C double bond, and another weaker band at 1657 cm^{-1} arising from the C=C stretch.

2.7 Synthesis of 4,5-dimethyl-1,2,4,6,7,8-hexahydroquinolizin-3-one (223)

In principle, the crucial introduction of the angular methyl group at C5 should be readily achieved by the use of dimethylcopper lithium, which is prepared from methyl lithium and copper iodide (molar ratio 2: 1). Piers and Keziere have reported that the reaction of octalone **224** with an excess of dimethylcopper lithium yielded eremophil-11-ene-3-one **180** in 77% yield (Scheme 2.17).[128] It should be noted that the stereoselective conversion of octalone **224** into eremophilene type **180** is of particular significance, since this reaction provides a simple and efficient method to install the vicinal dimethyl system found in

eremophilane-type sesquiterpenes. Methyl lithium alone would give the expected 1,2 addition rather than 1,4-addition, however, in the presence of copper salt the required conjugate, Michael-like addition was induced.
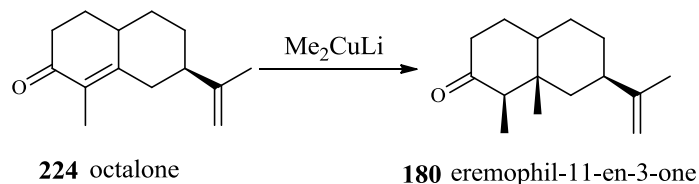
Scheme 2.17: *1,4- addition reaction of Me$_2$CuLi to octalone **224***

To our surprise, the reaction of enaminone **193** with an excess of dimethyl copper lithium gave an unexpected ring expansion reaction, yielding compound **225** (Scheme 2.18). ^{1}H-NMR, ^{13}C-NMR, 2D-NMR and HR-MS experiments were used to identify and structurally characterize this compound.
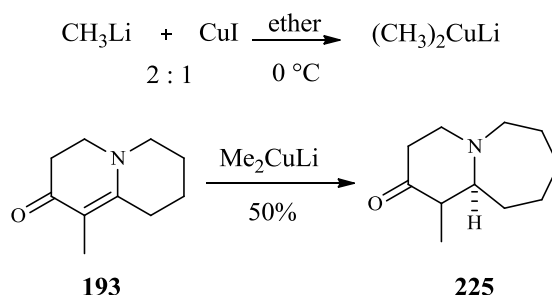
Scheme 2.18: *Ring expansion reaction of enaminone **193***

The ^{1}H-NMR spectrum of compound **225** revealed signals at δ 2.9-3.07 (m, 2H, CH$_2$N), 2.3-2.7 (m, 2H, CH$_2$N), 2.21-2.29 (m, 1H, CH$_3$C*H*), 1.70-1.72 (m, 1H, C*H*), and 0.99 (d. 3H, C*H$_3$*CH). The HMBC spectrum of amino ketone **225** showed three significant correlations peaks for the CH$_3$ protons on C-4 at 0.99 ppm with CH of C-5 at 67 ppm, correlation with the carbonyl carbon C=O at 210 ppm and correlation with C-4 at 55 ppm, and did not show any correlation peak between protons of CH$_3$ and C5 of CH$_2$ in structure B. These results confirmed the structure of this compound is A and not B (Figure 2.9).
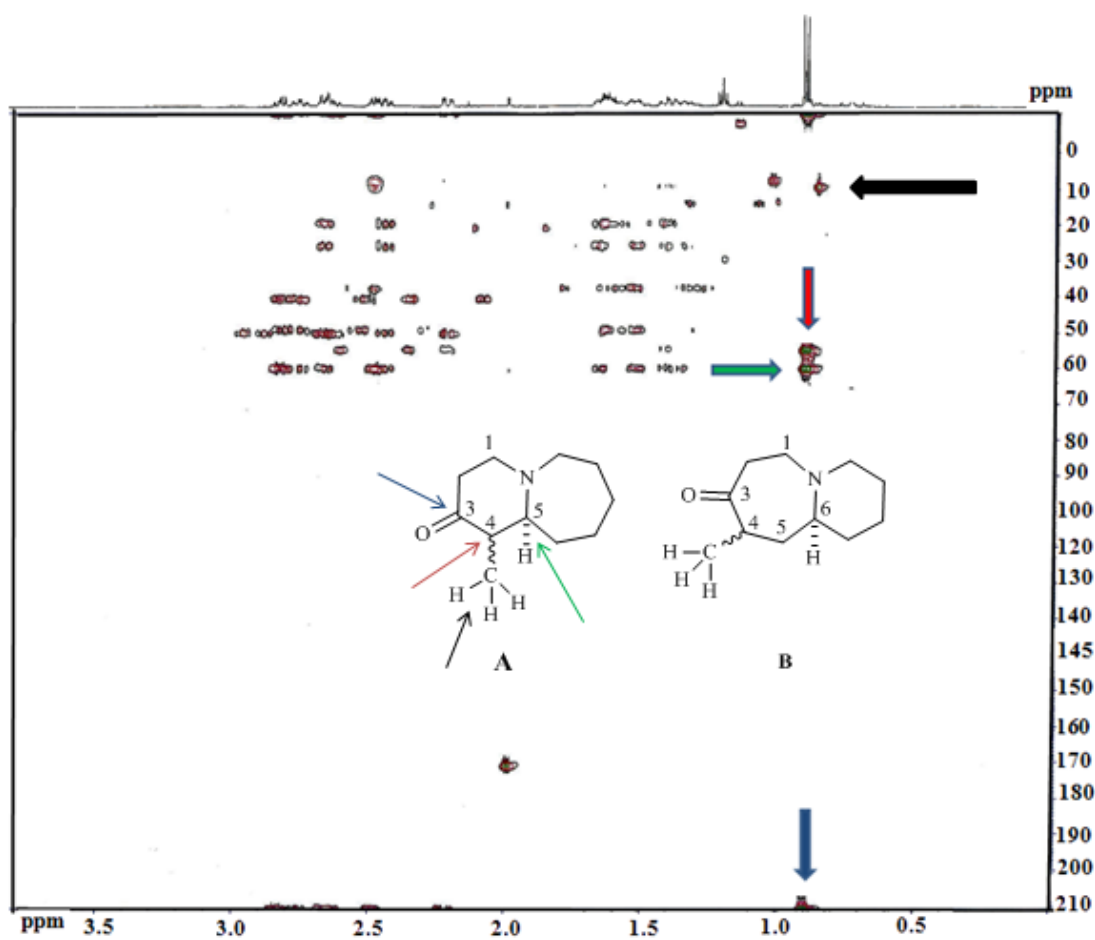
Figure 2.9: *HMBC spectrum of unexpected bicyclic compound **225***

A plausible mechanism is depicted in Scheme 2.19, this ring-expansion reaction could take place via the intermediacy of a copper (III) β-adduct, the a key intermediate proposed for the classical 1,4-addition of dimethyl lithium cuprate to enones.[129] The formation of this complex involves binding of copper to the π-system.
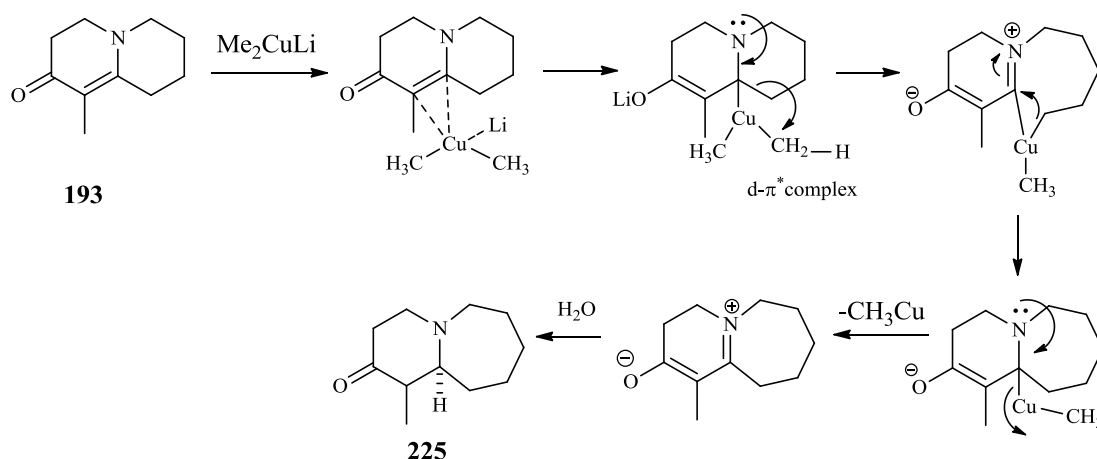
Scheme 2.19: *Proposed mechanism of expansion ring reaction of* **193**

Since the C-methylation of enaminone **193** was unsuccessful with Me$_2$CuLi, alternative strategies were tried to increase the reactivity of the β-position. Chloro silanes have frequently been used to trap the enolates formed by conjugate addition of organocuprate reagents to α, β-unsaturated carbonyl compounds.[129] TMSCl accelerates cuprate-enone conjugate addition by increasing the electron deficiency of the α,β-double bond. In this case, however, no reaction was observed when TMSCl was added to mixture of enaminone and dimethylcopper lithium. Boron trifluoride etherate (BF$_3$.OEt$_2$) has also been used as a Lewis acid, [130] aimed at activating **193** toward Michael alkylation. Unfortunately again, the addition of BF$_3$.OEt$_2$ to the reaction mixture at -78 °C, did not give the desired compound **223**. Furthermore, changing the copper (I) salt and the nucleophile, did not lead to any reaction as observed by TLC analysis or NMR spectroscopy. For example, when enaminone was added to a mixture of copper (I) bromide dimethyl sulphide complex (CuBr. SMe$_2$), MeLi and BF$_3$.OEt$_2$ at -78 °C, or MeLi was replaced with MeMgBr, the reactions only afforded unreacted starting material.[130]

2.8 Iminium salts from enaminones such as 193

Since the term enaminone refers to any compound containing the conjugated N-C=C-C=O,[131] it should be possible to convert enaminone to an iminium salt by using a strong Bronsted acid such as trifluoroacetic acid (TFA). This conversion allows 1,4-addition of methyl group to iminium salt. Although, in acyclic enaminone, there are four possible isomers as depicted in Figure 2.10, enaminone **193** display a *cis-trans* conformation.
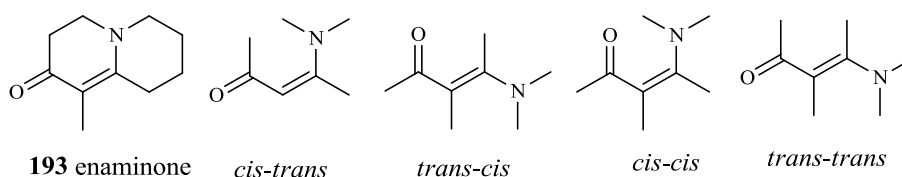
Figure 2.10: *Conformations of enaminone 193*

As expected, Mayers and co-workers[132] found that the reaction of *cis-trans* enaminone **226** with methyl magnesium bromide gave the enamine alcohol **227** in high yield, as a consequence of an exclusive 1,2-addition. However, with methyl magnesium iodide 10% of the 1,4 addition product **228** was obtained together with unreacted starting material and a mixture of unidentified compounds (Scheme 2.20). In contrast, the conversion of the enaminone **226** to its O-acetyl iminium salt **229** allows preparation of amino ketone **228** in a useful yield of 60 to 65% yield.[132]

Following Mayers and co-workers strategy, the reaction of enaminone **193** with 1.2 equivalents of acetyl chloride in dry THF[133] gave a mixture (2:1) of O-acetyl iminium salt **230** and N-acetyl enaminone salt **231** after 5 min in 90% as total yield (Scheme 2.21). Resonances arising from both **230** and **231** were visible in the ^{1}H-NMR spectrum of acetylated iminum salt mixture. The major compound was the unwanted N-acylated salt in 66% yield and the minor compound was O-acylated salt (33%). The signals assigned to **230** were: δ 1.72 (CH_3C=C), 2.0 (CH_3CON), 3.1-3.2 (CH_2N) in ring A, 3.70-3.72 (CH_2N) in ring B, and the signals assigned to **231** were: δ 1.89, 2.23, 3.92 and 4.10 for CH_3C=C-O, CH_3COO, CH_2N, CH_2N respectively.
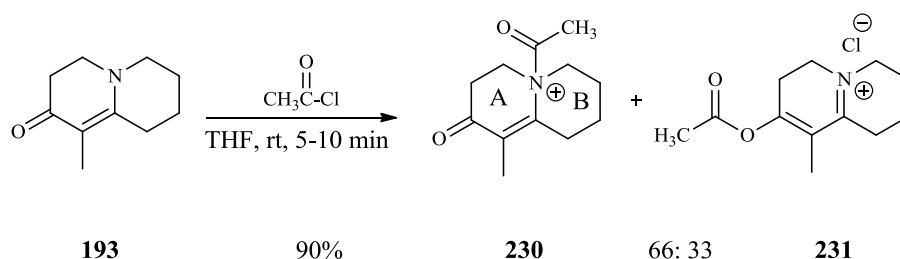
Scheme 2.21: *Reaction of enaminone 193 with acetyl chloride*

Comparing the nucleophilicity of a carbonyl group C=O and that of a tertiary amine, it is expected that of the enolate anion and the amine would have comparable nucleophilic reactivity. In addition, conformational analysis of bicyclic enaminone indicates that the three substituents of the N atom at the bridgehead position in the most stable *cis-trans* conformation are locked by the bicyclic skeleton, thus the lone pair electrons of the nitrogen atom are more exposed to the electrophiles (CH$_3$COCl, MeI etc) than normal tertiary free amines, which can freely rotate their alkyl substituents. This explains the larger amount of the N-acylate salt **230**. In addition, the reaction of O-methylated iminium salt **232** with methyl magnesium bromide, did not give the 1,4-addition product **223** after 24 h at room temperature (Scheme 2.23). Similarly, The TFA iminium salt **233**, which was prepared from **193** with TFA in high yield (90%) at room temperature, did not react with excess of MeMgBr at room temperature. Fortunately, when the temperature was

increased to 66 °C (refluxing THF), the formal 1,4-conjugate addition of MeMgBr took place giving racemic amine **223** in 65% yield (Scheme 2.22).

It is known that 10-quinolizidines with a *trans* ring fusion display characteristic absorption bands in the 2800-2700 cm^{-1} region of the infrared spectrum. These absorptions, termed the Bohlmann bands (discussed in chapter one) result from a specific interaction between the nitrogen lone pair and at least two axial hydrogens.[94] Quinolizidines with *cis* ring fusion either show much weaker or no Bohlmann bands at all. The amino ketone **223** showed Bohlmann bands at 2761-2927 cm^{-1}, thus indicating, that it was most likely in the trans-configuration (Figure 2.11).
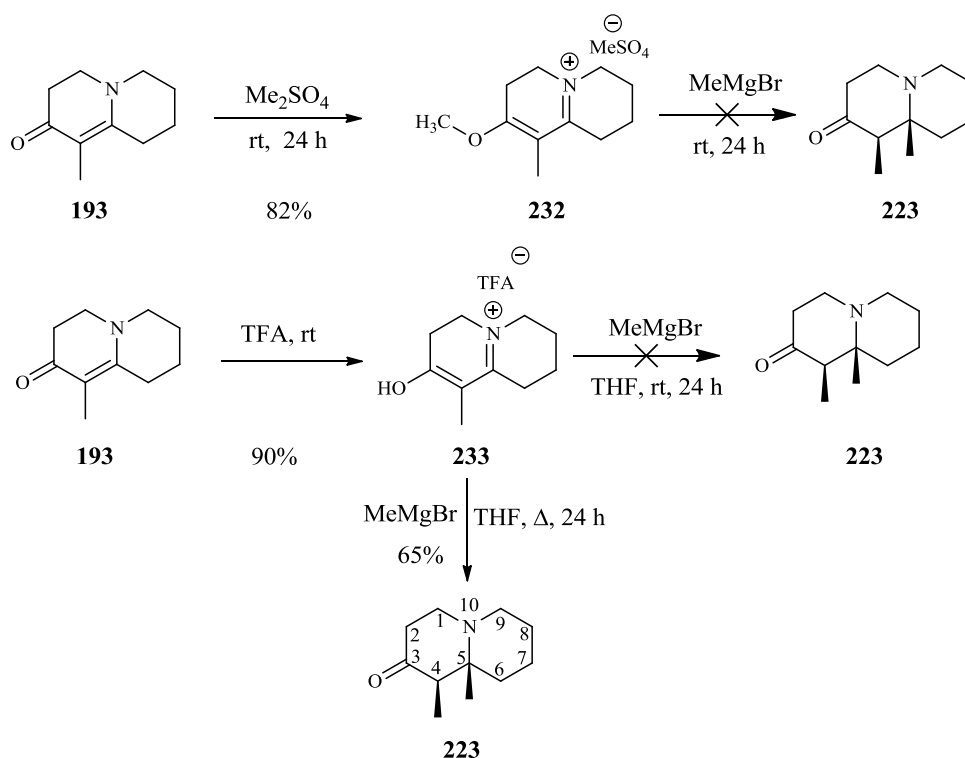
Scheme 2.22: *Introduction of an angular methyl group to enaminone through iminium salt* ***233*** *to generate 4,5-dimethyl-1,2,4,6,7,8-hexahydroquinolizin-3-one (**223**)*
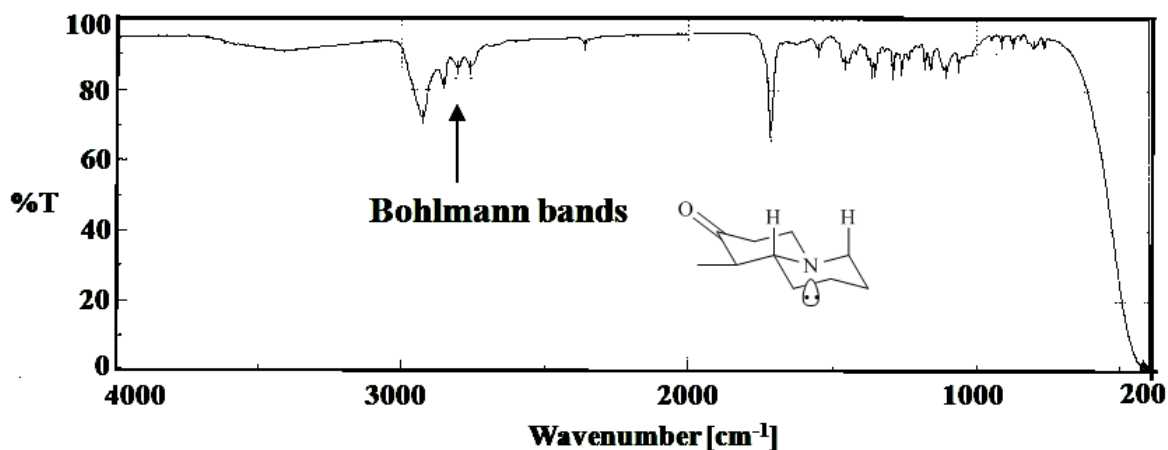
Figure 2.11: *Infra-red spectrum of amino ketone **223** showing Bohlmann bands at 2761-2927 cm^{-1}*

The ^{1}H-NMR and ^{13}C-NMR spectroscopic analyses of 4,5-dimethyl quinolizidine-3-one (**223**) confirmed the structure of **223** with characteristic ^{1}H-NMR signals at δ 0.72 [3H, s, C(C*H$_3$*)], 0.87 (3H, d, (C*H$_3$*)CH), 2.18-2.22 (1H, C*H*(CH$_3$), 2.63-2.85 (4H, m, 2C*H$_2$*N). The relative *cis*-orientation of the two vicinal methyl groups at C4 and C5 of **223** was unambiguously established by nOe-measurements. Irradiation of the methyl doublet at δ 0.87 ppm led to nOe enhancements (3%) of the CH$_3$ singlet at 0.72 ppm, likewise a nOe-enhancement was observed for CH$_3$ doublet (4%) when the CH$_3$ singlet at 0.72 ppm was irradiated. Thus, allowing both methyl groups to be assigned as *syn* relative to each other (Figure 2.12).
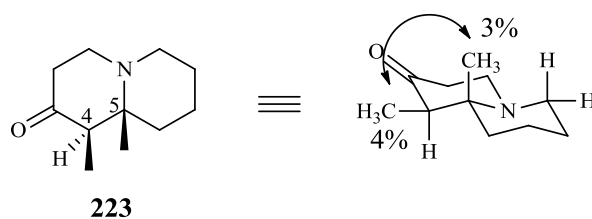
Figure 2.12: *Relative stereochemistry of the 4,5-dimethyl quinolizinone (**223**)*

2.9 Huang-Minlon modification of the Wolff-Kishner reduction

The final step *en route* to quinolizidine **105** was the removal of the ketone group in **223**. There are several well-established methodologies for the selective removal of the ketone carbonyl function. All of them require activation of the ketone first, followed by different types of metal reductions. Among others, conversion of a ketone to its thioketal followed by Raney Ni reduction is a commonly used method. Formation of thioketal is usually catalysed by acetic acid or $BF_3.OEt_2$. Indeed, when the amino ketone **223** was treated with ethanedithiol in the presence of 3 equivalents of $BF_3.OEt_2$, amino thioketal **234** was produced in good yield 80% (Scheme 2.23).[134] The condensation reaction between ethanedithiol and and amino ketone **223** took place with nucleophilic attack of the carbonyl group of **223** by a thiol group of ethandithiol followed by elimination of water to give compound **234**. ^{1}H-NMR,^{13}C-NMR and DEPT spectra where in full agreement with the structure of **234**. Heating of **234** with Raney-Ni in refluxing ethanol for 2-4 h,[134] did not give the desired compound **105** (Scheme 2.23), even though an excess of Raney-Ni was added. It is uncertain what caused the failure of this desulfurization reduction. Quite a few modifications of this reaction were tried unsuccessfully. Clearly, another strategy was needed for this reduction.
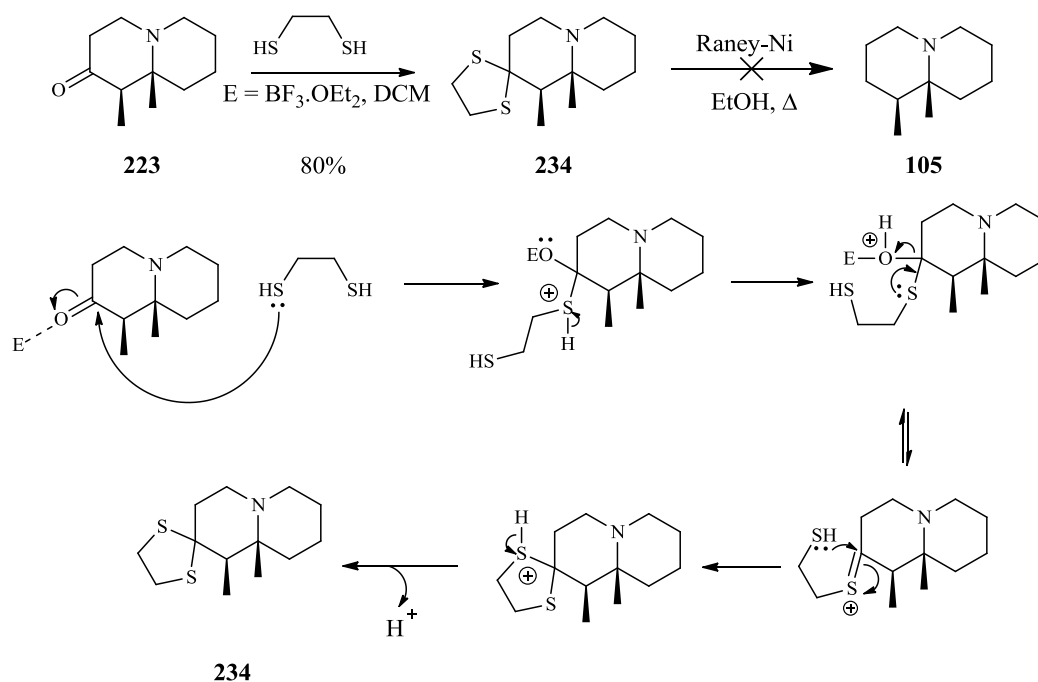
Scheme 2.23: *Formation of amine thioketal **234***

Tosyl hydrazones of aldehydes and ketones are readily obtained as crystalline compounds and easily purified. It has been previously shown that tosyl hydrazones react with bases at high temperature yielding p-toluensulphinic acid, nitrogen and alkanes.[135] Reaction of amino ketone **223** with $MeC_6H_4SO_2NHNH_2$ in EtOH at reflux temperature for 24 h gave the tosyl hydrazone derivative **235** in good yield (79%) (Scheme 2.24).[136] The condensation reaction took place through the nucleophilic attack of the carbonyl group of **223** by the NH_2 group of tosyl hydrazide, followed by elimination of water to yield compound **235**. However, attempts to reduce tosyl hydrazone **235** with lithium aluminium hydride ($LiAlH_4$) and sodium borohydride ($NaBH_4$) were unsuccessful at room temperature. When the reaction time and temperature of the $LiAlH_4$ reduction was increased, tosyl hydrazone **235** reacted via Shapiro elimination to afford the enamine **236** (Scheme 2.25).
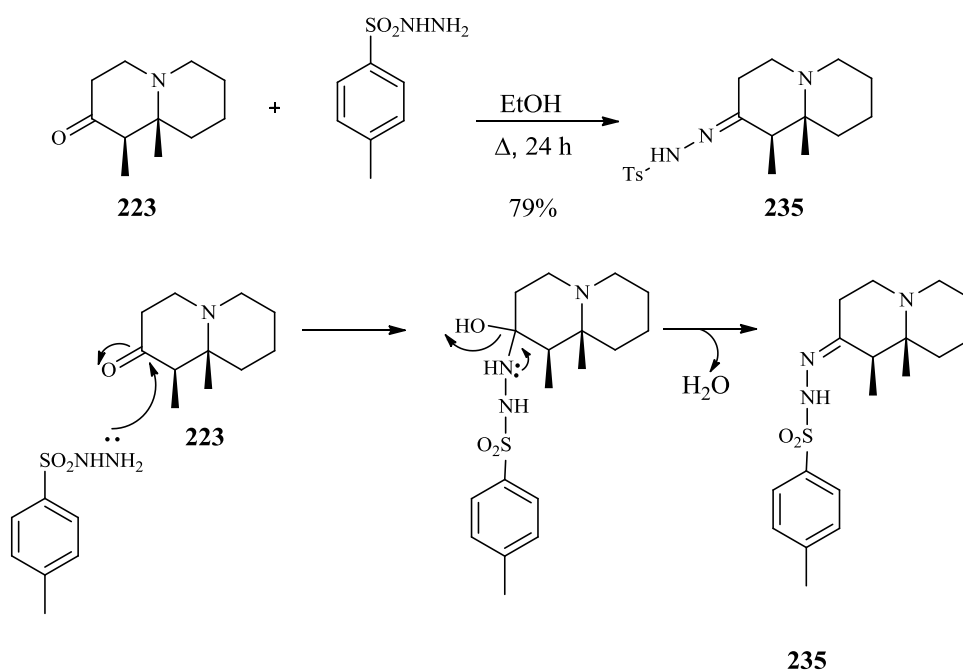
Scheme 2.24: *Formation of tosyl hydrazone **235**.*

However, in the Shapiro reaction the tosyl hydrazone group of **235** is used as the leaving group in the elimination reaction. The $LiAlH_4$ abstracts the first proton from hydrazone **235** and then the less acidic proton to produce a carbanion (Scheme 2.26). The carbanion

proceeds in an elimination reaction to create the C=C double bond, followed by expulsion of N_2 and the resulting vinyl amine reacts with water to give the enamine **236**.

These results indicated that the direct activation of the ketone group followed by reduction was not compatible with the functionalities of the molecule. Thus, a different strategy was needed to perform this transformation. It was envisioned that the C=O bond could be reduced in a two-step sequence by transformation to alcohol, then, after activation as tosylate, the alcohol might be reduced by $LiAlH_4$ to give the desired compound **105**.
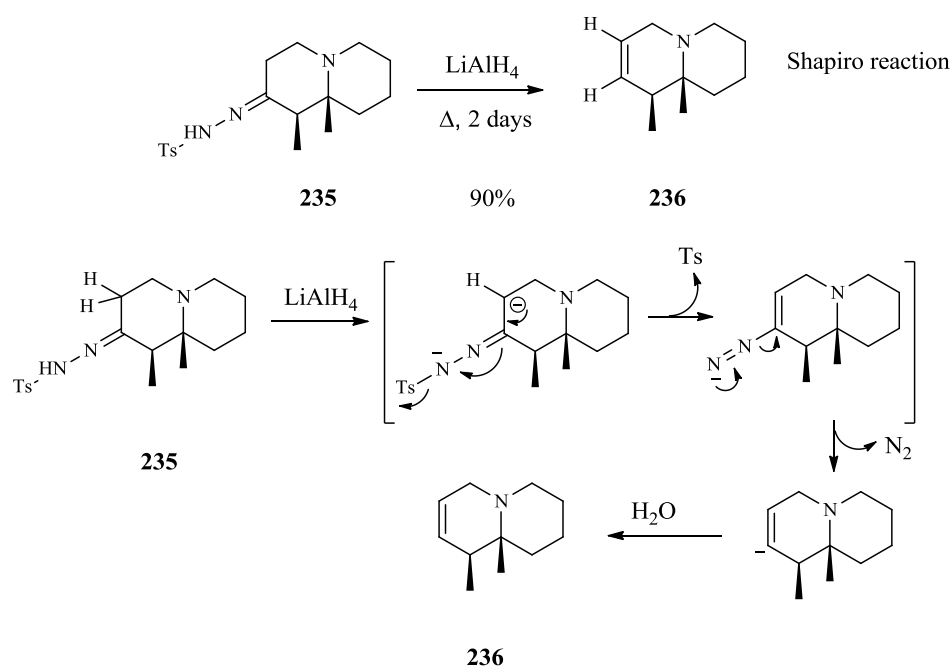
Scheme 2.25: *Proposed mechanism of Shapiro reaction of **235** to give **236**.*

Reduction of amino ketone **223** with lithium aluminium hydride in dry THF provided the diastereoisomers of amino alcohol **237** and **238** (9:1) in 90% total yield (Scheme 2.26). Both isomers are suitable for the following transformation, since this stereocenter will be erased after the reduction. The subsequent derivatisation of this epimeric mixture with tosyl chloride provided an epimeric mixture of tosylate salts **239**, that did not react with $LiAlH_4$ to yield the expected product **105** (Scheme 2.26).
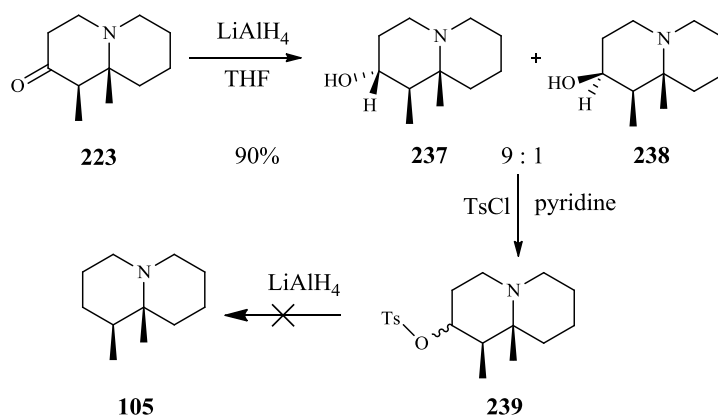
Scheme 2.26: *Conversion of aminoketone **223** to diastereoisomers of amino alcohol **237** and **238** and subsequently to tosylate salts **239**.*

Fernandez has reported another example of a related reduction of amino ketone **240** to compound **241**, using a mixture of potassium hydroxide, hydrazine hydrate and ethylene glycol at reflux, which afforded the amine **241** in 90% yield (Scheme 2.27).[137]
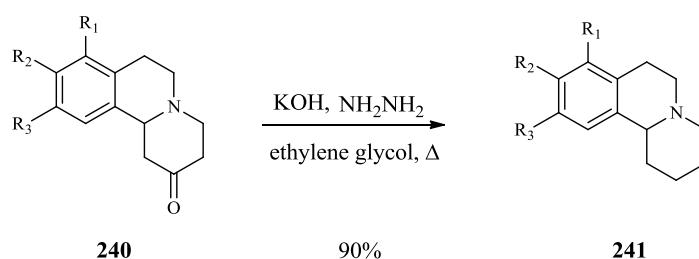
Scheme 2.27: *Fernandez procedure to remove the ketone functionality from **240**[138]*

Huang and Minlon reported a modification of the Wolff-Kishner reduction.[138] This procedure consists of refluxing the carbonyl compound in a moderate amount of diethylene or triethylene glycol, 85% hydrazine hydrate and three equivalents of sodium or potassium hydroxide. When these conditions (the Huang-Minlon modification), were applied to **223**, the final amine **105** was obtained in 74% yield (Scheme 2.28). The mechanism of this reaction first involved the formation of the hydrazone **242** (Scheme 2.28) in a mechanism that is analogous to the formation of an imine. Successive deprotonations eventually result in the expulsion of nitrogen gas.

Spectroscopic (IR and NMR) and mass spectrometric analyses confirmed the structure of amine **105**. The ^{13}C-NMR spectrum of amino ketone **223** showed the characteristic signal at 210 ppm for a ketone C=O group, a signal that disappeared in ^{13}C-NMR of amine **105**, also in the IR spectrum of amine **105** the stretching band of C=O at 1720 cm^{-1} also disappeared. The final amine **105** was stored at -20 °C under a nitrogen atmosphere.
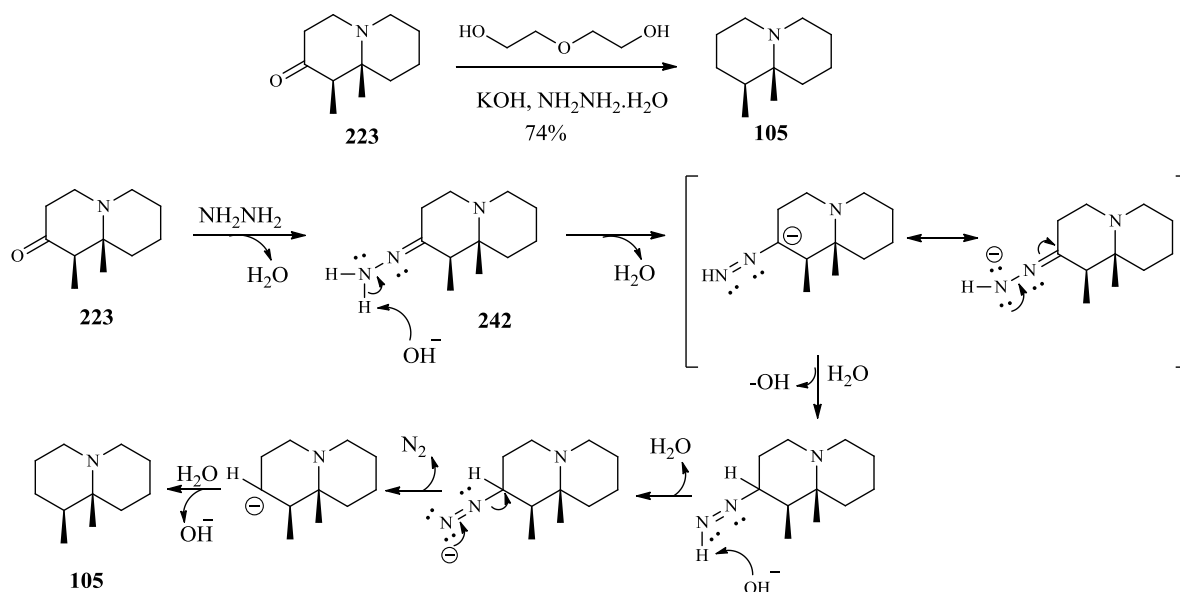
Scheme 2.28: *Mechanism of the Huang-Minlon reduction of amino ketone **223** to amine* ***105***.

For the kinetic studies with PR-AS, the final amine **105** was treated with 1 equivalent of TFA to yield the stable TFA salt **178** in 74% yield. ^{1}H-NMR and ^{13}C-NMR spectra of the salt showed a nice separation of all signals, as expected for the deshielding effect of TFA (Figures 2.13 and 2.14). The successful synthetic sequence leading to the bicyclic amine **105** and its salt **178** is summarised in Scheme 2.29.
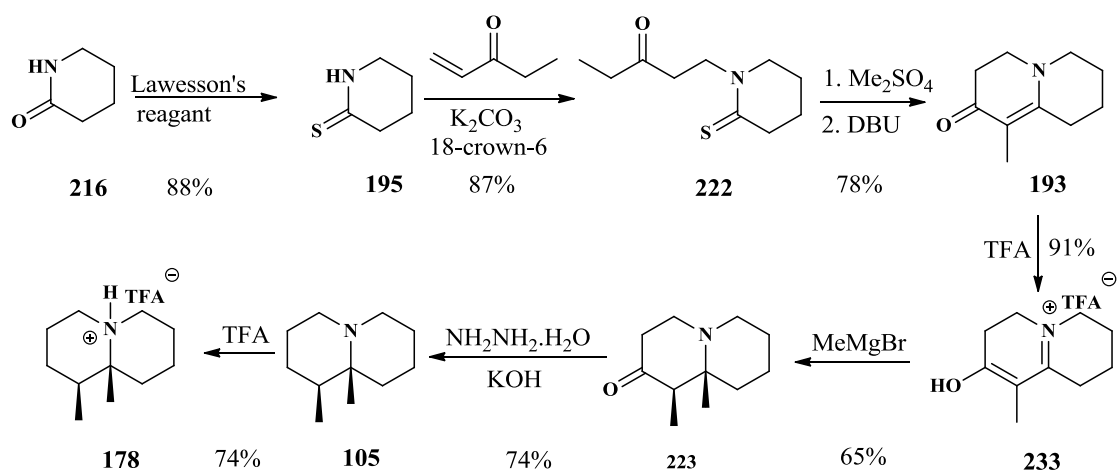
Scheme 2.29: *Synthesis of bicyclic tertiary amine 105 and its TFA salt 178*
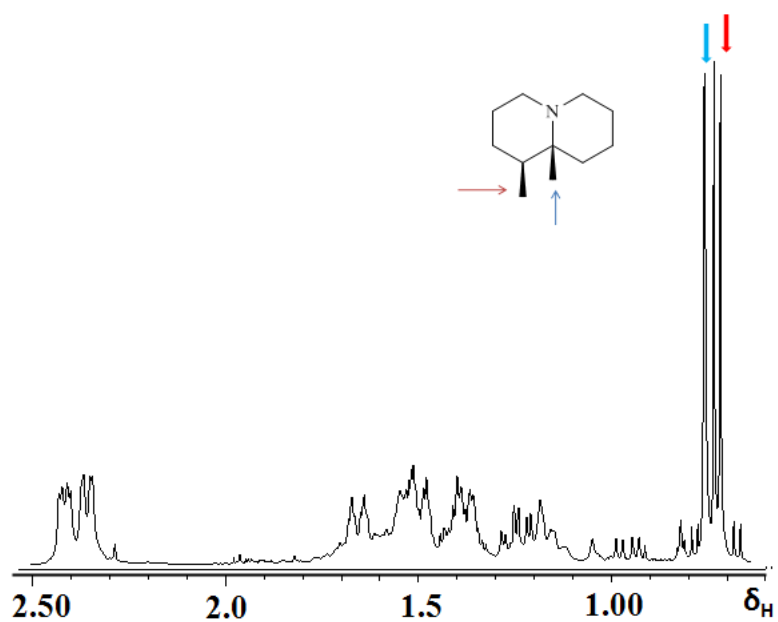
Figure 2.13: ¹*HNMR spectrum of 1,9-dimethyl-2,3,4,6,7,8-hexahydroquinolizidine (105) in*

the region δ$_H$ = 0.5 – 2.5 ppm
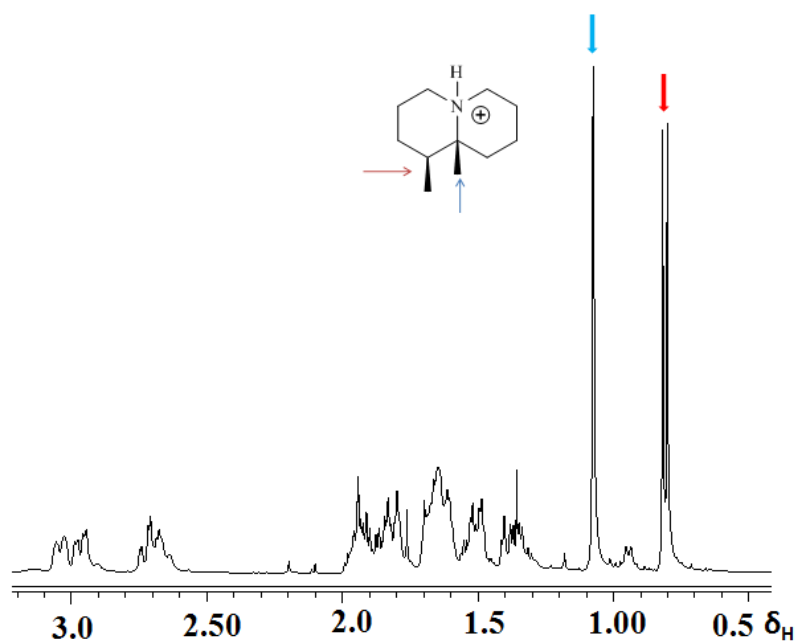
Figure 2.14: ¹-HNMR spectrum of 1,9-dimethyl-2,3,4,6,7,8-hexahydroquinolizidinium salt (178) in the region δ_H = 0.5 – 3.0 ppm

The relative configuration of the final ammonium salt was unambiguously verified by X-ray crystallography (Figure 2.15) using the picrate salt **243** (Scheme 2.30).
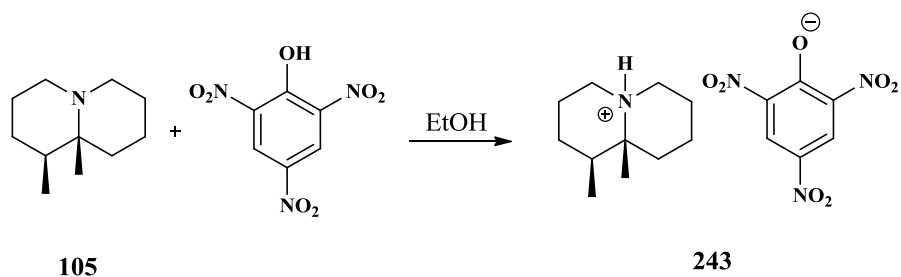
Scheme 2.30: *Preparation of picrate salt **243** for X-ray crystallography (performed by Dr. Juan A.Faraldos)*
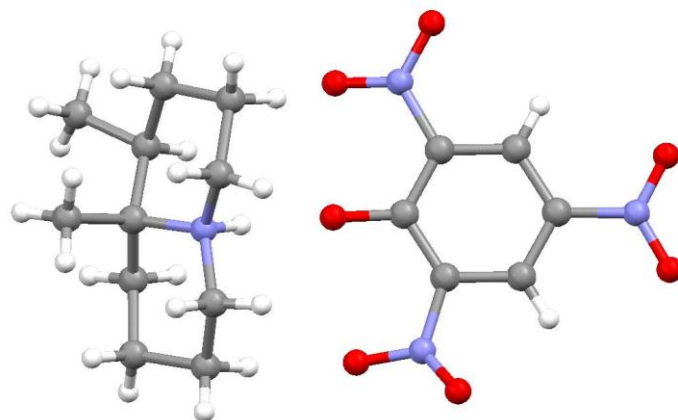
Figure 2.15: *Ball and stick representation of the X-ray crystal structure of the picrate salt* ***243*** *(solved by Dr. Benson Kariuki)*

2.10 Stereoselective synthesis of (7*R*,4*S*,5*S*)-84

Following the same synthetic sequence developed for the unsubstituted lactam **216**, lactam **183** was converted to quinolizidine **106** in six steps and 87% overall yield. Thiolactam **196** was obtained after purification and recrystallisation from *i*-PrOH in 77% as white crystals (Scheme 2.31).[126]
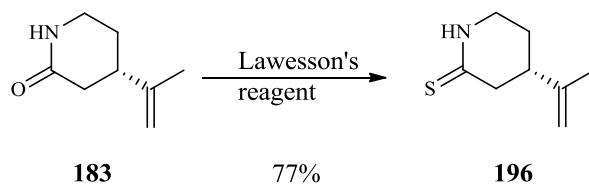
Scheme 2.31: *Conversion of lactam* ***183*** *to thiolactam* ***196***

The structure of **196** was verified by ^{1}H-NMR spectroscopy. The ^{1}H-NMR spectrum of thiolactam **196** was however slightly different from thiolactam **195**, due to the presence of chiral isopropylidene substituent on C7 as shown in Figure 2.16.
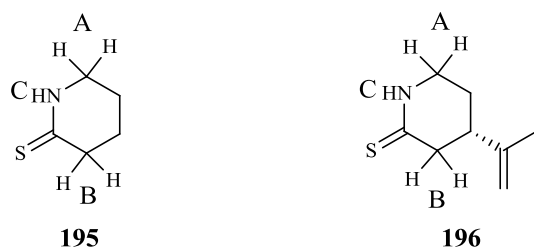
A δ 3.35 (2H, dt, $J = 6.0$ Hz, CH_2N)   3.27 (2H, m, CH_2N)

B δ 2.89 (2H, t, $J = 6.0$ Hz, $CH_2C=S$)   2.66 (1H, dd, $J = 4.0, 8.0$ Hz, HCHC=S)

      3.02 (1H, dd, $J = 4.5, 8.0$ Hz, HCHC=S)

C δ 8.90 (1H, br s, NH)   8.85 (1H, br s, NH)

Figure 2.16: *Comparison between the two thiolactams* **195** *and* **196**

Michael alkylation of thiolactam **196** with ethyl vinyl ketone in dry THF, anhydrous potassium carbonate and a catalytic amount of 18-crown-6 gave the Michael adduct **244** in 85% yield (Scheme 2.32).[123] The ^{1}H-NMR spectrum of the Michael adduct was in agreement with the chemical shifts recorded to the Michael adduct of the parent compound **222** as shown in Figure 2.17.
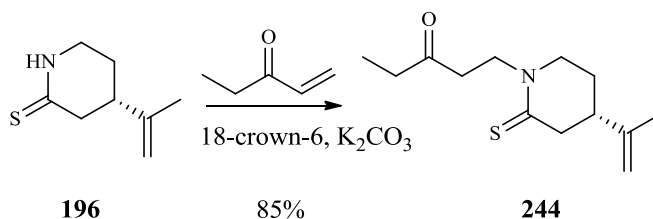
Scheme 2.32: *Formation of Michael adduct* **244**
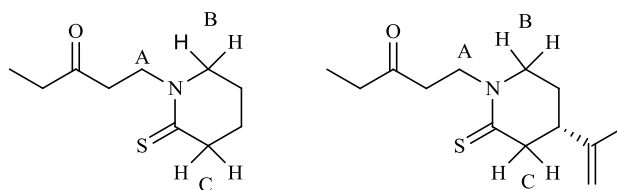
A δ	4.05 (2H, t, J = 6.5 Hz, CH$_2$N)	4.10 (2H, dt, J = 6.5, 13.0 Hz, CH$_2$N)
B δ	3.49 (2H, t, J = 6.0 Hz, CH$_2$N)	3.44 (1H, ddd, J = 2.0, 3.0, 6.0 Hz, HCHN)
		3.59 (1H, ddd, J = 4.0, 5.5, 13.0 Hz, HCHN)
C δ	2.95 (2H, m, CH$_2$C=S)	3.10 (2H, ddd, J = 5.0, 10, 13 Hz, CH$_2$C=S)

Figure 2.17: *Comparison between the two Michael adducts **222** and **244***

Next, **244** was activated for the intramolecular aldol condensation by treatment with dimethyl sulphate, generating in this manner the more reactive thioiminium ion, that further reacted with DBU to give the desired enaminone **194** in 54% as best yield after optimization (Scheme 2.33).[123] The low yield of enaminone **194** was a result of this enone undergoing isomerization under these conditions, which resulted in the formation of by-product **245**. Several modifications were tried to improve the yield of the reaction. First, Me$_2$SO$_4$ and DBU were distilled under reduced pressure and N$_2$ atmosphere, secondly DBU was replaced with other bases, such as Et$_3$N, 2,6-lutidine and 2,4,6-collidine.

As shown in Table 2.1, with the exception of 2,4,6-collidine, all bases could be used to generate the enolate that ultimately yielded the enaminone **193** after intramolecular cyclisation. However, no improvement of the yield was observed. When, the Michael adduct **244** was treated with dimethyl sulphate followed by treatment with triethylamine, the yield of enaminone **194** went down to 29% (Table 2.1). Since the isomerization of the enaminone **194** to the side-product **245** occurred at high temperature (boiling toluene, 140-150 °C), the solvent was changed to benzene, and the yield of enaminone rise up to 54%, by using Et$_2$O, the yield was slightly lower 41% as shown in Table 2.1.
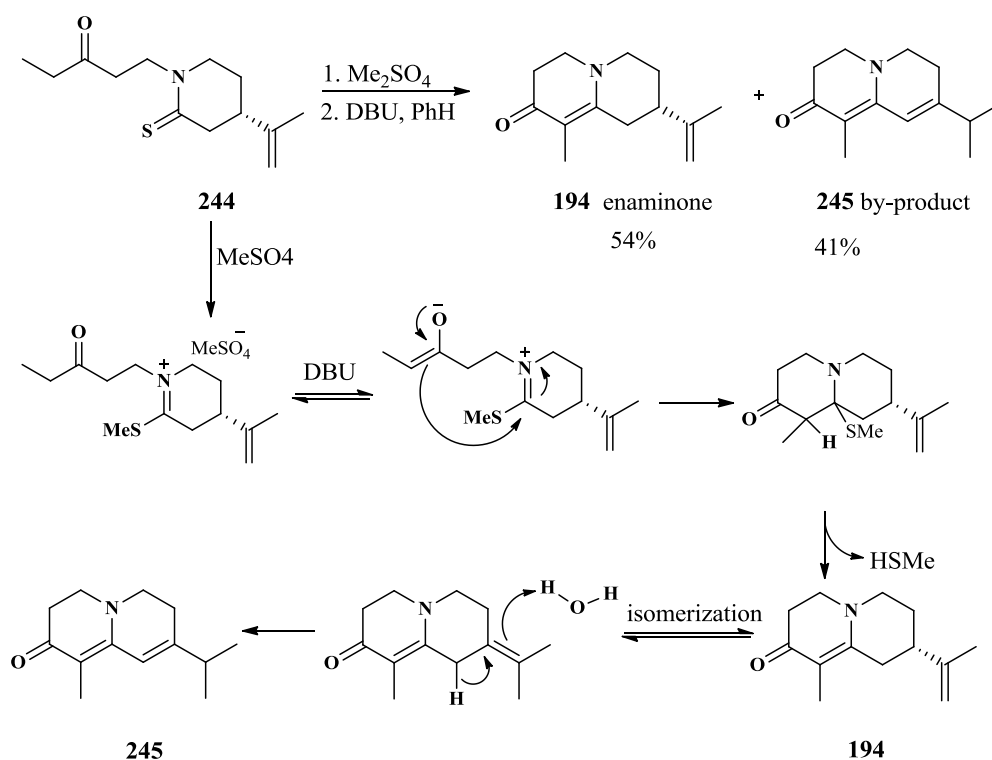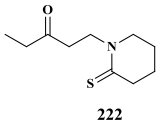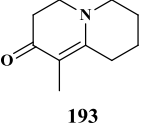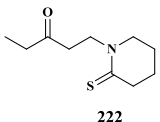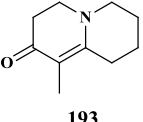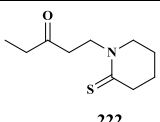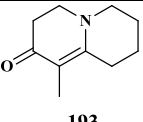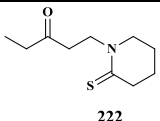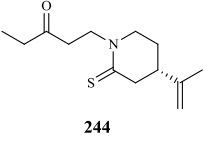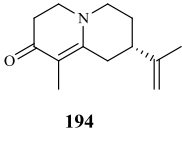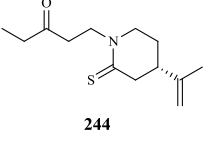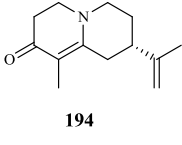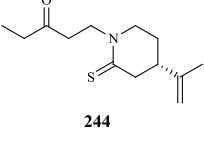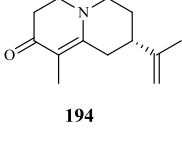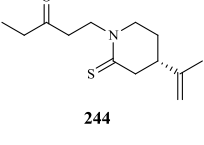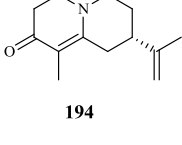
Scheme 2.33: *Aldol condensation of thioiminium salt generating enaminone **194** and by-product **245***

For comparison, the characteristic ^{1}H-NMR resonances of compounds **193** and **194** are given in Figure 2.18.

193

(A) δ 1.62 (3H, s, $CH_3C=CCO$)

(B) δ 2.37 (2H, m, CH_2CO)

(C) δ 3.12 (2H, t, $J = 5.0$ Hz, CH_2N)

(D) δ 3.25 (2H, t, $J = 7.0$ Hz, CH_2N)

194

1.52 (2H, s, $CH_3C=CCO$)

2.52 (2H, m, CH_2CO)

3.03-3.14 (4H, m, $2CH_2N$)

(E) 1.55 (3H, s, $CH_3C=C$)
(F) 4.6 and 4.8 (2H, br s, $CH_2C=C$)
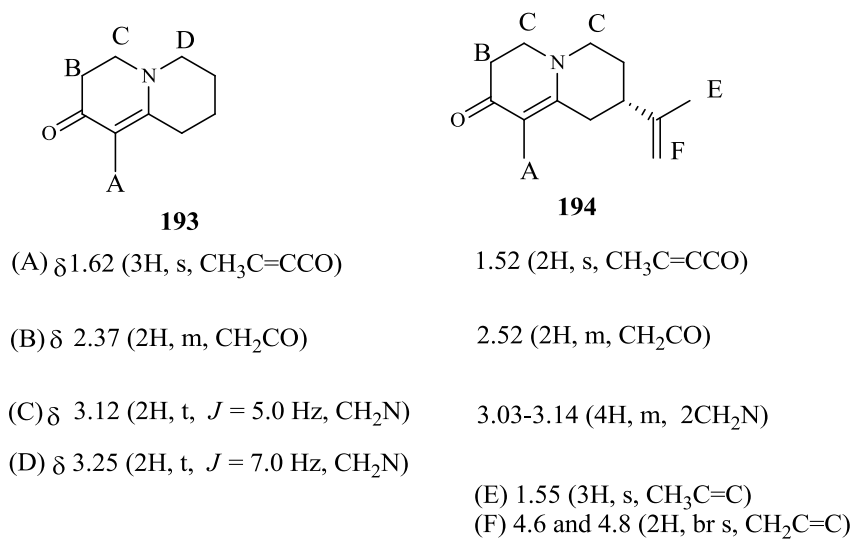
Figure 2.18: *^{1}H-NMR spectroscopic data for **193** and **194***

Attempt	Michael adduct	Solvent	Bases	Enaminone	Yield of enaminone	Yield of by-product
1.	**222**	toluene	DBU	**193**	78%	
2.	**222**	toluene	Et₃N	**193**	45%	
3.	**222**	toluene	2,6-lutidine	**193**	56%	
4.	**222**	toluene	2,4,6-collidine	No reaction		
5.	**244**	toluene	DBU	**194**	37%	62%
6.	**244**	toluene	Et₃N	**194**	29%	68%
7.	**244**	Et₂O	DBU	**194**	41%	51%
8.	**244**	benzene	DBU	**194**	54%	44%

Table 2.1: *Attempts to improve the yield of enaminone **194***

In same manner as the parent compound **193**, conversion of enaminone **194** to its salt **246** allowed the introduction of the angular methyl group, after reaction with methyl magnesium bromide to provide the vicinal dimethyl system **197** found in eremophilane-type sesquiterpenes in a useful yield of 64% (Scheme 2.34).
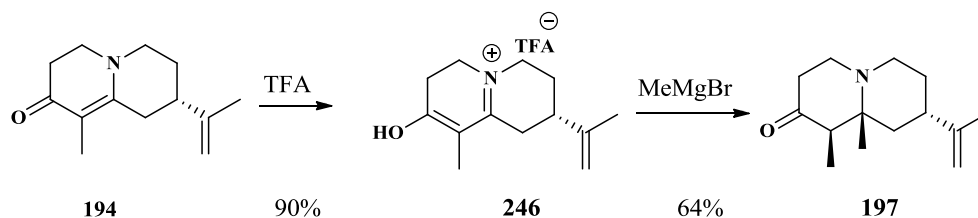
Scheme 2.34: *Conversion of enaminone **194** to amino ketone **197***

A combination of 1D and 2D-NMR experiments revealed that compound **197** was produced as single diastereoisomer. The ^{1}H-NMR spectrum of **197** displayed signals at δ 0.71 (s, 3H, CCH_3), 0.90 (d, J = 7.0 Hz, 3H, CHCH_3), 2.62-2.69 (m, 2H, COCH$_2$CH_2N), 2.80-2.86 (m, 2H, CH$_2$CH_2N). These values are in good agreement with those of the parent compound **223**, which displayed signals at δ 0.72 [3H, s, C(CH_3)], 0.87 [3H, d, J = 6.5 Hz, (C$H3$)CH], 2.42-2.64 (2H, m, COCH$_2$CH_2N), 2.61-2.85 (4H, m, COCH$_2$CH_2NCH_2) (Figure 2.19).
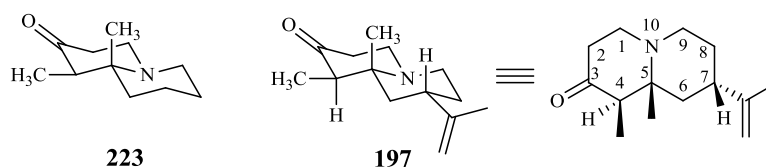
Figure 2.19: *Comparison between aminoketones **223** and **197***

The bicyclic amino ketone **197** showed Bohlmann bands at 2930-2793 cm^{-1} in the IR spectrum, which confirm this amino ketone **197** posses a *trans*- ring fusion configuration (Figure 2.20).[94]

197
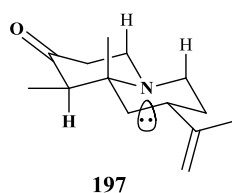
Figure 2.20: *Trans-fused quinolizidine **197** in which the nitrogen lone-pair is trans to at least two axial hydrogen atom (Bohlmann bands)*

The stereochemistry of compound **197** was confirmed by nOe-measurements (Figure 2.21). Irradiation of the CH$_3$ singlet at δ 0.71 ppm led to nOe enhancements of the CH$_3$ doublet (C4) (2%) at 0.91 ppm, and CH methane on C7 at 2.10 ppm (3.1%). A nOe was also observed for the protons of the CH$_3$ singlet (4.6%) at 0.71 ppm when the CH$_3$ doublet was irradiated, thus allowing the methyl at C4 to be assigned as *syn* relative to CH$_3$ at C5 and confirmed the *trans*-fused ring configuration.
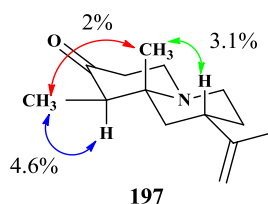
Figure 2.21: *Stereochemistry of amino ketone **197***

Conversion of the amino ketone **197** into the final amine **106** was carried out through Huang-Minlon reduction. Thus, after refluxing **197** in a mixture of potassium hydroxide, hydrazine hydrate, and ethylene glycol for 3 h, water was distilled off and the residue was heated to 180 °C for 3 h to yield **106** in 74% yield (Scheme 2.35).[137,138] The ^{13}C-NMR spectrum of amino ketone **197** showed characteristic signal at 210 ppm for ketone group C=O, which disappeared in ^{13}C-NMR of final amine **106**. The free amine **106** was stored at -20 °C under nitrogen atmosphere.

197   **74%**   **106**
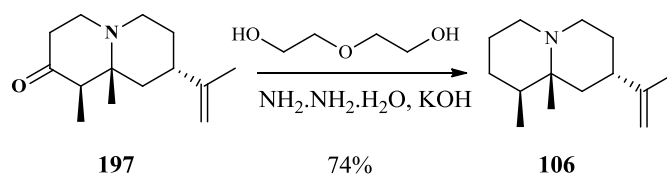
Scheme 2.35: *Conversion of amino ketone **197** to final free amine **106***

Amine **106** was treated with TFA to afford 10-aza-eremophilane salt (7*R*,4*S*,5*S*)-**84** in 70% yield (Scheme 2.36). The absolute configuration of the final ammonium salt was unambiguously verified by X-ray crystallography (Figure 2.22). For this purpose, another salt, was prepared by treating free amine with perchloric acid in EtOH to give perchlorate salt **247** (Scheme 2.36). The synthetic sequence leading to the bicyclic amine **106** is summarised in Scheme 2.37.
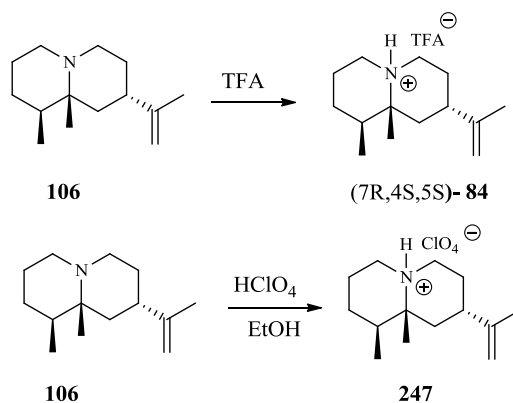
Scheme 2.36: *Formation of (7R,4S,5S)-**84** and perchlorate salt **247** (carried out by Dr. Juan A. Faraldos).*
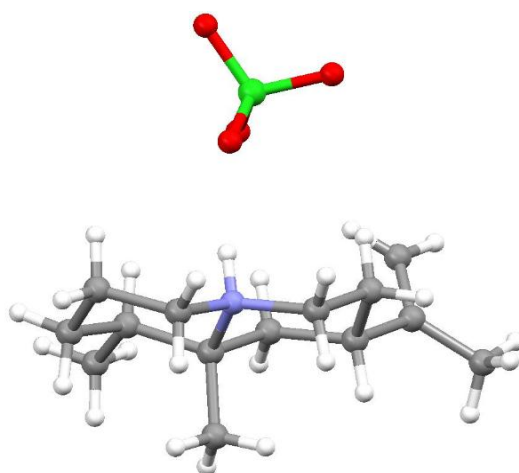
Figure 2.22: *Ball and stick representation of the X-ray crystal structure of the perchlorate salt **247** (solved by by Dr. Benson Kariuki)*
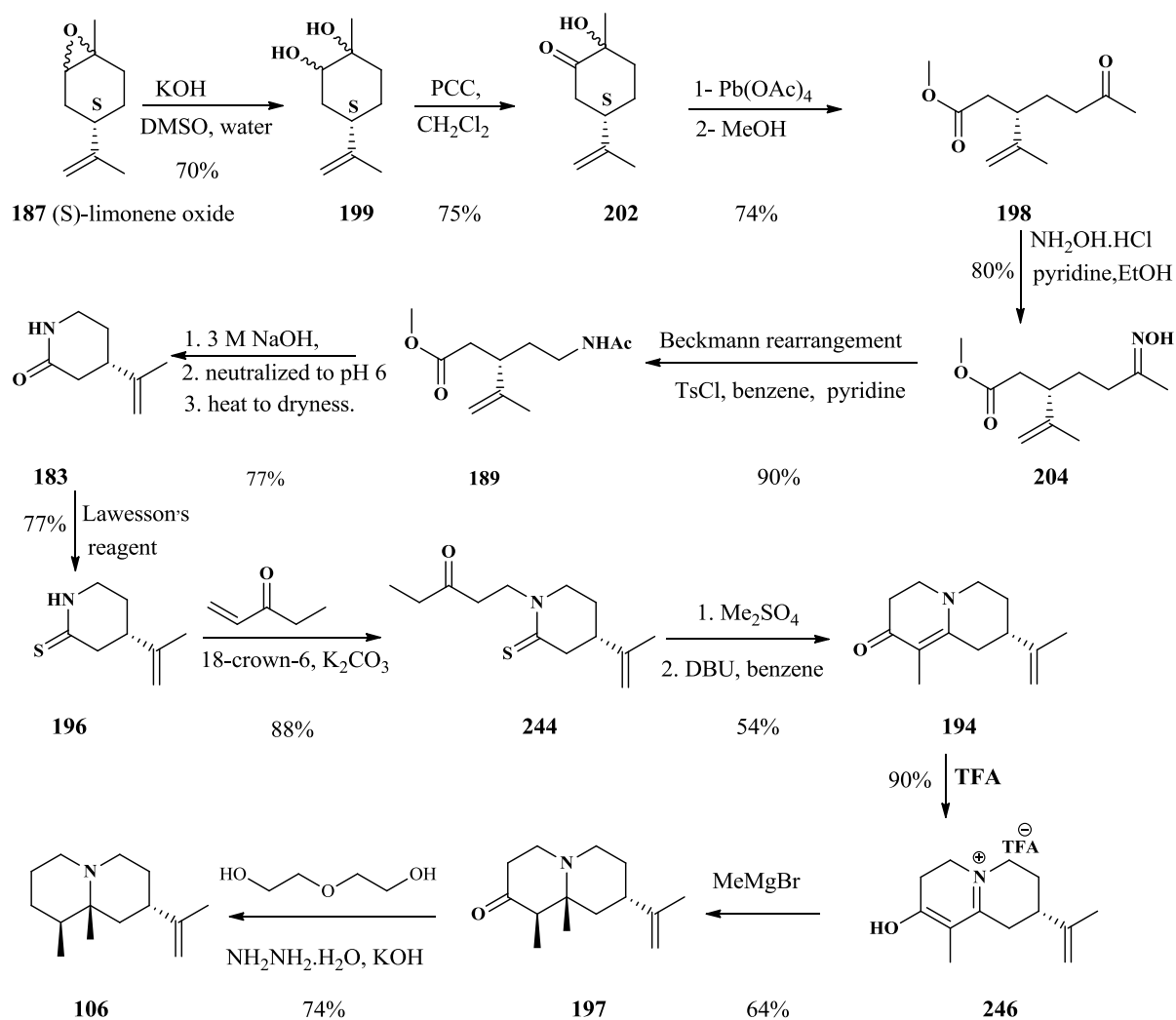
Scheme 2.37: *Stereospecific synthesis of bicyclic tertiary amine (7R,4S,5S)-4,5-dimethyl-7-(prop-1-en-2-yl) decahydroquinolizidine (**106**)*

(7*S*,4*R*,5*R*)-**84** was synthesised starting from *R*-(+)-limonene oxide (**248**) following the same synthetic sequence previously described for (7*R*,4*S*,5*S*)-**84**. The synthetic sequence leading to the bicyclic amine **107** and (7*R*,4*S*,5*S*)-**84** is summarised in Scheme 2.38. As before, For X-ray crystallography, the picrate salt **260** was prepared from the free amine **107** and picric acid, while perchlorate salt **261** was synthesised from reaction of free amine **107** and perchloric acid in ethanol (Scheme 2.39). These conversions were carried out by Dr. Juan A. Faraldos, Cardiff Unniversity. The absolute configuration of the final ammonium salts **260** and **261** were unambiguously verified by X-ray crystallography (Figures 2.23 and 2.24).
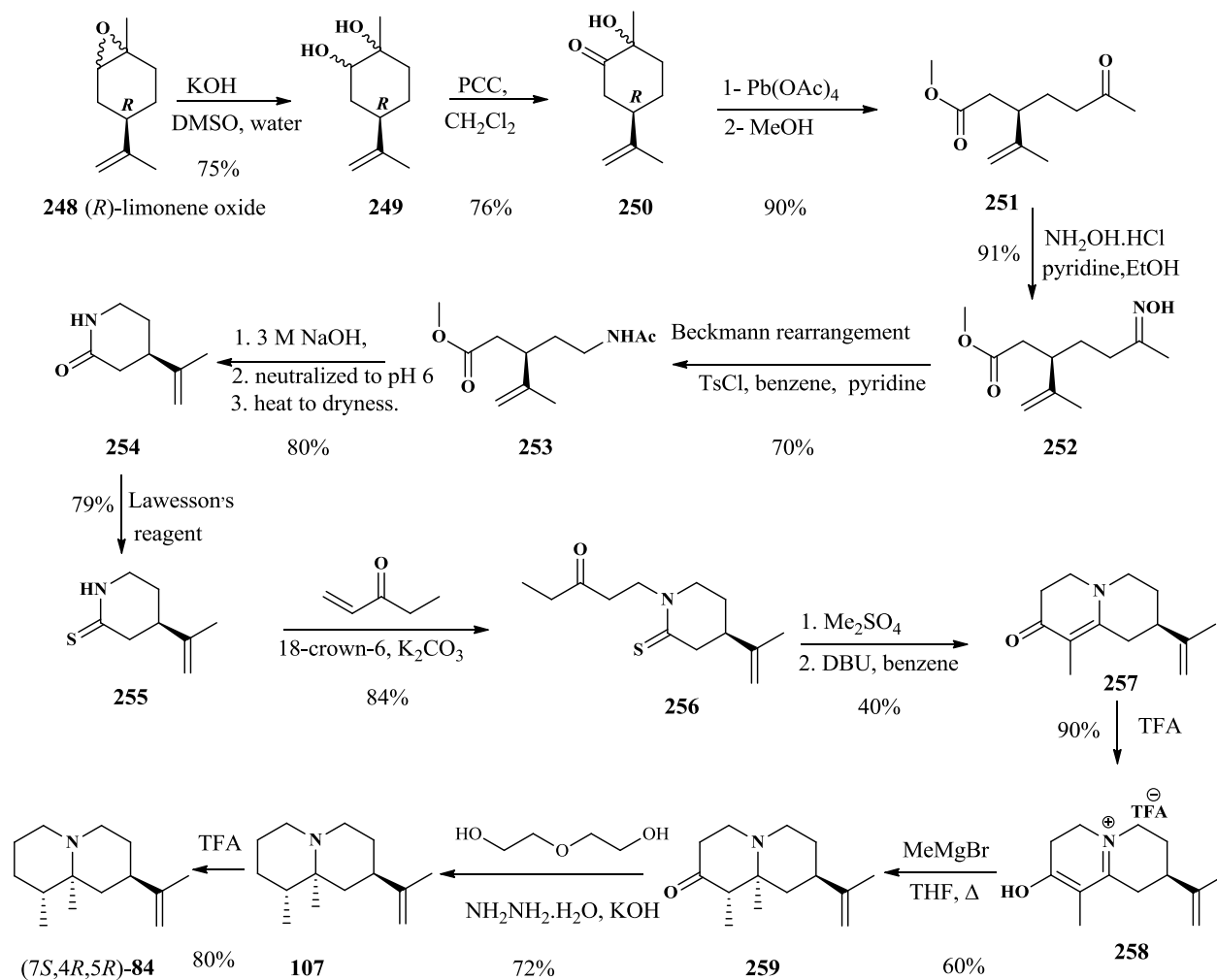
Scheme 2.38: *Stereoselective synthesis of bicyclic tertiary amine 107 and (7S,4R,5R)-84.*
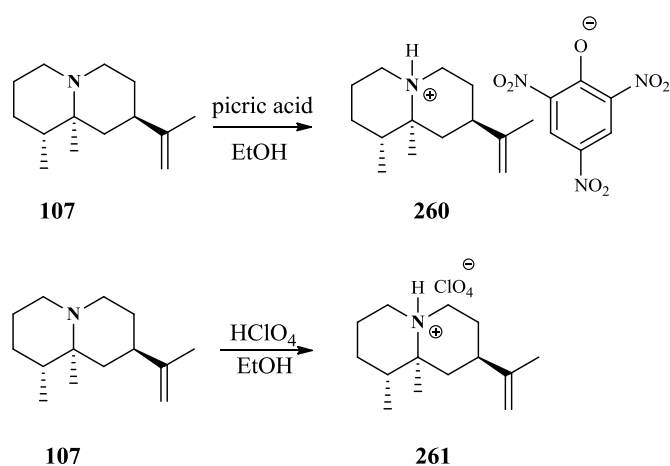
Scheme 2.39: *Picrate 260 and perchlorate 261 salts of amine 107 (carried out by Dr. Juan A. Faraldos)*
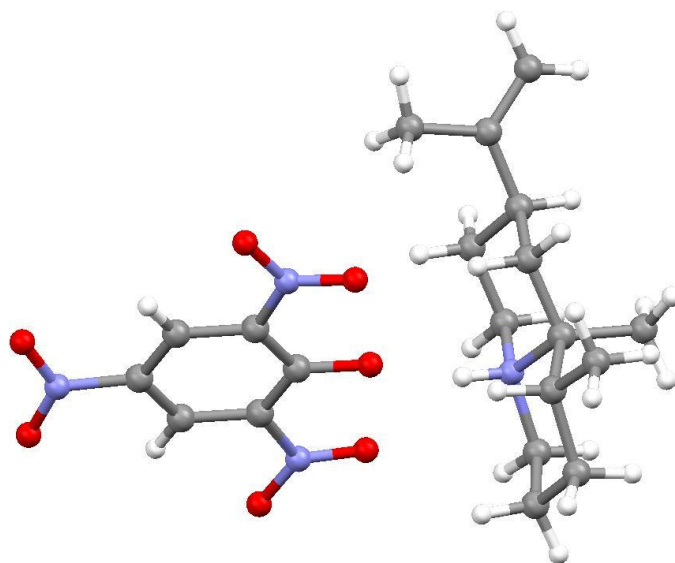
Figure 2.23: *Ball and stick representation of the X-ray crystal structure of the picrate salt 260 (solved by Dr. Benson Kariuki)*
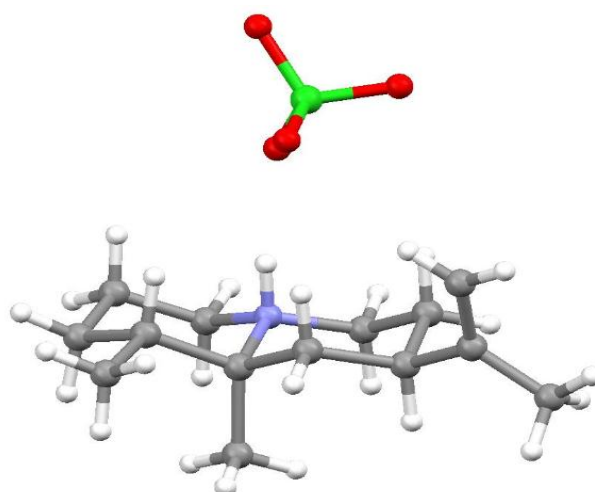
Figure 2.24: *Ball and stick representation of the X-ray crystal structure of the perchlorate salt 261 (solved by Dr. Benson Kariuki)*

After obtaining the three novel aza-analogues, **178**-(4*S*,5*S*)*,* (7*R*,4*S*,5*S*)-**84** and its mirror image (7*S*,4*R*,5*R*)-**84**, the next task was to evaluate them as potential inhibitors with aristolochene synthase. The analogue (7*R*,4*S*,5*S*)-**84** was expected to bind well to the active site of enzyme, since it was designed to mimic the eremophilane cation (**70**) involved in aristolochene biosynthesis. As introduced in the first chapter, many mechanistic details of

the cyclisation of FDP by aristolochene synthase from *P. roqueforti* have been studied, previously through the analysis of the reaction products generated by AS-mutants and FDP analogues. However there are still some mechanistic details that need further investigation. In particular regarding the reaction sequence from eudesmane cation that lead to the final hydrocarbon compound. Thus, in order to explore this, the three analogues were kinetically evaluated in the presence of fixed amounts of enzymes a described by Lineweaver-Burk.[139]

2.11 Inhibition studies of PR-AS with ammonium salt 178

The kinetic evaluation of these analogues was performed by Dr. Juan A. Faraldos (Cardiff University). In short, the kinetic steady state parameters of purified recombinant AS were measured in the presence of varying amounts of ammonium salt **178** by incubation with [1-^{3}H]FDP and monitoring the formation of tritiated, hexane extractable products. A double reciprocal plot indicated that the ammonium salt **178** lacking the isopropylidene unit was weak an inhibitor of PR-AS. The measured K_i of 2.86 ± 0.35 mM (no PPi) (Figure 2.25) was 5000-fold higher than the Michaelis-Menten constant for FDP (K_M = 0.53 ± 0.21 µM). Even in the presence of PPi (250 µM), ammonium salt **178** was weak an inhibitor of PR-AS [K_i of 1.66 ± 0.15 mM, (Figure 2.25)]. Since the aza-analogue ((7*R*,4*S*,5*S*)-**84**, Figure 1.12) was intended to mimic the topological and electrostatic properties of carbocation **70** presumably involved in the last step (Scheme 1.10) of aristolochene biosynthesis, the aza-analogue **178** is an imperfect mimic, because it lacks an isopropylidene group.
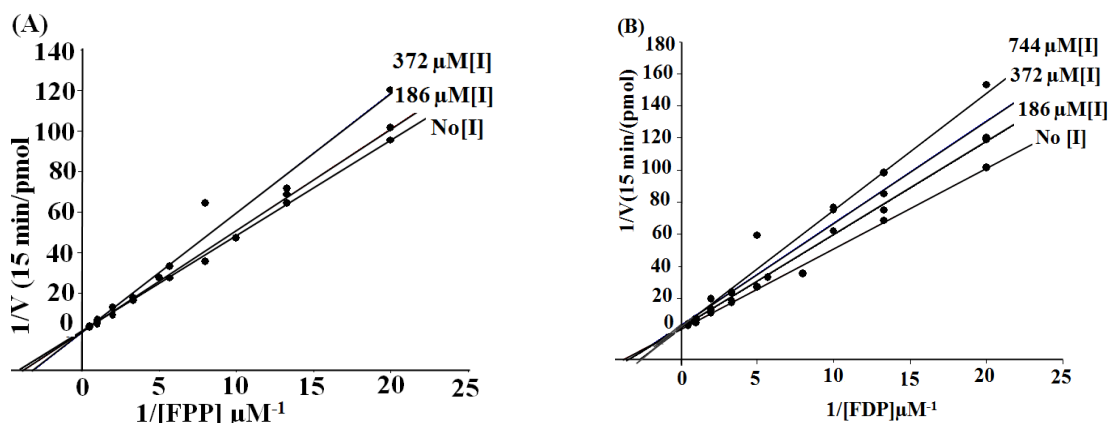
Figure 2.25: *Lineweaver-Burk plots of initial rate versus the concentration of substrate for AS catalysed turnover of FDP in the presence of 4,5-dimethyl-hexahydroquinolizidine.TFA salt (**178**) in (A) the absence of PPi (K_i = 2.86 ± 0.35 mM) and (B) the presence of 250 μM PPi (K_i = 1.66 mM ± 0.15). Initial rates were determined at increasing concentrations of analogue (0-25 μM). Assays were carried out (by Dr. Juan A. Faraldos) with purified wild-type AS (100 nM) in assay buffer (20 mM Tris, 5 mM MgCl$_2$, pH 7.5) and at room temperature (22 °C) for 12 min.*

2.12 Inhibition studies of PR-AS with ammonium salt (7*R*,4*S*,5*S*)-84

Inspection of the the kinetic plots (Figure 2.26 and Figure 2.27), obtained for compound (7*R*,4*S*,5*S*)-**84** and PR-AS revealed that this ammonium salt acted as moderate competitive inhibitor with a K_i = 27.7 ± 2.4 μM in the absence of PPi (Figure 2.26), K_i = 38 ± 4.1 μM (by Dixon plot, Figure 2.27). This was concluded because the individual plots intersect on the y-axis, indicating that V$_{max}$ remains constant in the presence of inhibitor, this is characterisitic of inhibitors that competes for the same binding site on the enzyme as the substrate.The measured K_i was 72-fold higher than the Michaelis-Menten constant measured for FDP (K_M = 0.53 ± 0.21 μM).

The inhibition potency of aza-analogues often increases by the addition of diphosphate PPi.[77,91] In order to mimic the complex of PR-AS with 10-aza-eremophillane cation, (7*R*,4*S*,5*S*)-**84** in the presence of PPi, the inhibition constant of ammonium salt for the PR-AS was measured in the presence of 250 μM of PPi. The K_i dropped to 2.5 ± 0.7 μM when PPi (250 μM) was added to the incubation mixture, hence it enhanced the effective

inhibition by a factor of 15.2 (Figures 2.26 and 2.27). This synergetic kinetic effect suggests the possible involvement of PPi in the stabilization of carbocation **70** (Figure 2.28) in aristolochene biosynthesis. This observation is consistent with the general strategy that has been suggested in terpene synthases, based on several crystal structures of terpene synthases aza analogues complexes.[76] Namely that stabilise carbocations generated during catalysis by the formation of carbocation-diphosphate ion pairs.[91] Compound (7*R*,4*S*,5*S*)-**84** mimic of eremophilane cation **70** binds moderately well to PR-AS in the presence of diphosphate. This could be a consequence of the possibility that the final carbocation intermediate in this terpenoid cyclisation reaction may be oriented toward the PPi anion, which may play a key role in quenching the final carbocation intermediate.
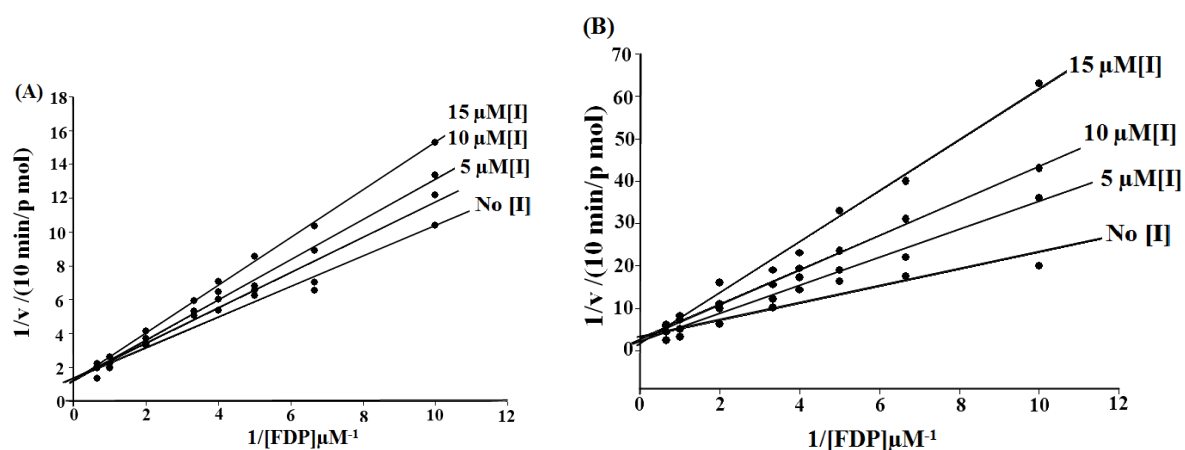
Figure 2.26: *Inhibition of AS by ammonium salt (7R,4S,5S)-**84**: Lineweaver-Burk plots of initial rate versus the concentration of substrate for AS catalysed turnover of FDP in the presence of inhibitor (7R,4S,5S)-**84** in (A) the absence of PPi (K_i = 27.7 ± 2.4 µM) and (B) the presence of 250 µM PPi (K_i = 2.9 ± 0.3 µM). Initial rates were determined at increasing concentrations of inhibitor (0-25 µM). Assays were carried out (by Dr. Juan. A. Faraldos) with purified wild-type AS (100 nM) in assay buffer (20 mM Tris, 5 mM MgCl$_2$, pH 7.5) and at room temperature (22 °C) for 12 min.*
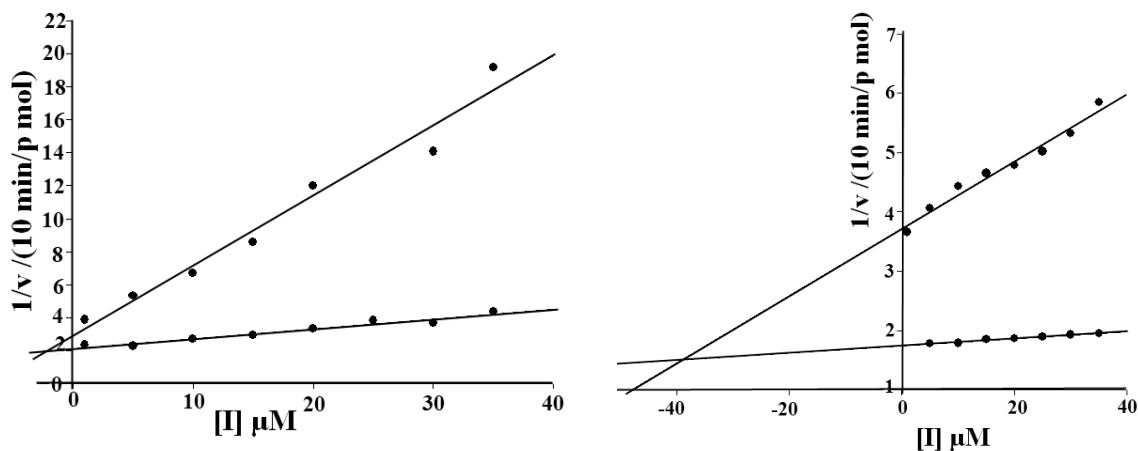
Figure 2.27: *Inhibition of AS by ammonium salt (7R,4S,5S)-**84**: Dixon plots for inhibition of PR-AS by (7R,4S,5S)-**84**, in the absence of PPi, (7R,4S,5S)-**84** acted a modest competitive inhibitor of PR-AS with K_i = 38 μM ± 4.1 (right plot). The K_i of (7R,4S,5S)-**84** dropped to 2.5 ± 0.7 μM when 250 mM diphosphate (left plot) was added demonstrating a strong synergistic inhibition. Assays were carried out by Dr. Juan A. Faraldos.*
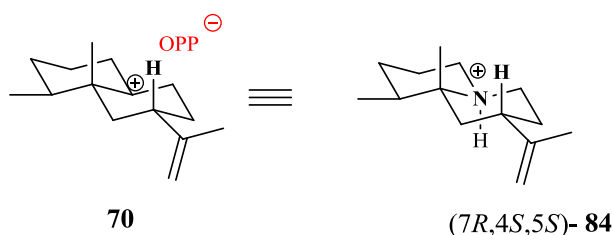
70 (7*R*,4*S*,5*S*)- **84**

Figure 2.28: *Ion-pair of eremophilane cation (**70**) with PPi and its analogue (7R,4S,5S)-**84***

2.13 Inhibition studies of PR-AS with ammonium salt (7*S*,4*R*,5*R*)-84

Inspection of the the kinetic plots (Figure 2.29), obtained for compound (7*S*,4*R*,5*R*)-**84** and PR-AS revealed, as somewhat expected, that this salt did not bind strongly to the active site of PR-AS either in the presence (K_i = 0.44 ± 0.18 mM) or absence (K_i = 1.03 ± 0.21 mM) of PPi (Figure 2.29). This enzymatic enantiomeric discrimination of aza-analogs highlights the chiral environment of the active site of PR-AS and provides evidence for a product-like

contour of this cavity that ultimately steers the electrophilic reaction cascade toward the production of a single enantiomer.
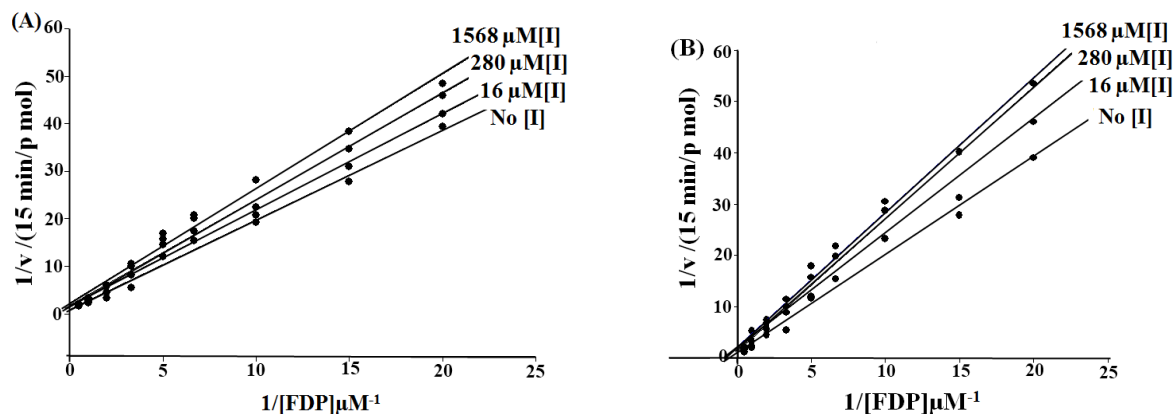
Figure 2.29: *Lineweaver-Burk plots of initial rate versus the concentration of substrate for AS catalysed turnover of FDP in the presence of (7S,4R,5R)-**84** in (A) the absence of PPi (K_i = 1.03 ± 0.21 mM) and (B) the presence of 250 µM PPi (K_i = 0.44 ± 0.18 mM). Initial rates were determined at increasing concentrations of analogue (0, 16, 280, and 1568 µM). Assays were carried out (by Dr. Juan A. Faraldos) with purified wild-type AS (100 nM) in assay buffer (20 mM Tris, 5 mM MgCl$_2$, pH 7.5) and at room temperature (22 °C) for 12 min.*

2.14 Crystal structures of *Aspergillus terreus* aristolochene synthase (AT-AS) complexed with (7*R*,4*S*,5*S*)-84 and (7*S*,4*R*,5*R*)-84

Our Inhibition studies with the mechanistically similar PR-AS have shown that only the aza-analog [(7*R*,4*S*,5*S*)-**84**] possessing the stereochemistry of the postulated carbocation binds efficiently to the active site, with the opposite enantiomer (7*S*,4*R*,5*R*)-**84** binding poorly.

More recent studies have reported the X-ray crystal structures of AT-AS complexed with amino analogues (7*R*,4*S*,5*S*)-**84**, (7*S*,4*R*,5*R*)-**84** (and **275**, chapter three).[140] Surprisingly, the active site of AT-AS was sufficiently flexible to accommodate analogues (7*R*,4*S*,5*S*)-**84**, (7*S*,4*R*,5*R*)-**84** and analogue **275** with partially or completely incorrect stereochemistry (Figure 2.30 a), (Figure 2.31 a). These studies show that the analogue (7*R*,4*S*,5*S*)-**84** binds in a region that is encircled by the faces of three aromatic residues Y61, F81 and F147 (Figure 2.31). Therefore, the binding of aza analogue (7*R*,4*S*,5*S*)-**84** with the correct stereocenters

to mimic eremophilane cation (**70**) suggest that Y61, F81 and F147 are ideally positioned to stabilise carbocation intermediates in the AT-AS reaction. The distances between the aza analogue (7*R*,4*S*,5*S*)-**84** and aromatic amino acids Y61, F81 and F147 are 3.4, 3.7 and 4.2 Å respectively. In order to accommodate the opposite enantiomer (7*S*,4*R*,5*R*)-**84** the aromatic ring of Y61 rotates approximately 90° and so the edge of this ring rather than the face is oriented towards the active site cavity (Figure 2.31). The distances between the aza analogue (7*S*,4*R*,5*R*)-**84** and aromatic amino acids Y61, F81 and F147 are 3.2, 3.5 and 4.01 Å respectively.

Another interesting observation was that the C8 methylene group is oriented toward the PPi anion.[140] This may imply that the PPi anion serves as a general base for the stereospecefic deprotonation of the H-8si atom in the cyclisation cascade. In addition, in each enzyme-inhibitor complex, the cationic amino group is oriented toward the PPi anion, so the binding orientation of each aza analogue appears to be governed by favourable electrostatic interactions.
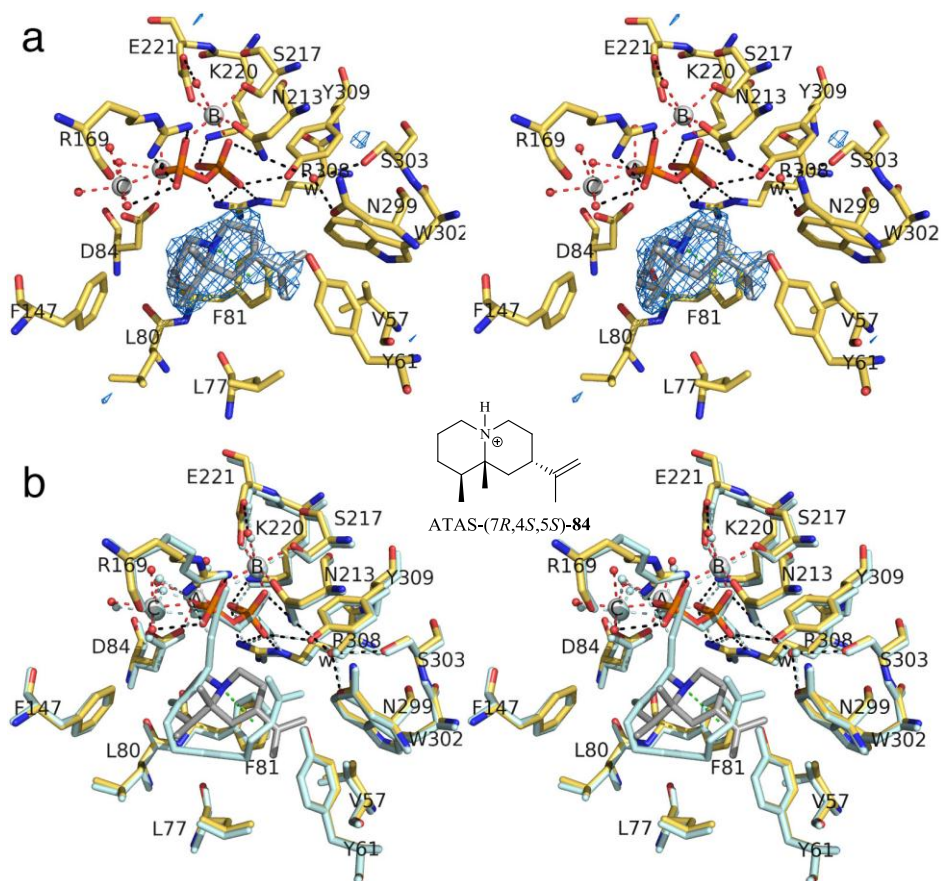
Figure 2.30: *Active site of AT-AS complexed with Mg^{2+}-PPi and tertiary amino cation (7R,4S,5S)-**84**. (a) Simulated annealing omit map of (7R,4S,5S)-**84** bound to monomer A in the AT-AS-(7R,4S,5S)-**84** complex. Analogue (7R,4S,5S)-**84**) is shown in gray, and Atoms are shown in the following colors: C = yellow (protein), O = red, N = blue, P = orange, S = yellow, Mg^{2+} ions = silver spheres, solvent molecules = red spheres. Water molecule "w" is trapped in the active site along with (7R,4S,5S)-**84**. (b) Superposition of the AT-AS-(7R,4S,5S)-**84** complex with the AT-AS-FSDP complex.[140] This structure was solved by the group of Prof. David W. Christianson, University of Pennsylvania.*
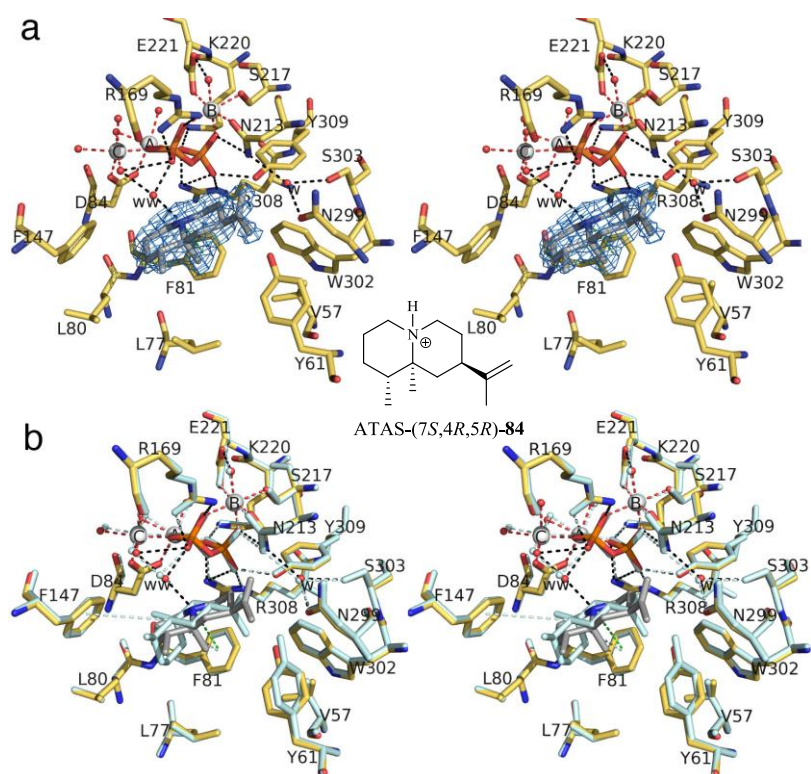
Figure 2.31: *Active site of AT-AS complexed with Mg^{2+}-PPi and tertiary amino cation (7S,4R,5R)-**84**. (a) Simulation of tertiary amino cation (7S,4R,5R)-**84** bound to monomer A in the AT-AS-(7S,4R,5R)-**84** complex. Analogue (7S,4R,5R)-**84** is shown in gray, and Atoms are shown in the following colors: C = yellow (protein), O = red, N = blue, P = orange, S = yellow, Mg^{2+} ions = silver spheres, solvent molecules = red spheres. Water molecule "w" is trapped in the active site along with (7S,4R,5R)-**84**. (b) Superposition of the AT-AS-(7S,4R,5R)-**84** complex with the AT-AS-FSDP complex.[140] This structure was solved by the group of Prof. David W. Christianson, University of Pennsylvania.*

CHAPTER THREE

APPROACHES TOWARDS THE SYNTHESIS OF 5-AZA-EUDESMANE CATION

3.1 Retrosynthetic analysis of 5-aza-eudesmane cation (83)

For the synthesis of **83**, iminium **262** salt (Figure 3.1) could be synthesised by kinetic deprotonation at the α-position of a cyclic imine **182**, followed by double alkylation with (*R*)-1,3-dibromobutane (**184**). Cyclic imine **182** could be obtained via cyclisation of carbamate **186**, which would be obtained via keto acid **211** through degradation of limonene oxide (**187**) and subsequent Curtius rearrangement of **211**.
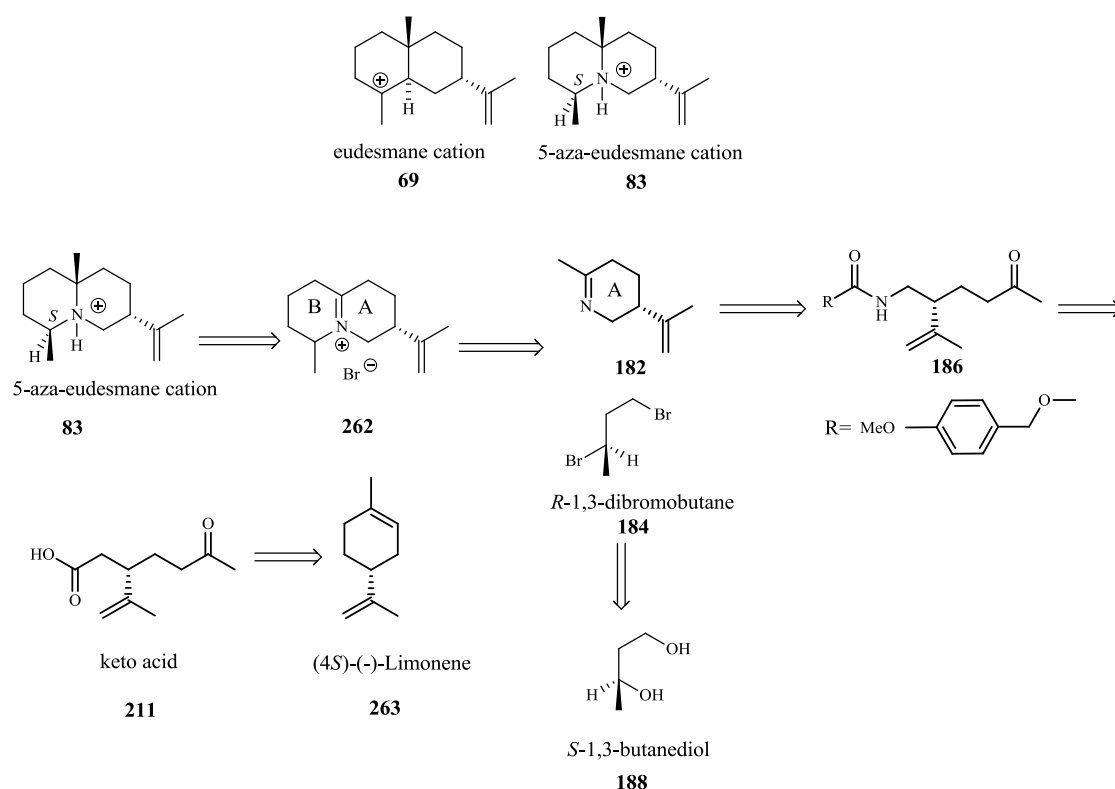
Figure 3.1: *Retrosynthetic analysis of 5-aza-edesmane cation (83)*

3.2 Preparation of monocyclic imine 182

The synthesis of ring A in **83** was constructed from (4*S*)-limonene (**263**) (Scheme 3.1). Epoxidation of limonene was carried out according to a literature procedure [77, 141] using *m*-CPBA in the presence of NaHCO$_3$ to provide a mixture of diastereoisomers of (4*S*)-limonene oxides (**187**) in 65% yield. Under these conditions, the double bond on the isopropylidine group was not oxidized by *m*-CPBA as it is less electron rich than the substituted double bond within the ring. The peroxide selectively attacks the top face of the ring opposite to the isopropenyl group on the bottom face. The *m*-CPBA reaction is a concerted electrophilic process via a 'butterfly' transition state where the oxygen is added and the proton shifted simultaneously (Scheme 3.1). As the reaction was performed without any stereochemical control the product was generated as a mixture of *cis*- and *trans*-isomers. The diastereoisomers are distinguishable by ^{1}H NMR spectroscopy. The lack of signals above 5 ppm (olefinic region) indicate the loss of the double bond on the cyclohexene ring, whilst the appearance of a doublet at 3 ppm and a triplet at 3.06 ppm, both of which integrate for 1H and correspond to the proton of the trisubstituted epoxide. The multiplets at 4.67 and 4.72 ppm both integrate to 1H and correspond to the methylene group. The singlets at 1.67 and 1.69 ppm correspond to the protons on the methyl group adjacent to the exo double bond. The olefinic CH$_3$ appeared downfield (1.67 and 1.69 ppm) when compared to the epoxide's methyl group (1.31 and 1.32 ppm) because the α-double bond has a greater deshielding effect than the β-oxygen of the epoxide (Figure 3.2).
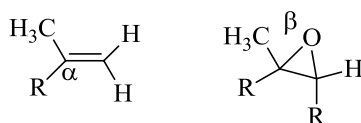
Figure 3.2: *Positions of α-double bond and β-oxygen with respect to the methyl group*
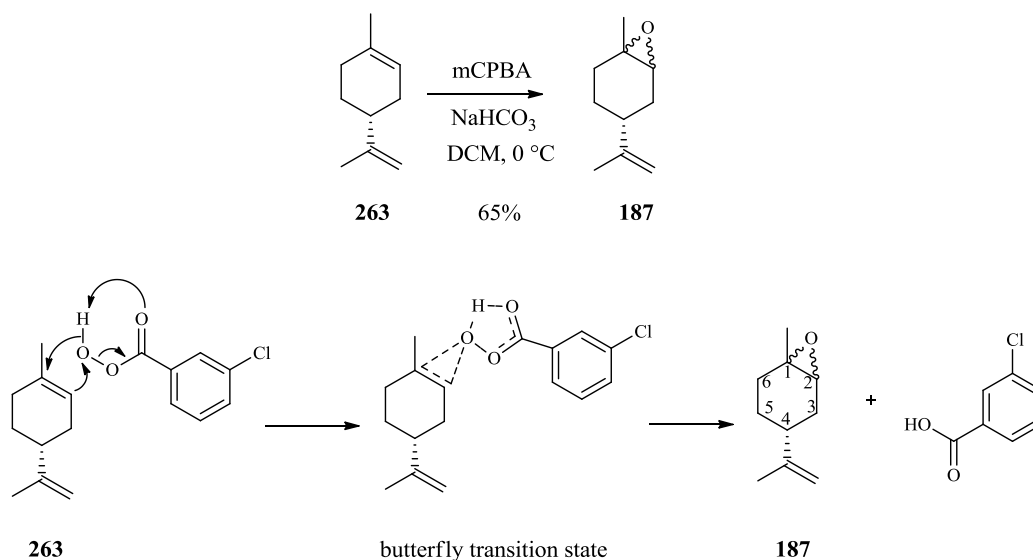
Scheme 3.1: *Epoxidation of (-)-limonene (263) to (-)-limonene oxide (187)*

Among the synthetic intermediates, the acyclic keto acid **211** is very important, since it is the precursor of the cyclic imine **182**. The preparation of keto acid **211** was reported by Kido and co-workers and has been discussed in chapter two.[114] (4*S*)-Limonene oxide (**187**) was converted to keto acid **211**,[114,142] as before (see chapter two) in four steps and 79% overall yield (Scheme 3.2).
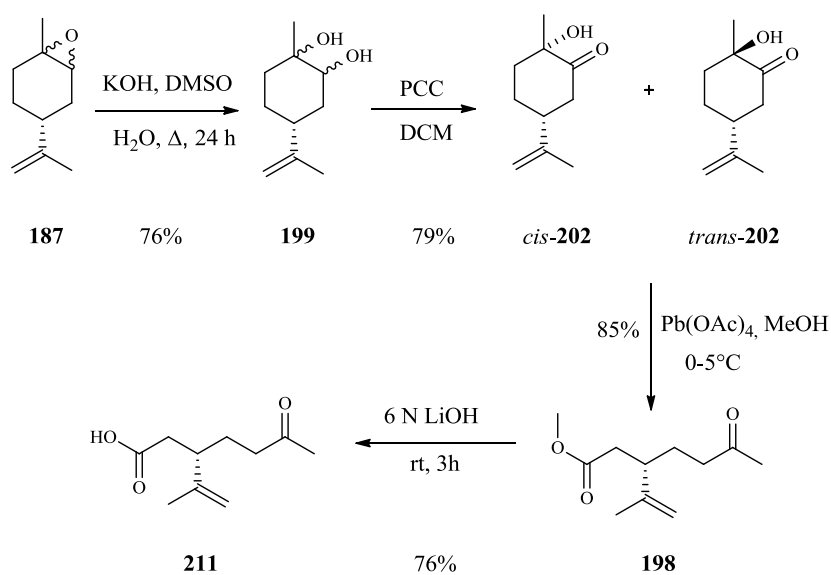
Scheme 3.2: *Conversion of (-)-limonene oxide (187) to keto acid 211*

Alternatively, the keto acid could also be obtained by direct oxidation of diol **199** with Jones' reagent (Scheme 3.3).[115] Jones' reagent is a solution of chromium trioxide in dilute sulfuric acid used for the general oxidation of primary and secondary alcohols to acids and ketones, respectively.
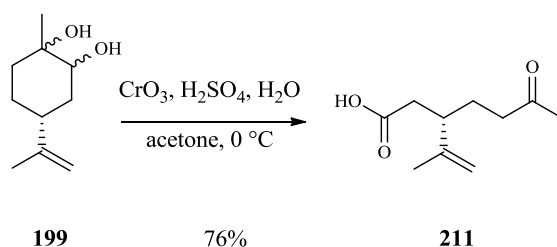
Scheme 3.3: *Synthesis of keto acid **211** by oxidation of diol **199** with Jones' reagent.*

The ^{1}H-NMR spectrum of keto ester **198** displayed a characteristic singlet at 3.65 ppm ascribed to COOCH_3. This signal was absent in the ^{1}H-NMR spectrum of keto acid **211**. The ^{13}C-NMR spectrum of keto ester **198** showed a signal for COOCH$_3$ at 173.6 ppm. This signal was shifted downfield to 178.5 ppm for COOH in the ^{13}C-NMR spectrum of keto acid **211**. The IR spectrum of keto ester **198** showed two characteristic bands at 1710 and 1725 cm^{-1} assigned to the ketone C=O stretch and C=O ester, while the keto acid showed a very strong band at 3360 cm^{-1} owing to the OH stretch, and another two bands at 1738 and 1715 cm^{-1} due to the C=O stretches of the acid and CO ketone groups, respectively.

3.2.1 Curtius rearrangement

With the keto acid **211** in hand, the next synthetic objective was to introduce the amine functionality regioselectively at the acid site, and then induce the cyclisation to form the advanced cyclic imine **182**. The keto acid **211** was converted to isocyanate **265** under Curtius rearrangement conditions when treated with diphenyl phosphoryl azide and triethyl amine in refluxing toluene (Scheme 3.4). The unstable isocyanate was quenched *in situ* with *p*-methoxy benzyl alcohol and the mixture was heated under reflux for 24 h.[143] TLC analysis of the crude mixture showed three spots, the middle one was identified as *p*-methoxy benzyl alcohol, and the UV active spot at the bottom was identified as the urethane **186** as determined by ^{1}H-NMR spectroscopy after purification. The product was purified by chromatography on silica to give the desired compound **186** in 61% yield.
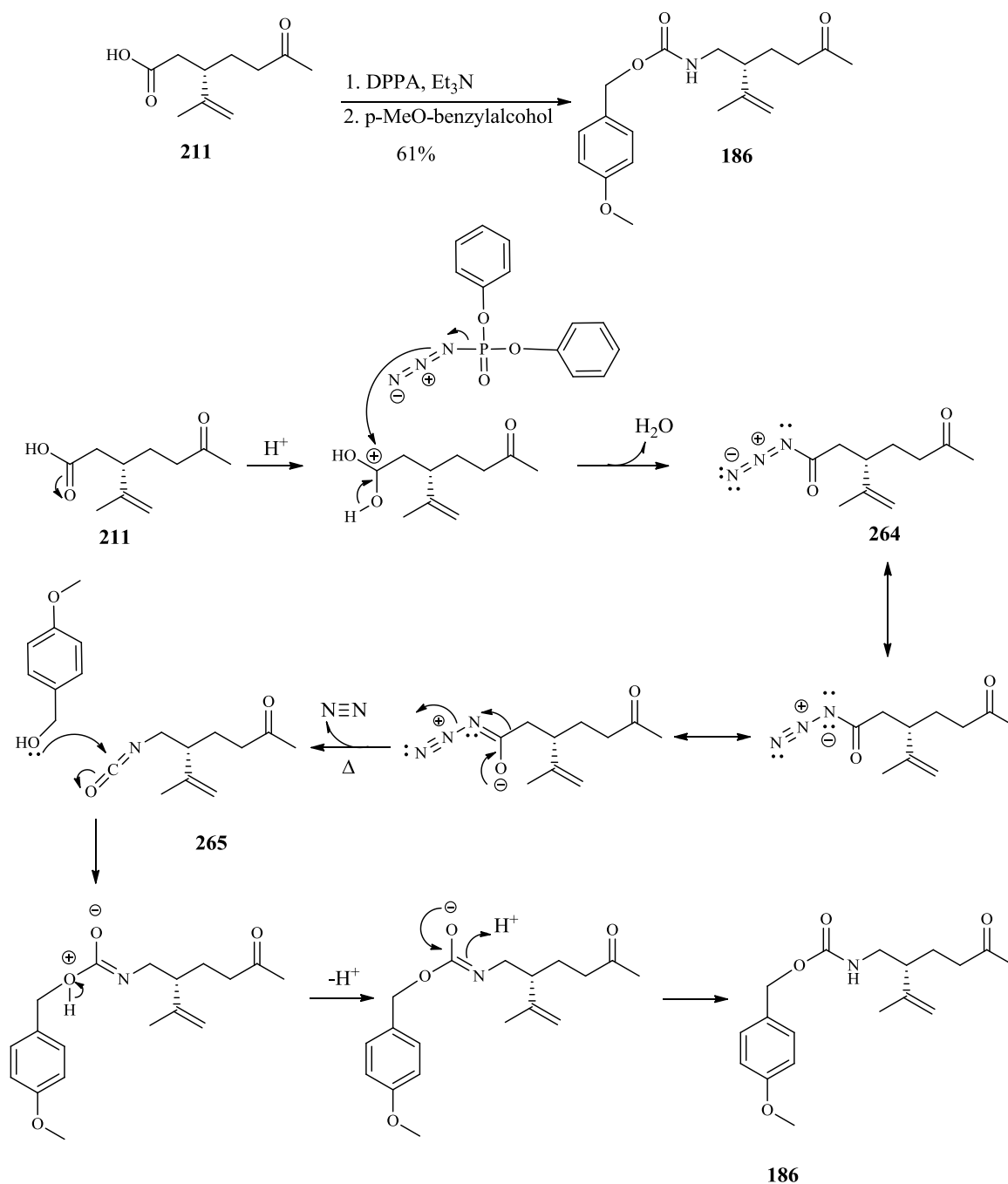
Scheme 3.4: *Mechanism of the Curtius rearrangement of keto acid **211***

The Curtius degradation of acyl azide **264** (Scheme 3.4) consists of the thermolysis of the "inner" N=N double bond. This thermolysis expels a nitrogen molecule and at the same time leads to the [1,2]-rearrangement of the substituent attached to the carboxyl carbon. It is the simultaneous occurrence of these two events that prevents the formation of an energetically disfavoured acylnitrene intermediate. This one-pot procedure was convenient because there was no need to isolate the potentially explosive acyl azide

264.[118] The isocyanate **265** can be reacted with heteroatom-nucleophiles *in situ*. In this case, the nucleophile (*p*-methoxybenzyl alcohol) was added to the C=N double bond of the isocyanate **265** to afford carbamate **186**.

3.2.2 Cyclic imine-enamine ring formation

Hydrolysis of urethane **186** with 10% mol of *p*-TsOH.H$_2$O in benzene at reflux resulted in the formation of enamine compound **266** (Scheme 3.5). Treatment of **266** with 5 equivalents of aqueous potassium hydroxide in DMSO gave cyclic imine **182** in 46% yield after purification by chromatography.[144]
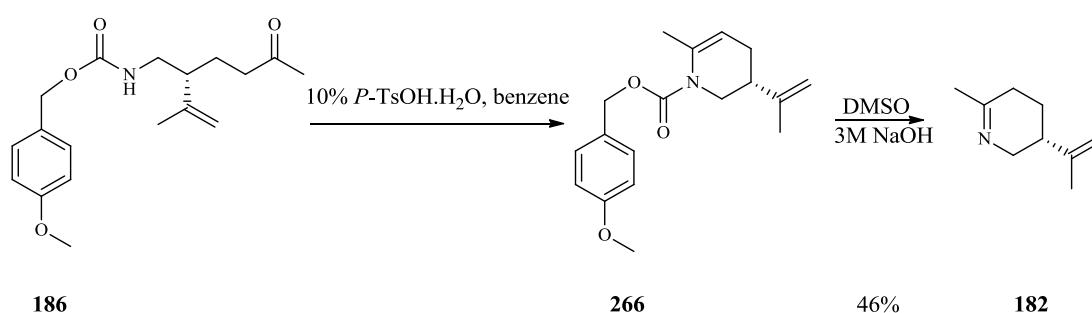
Scheme 3.5: *Cyclisation of urethane 186 to imine 182*

To optimise the yield of cyclic imine, the Albericio[145] method was used to remove the protecting group in **186**. This involved deprotection with 10% trifluoroacetic acid in DCM at RT for 10 min followed by cyclisation during basic work up (aqueous KOH, 0 °C, 20 min) to produce cyclic imine **182** (Scheme 3.6) in 74% yield and excellent purity (without further purification). The product was stored at -20 °C under N$_2$.

The ^{1}H-NMR spectrum of cyclic imine **182** revealed signals at δ 3.10-3.25 of H_aCHN, 3.65-3.78 of HCH_bN, 1.87 of CH$_3$C=N and 2.15-2.25 of CH$_2$C=N. These values were in good agreement with those previously reported for the 2-methyl-3,4,5,6-tetrahydropyridine **165** (Figure 3.3).[146]
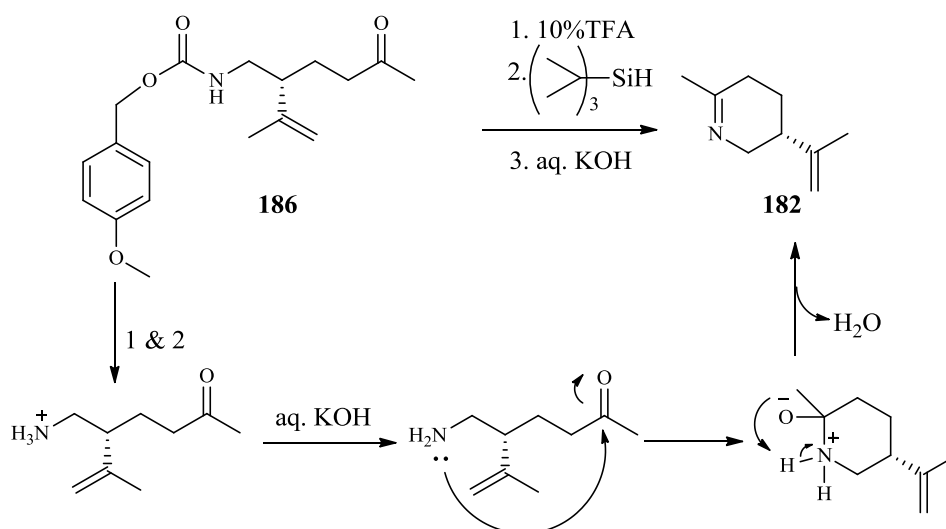
Scheme 3.6: *Intramolecular cyclisation of urethane **186** to cyclic imine **182** in 74% yield*
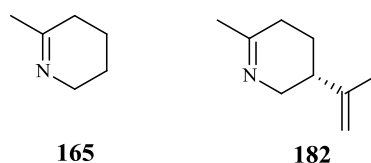
Figure 3.3: *Structures of imines **165** and **182***

3.3 Attempted stereospecific synthesis of (*R*)-1,3-dibromobutane

The synthesis of amine **267** would require the stereospecific synthesis of (*R*)-1,3-dibromobutane (**184**). The general strategy to introduce ring B consisted of the deprotonation of the methyl group at the α-position of 3*S*-(prop-1-en-2-yl)-6-methyl-2,3,4,5-tetrahydropyridine (**182**), followed by alkylation with (*R*)-1,3-dibromobutane (**184**) to generate a new chiral centre at C4 with an inverted configuration (Figure 3.4).

(4*S*,10*S*)-dimethyl-7*R*-(prop-1-en-2-yl) octahydroquinolizidine
267

(*R*)-1,3-dibromobutane
184

cyclic imine
182
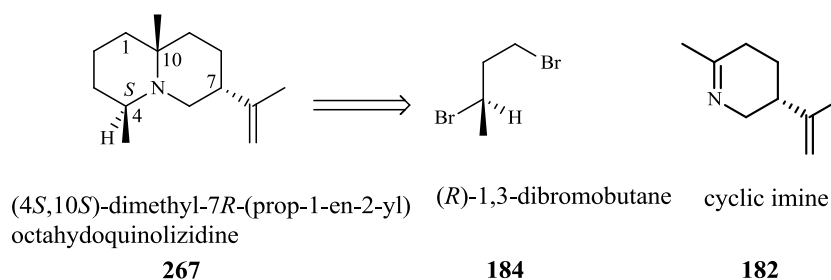
Figure 3.4: *General scheme for the stereospecific synthesis of amine **267***

Paquette and Freemann have reported the synthesis of (R)-1,3-dibromobutane (**184**).[147] Following the same procedure, (S)-(+)-1,3-butanediol (**188**) $[\alpha]^{24}_D$ = +10.1 (c 10.17, CHCl$_3$) was treated with 2 equivalents of freshly distilled methanesulfonyl chloride in dry pyridine at -5 °C to afford (S)-1,3-butanediol bis-methanesulfonate (**268**) in 70% yield with optical rotation $[\alpha]^{22}_D$ = + 30.1 (c 12.5, CHCl$_3$) and is consistent with that reported in the literature $[\alpha]^{22}_D$ = + 10.1 (c 10.17, CHCl$_3$)[147] (Scheme 3.7). The ^{1}H-NMR spectrum of dimesylate **268** displayed similar values to those reported by Paquette and Freemann.

Dimesylate **268** was treated with lithium bromide (5 equivalents) in dry THF at reflux to give racemic 1,3-dibromobutane instead of desired (R)-(-)-1,3-dibromobutane (**184**) in 75% yield. The optical rotation obtained for racemic 1,3-dibromobutane was $[\alpha]^{24}_D$ = 0. Paquette and Freemann reported the optical rotation for (R)-(-)-1,3-dibromobutane as $[\alpha]^{24}_D$ = -29.9 (c 17.7, CHCl$_3$) (Scheme 3.7).[147] However, attempts to prepare (R)-(-)-1,3-dibromobutane from dimesylate **268** by changing the number of equivalents of lithium bromide, temperature and solvent were unsuccessful. It seemed that this reaction took place with anchimeric (neighbouring group participation) assistance from the primary bromine atom, forming the bromonium ion intermediate (Scheme 3.8). This allows for the nucleophilic attack of a second Br⁻ to the primary electrophilic centre, yielding the (S)-enantiomer of 1,3-dibromobutane. Equilibration of the forward and backward reactions of this process racemise 1,3-dibromobutane from chiral diol **188**.

188 (S)-1,3-butandiol   **268** (S)-1,3-butandiol dimesylate   **184** (R)-1,3-dibromobutane   (S)-1,3-dibromobutane
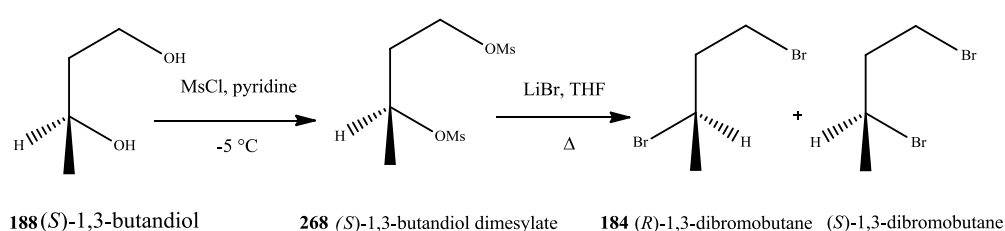
Scheme 3.7: *Conversion of (S)-1,3-butanediol (**188**) to racemic 1,3-dibromobutane*
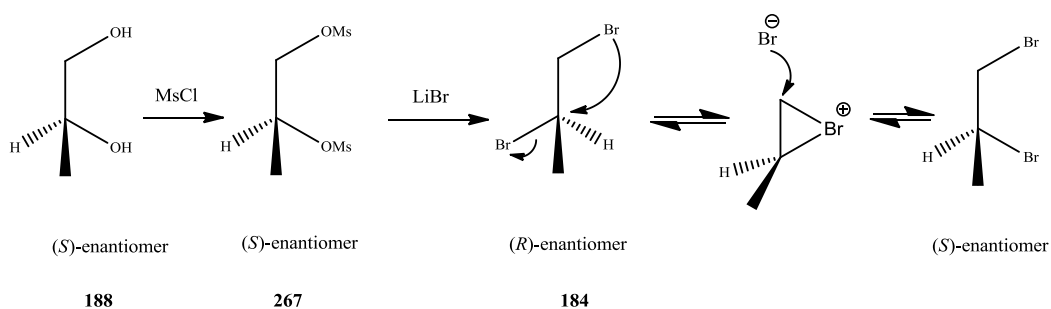
Scheme 3.8: *Proposed mechanism for conversion of chiral diol 188 to racemic 1,3-dibromobutane*

3.4 Synthesis of dehydroquinolizidinium salt 262

Kinetic deprotonation of 3*S*-(prop-1-en-2-yl)-6-methyl-2,3,4,5-tetrahydropyridine (**182**) was carried out at -35 °C with 1.5 equivalents of LDA in dry THF under argon for 30 min, followed by alkylation with 1,3-dibromobutane at -78 °C, the mixture was then allowed to warm to room temperature and stirred for 24 h.[148,149] Work-up was carried out by pouring the mixture into a solution of 0.5 M aqueous sodium hydroxide. After extraction and purification by alumina column chromatography, compound **270** was obtained in 71% yield (Scheme 3.9). A more polar compound was also obtained and determined by ^{1}H-NMR spectroscopy to be bicyclic enamine **271** in 20% yield.

In another experiment, cyclic imine **182** was treated with 1.1 equivalents of LDA at -35 °C for 30 min, followed by reaction with 1,3-dibromobutane at -78 °C. The reaction mixture was stirred at room temperature for 24 h and iminum salt **262** was obtained as a yellow-orange salt in 74% yield without using 0.5 M aqueous sodium hydroxide (Scheme 3.9). The solvent was evaporated under reduced pressure and the final traces of solvent under high vacuum for 2-3 h. Because of the hygroscopic nature of iminum salt **262**, it was difficult to measure the melting point. The purity of this salt was sufficient for use in the next step.
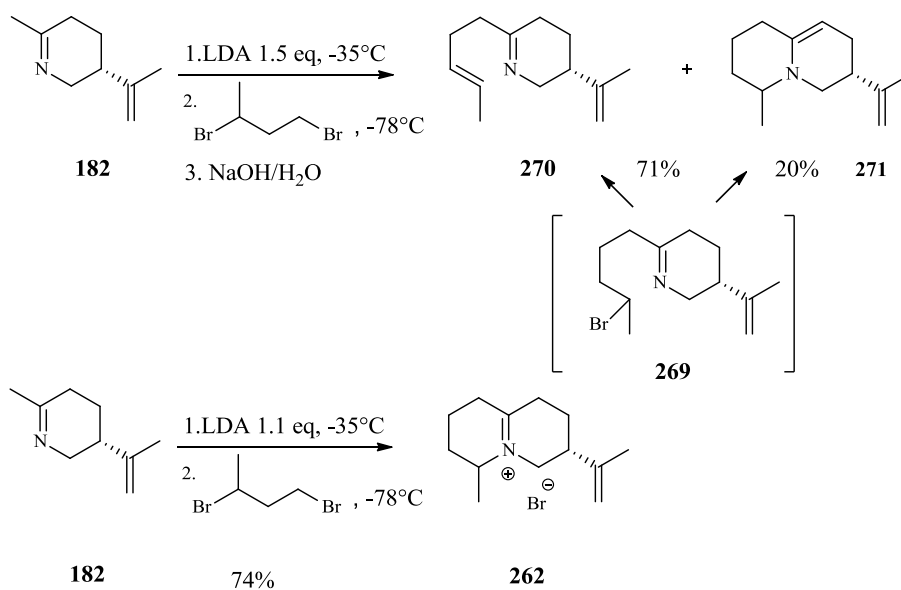
Scheme 3.9: *Reaction of cyclic imine **182** with racemic 1,3-dibromobutane*

Apparently after alkylation, the small excess of LDA (~0.4 eq) led to dehydrohalogenation, thus generating compound **270** (Scheme 3.9). The alkylated compound **269** is a secondary alkyl bromide (Scheme 3.10), therefore the HBr elimination reaction could take place either via a concerted E_2 mechanism or a stepwise E_1 mechanism (Scheme 3.10).
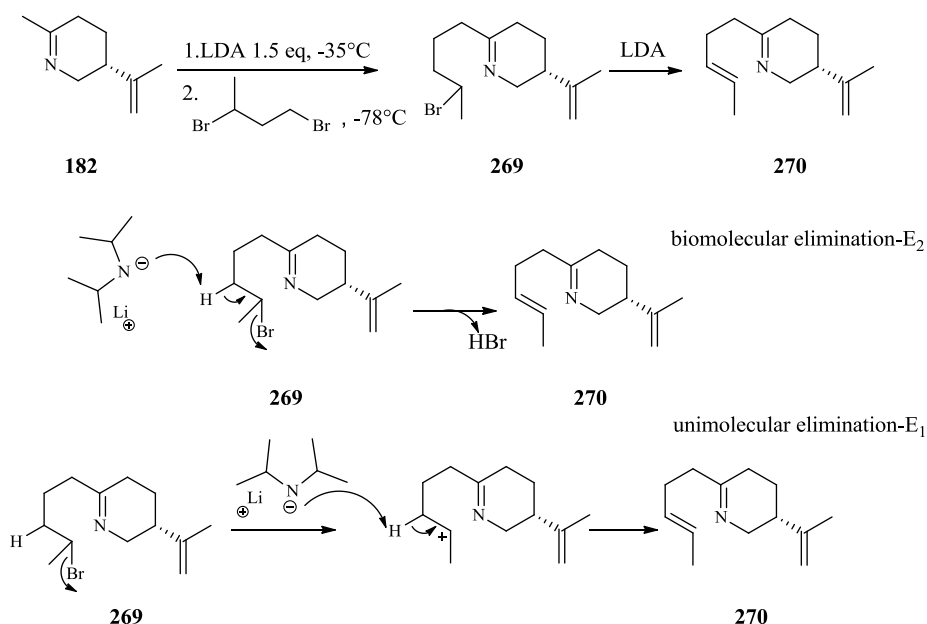
Scheme 3.10: *Possible elimination reaction mechanisms of alkylated compound **269***

3.5 Introduction of bridgehead methyl group to iminium salt 262

Introduction of the bridgehead methyl group, and the formation of 10-methylquinolizidine was performed by treatment of dehydroquinolizidinium salt **262** with methylmagnesium bromide in dry refluxing THF for 24 h.[99] TLC analysis on alumina of the crude mixture showed two spots corresponding to **108** and **109** (Scheme 3.11). The mixture of isomers was isolated by basic alumina-column chromatography. The two diastereomeric isomers were formed in the ratio 6:4 in 70% overall yield.
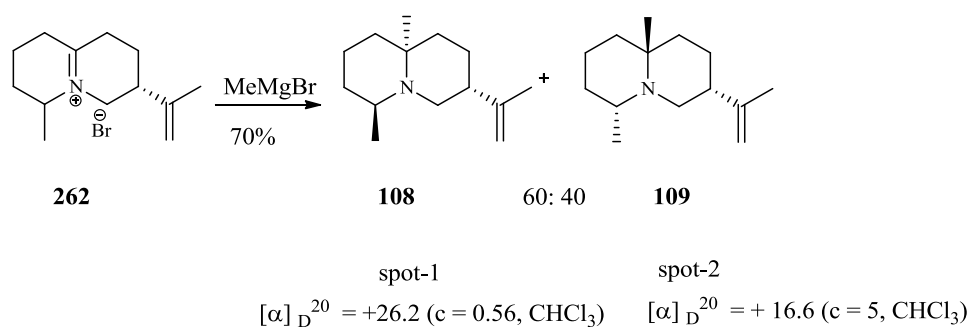
Scheme 3.11: *Conversion of iminium salt 262 to diastereoisomeric amines 108 and 109*

Four possibilities of 10-methyl quinolizidine in different configurations and conformations were predicted, due to the racemic form of iminium salt **262** (Scheme 3.12). The most stable isomers, amines **108** and **109** were characterised by nOe difference spectra and NOESY experiments and identified unambiguously by X-ray crystallography.
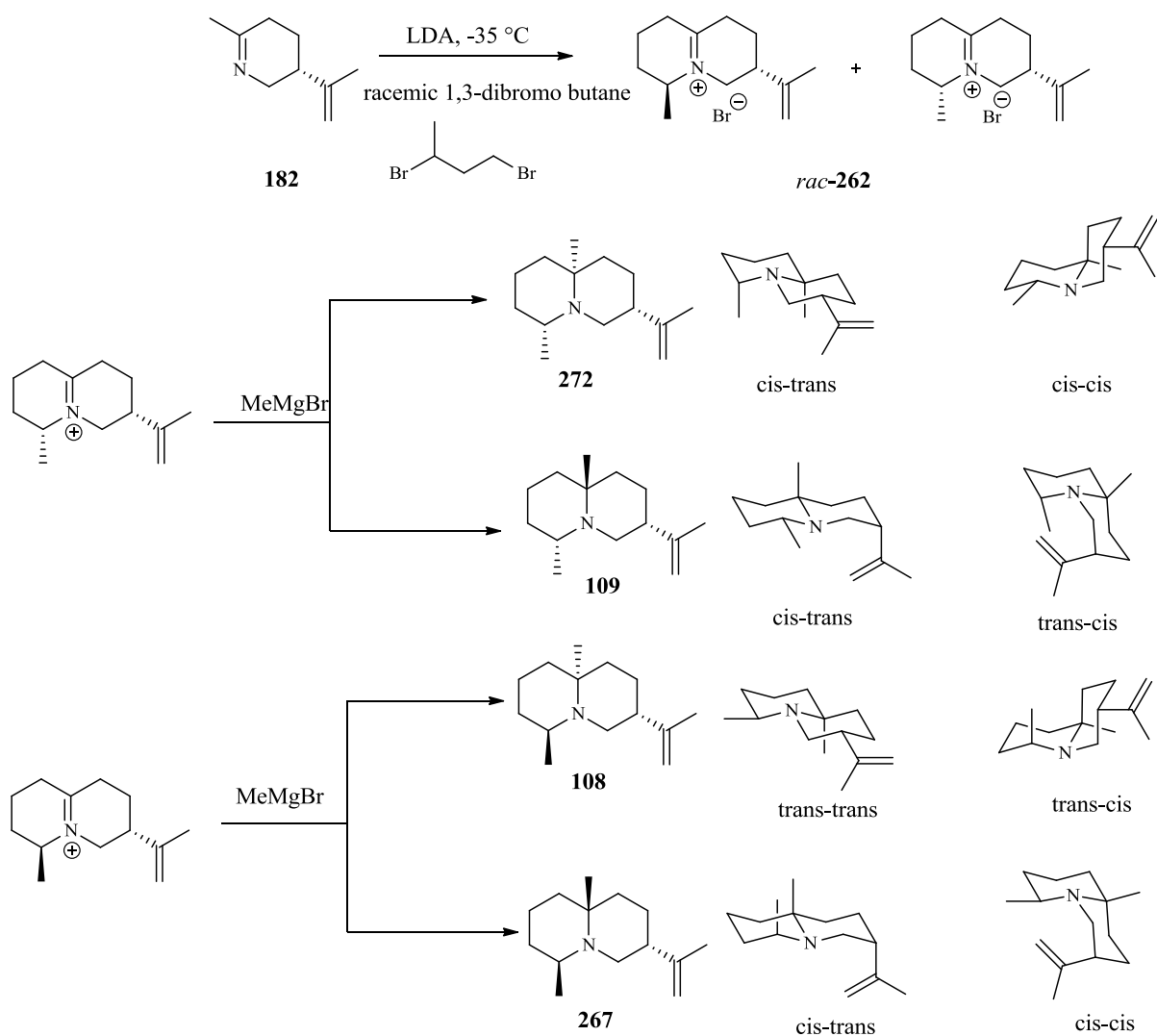
Scheme 3.12: *The configuration and conformational possibilities of 4,10-dimethyl quinolizidines 272, 109, 108 and 267*

In the infrared spectrum, the typical Bohlmann bands appeared at 2791-2856 cm^{-1} for the isomer **108**, thus, indicating that the bicyclic structure of this isomer was most likely trans-fused. The streochemistry of isomer **108** was determined using nOe difference spectra and NOESY experiments. Irradiation of CH_2=C at 4.65 ppm led to nOe enhancement on Hα (2.1%) of CH$_2$N at 2.13 ppm and CHN (2.4%) on C4 at 2.87-2.90 ppm (Figure 3.5), nOe were also observed for the protons of CH$_3$ (3.5%) on C4 at 0.96 ppm when Hβ of CH$_2$N at 2.35 ppm was irradiated. Irradiation of the protons of the C4 CH$_3$ doublet at 0.96 ppm did not enhance the CH$_3$ singlet on C10, also no nOe was observed for the CH$_3$ singlet when the

CH$_3$ doublet was irradiated, thus allowing the methyl group on C4 to be assigned as *anti* relative to CH$_3$ at C10.
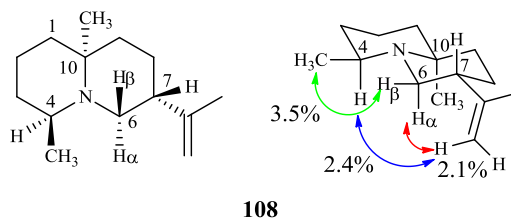
Figure 3.5: *Stereochemistry of amine 108*

The NOESY spectra of amine **108** showed a cross-peak between the signal at 4.65 ppm (C*H$_2$*=C) in one-dimension and the signal at 2.35 ppm (C*H*N) in the other dimension. A cross-peak between C*H*N and C*H$_3$*C also occurred. The absolute stereochemistry of isomer **108** was determined unequivocally by X-ray crystallography (Figure 3.6), using the perchlorate salt **273** prepared by treating free amine **108** with perchloric acid in ethanol (Scheme 3.13).
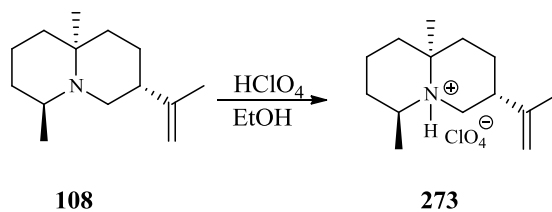
Scheme 3.13: *Formation of perchlorate salt 273 (carried out by Dr. Juan. A. Faraldos)*
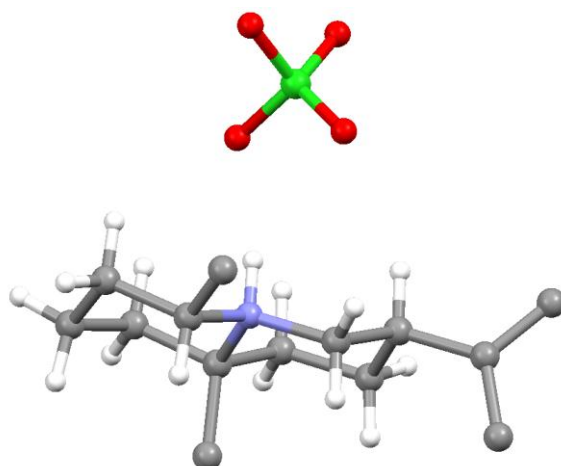
Figure 3.6: *Ball and stick representation of the X-ray crystal structure of the perchlorate salt 273 (solved by Dr. Benson Kariuki)*

The IR spectrum of isomer **109** did not show Bohlmann bands at 2700-2870 cm^{-1}, indicating that the bicyclic structure of this isomer was most likely cis-fused. The stereochemistry of isomer **109** was determined by NOESY and nOe difference spectra experiments. Irradiation of the protons of CH_2=C at 4.74 ppm led to enhancement of Hα of CH$_2$N at 2.41 ppm (2%) and of the C4 CH_3 doublet at 0.98 ppm (3.1%) (Figure 3.7). Another nOe was observed for Hβ of CH$_2$N at 2.66 ppm (2.4%) when the C7 CH proton at 2.01 ppm was irradiated. There was no nOe between the CH$_3$ singlet and CH$_3$ doublet, thus allowing the methyl group on C10 to be assigned also as *anti* relative to the methyl at C4.
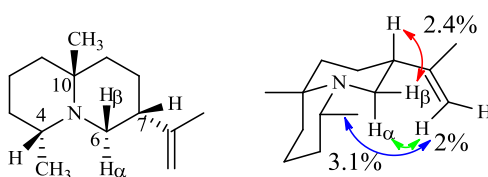
Figure 3.7: *Stereochemistry of amine 109*

The NOESY spectra of amine **109** displayed cross-peaks between the signal at 3.14 ppm (CHN) and the C10 CH$_3$ signal at 1.13 ppm. A cross-peak between CH_3 on C4 and Hβ of CH$_2$N also occurred. The absolute stereochemistry of isomer **109** was unambiguously determined by X-ray crystallography (Figure 3.8), the perchlorate salt **274** prepared from **109** as before (Scheme 3.14).
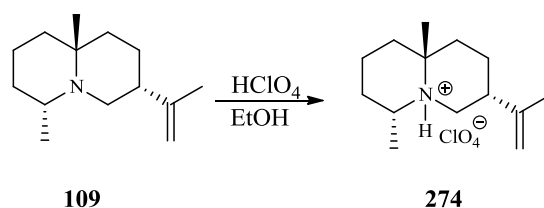
Scheme 3.14: *Formation of perchlorate salt 274 (carried out by Dr. Juan. A. Faraldos)*
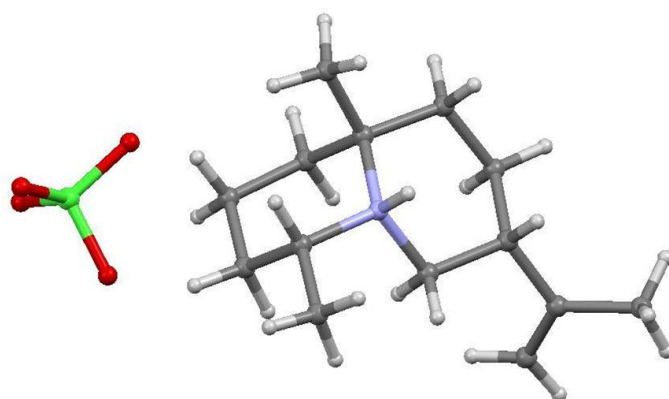
Figure 3.8: *Ball and stick representation of the X-ray crystal structure of the perchlorate salt 274 (solved by Dr. Benson Kariuki)*

All possible isomeric monomethylated quinolizidines have been subjected to a thorough investigation, and are known to exist predominantly in the trans-fused configuration, except for 4-methyl quinolizidine (Figure 3.9).[93] Thus, all the compounds, with the exception of 4-methyl quinolizidine showed Bohlmann bands. However, another study[150] has shown that 4-methylquinolizidine exists in a predominantly trans-fused ring conformation at room temperature as indicated by an IR band at 2850 cm^{-1}, which is probably a trans band. Therefore, the Bohlmann criterion must be used with caution when dealing with 4-substituted quinolizidines such as **108** and **109**.

1-methylquinolizidine   2-methylquinolizidine   3-methylquinolizidine   4-methylquinolizidne
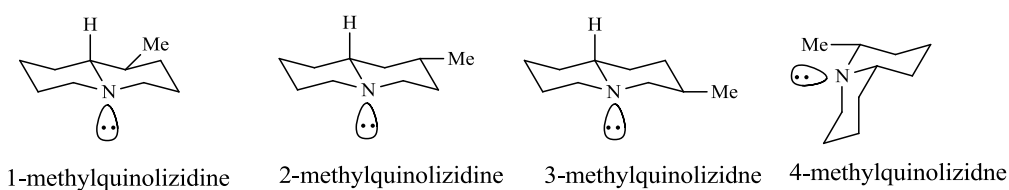
Figure 3.9: *Conformations of 1-, 2-, 3- and 4-methylquinolizidines*

The chemical shift of the methyl doublet and the apparent coupling constant are an excellent indication of the equatorial or axial orientation of the methyl group in monomethyl quinolizidines. It is known that the axial methyl group resonates at lower field[151] and shows a larger J coupling than its corresponding epimer.[151] Thus, the chemical shift and coupling constant of the CH_3CH doublet at C4 for isomer **109** are greater than the isomer **108** (Figure 3.10). Hence, the C4-methyl in amine **109** must be axial. The synthetic sequence leading to the bicyclic amines **108** and **109** is outlined in (Scheme 3.15).

108   **109**

δ 0.97 (3H, d, $J_{\text{CH-Me}}$ 6.0 Hz, CH_3CH) δ 1.00 (3H, d, $J_{\text{CH-Me}}$ 7.0 Hz, CH_3CH)
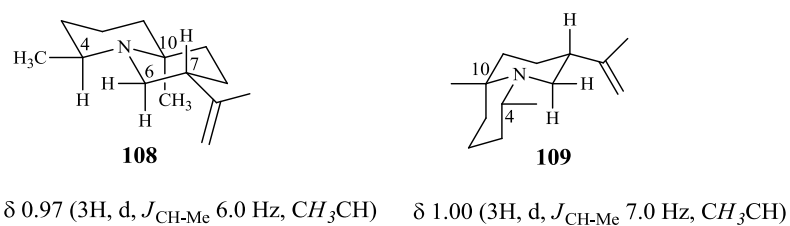
Figure 3.10: *Comparison of coupling constant of CH$_3$CH doublets between distereoisomers* **108** *and* **109**
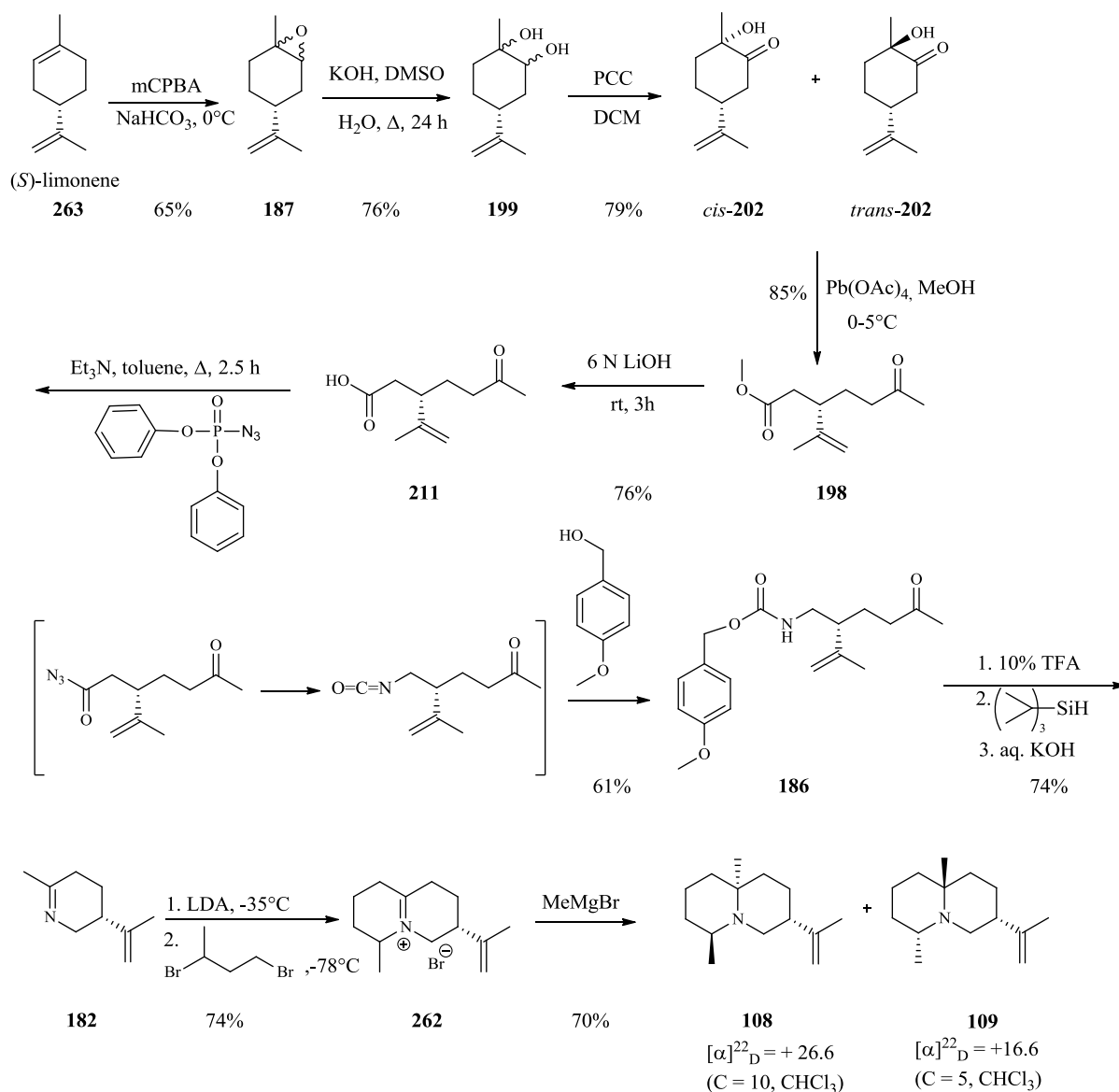
Scheme 3.15: *Stereoselective synthesis of trans-fused-quinolizidine **108** and cis-fused-quinolizidine **109***

3.6 Crystal structure of AT-AS complexed with amino cation 275

Tertiary amino cation **275** partially mimics the possible 5-eudesmane cation intermediate (**69**) (Figure 3.11) that would be formed in a stepwise mechanism, in which 4-eudesmane cation (**69**) undergoes a 1,2-hydride shift to form a tertiary carbocation at the ring-junction carbon. However, compound **275** is an imperfect mimic, due to incorrect stereochemistry

at the C5 atom (*R* instead of *S)*, the protonated amino nitrogen is sp^3-hybridized rather than sp^2-hydridized and the analogue adopts a configuration identical to that of cis-decalin. In spite of these facts, the co-crystal structure of AT-AS-**275** complex (solved by the group of Prof David W. Christianson, University of Pennsylvania, Figure 3.12 b)[140] showed that the tertiary amino cation **275** binds at the active site of AT-AS. The simulated annealing omit map of the AT-AS-**275** complex revealed that the isopropylidine group is nestled within the cavity formed by the side chains of Y61, F81, and W302. The distances between the aza analogue **275** and aromatic amino acids Y61, F81 and W302 are 3.2, 3.5 and 5.9 Å respectively.[140] Although the conformations of surrounding residues are almost identical to those observed in previous structures (Figures 2.30 and 2.31), F81 moves slightly toward the bottom of the cleft to accommodate **275**. In addition, the C8 methylene group is oriented toward the PPi anion.[140] This suggests that the PPi anion could be acting as a general base for the stereospecific deprotonation of the H-8si atom in the cyclisation cascade leading to (+)-aristolochene formation as shown in Scheme 1.10.
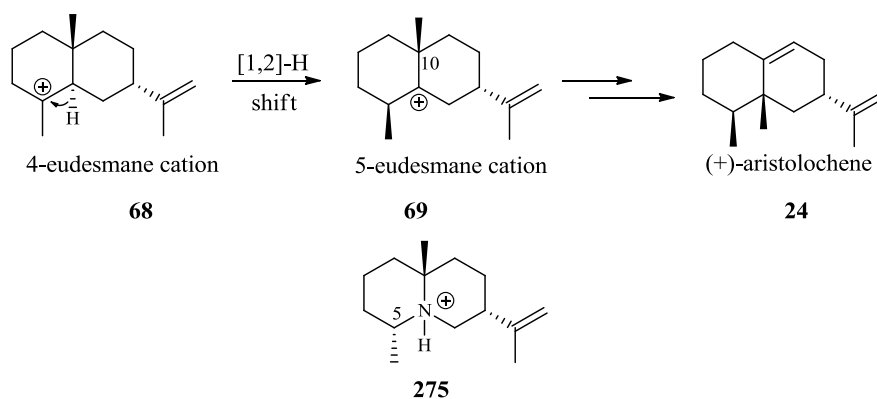
Figure 3.11: *Stepwise mechanism in AT-AS biosynthesis*
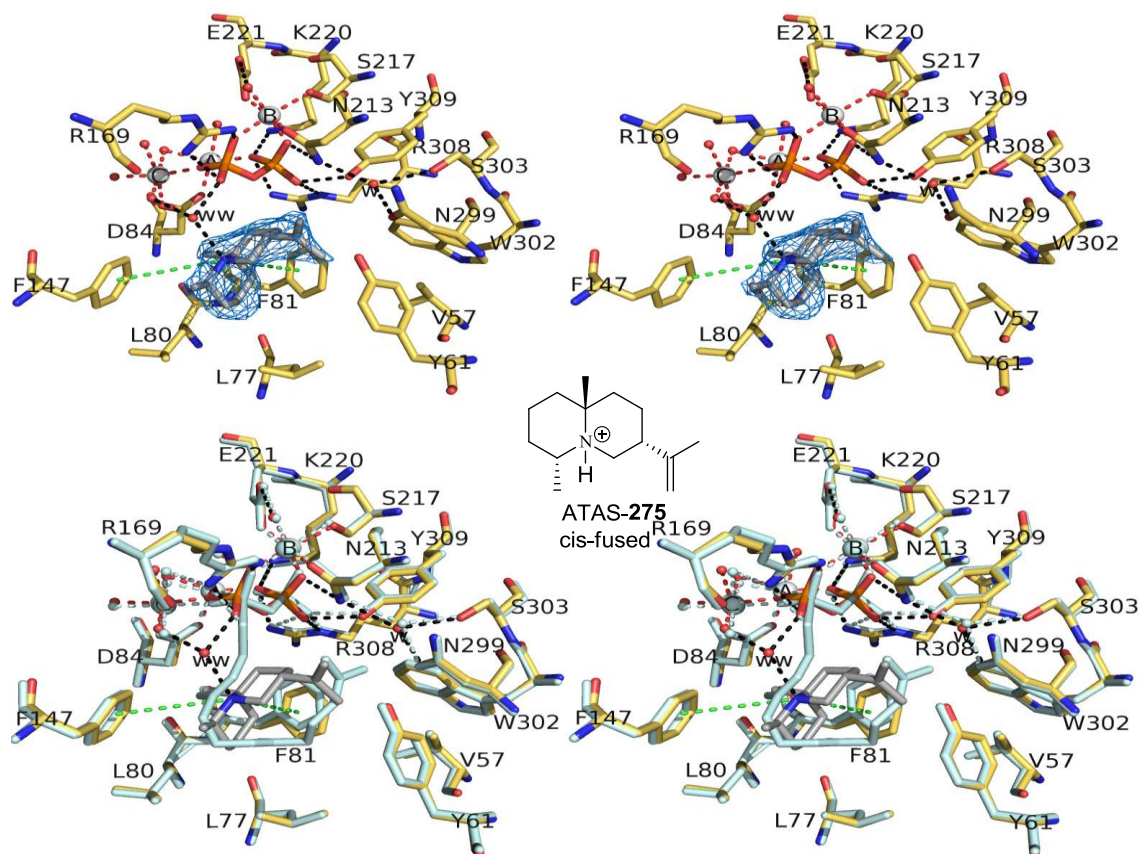
Figure 3.12: *Active site of AT-AS complexed with Mg²⁺-PPi and tertiary amino cation **275**. (a) Simulated annealing omit map of **275** bound to monomer A in the AT-AS-**275** complex. Analogue **275** is shown in grey, and atoms are shown in the following colours: C = yellow (protein), O = red, N = blue, P = orange, S = yellow, Mg²⁺ ions = silver spheres, solvent molecules = red spheres. Water molecule "w" is trapped in the active site along with **275**. (b) Superposition of the AT-AS-**275** complex with the AT-AS-FSDP complex.[140] This structure was solved by the group of Prof. David W. Christianson, University of Pennsylvania.*

3.7 Polonovski-Potier reaction of isomers 108 and 109

Treatment of a tertiary N-oxide **276** with an activating agent such as acetic anhydride, results in rearrangement where an *N,N*-disubstituted acetamide **277** and an aldehyde **278** are generated (Scheme 3.16). The central features of the Polonovski reaction are the transformation of an N-oxide to an iminum ion intermediate **279**. The reaction will either stop at this stage and the iminium ion becomes the Polonovski product, or HOAc elimination proceeds to afford an enamine.[152]
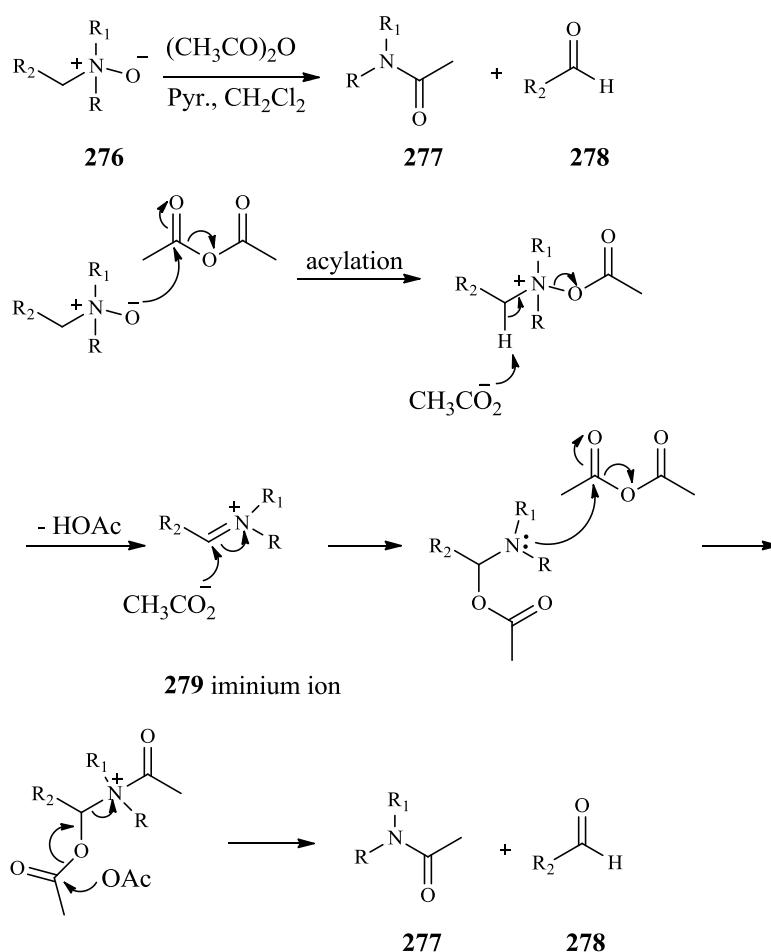
Scheme 3.16: *General scheme of Polonovski reaction of N-oxide 276*

In the first step of the Polonovski reaction, a tertiary amine is oxidized through the interaction of the pair of electrons on nitrogen with electrophile X, followed by elimination of HX to generate an iminium ion. Considering the rich chemistry and versatility of iminium

ions, many uses of this ion have been applied especially in the stereoselective synthesis of quionolizidines alkaloids.

The Polonovski-Potier reaction was applied to both diastereomeric isomers **108** and **109**, as a plausible means for the stereoselective synthesis of desired amine **266** (Figure 3.13).
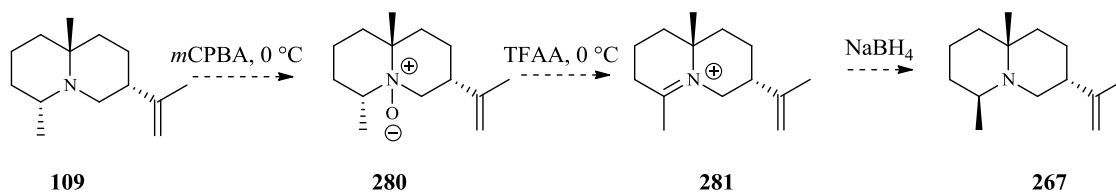
Figure 3.13: *Polonovski-Potier inversion of isomer **109***

3.7.1 Anti Polonovski-Potier inversion of bicyclic *trans*-fused quinolizidine 108

The *trans*-quinolizidine-N-oxide **282** was easily obtained by treating quinolizidine **108** with *m*-CPBA and K_2CO_3 in DCM at 0 °C for 2h (Scheme 3.17). The crude product was purified by basic alumina-column chromatography to give N-oxide **282** in 76% yield.[92,153]
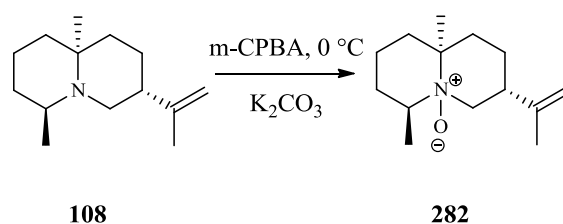
Scheme 3.17: *Synthesis of trans-fused-quinolizidine-N-oxide **282***

^{1}H-NMR, ^{13}C-NMR, DEPT and HSQC spectroscopic analyses of **282** were used to determine the structure of this compound. The signals of the ^{1}H- and ^{13}C-NMR spectra were shifted downfield when compared to those of the free amine, due to the deshielding effect of the N-O group. The IR spectrum of the N-oxide displayed characteristic Bohlmann bands at 2735-2822 cm^{-1}.

The ^{1}H-NMR spectrum of amine-N-oxide **282** revealed signals at δ 3.77 of C*H*N-O, 3.41 owing to HC*H*N, 3.18 of *H*CHN, 1.19 of CH$_3$CHN, these values were in a good agreement with those previously reported for cermizine C N-oxide (**283**) (Figure 3.14) at δ 3.63, 3.36, 3.07 and 1.24 arising from C*H*N-O, HC*H*N, *H*CHN and CH$_3$CHN, respectively.[92]

trans-fused quinolizidine-N-oxide

282

cis-fused cermizine C N-oxide

283
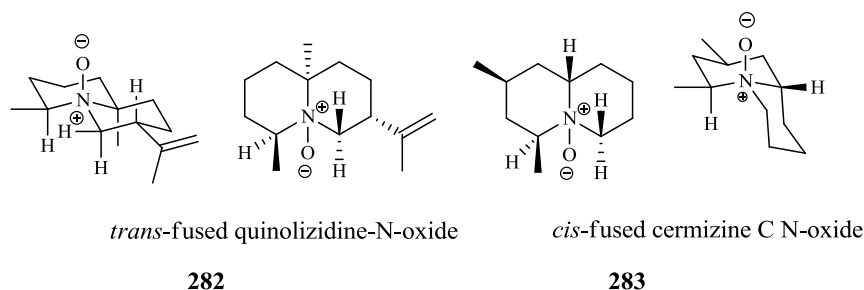
Figure 3.14*: Structures of trans-quinolizidine-N-oxide **282** and cermizine C N-oxide (**283**)*

The relative stereochemistry of isomer **282** was determined by NOESY experiments. The NOESY spectrum of amine-N-oxide **282** showed cross-peaks between the C*H$_3$* singlet at 1.42 ppm in one-dimension and the axial proton of CH$_2$N at 2.82 ppm in the other dimension (Figure 3.15). A cross-peak between the CH$_3$ singlet and CHN also occurred and another correlation was observed between the C*H$_3$* doublet at 1.19 ppm and both C*H* on C7 and the equatorial proton of CH$_2$N at 3.18 ppm.
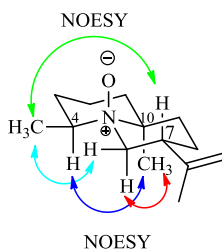
Figure 3.15*: Stereochemistry of amine N-oxide **282***

The next step in this inversion protocol was the generation of an iminium ion. Amine-N-oxide **282** was treated with trifluoroacetic anhydride (TFAA) in DCM at 0 °C for 4h followed by room temperature for 24 h to give iminium ion **112** in 90% yield (Scheme 3.18).[92,153,154] The purity of this compound **112** was sufficiently high to use in the next step without purification. It is worth mentioning that the same result was obtained when freshly distilled acetic anhydride was used instead of TFAA.
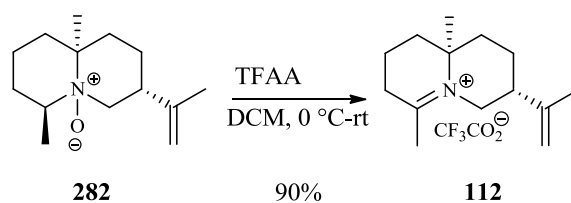
Scheme 3.18: *Synthesis of iminium ion 112*

The ^{1}H-NMR spectrum of iminium ion **112** displayed signals at δ 4.17 (HC*H*N$^+$), 3.51 (*H*CHN$^+$) and 2.44 ppm (C*H$_3$*C=N$^+$), these chemical shifts were in a good agreement with those previously reported for natural (-)-senepodine G (**114**) (Scheme 3.19) at δ 3.96, 3.53 and 2.45 ppm corresponding to HC*H*N$^+$, *H*CHN$^+$ and C*H$_3$*C=N$^+$ respectively.[92]
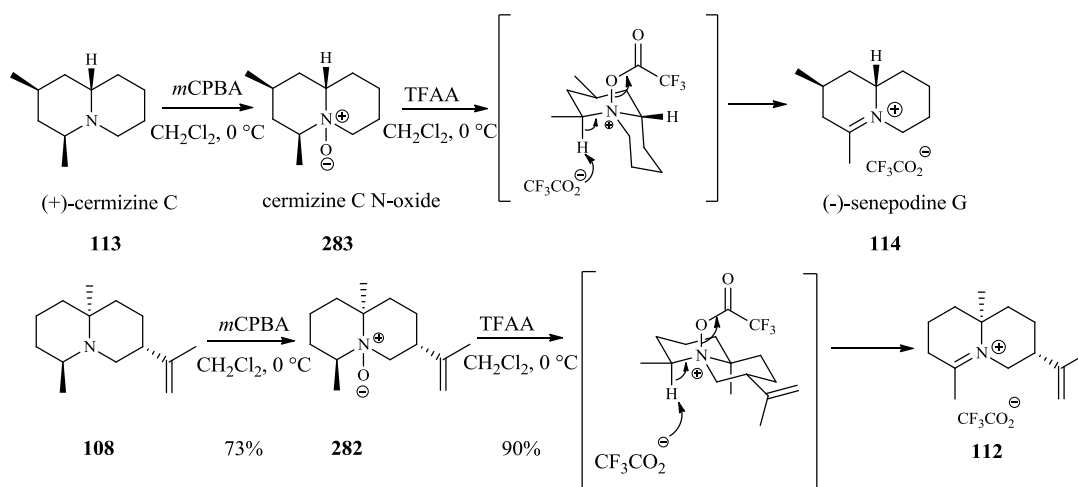
Scheme 3.19: *Synthesis of iminium ion 112 and comparison with (-)-senepodine G (114)*

Reduction of iminium ion **112** with NaBH$_4$ in MeOH at 25 °C for 10 min gave back the free amine **108**. Thus, hydride addition to iminum ion **112** took place stereospecifically by axial attack from the bottom face (Scheme 3.20).[155] The axial attack prevents the formation of the high energy isomer **284**.
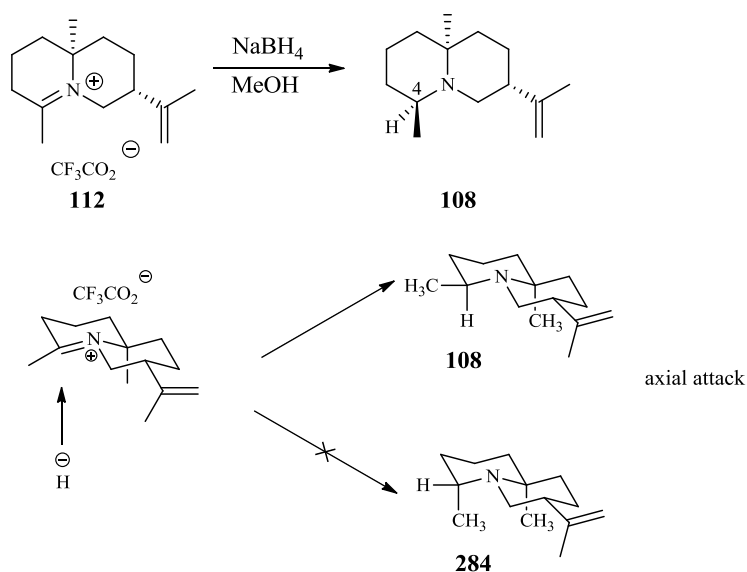
Scheme 3.20: *Reduction of iminium ion **112** with NaBH₄*

Hydride reductions of (-)-senepodine G (**114**) and *epi*-senepodine G (**156**) (Scheme 3.21) have been previously reported by Snider and Grabowski.[155] The reduction of **114** with NaBH₄ afforded (+)-cermizine C (**113**), thus, hydride addition to (-)-senepodine G also occurred by axial attack from the bottom face. Likewise, the reduction of *epi*-senepodine G (**156**) with NaBH₄ took place stereospecifically by axial attack from less hindered top face to give (±)-5-*epi*-cermizine C (**151**).
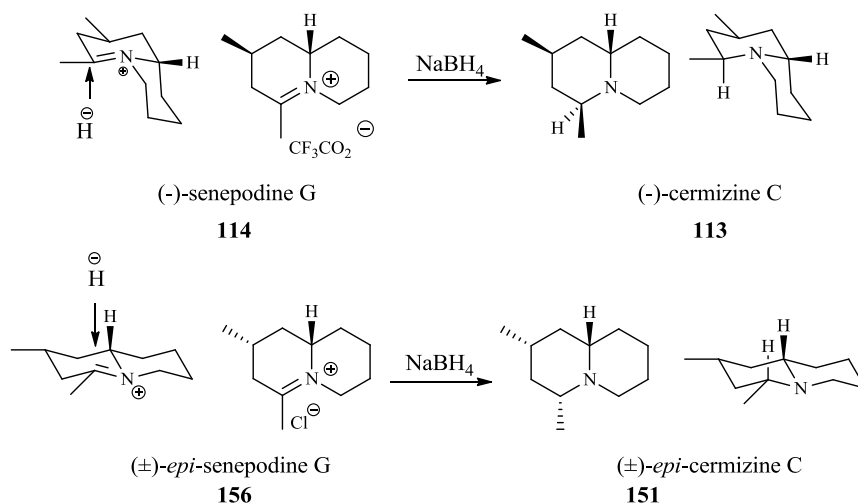
Scheme 3.21: *Stereospecifically addition of hydride to (-)-senepodine G (**114**) and (±)-epi-senepodine G (**156**)*

3.7.2 Anti Polonovski-Potier inversion of quinolizidine 109

cis-Quinolizidines have been reported to react with air to give N-oxide more readily than trans-quinolizidines.[156] Therefore, the *cis*-quinolizidne reacted with mCPBA and K_2CO_3 in DCM at 0 °C for 30 min to give cis-quinolizidine-N-oxide **280**. The crude mixture was purified on basic alumina-column to give pure N-oxide in 85% yield (Scheme 2.22).[92]
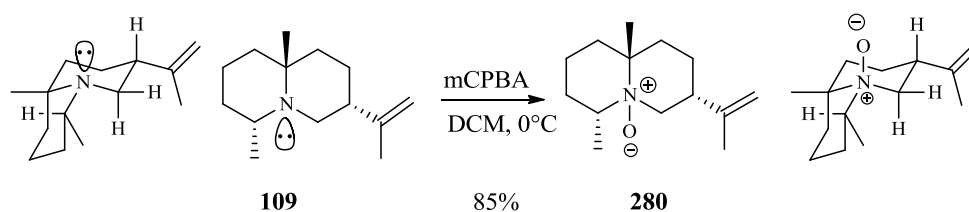
Scheme 3.22: *Synthesis of amine-N-oxide **280***

Generation of the iminium ion from N-oxide **280** was carried out following the same procedure as described for trans-quinolizidine-N-oxide **282**.[92] Reaction of *cis*-N-oxide **280** with TFAA in DCM at 0 °C and then stirring at room temperature for 24 h provided iminium ion **285** instead of iminum ion **281** (Scheme 2.23). The reason for elimination of the proton from C 6 in ring A instead of C 4, as expected was that the only proton situated in an *anti*-position to the N-O bond in N-oxide derivative **280** was on C 6. Iminium ion **285** isomerised to the unexpected conjugated iminum ion **286** when left with TFAA for another 24 h.
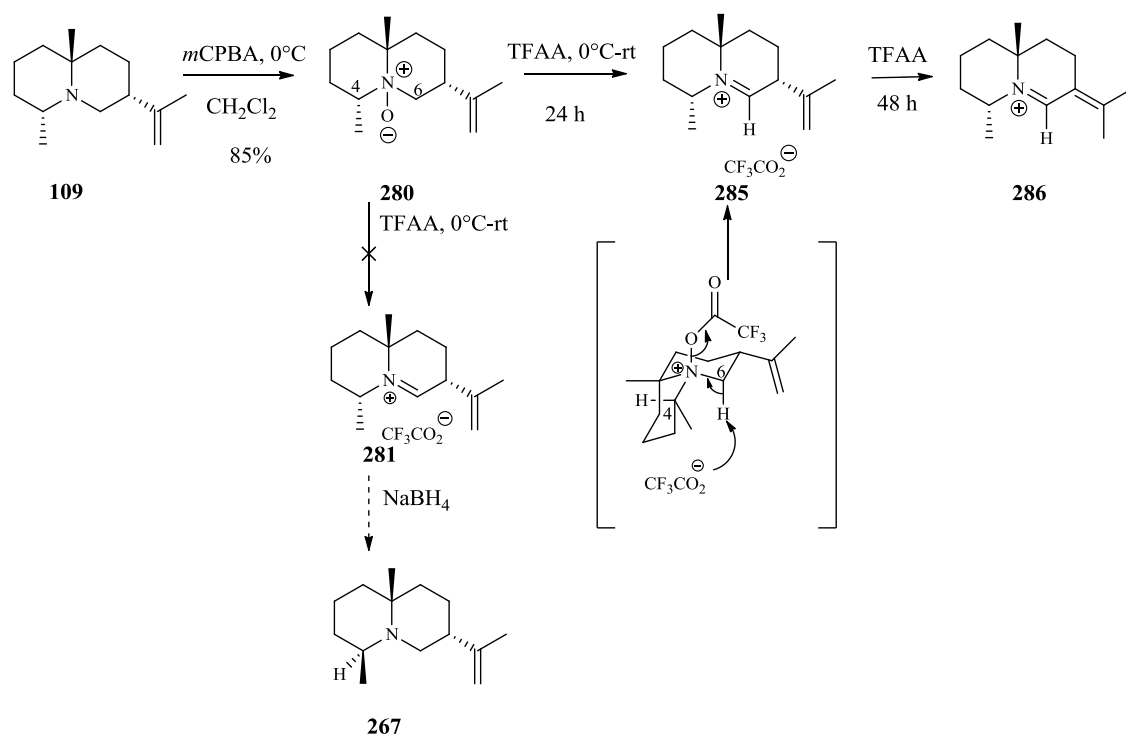
Scheme 3.23: *Conversion of cis-N-oxide **280** to iminum ion **285** and isomerization to unexpected conjugated iminum ion **286***

The ^{1}H-NMR spectrum of iminum ion **285** revealed characteristic a signal in the downfield region at 8.43 ppm owing to proton of CH=N$^+$. The two vinylic protons of CH_2=C of the isopropylidene unit were not observed in the proton NMR spectrum of conjugated iminum ion **286**, showing instead another two signals at 1.45 and 1.46 ppm arising from the two methyl groups attached to the *exo*-methylene double bond [(CH_3)$_2$C=C].

3.8 Stereoselective synthesis of (-)-5-aza-eudesemane cation

epi-Aristolochene synthase from tobacco (TEAS) catalyses conversion of farnesyl diphosphate FDP **5** to 5-*epi*-aristolochene (**287**) (Scheme 2.24). The complex reaction mechanism has been studied by site directed mutagenesis, providing evidence for intermediacy of the neutral hydrocarbon (+)-germacrene A (**288**) and the highly reactive bicyclic (-)-5-aza-eudesmane cation (**290**).[157]
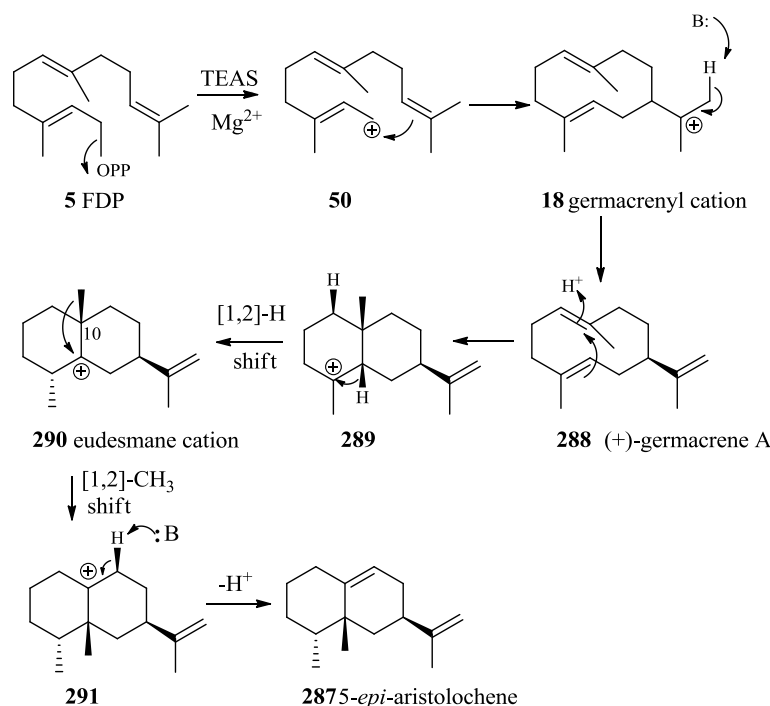
Scheme 3.24: *Biosynthesis of 5-epi-aristolochene (287)*

In order to explore the intermediacy of carbocation intermediate **290**, (-)-5-aza-eudesmane cation (**292**) was designed to mimic the electrostatic and geometric of putative carbocation **290** (Figure 3.16).
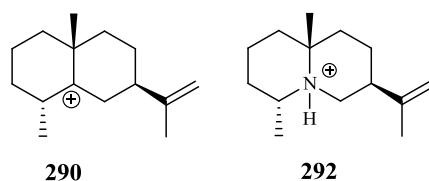
Figure 3.16: *Structures of (-)-5- eudesmane cation (290) and its ananlogue (-)-5-aza-eudesmane cation (292)*

(-)-5-Aza-eudesmane cation (**292**) was synthesized in eight steps following the same sequence of steps used to prepare the isomers **108** and **109**, starting from (*R*)-limonene (**293**). Epoxidation of limonene (**293**) was achieved by reaction of limonene with mCPBA and K_2CO_3 in DCM at 0 °C to produce limonene oxide (**248**) in 63% yield (Scheme 2.25). Hydrolysis of (*R*)-limonene oxide (**248**) with KOH and H_2O in DMSO for 24 h gave diastereomeric diaxial diol **249** in 72% yield. Jones oxidation of diol **249** in acetone at 0 °C afforded keto acid in 69% yield **294**. Treatment of keto acid **294** with diphenylphosphoryl azide and triethylamine in toluene yielded keto acyl azide **295**, that underwent Curtius rearrangement to produce keto isocyanate **296**, followed by addition of p-methoxybenzyl alcohol to give urethane **297** in 60% yield. Deprotection of urethane **297** was carried out by using 10% TFA, and then cyclisation was induced by use of an aqueous solution of KOH to produce cyclic imine **298** in 72% yield.

Kinetic deprotonation of 3*R*-(prop-1-en-2-yl)-6-methyl-2,3,4,5-tetrahydropyridine (**298**) was carried out at -35 °C with LDA, followed by subsequent alkylation with 1,3-dibromobutane to yield iminum ion salt **299** in 57% yield. Introduction of the angular methyl group was achieved by treating iminum ion **304** with methyl magnesium bromide to afford diastereomeric isomers **110** and **111** in 6:4 ratios in 52% as total yield. The synthetic sequence leading to the bicyclic amines **110** and **111** is outlined in (Scheme 3.25). *trans*-Quinolizidine isomer **110** and *cis*-quinolizidine **111** were treated with TFA to produce (-)-5-aza-eudesmane cation **292** in 82% yield and *cis*-quinolizidinum salt **300** in 84% yield respectively (Scheme 3.26).

Although four quinolizidines (**108**-**111**) were prepared in good yields, attempts to synthesise 5-aza-eudesmane cation (**83**) were unsuccessful. Annualation of cyclic imine **182** with 1,3-dibromobutane led to the formation of compounds **108** and **109**. Attempts at the stereospecific synthesis of (*R*)-1,3-dibromobutane were fruitless. Polonovski-Potier inversion of **109** caused loss of the isopropylidene group. Therefore, other methodologies are needed to complete the synthesis of the target compound **83**.
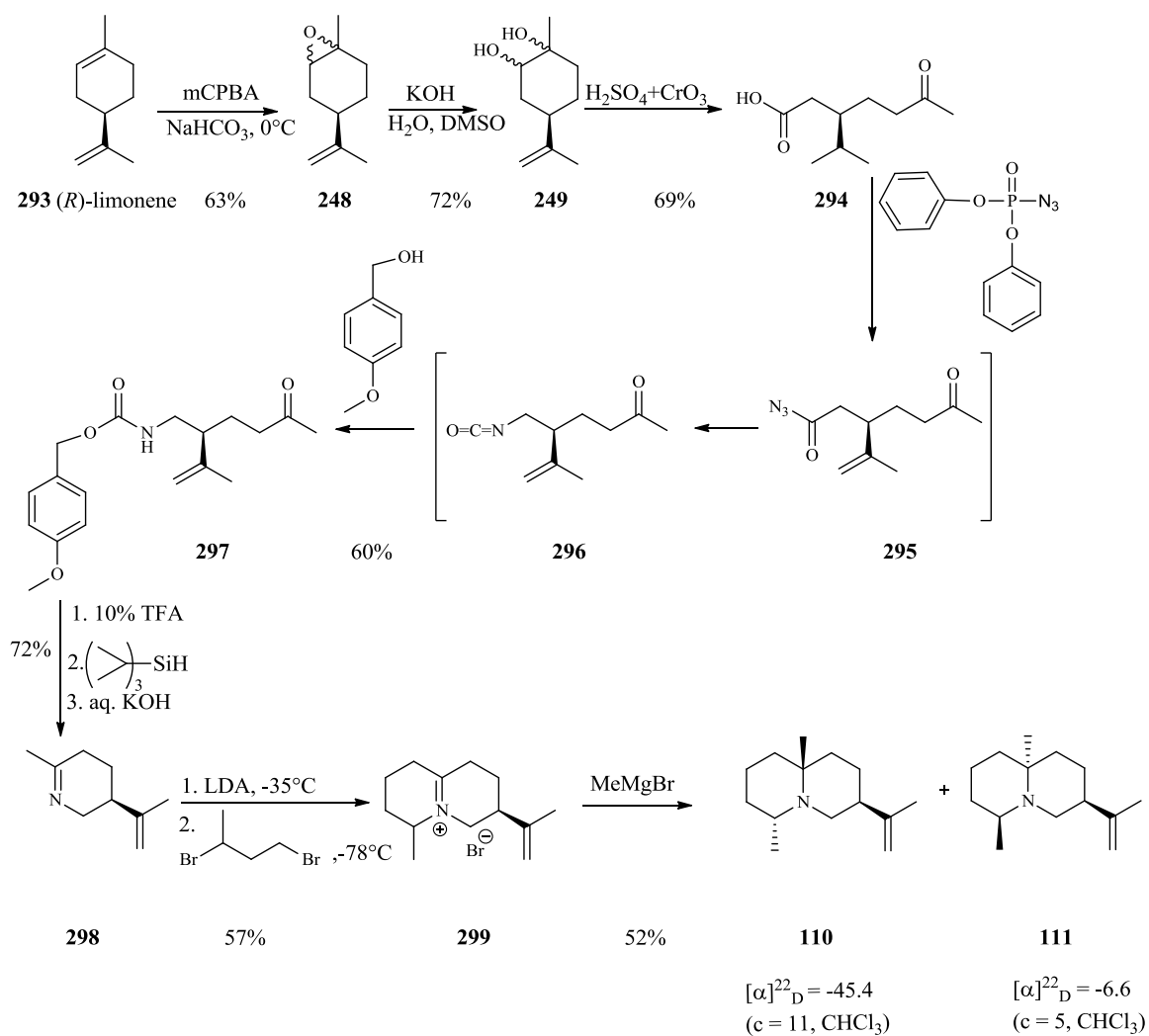
Scheme 3.25: *Stereoselective synthesis of trans-quinolizidine **110** and cis-quinolizidine **111***
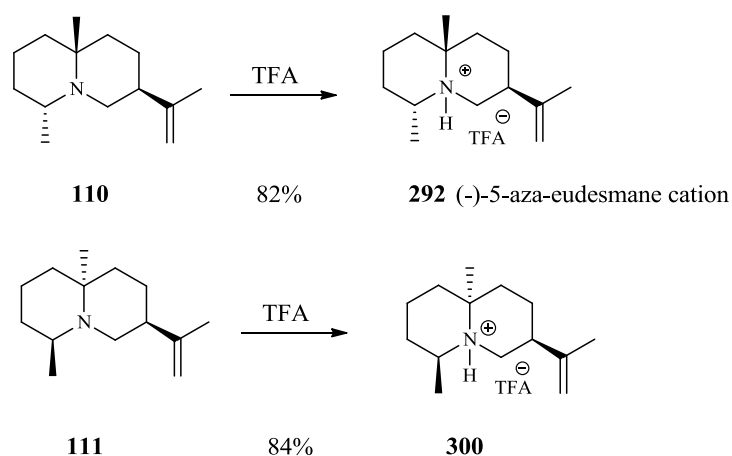
Scheme 3.26: *Preparation of 5-aza-eudesmane cation (**292**) and cis-quinolizidinium salt **300** (carried out by Dr. Juan. A. Faraldos)*

3.9 Another approach to the stereoselective synthesis of 5-aza-eudesmane cation 83

A new synthetic methodology was designed to synthesise 5-aza-eudesmane cation (**83**) with the correct stereochemistry regarding the two methyl groups. Since the introduction of the angular methyl group at C10 into the bicyclic iminium ion **262** in the first strategy was directed by the methyl group at C4, the methyl group at C10 needed to be introduced first, using the monocyclic compound **302** prior to cyclisation to the iminium ion **281** (Scheme 3.27).

This route also started with the kinetic deprotonation of cyclic imine **182**, followed by alkylation with bromo acetal **301** to afford imine acetal **302**. The introduction of a methyl group could potentially require activation of the imine acetal **302**. Cyclisation of secondary amine acetal **303** to Schiff base **281** should be induced with aqueous acid. Reduction of iminium ion **281** with NaBH$_4$ would then generate the desired compound **267**.
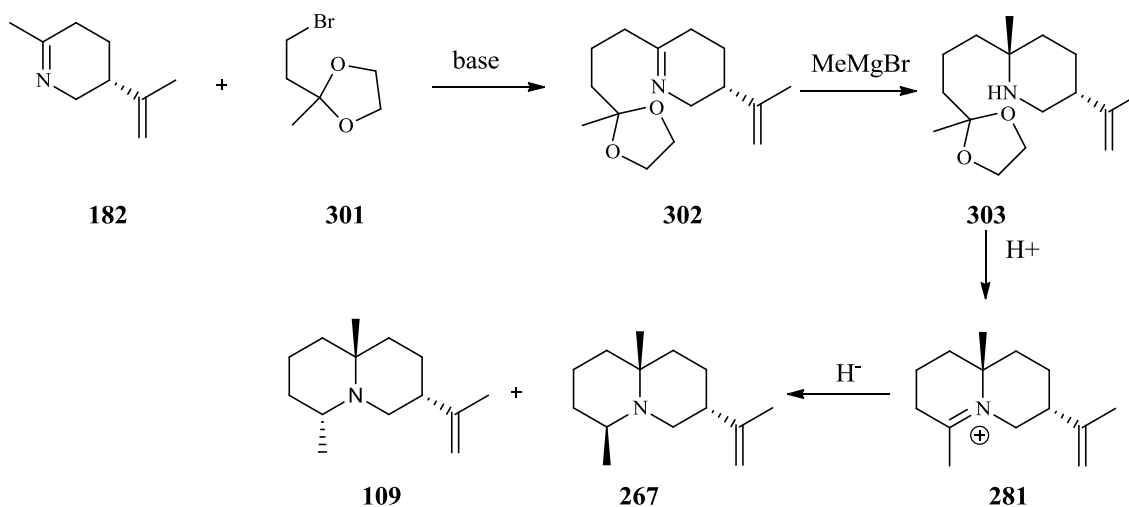
Scheme 3.27: *An alternative approach to the synthesis of bicyclic amine 266*

The kinetic deprotonation of cyclic imine **182** was carried out with LDA at -35 °C for 30 min, followed by alkylation with acetal bromide **301** at -78 °C and stirring at room temperature for 24 h to produce imine acetal **302** in 70% yield after purification of crude mixture on basic alumina-column chromatography (Scheme 3.28).[148]

Attempts to introduce a methyl group without activating imine acetal **302** were unsuccessful. The reaction of imine acetal **302** with methyl magnesium bromide in dry THF, did not give the desired compound **303**, even when the reaction mixture was heated under reflux for 24 h. Imine acetal was activated with anhydrous TFA at room temperature to afford iminum salt **304** (Scheme 3.28).[148] Reaction of iminum salt **304** with methyl magnesium bromide yielded the starting material, due to the reaction of methyl magnesium bromide with C=N$^+$H to produce CH_4 and imine acetal **302**.
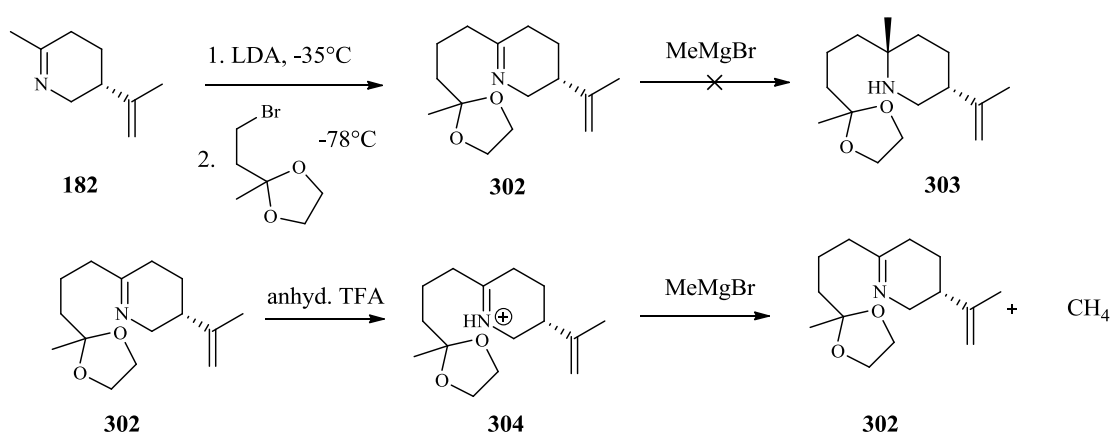
Scheme 3.28: *Synthesis of imine acetal 302 and attempts to introduce methyl group to 302*

A second attempt to activate imine acetal **302** towards the nucleophilic addition with methyl magnesium bromide was developed by oxidation to the nitrone **305** (Scheme 3.29). Nitrone **305** can then undergo reaction with nucleophiles like methyl magnesium bromide to produce α-methyl hydroxylamine **306**. This hydroxylamine **306** can then be converted to the corresponding secondary amine **303** upon treatment with a Lewis acid such as TiCl$_4$ in mixture of water and methanol.
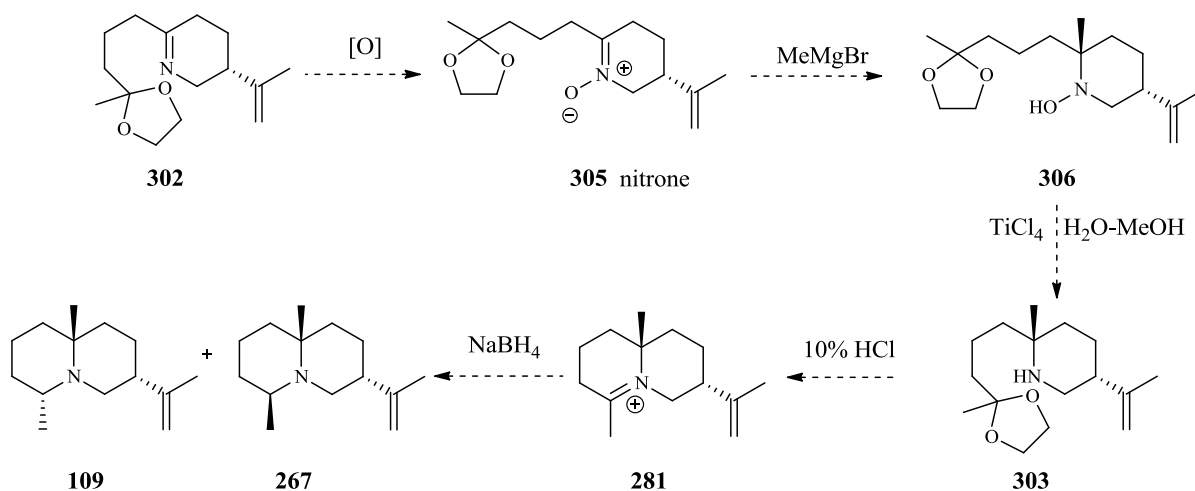
Scheme 3.29: *General strategy to activate imine acetal **302** as nitrone **305** towards addition of methyl magnesium bromide*

Thus, following a published protocol,[158] **302** was treated with a mixture of oxidizing agents, UHP (urea hydrogen peroxide) and a catalytic amount of MTO (methyltrioxorhenium)[158] in dry methanol at room temperature to give a mixture of compounds **307** and **308** instead of the expected nitrone **305** (Scheme 3.30). Although quite a few modifications were tried in efforts to get this reaction to work; such as variation the reaction time and temperature or the use of lower amounts of oxidizing agent, no significant difference in the outcome was observed. The signals of the two protons of the vinylic group in the isopropylidene unit in the proton NMR spectra of two epoxide compounds **307** and **308** disappeared, and two new signals appeared at 1.24 and 2.43 ppm. corresponding to the C*H₃*CO and C*H₂*O groups respectively.
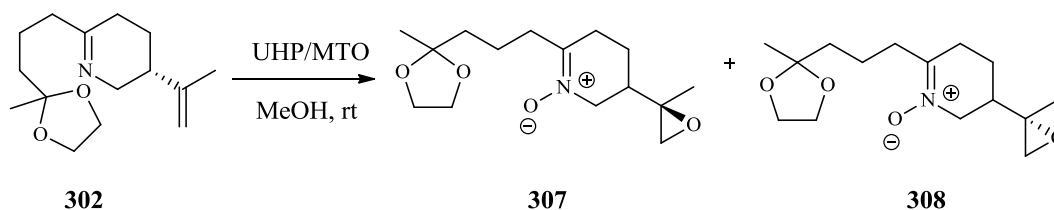
Scheme 3.30: *Epoxidation of vinylic group of imine acetal **302** to epoxides **307** and **308***

3.10 Summary and future work

A variety of quinolizidines analogues were prepared using both published protocols and novel methodologies. The synthesis of tertiary amines **108** and **109** were accomplished in 6 steps, starting from the known keto ester **198**. The syntheses of amine **106** and its mirror image **107** were accomplished in 8 steps, starting also from the keto ester **198** and its mirror image. The two enantiomers of **198** were obtained through degradation of (-)-limonene (**263**) and its mirror image.[77,114,139] The synthesis of **108** and **109** featured a modified Curtius rearrangement[141] that, after acid-promoted cyclisation, gave rise to a 3-alkylated cyclic amine **182**.[143] Cyclic imine **182** was easily converted to the final 3,7,10-alkyl substituted quinolizidines **108** and **109**, essentially as described by De Kimpe.[147] An identical synthetic protocol was repeated from (+)-limonene to give amines **110** and **111**.

Starting from keto ester **198**, the synthesis of **106** was carried out using a Beckmann rearrangement[117] that provided, after cyclisation, the enantiopure lactam **183**. The latter was then converted to the final quinolizidine **106** via a tandem aza-Robinson annulations/Michael alkylation/Wolff-Kishner reduction that installed the *syn* vicinal methyl groups of **106** with excellent stereospecficity.[123,137,138] An identical synthetic protocol was repeated from (+)-limonene to give amine **107**, the enantiomer of quinolizidine **106**. The absolute configuration of amines **106**-**109** was determined using a combination of 1D and 2D NMR experiments and confirmed by X-ray crystal structure determinations of the perchlorate salts of **108**, **109**, **110** and **111**.

In order to probe the transformation of eudesmane cation **68** to (+)-aristolochene (**24**), the three novel aza-analogues, **178**, (7*R*,4*S*,5*S*)-**84** and its mirror image (7*S*,4*R*,5*R*)-**84** were evaluated with aristolochene synthase. The kinetic results revealed that the tertiary amino cation (7*R*,4*S*,5*S*)-**84** acted as a moderate competitive inhibitor (K_i = 38 μM) while the compound (7*S*,4*R*,5*R*)-**84**, which has incorrect stereochemistry, did not act as inhibitor of PR-AS (K_i = 1.03 mM). The data obtained for this compound highlights the chiral environment of the active site of PR-AS. Interestingly, more recent studies have reported X-ray crystal structures of aristolochene synthase from *Aspergillus terreus* (AT-AS) complexed with three Mg^{2+} ions, inorganic diphosphate (PPi), and amino and imino

analogues (7*R*,4*S*,5*S*)-**84**, (7*S*,4*R*,5*R*)-**84** and an analogue **275** of bicyclic carbocation intermediates **69** and **70** proposed in the cyclisation cascade.[140] Surprisingly, the active site of AT-AS was sufficiently flexible to accommodate analogues (7*R*,4*S*,5*S*)-**84**, (7*S*,4*R*,5*R*)-**84** and analogue **275** with partially or completely incorrect stereochemistry. In addition, in each enzyme-inhibitor complex, the cationic amino group is oriented toward the PPi anion, so the binding orientation of each aza analogue appears to be governed by favourable electrostatic interactions.

Chapter three was focused on the design, and progress toward the stereoselective synthesis of 5-aza-eudesmane cation (**83**). This teriary amine **83** is a structural mimic of the 5-eudesmyl carbocation (**69**), a key intermediate in the biosynthesis of AS. However, this tertiary amine was not obtained with desired stereochemistry, namely cis-1,3-dimethyl quinolizidine. Instead, two different diastereoisomers were gained. Although four quinolizidines (**108**-**111**) were prepared in good yields, attempts to synthesise the 5-aza-eudesmane cation (**83**) with the required stereocenters were unsuccessful. Since the 5-eudesmane cation is an important analogue, efforts are still underway to synthesise this compound by other methodologies.

In the near future, work is underway to employ the efficient synthetic methodology described here to prepare libraries of novel multi-substituted quinolizidines and indolizines alkaloids. These will be used as mechanistic probes and protein crystallization aids of sesquiterpene synthases. The results gathered from this demanding approach, in combination with those obtained from site-directed mutagenesis and substrate analogues, will expand our current understanding of the complex chemistry exhibited by terpene synthase and will help in the major goal of designing and preparing terpene synthases of specific artificial activity. Ultimately, this knowledge may be applied to engineering yeast or bacterial organisms for the production of natural and non-natural valuable (sesqui)terpenes.

In addition, the synthetic efforts successfully applied here in the synthesis of aza-analogs (**108**-**111**) from commercial available chiral pools (eg. (*S*)- and (*R*)-limonene), could also be applied in the total synthesis of important natural alkaloids (*Lycopodium* alkaloids) of

commercial, pharmaceutical or medicinal value. At the same time, the future library of unnatural quinolizidine and indolizines alkaloids could be tested for biological activity using different cancer cell lines, or other biomedicinal targets.

CHAPTER FOUR

EXPERIMENTAL

4.1 General experimental

All chemicals were purchased from Sigma-Aldrich unless otherwise stated. Tetrahydrofuran (THF) was distilled from sodium/benzophenone ketyl under nitrogen; diethyl ether was distilled from sodium under nitrogen. Triethylamine, DCM and toluene were distilled from calcium hydride under nitrogen. DBU, Me_2SO_4 and TFAA were distilled under reduced pressure and a nitrogen atmosphere. Acetic anhydride was distilled from quinoline under reduced pressure and nitrogen atmosphere.

^{1}H-NMR spectra were measured on a Bruker Avance 500 MHz spectrometer or or a Bruker Avance DPX 400 NMR spectrometer and are reported as chemical shifts in parts per million (δ scale) downfield from tetramethylsilane (TMS). The following solvents and reference values in ppm were used in obtaining the NMR data: $CDCl_3$ (^{1}H, 7.26, [13]C 77.0), D_2O (^{1}H, 4.79), multiplicity (s = singlet, d = doublet, t = triplet, q = quartet, m = multiplet), coupling constant (to the nearest 0.5 Hz) and assignment respectively. The abbreviation "app" (apparent) in NMR data means that interpretation was based on first-order analysis of the multiplet in question and the data gives the appearance, positions, and spacing of the signals. ^{13}C-NMR spectra were measured on a Bruker Avance 500 MHz spectrometer and are reported as chemical shift downfield from tetramethylsilane, coupling constant where appropriate and assignment. The assignments are made to the limitations of COSY, DEPT 90/135, and gradient HSQC and gradient HMBC spectra. IR spectra were recorded on Perkin ELMER 1600 series FTIR spectrometer, and samples were prepared as thin films of neat liquid on NaCl discs for oils and as KBr disks for solids. EI[+] mass spectra were measured on a Micromass LCT premiere XE mass spectrometer, ES[-] mass spectra were provided by the UK EPSRC mass spectrometry service. The purity of purified compounds was judged to be > 95% by TLC and/or GC analyses and NMR spectroscopic analyses. TLC analyses were performed on plates pre-coated with 250 µM layers of either silica gel 60 F254 or alumina 60 F254. All retention factors (R_f) are on silica gel and alumina TLC plates. TLC visualisations were performed with 5% phosphomolybdic acid, CAM (ceric-ammonium-molybdate), $KMnO_4$, I_2 vapour, or UV light. Optical rotations were measured on a JASCO DIP-370 Digital Polarimeter at rt. Melting points were recorded with a melting apparatus and are quoted uncorrected.

4.2 Experimental

(1*S*,8*S*,9a*R*)-1,9a-Dimethyl-8-(prop-1-en-2-yl)decahydroquinolizin-5-ium2,2,2-trifluoroacetate (84)
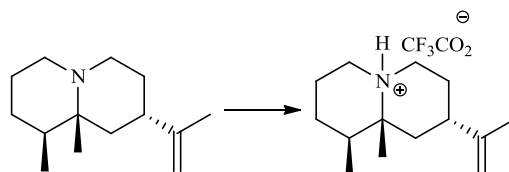
To a solution of the free amine **106** (20 mg, 0.09 mmol) in dry DCM (2 mL) was added TFA (8 μL, 0.09 mmol). After 15 min, the solvent was evaporated under reduced pressure, and the residue was purified by column chromatography on alumina (ethyl acetate-methanol, 15%, R_f 0.15) to give pure TFA salt **84** as yellow oil (28 mg, 90%): IR (thin film) cm^{-1} 3050 (m) (CH, stretch), 2670-2795 (s) (CH, stretch), 1660 (m) (C=C, stretch); ^{1}H-NMR (500 MHz, CDCl$_3$) δ_H 0.85-.86 (3H, d, *J* = 6.5 Hz, C*H*$_3$CH), 1.19 (3H, s, C*H*$_3$C), 1.18-1.29 (2H, m, C*H*$_2$), 1.36-1.41 (1H, m, C*H*CH$_3$), 1.52-1.63 (2H, m, C*H*$_2$CCH$_3$), 1.50-1.74 (4H, m, C*H*$_2$CH$_2$N, C*H*$_2$CH$_2$N), 1.65 (3H, s, C*H*$_3$C=C), 2.02-2.15 (1H, m, C*H*), 2.71-2.86 (2H, ddd, J = 7.5, 6.0, 5.5 Hz, C*H*$_2$N), 3.20-3.36 (2H, m, C*H*$_2$N), 4.69 (1H, s, C*H*$_a$H=C), 4.73 (1H, s, CH*H*$_b$=C), 9.28 (1H, broad s, NH); ^{13}C-NMR (125 MHz, CDCl$_3$) δ_C 9.8 (*C*H$_3$C), 15.6 (*C*H$_3$CH), 20.0 (*C*H$_3$C=C), 22.4 (*C*H$_2$CCH$_3$), 26.6 (*C*H$_2$CCH$_3$), 27.8 (*C*H$_2$CH$_2$N), 36.9 (*C*H$_2$CH$_2$N), 39.3 (*C*H), 39.4 (*C*HCH$_3$), 49.6 (*C*H$_2$N), 49.7 (*C*H$_2$N), 64.8 (*C*CH3), 111.0 (*C*H$_2$=C), 114.8-117.1 (q, *J* = 285 Hz, *C*F$_3$), 146.2 (*C*H$_2$=C), 161.0-161.3 (q, *J* = 39.0 H$_z$, *C*OO); HRMS(EI$^+$) found 208.2065, C$_{14}$H$_{26}$N requires 208.2065.

(1*S*,9a*R*)-1,9a-Dimethyloctahydro-1H-quinolizine (105)
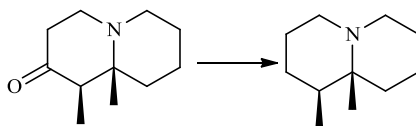
A stream of nitrogen was bubbled through a solution of amino ketone **223** (100 mg, 0.55 mmol), potassium hydroxide (129 mg, 1.7 mmol), diethylene glycol (1 mL), 85% hydrazine hydrate (0.2 mL, 1.7 mmol) and absolute ethanol (3 mL). The mixture was heated under reflux at (160-165 °C) for 3 h. The temperature was increased to 180 °C to distill off water

and excess hydrazine hydrate, and the residue was then heated under reflux for 4 hrs. After cooling, the mixture was poured into water (20 mL) and extracted with Et_2O (3 x 5 mL). The resulting ethereal layers were washed with 10% HCl (5 mL). The separated aqueous layer was adjusted to pH 12 with NaOH (pellets), and extracted with Et_2O (3× 10 mL). The combined ethereal layers were dried (K_2CO_3) and filtered, and the solvent was removed under reduced pressure. The residue was purified by column chromatography on alumina (hexane-ethyl acetate, 1:1, R_f 0.15) to give free amine **105** as pale yellow (68 mg, 74%): IR (NaCl) cm^{-1} 3050 (m) (CH, stretch), 2790-2927 (s) (stretch C-H), 1260 (m) (CN, stretch); ^{1}H-NMR (400 MHz, $CDCl_3$) δ_H 0.72-0.73 (3H, d, *J*= 7.0 Hz, C*H$_3$*CH), 0.76 (3H, s, C*H$_3$*C), 1.32-1.43 [1H, m, C*H*(CH$_3$)], 1.18-1.67 [10H, m, (CH$_2$)$_5$], 2.34-2.43 [4H, m, (CH$_2$)$_2$N]; ^{13}C-NMR (100 MHz, $CDCl_3$) δ_C 4.3 (*C*H$_3$C), 15.1 (*C*H$_3$CH), 19.4 [*C*H$_2$C(CH$_3$)], 24.8 [(*C*H$_2$CH$_2$C(CH$_3$)], 25.3 [*C*H$_2$CH(CH$_3$)], 28.3 (*C*H$_2$CH$_2$N), 36.7 (*C*H$_2$CH$_2$N), 41.1 (CH$_3$*C*H), 48.9 (*C*H$_2$N), 49.1 (*C*H$_2$N), 55.6 (CH$_3$*C*); HRMS(EI$^+$) found 167.1672, $C_{11}H_{21}N$ requires 167.1674.

(1*S*,8*S*,9a*R*)-1,9a-Dimethyl-8-(prop-1-en-2-yl)octahydro-1H-quinolizine (106)
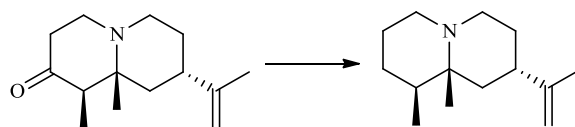
A stream of nitrogen was bubbled through a solution of amino ketone **197** (100 mg, o.45 mmol), potassium hydroxide (129 mg, 1.35 mmol), diethylene glycol (1 mL), 85% hydrazine hydrate (0.2 mL, 1.35 mmol) and absolute ethanol (3 mL). The mixture was heated under reflux at (160-165 °C) for 3 h. The temperature was increased to 180 °C to distill off the water and excess hydrazine hydrate, and the residue was heated under reflux for another 3h. After cooling, the mixture was poured into water (20 mL) and extracted with Et_2O (3 x 10 mL). To the pooled ethereal layers was added 10% HCl (5 mL) and the two phases were separated. The aqueous phase was adjusted to pH 12 with NaOH (pellets) and extracted with Et_2O (5 x 10 mL). The combined ethereal layers were dried (K_2CO_3) then filtered and the solvent was removed under reduced pressure. The crude was purified by chromatography on basic alumina (hexane-diethyl ether, 10%, R_f 0.22) to afford the final free amine **106** as colourless oil (65 mg, 74%): IR(thin film) (NaCl) cm^{-1} 3040 (m) (CH, stretch), 2700-2825 (s) (CH, stretch), 1640 (m) (C=C, stretch); ^{1}H-NMR (500 MHz, $CDCl_3$) δ_H

0.73 (3H, d, J = 6.5 Hz, CH_3CH), 0.77 (3H, s, CH_3C), 1.18-1.29 (2H, m, CH_2CHCH$_3$), 1.36-1.41 (1H, m, CHCH$_3$), 1.51-1.62 (2H, CH_2CCH$_3$), 1.50-1.74 (4H, m, CH_2CH$_2$N, CH_2CH$_2$N), 1.65 (3H, s, CH_3C=C), 2.02-2.15 (1H, CH), 2.31-2.40 (2H, ddd, J = 7.5, 6.5, 5.0 Hz, CH_2N), 2.52-2.55 (2H, m, CH_2N), 4.60 (1H, s, CH_aH=C), 4.65 (1H, s, CHH_b=C); ^{13}C-NMR (125 MHz, CDCl$_3$) δ_C 5.7 (CH_3C), 16.1 (CH_3CH), 20.6 (CH_3C=C), 22.3 (CH_2CH$_2$CH$_2$N), 25.8 (CH_2CHCH$_3$), 29.0 (CH_2CH$_2$N), 31.2 (CH_2CH$_2$N), 39.0 (CH), 42.9 (CHCH$_3$), 49.7 (CH$_2$N), 49.9 (CH$_2$N), 55.6 (CCH$_3$), 108.6 (CH$_2$=C), 150.0 (CH$_2$=C); HRMS(EI$^+$) found 208.2065, $C_{14}H_{25}N$ requires 208.2066.

(1R,8R,9aS)-1,9a-Dimethyl-8-(prop-1-en-2-yl)octahydro-1H-quinolizine (107)
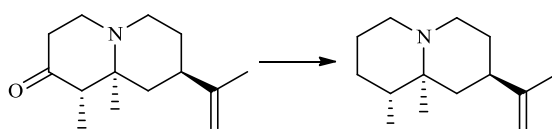
A stream of nitrogen was bubbled through a stirred mixture of amino ketone **259** (100 mg, o.45 mmol), potassium hydroxide (0.129 g, 1.35 mmol), diethylene glycol (1 mL), 85% hydrazine hydrate (0.2 mL, 1.35 mmol) and absolute ethanol (3 mL) . The mixture was heated under reflux at 160-165 °C for 3 h. The temperature was then increased to 180 °C to distill off the water and excess hydrazine hydrate, and the residue was heated under reflux for another 3h. After cooling, the mixture was poured into water and the resulting mixture was extracted with Et$_2$O (3 x 10 mL). To the pooled ethereal extracts was added 10% HCl (5 mL) and extracted and the two phases were separated. The aqueous phase was adjusted to pH 12 with NaOH (pellets) and extracted with Et$_2$O (5 x 10 mL). The combined ethereal extracts were dried (K$_2$CO$_3$) then filtered and the solvent was removed under reduced pressure. The crude product was purified by chromatography on basic alumina (Hexane-diethyl ether, 10%, R$_f$ 0.22) to afford the final free amine **107** as colourless oil (50 mg, 54%); IR(thin film) (NaCl) cm^{-1} 3060 (m) (CH, stretch), 2667-2825 (s) (CH, stretch), 1640 (m) (C=C, stretch); ^{1}H-NMR (500 MHz, CDCl$_3$) δ_H 0.73 (3H, d, J = 6.5 Hz, CH_3CH), 0.77 (3H, s, CH_3C), 1.18-1.29 (2H, m, CH_2CHCH$_3$), 1.36-1.41 (1H, m, CHCH$_3$), 1.51-1.62 (2H, CH_2CCH$_3$), 1.50-1.74 (4H, m, CH_2CH$_2$N, CH_2CH$_2$N), 1.65 (3H, s, CH_3C=C), 2.02-2.15 (1H, CH), 2.31-2.40 (2H, ddd, J = 7.5, 6.5, 5.0 Hz, CH_2N), 2.52-2.55 (2H, m, CH_2N), 4.60 (1H, s, CH_aH=C), 4.65 (1H, s, CHH_b=C); ^{13}C-NMR (125 MHz, CDCl$_3$) δ_C 5.7 (CH_3C), 16.1 (CH_3CH), 20.6 (CH_3C=C), 22.3 (CH_2CH$_2$CH$_2$N), 25.8 (CH_2CHCH$_3$), 29.0 (CH_2CH$_2$N), 31.2 (CH_2CH$_2$N), 39.0 (CH), 42.9 (CHCH$_3$),

49.7 (CH_2N), 49.9 (CH_2N), 55.6 (CCH_3), 108.6 (CH_2=C), 150.0 (CH_2=C); HRMS(EI$^+$) found 208.2065, $C_{14}H_{25}N$ requires 208.2066.

(3*R*,6*S*,9a*S*)-6,9a-Dimethyl-3-(prop-1-en-2-yl)octahydro-1H-quinolizine (108) and

(3*R*,6*R*,9a*R*)-6,9a-Dimethyl-3-(prop-1-en-2-yl)octahydro-1H-quinolizine (109)

108   60: 40   **109**
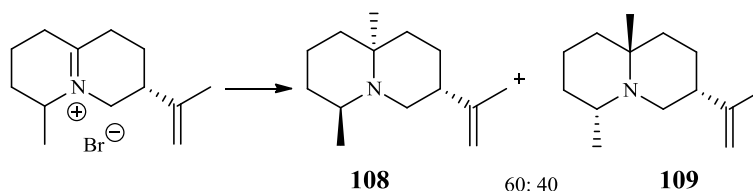
To a stirred solution of dehydroquinolizidinium bromide **262** (450 mg, 2.34 mmol) in dry THF (10 mL) at room temperature under argon was slowly added methylmagnesium bromide (2.5 M in diethyl ether, 2.8 mL, 7.03 mmol). The mixture was then heated under reflux for 24 h and after cooling, a saturated ammonium chloride (10 mL) and 10% NH_4OH (10 mL) were added and extracted with diethyl ether (4 x 10 mL). The combined ethereal extracts were dried over K_2CO_3 then filtered and concentrated under reduced pressure. The residue was purified by column chromatography on alumina (hexane-ethyl acetate, 10%, R_f 0.30) to give *trans*-fused-dimethylquinolizidine **108** as colourless oil (200 mg, 42%); IR (NaCl) cm^{-1} 3010 (m) (CH, stretch), 2750-2876 (m) (CH, stretch), 1660 (m) (C=C, stretch), 1346 (m) and 1241 (m) (C-N stretch); ^{1}H-NMR (400 MHz, CDCl$_3$) δ_H 0.89 (3H, s, CH_3), 0.96-0.97 (3H, d, *J* = 6.5 Hz, CH_3), 1.35-1.55 (10H, m, 5 x CH_2), 1.66 (3H, s, CH_3), 1.91-1.93 (1H, t, *J* = 6.0 Hz, CH), 2.13-2.14 (1H, m, HCHN), 2.35-2.36 (1H, m, HCHN), 2.87-2.90 (1H, dd, *J* = 6.5, 5.5 Hz, CHN), 4.64 (1H, s, CH_aH=C), 4.66 (1H, s, CHH_b=C); ^{13}C-NMR (100MHz, CDCl$_3$) δ 11.0 (CH_3C), 18.2 (CH_3CH), 20.1 (CH_2), 21.3 (CH_2), 25.2 (CH_3C=C), 35.9 (CH_2), 40.4 (CH_2), 40.7 (CH_2) 48.4 (CH), 51.0 (CH_2N), 51.3 (CHN), 53.3 (CN), 109.1 (CH_2=C), 148.6 (CH_2=C); HRMS(EI$^+$) found 207.1283, $C_{14}H_{25}N$ requires 207.1280; [α]$^{22}_D$ = + 26.6 (c = 10, CHCl$_3$).

A second elution with (hexane-ethyl acetate, 20%, R_f 0.23) gave *cis*-fused-dimethylquinolizidine **109** as colourless oil (134 mg, 27%): IR (thin film) cm^{-1} 3080 (m) (CH, stretch), 2925 (m) (CH, stretch), 1660 (m) (C=C, stretch), 1346 (m) and 1241 (m) (C-N, stretch)^{1}H-NMR (400 MHz, CDCl$_3$) δ_H 0.98-1.00 (3H, d, *J* = 7.0 Hz, CH$_3$CH), 1.13 (3H, s, CH_3C), 1.35-1.54 (10H, m, 5 x CH_2), 1.68 (3H, s, CH_3), 2.01-2.05 (1H, m, CH), 2.41-2.45 (1H, t, *J* = 6.5

Hz, *H*CHN), 2.60-2.66 (1H, dd, *J* = 6.0, 5.5 Hz, HC*H*N), 3.13-3.14 (1H, m, C*H*N), 4.70 (1H, s, C*H*aH=C), 4.74 (1H, s, CH*H*b=C); ^{13}C-NMR (100MHz, CDCl$_3$) δ$_C$ 21.3 (*C*H$_3$CH), 21.4 (*C*H$_3$C=C), 21.8 (*C*H$_2$) 23.6 (*C*H$_2$), 25.2 (*C*H$_3$C), 26.0 (*C*H$_2$), 26.8 (*C*H$_2$), 40.8 (*C*H), 44.0 (*C*H$_2$N), 44.7 (*C*H$_2$N), 50.9 (*C*HN), 53.4 (*C*N), 109.5 (*C*H$_2$=C), 148.5 (*C*H$_2$=C); HRMS(EI$^+$) found 207.1283, C$_{14}$H$_{25}$N requires 207.1280; [α]^{22}$_D$ = + 16.6 (c = 5, CHCl$_3$).

(3*S*,6*R*,9a*R*)-6,9a-Dimethyl-3-(prop-1-en-2-yl)octahydro-1H-quinolizine (110) and

(3*S*,6*S*,9a*S*)-6,9a-Dimethyl-3-(prop-1-en-2-yl)octahydro-1H-quinolizine (111)

110   60: 40   **111**
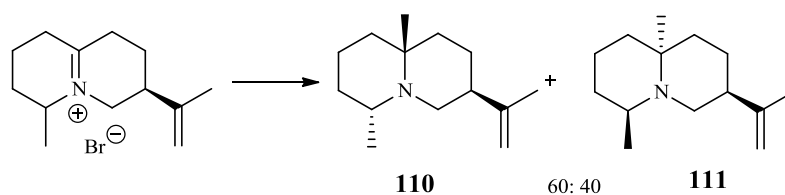
To a stirred solution of quinolizidinium bromide **299** (900 mg, 2.34 mmol) in dry THF (10 ml) at room temperature under argon was slowly added methylmagnesium bromide (2.5 M in diethyl ether, 2.8 mL, 7.03 mmol). The mixture was then heated under reflux for 24 h and after cooling, a saturated ammonium chloride (30 mL) and 10% NH$_4$OH (30 mL) were added and the mixture was extracted with DCM (4 x 10 mL). The combined DCM extracts were dried over K$_2$CO$_3$ then filtered and concentrated under reduced temperature. The residue was purified by column chromatography on alumina (hexane-ethyl acetate, 10%, R$_f$ 0.30) to give *trans*-fused-dimethylquinolizidine **110** as colourless oil (485 mg, 52% yield); IR (NaCl) cm^{-1} 3010 (m) (CH, stretch), 2750-2876 (m) (CH, stretch), 1667 (m) (C=C, stretch); ^{1}H-NMR (400 MHz, CDCl$_3$) δ$_H$ 0.89 (3H, s, C*H$_3$*), 0.96-0.97 (3H, d, *J* = 6.5 Hz, C*H$_3$*), 1.35-1.55 (10H, m, 5C*H$_2$*), 1.66 (3H, s, C*H$_3$*), 1.91-1.93 (1H, t, *J* = 6.0 Hz, C*H*), 2.13-2.14 (1H, m, *H*CHN), 2.35-2.36 (1H, m, HC*H*N), 2.87-2.90 (1H, dd, *J* = 6.5, 5.5 Hz, C*H*N), 4.64 (1H, s, C*H*aH=C), 4.66 (1H, s, CH*H*b=C); ^{13}C-NMR (100MHz, CDCl$_3$) δ 11.0 (*C*H$_3$C), 18.2 (*C*H$_3$CH), 20.1 (*C*H$_2$), 21.3 (*C*H$_2$), 25.2 (*C*H$_3$C=C), 35.9 (*C*H$_2$), 40.4 (*C*H$_2$), 40.7 (*C*H$_2$) 48.4 (*C*H), 51.0 (*C*H$_2$N), 51.3 (*C*HN), 53.3 (*C*N), 109.1 (*C*H$_2$=C), 148.6 (*C*H$_2$=C); HRMS(EI$^+$) found 207.1283 C$_{14}$H$_{25}$N requires 207.1280;

A second elution with (hexane-ethyl acetate, 20%, R$_f$ 0.23) to give *cis*-fused-dimethylquinolizidine **111** as colourless oil (185 mg, 38%): IR (NaCl) cm^{-1} 3030 (m) (CH,

stretch), 2740-2856 (m) (CH, stretch), 1667 (m) (C=C, stretch); ^{1}H-NMR (400 MHz, CDCl$_3$) δ_H 0.98-1.00 (3H, d, J = 7.0 Hz, CH$_3$CH), 1.13 (3H, s, CH_3C), 1.35-1.54 (10H, m, 5CH_2), 1.68 (3H, s, CH_3), 2.01-2.05 (1H, m, CH), 2.41-2.45 (1H, t, J = 6.5 Hz, HCHN), 2.60-2.66 (1H, dd, J = 6.0, 5.5 Hz, HCHN), 3.13-3.14 (1H, m, CHN), 4.70 (1H, s, CH_aH=C), 4.74 (1H, s, CHH_b=C); ^{13}C-NMR (100MHz, CDCl$_3$) δ_C 21.3 (CH$_3$CH), 21.4 (CH$_3$C=C), 21.8 (CH$_2$) 23.6 (CH$_2$), 25.2 (CH$_3$C), 26.0 (CH$_2$), 26.8 (CH$_2$), 40.8 (CH), 44.0 (CH$_2$N), 44.7 (CH$_2$N), 50.9 (CHN), 53.4 (CN), 109.5 (CH$_2$=C), 148.5 (CH$_2$=C); HRMS(EI$^+$) found 207.1283 C$_{14}$H$_{25}$N requires 207.1280; $[\alpha]^{22}_D$ = -6.6 (c = 5, CHCl$_3$).

(1S,9aR)-1,9a-Dimethyldecahydroquinolizin-5-ium 2,2,2-trifluoroacetate (178)
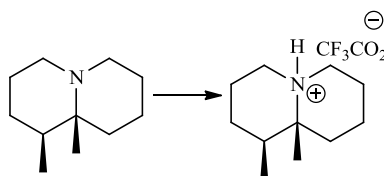
To a solution of free amine **105** (68 mg, 0.4 mmol) in anhydrous DCM (2 mL) was added trifluoroacetic acid (22 µL, 0.4 mmol) at room temperature. After 5 min, solvent was removed under reduced pressure, and the residue was purified by column chromatography on alumina (diethyl ether-methanol, 15%, R$_f$ 0.12) to afford the TFA salt **178** as yellow-orange oil (80 mg, 70%); IR (NaCl) cm^{-1} 3060 (m) (CH, stretch), 2785-2935 (s) (CH, stretch), 1225 (m) (CN, stretch); ^{1}H-NMR (400 MHz, CDCl$_3$) δ_H 0.80-0.81 (3H, d, J = 6.5 Hz, CH_3CH), 1.07 (3H, s, CH_3C), 1.33-1.98 (11H, m, (CH_2)$_5$CH, CH(CH$_3$)), 2.67-2.74 (2H, m, CH_2N), 2.94-3.05 (2H, m, CH_2N), 9.28 (1H, broad s, NH); ^{13}C-NMR (100 MHz, CDCl$_3$) δ_C 15.6 (CH$_3$C), 18.7 (CH$_3$CH), 23.0 [CH$_2$C(CH$_3$)], 23.5 [(CH$_2$CHC(CH$_3$)], 27.0 [CH$_2$CH(CH$_3$)], 27.4 (CH$_2$CH$_2$N), 34.8 (CH$_2$CH$_2$N), 39.0 (CH$_3$CH), 48.9 (CH$_2$N), 49.12 (CH$_2$N), 55.6 (CH$_3$C), 115.7-118.0 (q, $^2J_{CF}$ = 285 HZ, CF$_3$), 162.0-162.3 (q, $^3J_{CF}$ = 38.0 HZ, COO); HRMS(EI$^+$) found 168.1753, C$_{11}$H$_{22}$N requires 168.1752.

(R)-6-Methyl-3-(prop-1-en-2-yl)-2,3,4,5-tetrahydropyridine (182)
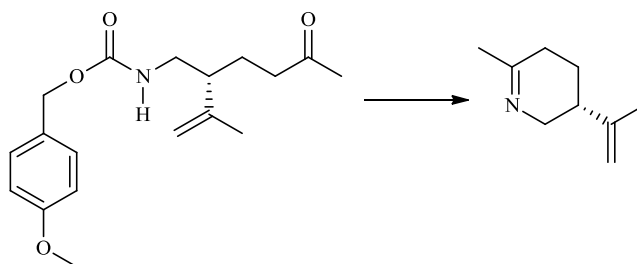
Method 1

To a solution of urethane **186** (200 mg, 0.62 mmol) in benzene (5 mL) was added *p*-toluenesulfonic acid (45 mg, 0.50 mmol), and the reaction mixture was stirred at 65 °C under Dean-Stark condition for 1.5 h. The reaction temperature was cooled to 45 °C and dimethyl sulfoxide (10 mL) was added followed by aqueous 3M NaOH solution (9 mL, 27 mmol). The red reaction mixture was then stirred for 3 h before being cooled to room temperature and diluted with a saturated aqueous solution of ammonium chloride (10 mL). The mixture was extracted with Et_2O (5 x 5 mL). The combined organic layers were washed with brine (4 x10 mL), dried over K_2CO_3 then filtered and concentrated under reduced pressure. The residue was purified on basic alumina column (1: 1 hexane: ether, R_f 0.2) to give cyclic imine **182** as yellow oil (40 mg, 47%).

Method 2:

To a stirred solution of urethane **186** (1.0 g, 3.1 mmol) in DCM (40 mL) was added, dropwise, a solution of TFA (8 mL) in DCM (40 mL) to give a bright orange solution. After 10 min, triisopropylsilane (1.2 mL) was added and stirring was continued for 5 min before ice-water (100 mL) was added. The aqueous phase was washed with DCM (2 x 20 mL) and then adjusted to pH 12 with KOH pellets. The aqueous layer was extracted with DCM (4 x 20 mL). The combined DCM extracts were dried over K_2CO_3 and concentrated under reduced pressure. The crude product was purified by chromatography on basic alumina (hexane-Et_2O, 50%, R_f 0.35) to give cyclic imine **182** as yellow oil (316 mg, 74%); IR (NaCl) cm^{-1} 3060 (m) (CH, stretch), 2975 (s) (CH, stretch), 1616 (m) (C=C, stetch), 1660 (m) (C=C, stretch); ^{1}H-NMR (400 MHz, CDCl$_3$) δ_H 1.42-1.60 (1H, m, HC*H*CH$_2$C=N), 1.65 (3H, s, C*H$_3$*C=C), 1.70-1.81 (1H, m, *H*CHCH$_2$C=N), 1.87 (3H, s, C*H$_3$*C=N), 2.01-2.11 (1H, m, C*H*), 2.15-2.25 (2H, m,

CH_2C=N), 3.10-3.25 (1H, m, HCHN), 3.65-3.78 (1H, m, HCHN), 4.67 (1H, s, CH_aH=C), 4.78 (1H, s, CHH_b=C); ^{13}C-NMR (100MHz, CDCl$_3$) δ_C 20.0 (CH$_3$C=C), 24.4 (CH$_3$C=N), 27.0 (CH$_2$CH$_2$C=N), 30.3 (CH$_2$C=N), 39.7 (CHCH$_2$), 54.1 (CH$_2$N), 110.0 (CH$_2$=C), 147.2 (CH$_2$=C), 167.5 (C=N); HRMS(EI$^+$) found 138.1283, C$_9$H$_{15}$N requires 138.1280.

(S)-4-(Prop-1-en-2-yl)piperidin-2-one (183)
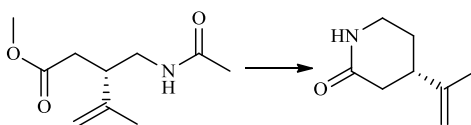
A stirred mixture of acetamide **189** (267 mg, 1.3 mmol) and 3 M sodium hydroxide solution (30 mL, 90 mmol) was heated under reflux for 3 h. After cooling the solution was adjusted to pH 6 with 1M HCl. The resulting mixture was evaporated under reduced pressure to dryness and the residue was heated at 130 °C for 3 h, the solid was extracted with petroleum ether (12 × 25 mL). The combined organic extracts were concentrated under reduced pressure and the residue was purified by chromatography on silica gel (diethyl ether, R$_f$ 0.35) to give the lactam **183** as a white crystalline solid (140 mg, 77%); mp 53-55˚C; IR (NaCl) cm^{-1} 3212 (s) (NH, stretch), 3083 (m) (CH, stretch), 2923 (m) (CH, stretch), 1668 (s) (lactam C=O, stretch), 1645 (s) (C=C, stretch); ^{1}H-NMR (400 MHz, CDCl$_3$) δ_H 1.69 (3H, s, CCH_3), 1.18-1.88 (1H, m, CH), 2.15-2.23 (2H, q, J = 6.0, 5.5 Hz, CHCH_2CH$_2$), 2.37-2.46 (2H, m, CHCH_2CO), 3.27-3.28 (2H, m, CH_2N), 4.68 (1H, s, CH_aH=C), 4.76 (1H, s, CHH_b=C) and 6.38 (1H, br s, NH); ^{13}C-NMR (100 MHz, CDCl$_3$) δ_C 21.0 (CH$_3$C), 27.2 (CH$_2$CHCH$_2$), 36.8 (CH$_2$CHCH$_2$), 39.6 (CH$_2$CO), 41.5 (CH$_2$NH), 110.6 (C=CH$_2$), 146.8 (C=CH$_2$) and 173.0 (C=O lactam); HRMS(EI$^+$) found 139.0996, C$_8$H$_{13}$NO requires 139.0997; $[\alpha]^{22}_D$ = -6.8 (c 3.22, CHCl$_3$).

(*R*)-4-Methoxybenzyl (5-oxo-2-(prop-1-en-2-yl)hexyl)carbamate (186)
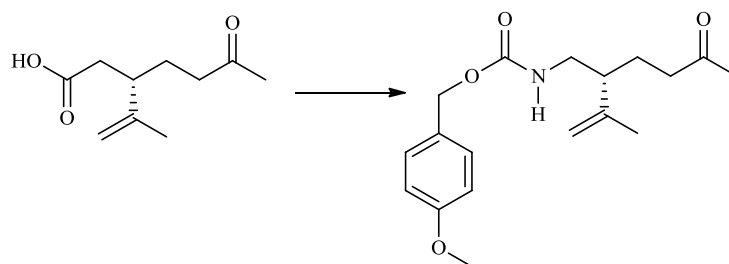
To a stirred solution of keto acid **211** (700 mg, 3.8 mmol) in dry toluene (10 mL) was added Et$_3$N (1.1 mL, 7.98 mmol) followed by diphenylphosphoryl azide (2.55 mL, 11. 8 mmol), with stirring under nitrogen. After stirring for 15 min at room temperature, the solution was heated at reflux for 2.5 h, after which time, the starting material was converted completely to the isocyanate as judged by TLC (eluent hexane-ethyl acetate, 25%, R$_f$ 0.37). *p*-Methoxybenzyl alcohol (0.94 mL, 7.6 mmol) was then added and the resulting mixture was heated under reflux for 24 h. The solvent was evaporated under reduced pressure to give a black oil that was purified by flash chromatography on silica-gel (hexane-ethyl acetate, 25%, Rf 0.28) to give the urethane **186** as a yellow oil (730 mg, 61%); IR (NaCl) cm^{-1} 3120 (m) (NH, urethane, stretch), 2975 (m) (CH, stretch), 1716 (C=O, stretch), 1665 (m) (C=C stretch); ^{1}H-NMR (400 MHz, CDCl$_3$) δ$_H$ 1.52 (3H, s, C*H$_3$*C=C), 2.14 (3H, s, C*H$_3$*C=O), 1.80-2.72 [5H, m, (C*H$_2$*)$_2$C*H*], 2.91-3.10 (1H, m, C*H*NH), 3.20-3.31 (1H, m, *H*CNH), 3.75 (3H, s, OC*H$_3$*), 4.74 (1H, s, CH$_a$H=C), 4.80 (1H, s, CH*H$_b$*=C), 5.25 (2H, s, OC*H$_2$*), 6.85 (2H, d, *J* = 8.5 Hz), 7.27 (2H, d, *J* = 8.5 Hz); ^{13}C-NMR (100 MHz, CDCl$_3$) δ$_C$ 18.2 (*C*H$_3$C=C), 23.9 (*C*H$_3$CO), 30.0 (*C*H$_2$CH), 40.9 (*C*H$_2$CO), 43.1 (*C*H), 46.6 (*C*H$_2$N), 55.2 (O*C*H$_3$), 66.4 (O*C*H$_2$), 113.9 (*C*H$_2$=C), 114.2 (Ar*C*H, Ar*C*H), 128.7 (Ar*C*CH$_2$O), 129.9 (Ar*C*H, Ar*C*H), 144.3 (CH$_2$=*C*), 156.3 (*C*OO), 159.6 (Ar*C*OCH$_3$), 208.3 (*C*=O);HRMS(EI$^+$) found 319.1812, C$_{18}$H$_{25}$NO$_4$ requires 319.1811.

(4S)-Limonene oxide [(4S)-4-isopropyl-1-methyl-7-oxabicyclo[4.1.0]heptane] (187)
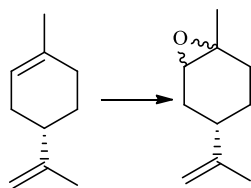
A mixture of (20.5 g, 150 mmol) of (-)-(*S*)-limonene **263** and (25.2 g, 300 mmol) of NaHCO$_3$ in DCM (150 mL) was stirred at 0-5 °C, as a solution of 75% m-CPBA (47.0 g, 150 mmol) in DCM (250 mL) was added over 50 min. The mixture was stirred at 0 °C for 30 min and then a solution of Na$_2$SO$_3$ (10 g) in water (100 mL) was added. The mixture was stirred for 30 min at room temperature and diluted with water (100 mL) before separating the organic fraction. The aqueous layer was extracted with DCM (3 x 100 mL) and the combined organic layers were dried (MgSO$_4$) and concentrated under reduced pressure. The residue was purified by chromatography on silica gel (hexane-ethyl acetate, 5%, R$_f$ 0.40) to give limonene oxide **187** as a colourless oil which was a 60: 40 mixture of two isomers (14.42 g, 63%); IR (thin film) cm^{-1} 3070 (m) (CH, stretch), 2918 (m) (CH, stretch), 1655 (m) (C=C, stretch); ^{1}H-NMR (500 MHz, CDCl$_3$) δ_H 1.23 and 1.25 (3H, s, C*H$_3$*CO), 1.60 and 1.64 (3H, s, C*H$_3$*C=C), 1.43-2.18 (7H, m, 3C*H$_2$*, C*H*), 3.00 and 3.02 (1H, dd, *J* = 6.5 Hz, C*H*O), 4.68 (1H, s, CH$_a$H=C), 4.74 (1H, s, CHH$_b$=C); ^{13}C-NMR (125 MHz, CDCl$_3$) δ_C 17.1 (*C*H$_3$CO), 21.3 (*C*H$_3$C=C), 23.8 (*C*H$_2$CHO), 27.9 (*C*H$_2$CCH$_3$), 28.6 (*C*H$_2$CH), 39.3 (*C*H), 60.3 (CH$_3$*C*O), 63.7 (*C*HO), 110.4 (*C*H$_2$=C), 147.8 (CH$_2$=*C*); HRMS(EI$^+$) found 152.2303, C$_{10}$H$_{16}$O requires 152.2301

(*S*)-Methyl 3-(2-acetamidoethyl)-4-methylpent-4-enoate (189)
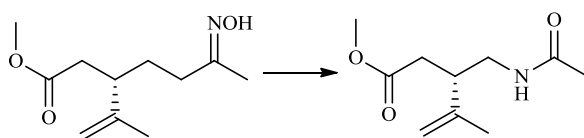
p-Toluene sulfonyl chloride (231 mg, 1.21 mmol) was added in one portion to a solution of freshly prepared oxime **204** (130 mg, 0.61 mmol) in dry benzene (4 mL) and pyridine (2 mL). The mixture was stirred at room temperature in the dark for 7 days. The solvent was removed under reduced pressure and the residue was dissolved in ethyl acetate (50 mL) and washed with 10% hydrochloric acid (10 mL). The organic layer was dried over anhydrous Na$_2$SO$_4$ then filtered and the solvent was removed under reduced pressure. The

residue was purified by chromatography on silica gel (ethyl acetate, R_f 0.18) to give acetamide **189** as a colourless oil (116 mg, 90%); IR (thin film) cm^{-1} 3296 (s) (NH, stretch), 3078 (m) (CH, stretch), 2950 (m) (CH, stretch), 1739 (s) (ester C=O, stretch), 1647 (s) (amide, C=O, stretch), 1558 (s) (C=C, stretch); ^{1}H-NMR (400 MHz, CDCl$_3$) δ_H 1.65 (3H, s, CCH_3), 1.99 (3H, s, COCH_3), 2.35-2.65 (3H, m, CH_2, CH), 3.01-3.25 (2H, m, CH_2NH), 3.65 (3H, s, OCH_3), 4.74 (1H, s, CH$_a$H=C), 4.80 (1H, s, CHH$_b$=C) and 5.56 (1H, br s, NH); ^{13}C-NMR (100 MHz, CDCl$_3$) δ_C 18.6 (CH$_3$C), 23.4 (COCH$_3$), 38.4 (CH), 39.2 (CH$_2$COO), 41.8 (CH$_2$NH), 52.1 (OCH$_3$), 113.3 (C=CH$_2$), 145.7 (C=CH$_2$), 170.7 (C=O amide) and 173.7 (CO ester); HRMS(EI$^+$) found 214.1446, C$_{10}$H$_{20}$NO$_3$ requires 214.1443; $[\alpha]^{22}_D$ = -6.3 (c 2.07, CHCl$_3$).

9-Methyl-3,4,6,7-tetrahydro-1H-quinolizin-8(2H)-one (193)
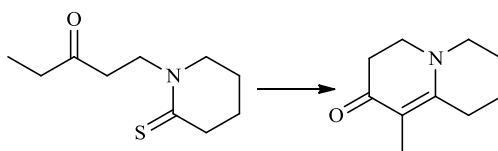
Oxo-thione **222** (2.5 g, 12.6 mmol) was suspended under nitrogen atmosphere in anhydrous toluene (80 mL), and then Me$_2$SO$_4$ (2.1 mL, 21.4 mmol) was added dropwise by a syringe at room temperature and under stirring. After the addition was complete, the flask was placed into an oil bath at 140-150 °C. After refluxing for 15 min, 1,8-diazabicyclo [5.4.0] undec-7ene (DBU) (3.1 mL, 21.4 mmol) was added dropwise by syringe and the resulting solution heated under reflux for a further 20 min. After cooling to room temperature, the solution was diluted with CH$_2$Cl$_2$ (100 mL), and washed with water (100 mL). The organic layer was dried over sodium sulfate, filtered, and concentrated under reduced pressure. The resulting crude oil was purified by flash chromatography on basic alumina (hexane: diethyl ether, 10%, R_f 0.27) to give the enaminone **193** as a yellow oil (1.8 g, 78%); IR (NaCl) cm^{-1} 3060 (m) (CH, stretch), 2946 (s) (CH, stretch), 1711 (s) (ketone C=O, stretch), 1657 (s) (C=C, stretch), 1326 (m) and 1252 (s) (CN, stretch); ^{1}H-NMR (400 MHz, CDCl$_3$) δ_H 1.61 (2H, m, CH$_2$CH_2CH$_2$N), 1.62 (3H, s, C=C-CH_3), 1.70 (2H, m, CH_2), 2.37 (4H, m, CH_2CO, CH_2C=C), 3.12 (2H, t, J = 5.0 Hz, O=CCH_2CH$_2$N) and 3.25 (2H, t, J = 7.0 Hz, CH$_2$CH_2N); ^{13}C-NMR (100 MHz, CDCl$_3$) δ_C 9.4 (C=C-CH$_3$), 19.6 (CH$_2$$CH_2CH_2$N), 22.7 ($CH_2CH_2CH_2$), 26.9 ($CH_2$CO), 35.1 ($CH_2$C=C), 50.3 (CO$CH_2CH_2$N), 50.7 (CH$_2$$CH_2$N), 103.1 (C=$C$-CH$_3$), 160.3 (C$C$=C-CH$_3$) and 188.7 (C=O); HRMS(EI$^+$) found 166.1238, C$_{10}$H$_{15}$NO requires 166.1232.

(_S_)-9-Methyl-2-(prop-1-en-2-yl)-3,4,6,7-tetrahydro-1H-quinolizin-8(2H)-one (194)
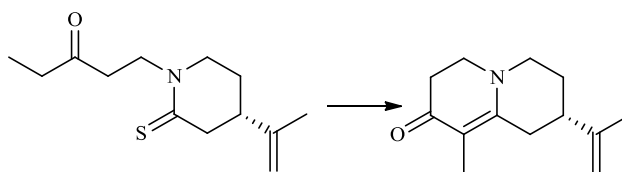
To a stirred suspension of oxo-piperidine-2-thione **244** (500 mg, 2.09 mmol) in anhydrous benzene (10 mL) under nitrogen was added freshly distilled Me_2SO_4 (0.33 mL, 3.55 mmol) drop wise. The mixture was heated under reflux for 30 min, and then 1, 8-diazabicyclo [5.4.0] undec-7-ene (DBU) (0.53 mL, 3.55 mmol) was added drop wise. The resulting solution was heated under reflux for a further 1 h. After cooling to room temperature, the solution was diluted with DCM (100 mL), and washed with water (100 mL). The organic layer was dried over K_2CO_3, filtered and concentrated under reduced pressure. The residue was dissolved in Et_2O (10 mL) and then adjusted to pH 2 with 10% HCl (5 mL) and extracted with Et_2O (3× 10 mL). The aqueous phase was adjusted to pH 12 with NaOH (pellets) and extracted with Et_2O (5 x 10 mL). The combined ethereal layers were dried (K_2CO_3) and filtered, and the solvent was removed under reduced pressure. The crude was purified by chromatography on alumina (hexane: diethyl ether, 10%, R_f 0.35). The by-product **245** eluted first and was isolated as a yellow oil (185 mg, 41%). Further elution (hexane-diethyl ether, 30%, R_f 0.27) gave the bicyclic enone **194** as a colourless oil (221 mg, 54%); IR (thin film) cm^{-1} 3080 (m) (CH, stretch), 2925 (m) (CH, stretch), 1660 (m) (C=C, stretch), 1643 (m) (ketone C=O, stretch), 1346 (m) and 1241 (m) (C-N stretch); ^{1}H-NMR (400 MHz, $CDCl_3$) δ_H 1.52 [3H, s, C=C(CH_3)CO], 1.55 (3H, s, C=CCH_3), 1.81 (1H, m, CH), 2.08 (2H, d, J = 3.5 Hz, CHCH_2C), 2.252 (2H, q, J = 6.0, 5.5 Hz, CHCH_2CH$_2$), 2.52 (2H, m, CH_2CO), 3.02-3.14 (4H, m, CH$_2$CH_2NCH_2), 4.63 (1H, s, CH_aH=C), 4.73 (1H, s, CHH_b=C); ^{13}C-NMR (100MHz, $CDCl_3$) δ_C 9.6 (CH$_2$=CCH$_3$), 20.6 [C=C(CH$_3$)CO], 27.4 (CH$_2$$CHCH_2$), 32.2 (CH$CH_2CH_2$N), 35.1 (CH$CH_2$C), 38.1 (CO$CH_2CH_2$), 50.2 (CO$CH_2$$CH_2$N), 50.6 (CH$_2$$CH_2$N), 103.0 ($CH_2$=C$CH_3$), 110.5 [C=$C$(CH$_3$)CO], 146.9 (C=$CCH_3$), 160.3 [$C$=C(CH$_3$)CO] and 189.0 (CO ketone); HRMS(EI$^+$) found, 206.1540 $C_{13}H_{19}NO$ requires 206.1545; $[\alpha]^{22}_D$ = -9.1 (_c_ 4.6, $CHCl_3$).

Piperidone-2-thione (195)

A mixture of 2-piperidone (**216**) (4 g, 40.3 mmol) and Lawesson's reagent (8.1 g, 20.1 mmol) was suspended in anhydrous toluene (200 mL), then heated under reflux under nitrogen atmosphere for 30 min. The solution was then cooled to room temperature and concentrated under reduced pressure. The residue was purified by flash chromatography on silica gel (eluent DCM-light petroleum ether, 10%, R_f 0.34) providing compound **195** as a pale yellow solid. After recrystillasation with isopropanol, **195** was isolated as white crystals (3.5 g, 88%); mp 110-113 °C; IR (NaCl) cm^{-1} 3186 (s) (NH, stretch), 2948 (m) (CH, stretch), 1265 (s) and 1167 (s) (C=S, stretch); ^{1}H-NMR (400 MHz, CDCl$_3$) δ_H 1.74-1.77 (2H, m, CCH_2CC=S), 1.79-1.84 (2H, m, NCCH_2C), 2.89 (2H, t, J = 6.0 Hz, CH_2C=S), 3.35 (2H, dt, J = 6.0 Hz, CH_2N) and 8.90 (1H, br s, NH); ^{13}C-NMR (100 MHz, CDCl$_3$) δ_C 20.3 (CH$_2$CH$_2$C=S), 20.9 (CCH$_2$N), 39.2 (CH$_2$C=S), 44.2 (CN) and 202.9 (C=S). HRMS(EI$^+$) found 116.0531, C$_5$H$_9$NS requires 116.0534.

(*S*)-4-(Prop-1-en-2-yl)piperidine-2-thione (196)

A mixture of lactam **183** (200 mg, 1.43 mmol) and Lawesson's reagent (250 mg, 0.72 mmol) was suspended in anhydrous toluene (10 mL), and heated under reflux for 1 h under nitrogen. The resulting mixture was cooled to room temp, and then solvent was removed under reduced pressure. The residue was purified by chromatography on slica-gel (DCM: petroleum ether, 2:1, R_f 0.33) to give a yellow powder. Recrystallisation from *i*-PrOH produced analytically pure white needles of thiolactam **196** (170 mg, 77%); mp 93-95 ˚C; IR (NaCl) cm^{-1} 3169 (s) (NH, stretch), 3086 (m) (CH, stretch), 2952 (m) (CH, stretch), 1645 (s) (C=C, stretch), (m) (C=C, stretch), 1258 (m) and 1119 (s) (C=S); ^{1}H-NMR (400 MHz, CDCl$_3$) δ_H 1.65 (3H, s, CH_3C=C), 1.70-1.89 (1H, m, CH), 2.32 (2H, m, CH_2), 2.69 (1H, dd, J = 4.0, 8.0 Hz, HCHC=S), 3.06 (1H, dd, J = 4.5, 8.0 Hz, HCHC=S), 3.27-3.40 (m, 2H, CH_2N), 4.85 (1H, s,

CH$_a$H=C), 4.94 (1H, s, CHH$_b$=C) and 8.85 (1H, br s, NH); ^{13}C-NMR (100 MHz, CDCl$_3$) δ$_C$ 20.2 (CH$_3$C), 26.3 (CH$_2$CHCH$_2$), 38.7 (CHCH$_2$CH$_2$), 41.2 (CH$_2$NH), 45.7 (CH$_2$C=S), 112.8 (C=CH$_2$), 145.7 (C=CH$_2$) and 206.9 (C=S); HRMS(EI$^+$) found 156.0847, C$_8$H$_{13}$NS requires 156.0847; [α]^{22}$_D$ = -3.4 (c 0.62, CHCl$_3$).

(1R,8S,9aR)-1,9a-Dimethyl-8-(prop-1-en-2-yl)hexahydro-1H-quinolizin-2(6H)-one (197)

To a solution of the freshly prepared TFA salt **246** (350 mg, 1.09 mmol) in dry THF (5 mL) was added methylmagnesium bromide (3M in diethyl ether, 1.8 mL, 5.45 mmol) at room temperature under argon. The resulting mixture was heated under reflux for 24 h, and then a solution of NH$_4$Cl (10 mL) and 10% NH$_4$OH (10 mL) were added and extracted with Et$_2$O (8 x 10 mL). The resulting residue was dissolved in Et$_2$O (10 mL) and then adjusted to pH 2 with 10% HCl (5 mL) and extracted with Et$_2$O (3 x 10 mL). The aqueous phase was adjusted to pH 12 with NaOH (pellets) and extracted with Et$_2$O (5 x 10 mL). The combined ethereal layers were dried (K$_2$CO$_3$) then filtered and the solvent was removed under reduced pressure. The crude product was purified by chromatography on alumina (hexane-ethyl acetate; 20%, R$_f$ 0.26) to give amino ketone **197** as pale yellow oil (156 mg, 64%); IR (thin film) cm^{-1} 3050 (m) CH, stretch), (2790-2966 (s) (CH, stretch), 1718 (s) (C=O, stretch), 1600 (m) (C=C, stretch), 1326 (m) and 1252 (s) (CN, stretch); ^{1}H-NMR (500 MHz, CDCl$_3$) δ$_H$ 0.71 (3H, s, CCH$_3$), 0.90 (3H, d, J = 7.0 Hz, CH$_3$CH), 1.12-1.15 [2H, m, C(CH$_3$)CH$_2$CH], 1.17-1.25 (2H, m, CH$_2$CH), 1.50-1.55 (2H, ddd, J = 7.0, 6.5, 5.0 Hz, CH$_2$CO), 1.63 (3H, s, CH$_3$C=C), 1.95-2.01 (1H, m, CH$_2$CHCH$_2$), 2.41-2.50 (1H, dddd, J = 8.0, 7.5, 6.0 Hz, CHCH$_3$), 2.62-2.69 (2H, m, CH$_2$N), 2.80-2.86 (2H, m, CH$_2$N), 4.65 (1H, s, CH$_a$H=C), 4.69 (1H, s, CHH$_b$=C); ^{13}C-NMR (125 MHz, CDCl$_3$) δ$_C$ 14.0 (CH$_3$C), 15.2 (CH$_3$CH), 20.6 (CH$_3$C=C), 31.9 (CH$_2$CH$_2$N), 37.6 (CH$_2$CCH$_3$), 41.2 (CH$_2$CO), 43.3 (CH$_2$CHCH$_2$), 49.7 (CH$_2$N), 50.0 (CH$_2$N), 56.5 (CHCH$_3$), 60.0 (CCH$_3$), 109.1 (CH$_2$=C), 149.1 (CH$_2$=C), 210.6 (C=O); HRMS(EI$^+$) found 221.1783, C$_{14}$H$_{23}$NO requires 221.1781; [α]^{22}$_D$ = -1.6. (c 0.12, CHCl$_3$).

(S)-Methyl-6-oxo-3-(prop-1-en-2-yl)-heptanoate (198)

To a stirred solution of hydroxy ketone **202** (5 g, 25 mmol) in methanol (40 mL) was slowly added lead tetraacetate (15 g, 33 mmol) at -5 °C over 30 min. The reaction mixture was stirred at 0 °C for an additional 1 h and then diluted with water (40 mL) and brine (20 mL). The product was extracted with Et_2O (4 × 20 mL) and the combined ethereal extracts were dried with Na_2SO_4, filtered and concentrated under reduced pressure. The residue was purified by silica gel column chromatography (hexane- ethyl acetate; 10%, R_f 0.26) to give methyl ester **198** as a colourless oil (3.7 g, 74%); IR (thin film) cm^{-1} 3067 (m) (CH, stretch), 1738 (s) (ester C=O, stretch), 1716 (s) (ketone C=O, stretch), 1646 (m) (C=C, stretch); ^{1}H-NMR (400 MHz, CDCl$_3$) δ_H 1.66 (3H, s, CH_3C=C), 2.15 (3H, s, CH_3CO), 1.85-2.75 [7H, m, 3 x CH_2, CH), 3.65 (3H, s, OCH_3) and 4.74 (1H, s, CH_aH=C), 4.80 (1H, s, CHH_b=C); ^{13}C-NMR (100 MHz, CDCl$_3$) δ_C 18.7 (CH$_3$C=CH$_2$), 26.6 (CH$_3$CO), 30.4 (CH$_2$CHCH$_2$), 39.3 (CH$_2$$CHCH_2$), 41.5 ($CH_2$COO), 43.4 ($CH_2$CO), 51.9 (O$CH_3$), 113.3 (C=$CH_2$), 145.7 (CH$_2$=$C$), 173.1(CO ester) and 208.8 (CO ketone); HRMS(EI$^+$) found 199.1328, C$_{11}$H$_{18}$O$_3$requires 199.1334.
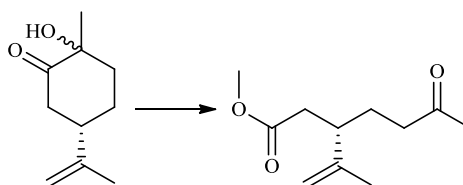
(4S)-1-Methyl-4-(prop-1-en-2-yl)-cyclohexane-1, 2-diol (199)
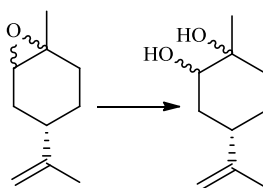
A mixture of (-)-limonene oxide **187** (25 g, 0.16 mol), KOH (54.5 g, 1.36 mol), DMSO (82 mL) and water (75 mL) was heated at 110 °C for 24 h. The mixture was cooled to room temperature and cooled in an ice-bath to precipitate the diol as white crystals. Crystals were collected by filtration under reduced pressure. The filtrate was extracted with Et_2O (6 x 100 mL) and the combined organic layers were dried over Na_2SO_4, filtered and concentrated under reduced pressure. The extracted diol, in addition to the first batch of crystals gave the diol **199** in a combined yield of 20 g (hexane:ethyl acetate, 20%, R_f 0.25, 70%); mp 70-74 °C; IR (thin film) cm^{-1} 3350 (s) (br), (OH, stretch), 3080 (m) (CH, stretch),

2924 (m) (CH, stretch), 1653 (m) (C=C, stretch), 1375 (m) and 1265 (m); ^{1}H-NMR (400 MHz, CDCl$_3$) δ$_H$ 1.25 [3H, s, C(OH)CH_3], 1.72 [3H, s, CH_3C=C], 1.42-2.85 [9H, m, 3 x CH_2, CH, 2 x OH], 3.62 [1H, s, CH(OH)] and 4.74 (2H, br s, CH_2=C); ^{13}C-NMR (100 MHz, CDCl$_3$) δ$_C$ 21.1 [C(OH)CH$_3$], 26.2 (CH$_3$C=CH$_2$), 26.7 (CHCH$_2$CH$_2$), 33.6 (CH$_2$CHCH$_2$), 34.0 [C(OH)CH$_2$CH], 37.4 [C(OH)CH$_3$$CH_2$], 71.3 [$C$(OH)CH$_3$], 73.9 [$C$(OH)], 109.0 ($CH_2$=C) and 149.3 (CH$_2$=$C$); HRMS(EI$^+$) found 170.1308, C$_{10}H_{18}O_2$ requires 170.1307.

(5*S*)-2-Hydroxy-2-methyl-5-(prop-1-en-2-yl)-cyclohexanone (202)

To a stirred suspension of PCC (45 g, 0.2 mol) in CH$_2$Cl$_2$ (250 mL) was added dropwise at room temperature a solution of freshly prepared diol **199** (13 g, 0.07 mol) in DCM (250 mL). After stirring for 2 h, the reaction mixture was filtered through a short silica-gel column using DCM. The filtrate was concentrated under reduced pressure. Purification of the residue by flash-column chromatography on silica gel (hexane-ethyl acetate, 20%, R$_f$ 0.30) gave the hydroxyl ketone **202** as a colourless oil (10 g, 75%); IR (thin film) cm^{-1} 3423 (s) (OH, stretch), 3083 (m) (CH, stretch), 2973 (m) (CH, stretch), 1717 (s) (C=O, stretch), 1645 (m) (C=C, stretch) and 1375 (m); ^{1}H-NMR (400 MHz, CDCl$_3$) δ$_H$ 1.37 [3H, s, C(OH)CH_3], 1.75 (3H, s, CH_3C=C), 1.65-2.95 [7H, m, 3 x CH_2, CH], 3.62 (1H, s, OH), 4.70 (1H, s, CH$_a$H=C), 4.86 (1H, s, CHH$_b$=C); ^{13}C-NMR (100 MHz, CDCl$_3$) δ$_C$ 21.5 (CH$_3$C=CH$_2$), 24.9 [C(OH)CH$_3$], 25.2 (CH$_2$CHCH$_2$), 40.7 (CH$_2$$CHCH_2$), 44.1 [C(OH)CH$_3$$CH_2$], 46.2 ($CH_2$CO), 75.6 [$C$(OH)CH$_3$], 110.6 ($CH_2$=C), 146.13 (CH$_2$=$C$) and 209.64 (C=O); HRMS(EI$^+$) found 168.1152, C$_{10}$H$_{16}$O$_2$ requires 168.1150.

(S)-Methyl-6-(hydroxyimino)-3-(prop-1-en-2-yl)-heptanoate (204)

Hydroxylamine hydrochloride (232 mg, 3.3 mmol) was added in one portion to a stirred solution of methyl ester **198** (444 mg, 2.2 mmol) in pyridine (1.5 mL) and ethanol (1 mL). The resulting mixture was stirred for 6 h and then diluted with water (5 mL) and extracted with ethyl acetate (6 x 5 mL). The combined organic extracts were washed with aqueous hydrochloric acid (10%, 5 mL), saturated sodium hydrogen carbonate (2 mL) and brine (5 mL). The organic layer was dried (Na_2SO_4), filtered and concentrated under reduced pressure. The residue was purified by silica-gel column chromatography (hexane-ethyl acetate; 10%, Rf 0.30) to give a mixture of E/Z oximes **204** as a colourless oil (197 mg, 80%); IR (thin film) cm^{-1} 3377 (s) (OH, stretch), 3086 (m) (CH, stretch), 2931 (m) (CH, stretch), 1716 (s) (ester C=O, stretch), 1645 (s) (C=N, stretch), 1656 (m) (C=C, stretch); ^{1}H-NMR (400 MHz, CDCl$_3$) δ$_H$ 1.56 and 1.57 (3H minor and major isomers, 2 x s, CH_3C=C), 1.75 and 1.76 (3H, minor and major isomers, 2 x s, N=CCH_3), 1.80-2.72 (7H, minor and major isomers, m, 3 x CH_2, CH), 3.64 and 3.65 (3H, minor and major isomers, 2 x s, OCH_3), 4.70, 4.74 and 4.75 (2H, br s, minor and major isomers, CH_2=C); ^{13}C-NMR (100 MHz, CDCl$_3$) δ$_C$ 14.0 (CH_3C), 18.9 and 18.8 (major and minor isomer, CH_3CN), 29.4 and 28.6 (major and minor isomer, CHCH_2CH$_2$), 33.9 (CHCH$_2$CH_2), 39.9 and 39.4 (CH_2CHCH$_2$), 43.6 and 44.2 (major and minor isomer, CH_2COOCH$_3$), 51.2 (OCH_3), 113.2 and 113.1 (C=CH_2), 145.7 (C=CH$_2$), 158.9 and 158.5 (major and minor isomer, C=N) and 173.3 (CO ester); HRMS(EI$^+$) found 213.1360, $C_{11}H_{19}NO_3$ requires 213.1365.

(S)-6-Oxo-3-(prop-1-en-2-yl)heptanoic acid (211)

To a solution of methyl ester **198** (1.03 g, 5.0 mmol) in methanol (6 mL) was added a solution of 6 M LiOH (6 mL) with stirring. After stirring for 3 h, methanol was removed under reduced pressure and a solution of 1 M HCl (10 mL) was added. The mixture was

extracted with ethyl acetate (3 x 10 mL) and the combined organic extracts were dried over Na_2SO_4, filtered, and concentrated under reduced pressure. The residue was purified by silica-gel column chromatography (hexane-ethyl acetate; 15%, R_f 0.21) to give keto acid **221** as a colourless oil (0.74 g, 80%); IR (thin film) cm^{-1} 3300 (vs) (OH, stretch), 2845 (m) (CH, stretch), 1738 (s) (acid C=O, stretch), 1715 (s) (ketone C=O, stretch), 1660 (m) (C=C, stretch); ^{1}H-NMR (400 MHz, $CDCl_3$) δ_H 1.56 (3H, s, CCH_3), 1.8-2.7 (7H, m, 3 x CH_2, CH), 2.15 (3H, s, COCH_3) and 4.74 (1H, s, CH_aH=C), 4.80 (1H, s, CHH$_b$=C); ^{13}C-NMR (100 MHz, $CDCl_3$) δ_C 18.8 (CH$_3$C), 26.6 (CH$_3$CO), 30.4 (CH$_2$CH$_2$CO), 39.2 (CH$_2$CHCH$_2$), 41.5 (CH$_2$COO), 43.1 (CH$_2$CO), 113.5 (C=CH$_2$), 145.4 (CH$_2$=C), 178.5 (CO acid), 209.3 (CO ketone); HRMS(EI$^+$) found 185.1178, $C_{10}H_{16}O_3$ requires 185.1178.

Jones oxidation of diol 199 to (*S*)-6-oxo-3-(prop-1-en-2-yl)heptanoic acid (211)

Jones reagent: 25 g of CrO_3 was dissolved in concentrated H_2SO_4 (25 mL). This solution was added very slowly to H_2O (75 mL) that had been cooled to 0 °C with stirring.

To a stirred solution of diol **199** (22.3 g, 0.13 mol) in acetone (200 mL) was slowly added Jones reagent (~50 mL) at 0 °C for 20 min. The addition was continued until the characteristic orange colour of Jones reagent persisted for about 20 min; the reaction was monitored by TLC (hexane-ethyl acetate; 15%, R_f 0.21). A solution of $NaHCO_3$ (1N, 100 mL) was added, and the suspension was stirred vigorously until the pH of reaction mixture tested neutral. The suspension was filtered and the residue was washed with acetone (100 mL). H_2O (150 mL) was added to the filtrate and the solution was then extracted with DCM (5 x 100 mL). The organic layers were dried over anhydrous $MgSO_4$, filtered and concentrated under reduced pressure. The crude product was purified by chromatography on silica gel (hexane-ethyl acetate, 15%) to give pure keto acid as colourless oil (18.8 g, 78%); IR (thin film) cm^{-1} 3300 (vs) (stretch OH), 2845 (m) (C-H stretch), 1738 (s) (acid C=O, stretch), 1715 (s) (ketone C=O stretch), 1660 (m) (C=C stretch); ^{1}H-NMR (400 MHz, $CDCl_3$) δ_H 1.56 (3H, s, CCH_3), 1.8-2.7 (7H, m, 3 x CH_2, CH), 2.15 (3H, s, COCH_3) and 4.74 (1H, s,

CH_aH=C), 4.80 (1H, s, CHH_b=C); ^{13}C-NMR (100 MHz, CDCl$_3$) δ$_C$ 18.8 (*C*H$_3$C), 26.6 (*C*H$_3$CO), 30.4 (*C*H$_2$CH$_2$CO), 39.2 (*C*H$_2$CHCH$_2$), 41.5 (*C*H$_2$COO), 43.1 (*C*H$_2$CO), 113.5 (C=*C*H$_2$), 145.4 (CH$_2$=*C*), 178.5 (*C*O acid), 209.3 (*C*O ketone); HRMS(EI$^+$) found 185.1178, C$_{10}$H$_{16}$O$_3$ requires 185.1178.

1-(3-Oxopentyl) piperidine-2-thione (222)

Piperidine-2-thione (**195**) (2 g, 17.4 mmol), anhydrous K$_2$CO$_3$ (5.2 g, 38.2 mmol) (kept at 140 °C for 12 h before use), and 18-crown-6 (0.58 g, 2.20 mmol) were suspended in anhydrous THF (100 mL) under N$_2$. After cooling to 0 °C, a first portion of ethyl vinyl ketone (2.3 mL, 23.5 mmol) was added drop wise under stirring. After the addition was complete, the solution was left at 0 °C for 5 min and then at room temperature for 1 h. The solution was cooled again to 0 °C, and a second portion of ethyl vinyl ketone (2.3 mL, 23.5 mmol) was added, the solution was left under stirring for 3 h at room temperature, monitoring the reaction by TLC. Sodium sulfate was added and the solution was filtered and concentrated under reduced oressure. The crude material was purified by chromatography on silica gel (CH$_2$Cl$_2$, R$_f$ 0.25) to give oxo-thione **222** as a light yellow oil (3.2 g, 87%); IR (NaCl) cm^{-1} 3030 (m) (CH, stretch), 2942 (s) (CH, stretch), 1710 (s) (ketone C=O, stretch), 1329 (m), 1265 (m) and 1159 (m) (C=S stretch); ^{1}H-NMR (400 MHz, CDCl$_3$) δ$_H$ 1.03 (3H, t, *J* = 7.0 Hz, COCH$_2$CH_3), 1.61 (2H, m, CH$_2$CH_2CH$_2$CS), 1.84 (2H, m, CH$_2$CH_2CH$_2$N), 2.44 (2H, q, *J* = 7.0 Hz, CH_2CH$_3$), 2.93 (2H, t, *J* = 6.5 Hz, CH$_2$CH_2CO), 2.95 (2H, m, CH_2C=S), 3.49 (2H, t, *J* = 6.0 Hz, CH_2N) and 4.10 (2H, t, *J* = 6.5 Hz, CH_2N); ^{13}C-NMR (100 MHz, CDCl$_3$) δ$_C$ 7.8 (COCH$_2$*C*H$_3$), 20.5 (*C*H$_2$CH$_2$CS), 23.0 (*C*H$_2$CH$_2$N), 36.2 (CH$_3$*C*H$_2$CO), 38.6 (*C*H$_2$CH$_2$CO), 41.9 (*C*H$_2$CS), 50.3 (COCH$_2$*C*H$_2$N), 52.2 (*C*H$_2$N), 199.7 (*C*O ketone), and 209.7 (*C*=S); HRMS(EI$^+$) found 200.1118, C$_{10}$H$_{17}$NOS requires 200.1109.

(1*R*,9a*R*)-1,9a-Dimethylhexahydro-1H-quinolizin-2(6H)-one (223)

To a solution of TFA salt **233** (630 mg, 2.3 mmol) in dry THF (15 mL) was added methylmagnesium bromide (3 M in diethyl ether, 3.7 mL, 11.3 mmol) at room temperature under an argon atmosphere. After the mixture was heated at reflux temperature for 24 h, a solution of saturated ammonium chloride (20 mL) and 10% NH_4OH (20 mL) were added and the solution extracted with Et_2O (5 x 10 mL), the combined organic layers were dried over anhydrous K_2CO_3 then filtered and concentrated under reduced pressure. The resulting residue was dissolved in Et_2O (10 mL) and adjusted to pH 2 with 10% HCl (5 mL) and extracted with Et_2O (3 x 10 mL). The aqueous phase was adjusted to pH 12 with NaOH (pellets) and extracted with Et_2O (5 x 10 mL). The combined ethereal layers were dried (K_2CO_3) and filtered, and the solvent was removed under reduced pressure. The crude material was purified by chromatography on alumina (hexane-ethyl acetate; 1:1, R_f 0.30) to give compound **223** as pale yellow oil (273 mg, 65%); IR (thin film) cm^{-1} 2790-2928 (s) (CH, stretch), 1718 (s) (C=O, stretch), 1326 (m) and 1252 (s) (CN, stretch); ^{1}H-NMR (400 MHz, CDCl$_3$) δ_H 0.72 [3H, s, C(C*H$_3$*)], 0.87 (3H, d, *J* = 6.5 Hz, (C*H$_3$*)CH), 1.33 -1.50 (6H, m, 3C*H$_2$*), 1.57-1.66 (1H, dddd, *J* = 6.5, 6.0, 5.5 Hz, C*H*(CH$_3$), 2.42-2.64 (2H, m, C*H$_2$*CO), 2.63-2.85 (4H, m, 2C*H$_2$*N); ^{13}C-NMR (100 MHz, CDCl$_3$) δ_C 8.1 (*C*H$_3$)C, 10.1 (*C*H$_3$CH), 20.1 (*C*H$_2$CH$_2$CH$_2$N), 26.2 (CH$_2$*C*H$_2$CH$_2$N), 37.70 [*C*H$_2$C(CH$_3$)], 40.68 (CO*C*H$_2$CH$_2$N), 49.33 (CH$_2$CH$_2$*C*H$_2$N), 50.33 (CO*C*H$_2$CH$_2$N), 55.80 [*C*H(CH$_3$)], 60.17 [*C*(CH$_3$)], 210.90 (C=O, ketone); HRMS(EI$^+$) found 182.1554, C$_{11}$H$_{19}$NO requires 182.1545.

1-Methyloctahydropyrido[1,2-a]azepin-2(1H)-one (225)

CuI (80.8 mg, 0.42 mmol) was suspended in dry Et$_2$O (3 mL) at 0 °C under argon atmosphere, and then MeLi (2 M in diethyl ether, 0.5 mL, 0.84 mmol) was added drop wise at 0 °C, a yellow precipitate appeared, and then disappeared after the complete addition of MeLi. Enone **193** (70 mg, 0.42 mmol) was added to the above solution of dimethyl copper lithium at 0 °C. After stirring for 90 min at 0°C and 2 h at room temperature, a solution of ammonium chloride (10 mL) and 10% ammonium hydroxide (10 mL) were added and the solution was extracted with Et$_2$O (5 × 10 mL), the combined organic layers were dried over anhydrous K$_2$CO$_3$, filtered and concentrated under reduced pressure. The resulting residue was adjusted to pH 2 with 10% HCl (5 mL) and extracted with Et$_2$O (3 × 10 mL). The aqueous phase was adjusted to pH 12 with NaOH (pellets) and extracted with Et$_2$O (3 x 5 mL), the combined ethereal layers were dried (K$_2$CO$_3$) then filtered and the solvent was removed under reduced pressure. The crude material was purified by chromatography on alumina column (hexane-ethyl acetate; 10%, R$_f$ 0.30) to give compound **225** as pale yellow oil (40 mg, 52%): IR (thin film) cm^{-1} 3040 (m) (CH, stretch), 2760-2800 (m) (CH, stretch), 1718 (s) (ketone C=O, stretch): ^{1}H-NMR (400 MHz, CDCl$_3$) δ$_H$ 0.99 (3H, d, J = 7.0 Hz, CH_3CH), 1.6-1.64 (2H, m, CH_2), 1.70-1.72 (1H, m, CH$_3$CH), 1.73-1.76 (2H, m, CH_2), 2.21-2.29 (1H, m, CH), 2.32-2.39 (4H, m, CH_2CH$_2$CH$_2$N), 2.70-2.2.73 (2H, m, CH_2CO), 2.90-2.95 (2H, m, CH_2N), 3.01-3.09 (2H, m, CH_2N); ^{13}C-NMR (100 MHz, CDCl$_3$) δ$_C$ 8.8 (CH_3CH), 22.4 (CH_2), 24.2 (CH_2), 28.2 (CH_2), 30.4 (CH_2), 40.2 (CH_2CO), 55.60 (CHCH$_3$), 57.7 (CH_2N), 58.0 (CH_2N), 67.3 (CH), 210.0 (C=O); HRMS(EI$^+$) found 181.1554, C$_{11}$H$_{19}$NO requires 181.1553.

8-Hydroxy-9-methyl-1,2,3,4,6,7-hexahydroquinolizin-5-ium 2,2,2-trifluoroacetate (233)

To a solution of enaminone **193** (420 mg, 2.5 mmol) in dry THF (5 mL) was added trifluoroacetic acid (0.20 mL, 2.5 mmol) at room temperature. After stirring for 10 min, the solvent and excess TFA was removed under reduced pressure, and the residue placed under high vacuum to give salt of enone **233** as yellow-orange oil (630 mg, 90%, R_f 0.15); IR (thin film) cm^{-1} 3050 (m) (CH, stretch), 2828 (s) (C-H stretch); ^{1}H-NMR (400 MHz, CDCl$_3$) δ_H 1.71 (3H, s, C*H$_3$*C=C), 1.76-1.80 (2H, m, C*H$_2$*CH$_2$CH$_2$) 1.84-1.91 (2H, m, CH$_2$C*H$_2$*CH$_2$N), 2.6-2.7 (2H, t, *J* = 7.0 Hz, C*H$_2$*COH), 2.8-2.89 (2H, t, *J* = 6.5 Hz, C*H$_2$*C=N), 3.50-3.55 (2H, t, *J* = 5.5 Hz, HOCC*H$_2$*CH$_2$N), 3.60-3.65 (2H, t, *J* = 5.5 Hz, CH$_2$C*H$_2$*N); ^{13}C-NMR (100 MHz, CDCl$_3$) δ_C 8.6 (*C*H$_3$), 16.5 (*C*H$_2$CH$_2$CH$_2$N), 20.0 (CH$_2$*C*H$_2$CH$_2$N), 25.8 (*C*H$_2$COH), 27.5 (*C*H$_2$C=N), 48.6 (CH$_2$CH$_2$*C*H$_2$N), 51.2 (COH*C*H$_2$CH$_2$N), 102.6 (*C*=COH), 111.1 (q, *C*F$_3$), 158.9 (*C*OO), 172.1 (*C*=N), 174.2 (*C*OH=C). This salt was used forward in the next step without purification.

(1'*R*,9a'*R*)-1',9a'-Dimethyloctahydrospiro[[1,3]dithiolane-2,2'-quinolizine] (234)

To a solution of amino ketone **223** (70 mg, 0.4 mmol) in dry DCM (5 mL) were added 1,2-ethanedithiol (0.3 mL, 3.8 mmol) and BF$_3$.OEt$_2$ (2 M in diethyl ether, 0.14 mL, 1.16 mmol) at room temperature under a nitrogen atmosphere. The mixture was stirred for 24 h, and then a solution of 1N NaOH (5 mL) was added and the mixture was extracted with DCM (5 x 3 mL). The combined organic layers were dried (K$_2$CO$_3$), filtered and concentrated under reduced pressure. The crude material was purified by chromatography on silica gel (hexane: ethyl acetate, 20%, R_f 0.34) to give the compound **234** as white solid (80 mg, 80%); IR (thin film) cm^{-1} 3060 (m) (CH, stretch), 2790-2928 (s) (CH, stretch); ^{1}H-NMR (400 MHz, CDCl$_3$) δ_H 0.88 (3H, s, C*H$_3$*C), 1.08-1.10 (3H, d, *J* = 7.0 Hz, C*H$_3$*CH), 1.45-1.60 (6H, m, 3C*H$_2$*), 1.92-1.93 (1H, q, *J* = 7.0, 13.5 Hz, C*H*CH$_3$), 2.00-2.01 (1H, m, *H*CHCS$_2$), 2.30-2.46 (4H,

m, HC*H*CS$_2$, C*H$_2$*N, *H*CHN), 2.64-2.65 (1H, m, HC*H*N), 2.98-3.26 (4H, m, SC*H$_2$*C*H$_2$*S); ^{13}C-NMR (100 MHz, CDCl$_3$) δ$_C$ 6. 9 (*C*H$_3$C), 11.6 (*C*H$_3$CH), 19.6 (*C*H$_2$), 25.8 (*C*H$_2$), 38.0 (*C*H$_2$), 38.3 (*C*H$_2$CS$_2$), 40.5 (*C*HCH$_3$), 46.2 (*C*H$_2$S), 49.3 (*C*H$_2$S), 49.5 (*C*H$_2$N), 51.7 (*C*H$_2$N), 58.0 (*C*S$_2$), 72.5 (*C*CH$_3$); HRMS(EI$^+$) found 258.1359, C$_{13}$H$_{23}$NS$_2$ requires 258.1350.

(1*R*,2*R*,9a*R*)-1,9a-Dimethyloctahydro-1H-quinolizin-2-ol (237) and
(1*R*,2*S*,9a*R*)-1,9a-Dimethyloctahydro-1H-quinolizin-2-ol (238)

To a stirred solution of amino ketone **223** (100 mg, 0.5 mmol) in dry THF (4 mL) was added LiAlH$_4$ (18 mg, 5.5 mmol) at room temperature under N$_2$. The reaction mixture was stirred at room temperature for 2 h, and then a solution of 5% of NaOH (5 mL) was added slowly to precipitate the aluminium salt by-product. The white salt removed by filtration under reduced pressure and the residue washed with additional THF (5 mL). To the resulting THF filtrate was added 10% HCl (5 mL) and the mixture was stirred for 5 min. DCM (10 mL) was added and the two phases were separated. The aqueous layer was adjusted to pH 12 with NaOH (pellets), and extracted with Et$_2$O (4 x 5 mL). The combined ethereal layers were dried (K$_2$CO$_3$) and filtered, and the solvent was removed under reduced pressure. The crude product was purified by chromatography on alumina (ethyl acetate-methanol, 10%, R$_f$ 0.17) to give the amino alcohol mixture (**237** and **238**) as a colourless oil (92 mg, 90%); IR (thin film) cm^{-1} 3396 (s) (br), (OH, stretch), 2760-2866 (s) (CH, stretch), 1220 (m) (CN, stretch); ^{1}H-NMR (400 MHz, CDCl$_3$) δ$_H$ 0.74 (3H, s, C*H$_3$*C, 10%) and 1.00 (3H, s, C*H$_3$*C, 90%), 0.89 (3H, d, *J* = 7.0 Hz, C*H$_3$*CH, 10%) and 0.92 (3H, d, *J* = 12.0 Hz, C*H$_3$*CH, 90%), 1.45-1.50 (6H, m, 3C*H$_2$*), 1.52-1.60 [1H, m, C*H*(CH$_3$)], 2.00-2.44 (2H, m, C*H$_2$*COH), 2.46-2.50 (2H, m, C*H$_2$*N), 2.53-2.75 (2H, m, C*H$_2$*N), 3.36-3.37 (1H, tt, *J* = 10.0 Hz, C*H*OH, 10%) and 3.80-3.82 (1H, td, *J* = 11.0 Hz, C*H*OH, 90%); ^{13}C-NMR (100 MHz, CDCl$_3$) δ$_C$ 12.5 (*C*H$_3$C), 14.8 (*C*H$_3$CH), 19.6 (*C*H$_2$CH$_2$CH$_2$N), 26.8 (*C*H$_2$CH$_2$N), 33.2 (*C*H$_2$CH$_2$N), 37.5 (COH*C*H$_2$CH$_2$N), 45.0 (*C*HCH$_3$), 49.6 (*C*H$_2$N), 56.8 (*C*H$_2$N), 60.4 (*C*CH$_3$), 70.6 (*C*OH); HRMS(EI$^+$) found 184.1325, C$_{11}$H$_{21}$NO requires 184.1320.

(1S,9aR)-1,9a-Dimethyldecahydroquinolizin-5-ium 2,4,6-trinitrophenolate (243)

This salt was prepared by Dr.Juan. A. Faraldos: To a stirred solution of free amine **105** (68 mg, 0.4 mmol) in ethanol (4 mL) was added picric acid (91.6 mg, 0.4 mmol) at room temperature. After stirring for 1h, the mixture was filtered under reduced pressure to give the picrate salt **243** as yellow crystals (115 mg, 77%); mp 220 °C; IR (NaCl) cm^{-1} 3060 (m) (CH, stretch), 2780-2940 (s) (stretch C-H), 1230 (m) (CN, stretch); ^{1}H-NMR (500 MHz, CDCl$_3$) δ_H 0.89-0.90 (3H, d, J = 7.0 Hz, CH_3CH), 1.21 (3H, s, CH_3C), 1.42-1.44 (2H, m, CH_2CH$_2$CH$_2$N), 1.57-1.59 (1H, m, CH$_3$CH), 1.70-1.72 [2H, m, CH_2C(CH$_3$)N], 1.87-1.91 (2H, m, CH_2CH$_2$N), 2.08-2.33 (4H, m, 2 x CH_2CH$_2$N), 2.80-2.90 (2H, m, CH_2N), 3.22-3.24 (2H, m, CH_2N), 8.83 (2H, s, ArH), 9.56 (broad s, NH); ^{13}C-NMR (125 MHz, CDCl$_3$) δ_C 9.3 (CH$_3$CH), 15.7 (CH$_3$C), 18.8 (CH$_2$CH$_2$CH$_2$N), 22.7 (CH$_2$CH$_2$CH$_2$N), 22.9 (CH$_2$CH$_2$CH$_2$N), 26.9 [CH$_2$CH(CH$_3$)], 33.7 [CH$_2$C(CH$_3$)CN], 38.9 (CHCH$_3$), 50.3 (CH$_2$N), 50.4 (CH$_2$N), 65.4 (CH$_3$C), 126.6 (ArCH, ArCH), 127.8 (ArCNO$_2$), 141.8 (ArCNO$_2$, ArCNO$_2$), 161.6 (ArCO$^-$); HRMS(EI$^+$) found 168.1753, C$_{11}$H$_{22}$N requires 168.1752.

(S)-1-(4-(Prop-1-en-2-yl)-2-thioxopiperidin-1-yl)pentan-3-one (244)

Piperidine-2-thione (**196**) (100 mg, 0.64 mmol), anhydrous K$_2$CO$_3$ (190 mg, 1.4 mmol) (kept at 140 ˚C for 12 h before use), and 18-crown-6 (20 mg, 0.08 mmol) were suspended in anhydrous THF (10 mL). After cooling to 0 °C, a first portion of ethyl vinyl ketone (0.1 mL, 0.86 mmol) was added dropwise with stirring under nitrogen. After the addition was complete, the solution was left at 0 °C for 5 min and then at room temperature for 1 h. The solution was cooled again to 0 °C, and a second portion of ethyl vinyl ketone (0.1 mL, 0.86 mmol) was added. Stirring was continued for 1 h at room temperature, monitoring the

reaction by TLC. Anhydrous Na_2SO_4 was then added and the solution was filtered and concentrated under reduced pressure. The crude product was purified by chromatography on silica gel (DCM, R$_f$ 0.25) to give pure oxo-piperidine-2-thione **244** as a light yellow oil (130 mg, 84%): IR (thin film) cm^{-1} 3085 (m) (CH, stretch), 1712 (s) (ketone C=O, stretch), 1645 (s) (C=C, stretch), 1348 (s) and 1161 (m) (C=S); ^{1}H-NMR (400 MHz, CDCl$_3$) δ_H 1.03 (3H, t, J = 5.0 Hz, COCH$_2$CH_3), 1.65 (3H, s, CH_3C=C), 2.01 (1H, m, CH), 2.44 (2H, q, J = 7.0, 6.0 Hz, COCH_2CH$_3$), 2.65 (2H, t, J = 6.5 Hz, CH_2CH$_2$N), 2.97 (2H, dt, J = 6.5, 4.0 Hz, CH$_2$CH_2CO), 3.10 (2H, ddd, J = 2.0, 3.0, 6.0 Hz, CH_2CS), 3.59 (1H, app ddd, J = 4.0, 5.5, 13.0 Hz, CHN), 3.44 (1H, app ddd, J = 5.0, 10.0, 13.0 Hz, CHN), 4.10- 4.20 (2H, dt, J = 6.5, 13.0 Hz, NCH_2CH$_2$CO) and 4.74 (1H, s, CH_aH=C), 4.80 (1H, s, CHH_b=C); ^{13}C-NMR (100 MHz, CDCl$_3$) δ_C 7.7 (COCH$_2$$CH_3$), 20.6 (CH$_2CH_2$CN), 27.5 ($CH_3$CH=CH$_2$), 36.1 ($CH_2$CHCH$_2$), 38.4 ($CH_2CH_2$CO), 38.6 (CO$CH_2CH_3$), 46.7 ($CH_2$CS), 49.9 (CN$CH_2CH_2$), 51.8 ($CH_2$CN), 110.5 ($CH_2$=CH), 145.8 ($C$=CH$_2$), 198.9 (C=O) and 209.8 (C=S); HRMS(EI$^+$) found 239.1352, C$_{13}$H$_{21}$NOS requires 239.1344; [α]$^{22}_D$ = -28.4 (c 2.27, CHCl$_3$).

(S)-8-Hydroxy-9-methyl-2-(prop-1-en-2-yl)-1,2,3,4,6,7-hexahydroquinolizin-5-ium (246)
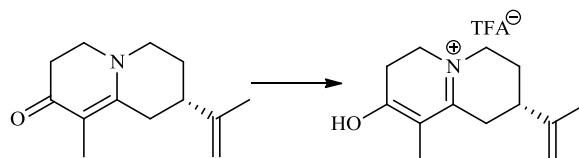
To a solution of bicyclic enone **194** (250 mg, 1.21 mmol) in dry DCM (3 mL) was added TFA (0.1 mL, 1.21 mmol). After stirring for 5 min, the excess of TFA and solvent were removed under reduced pressure and the residue was placed under high vacuum to give the TFA salt **246** as yellow-orange oil (350 mg, 91%); IR (thin film) cm^{-1} 3340 (m) (OH, stretch) 3085 (m) (CH stretch), 2822 (m) (CH, stretch), 1640 (m) (C=C, stretch), 1346 (m) and 1241 (m) (C-N stretch); ^{1}H-NMR (400 MHz, CDCl$_3$) δ_H 1.82 [3H, s, C=C(CH_3)CO], 1.85 (3H, s, C=CCH_3), 2.11 (1H, m, CH), 2.48 (2H, d, J = 3.5 Hz, CHCH_2C), 2.61 (2H, q, J = 6.0, 5.0 Hz, CHCH_2CH$_2$), 2.92 (2H, m, CH_2CO), 3.62-3.84 (4H, m, CH$_2$CH_2NCH_2), 4.75 (1H, s, CH_aH=C), 5.13 (1H, s, CHH_b=C); ^{13}C-NMR (100 MHz, CDCl$_3$) δ_C 8.4 (CH$_3$C=COH), 22.5 (CH$_3$C=C), 31.3 (CH$_2$C=N), 32.1 (CH$_2$CH$_2$N), 33.8 (CH$_2$CH$_2$N), 38.5 (CH), 44.6 (CH$_2$N), 45.9 (CH$_2$N), 105.7 (C=COH), 105.1

(CH_2=CCH$_3$), 111.1-115.9 (q, J = 285 Hz, CF$_3$), 147.9 (C=CCH$_3$), 158.9-159.9 (q, J = 38 Hz, COO), 172.1 (C=N), 174.2 (COH=C). This salt was used in the next step without purification.

(1*S*,8*S*,9a*R*)-1,9a-Dimethyl-8-(prop-1-en-2-yl)decahydroquinolizin-5-ium perchlorate (247)
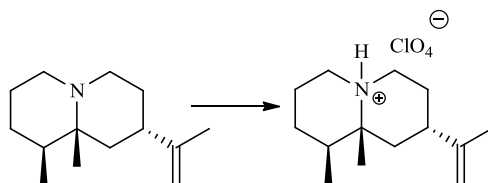
This salt was prepared by Dr. Juan. A. Faraldos: To a solution of the free amine **106** (20 mg, 0.09 mmol) in dry Et$_2$O (4 mL) was added perchloric acid (9.0 mL, 0.09 mmol) under a nitrogen. After stirring for 15 min, the crystals were filtered and washed with dry ether (10 mL) to give perchlorate salt **247** (25 mg, 90%) as white crystals; IR (thin film) cm^{-1} 3050 (m) (CH, stretch), 2695-2770 (s) (CH, stretch), 1660 (m) (C=C, stretch); ^{1}H-NMR (500 MHz, D$_2$O) δ$_H$ 0.80-0.81 (3H, d, J = 6.5 Hz, CH_3CH), 1.18 (3H, s, CH_3C), 1.36-1.41 (1H, m, CHCH$_3$), 1.45-1.59 (4H, 2 x CH_2), 1.60 (3H, s, CH_3C=C), 1.73-2.05 (4H, m, CH_2CH$_2$N, CH_2CH$_2$N), 2.35 (1H, m, CH), 2.92-3.02 (3H, m, CH_2N, CHN), 3.11-3.19 (1H, ddd, J = 3.5, 3.0, 2.0 Hz, CHN), 4.66 (1H, s, CH_aH=C), 4.71 (1H, s, CHH_b=C); ^{13}C-NMR (125 MHz, D$_2$O) δ$_C$ 9.8 (CH$_3$CH), 15.4 (CH$_3$C), 20.7 (CH$_3$C=C), 24.1 (CH$_2$CHCH$_3$), 27.5 (CH$_2$CCH$_3$), 29.2 (CH$_2$CH$_2$N), 37.7 (CH$_2$CH$_2$N), 41.5 (CH), 42.3 (CHCH$_3$), 50.8 (CH$_2$N), 50.9 (CH$_2$N), 66.8 (CCH$_3$), 110.4 (CH$_2$=C), 148.4 (CH$_2$=C); HRMS(EI$^+$) found 208.2058, C$_{14}$H$_{26}$N requires 208.2065.

(4*R*)-Limonene oxide[(4*R*)-1-methyl-4-(prop-1-en-2-yl)-7-oxabicyclo[4.1.0]heptanes] (248)
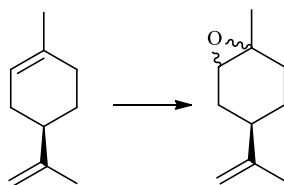
A mixture of (*R*)-limonene (30.1 g, 220 mmol) and NaHCO$_3$ (37.8 g, 450 mmol) in DCM (150 mL) was stirred at 0-5 °C, as a solution of 75% m-CPBA (70.0 g, 223 mmol) in DCM (250 mL) was added over 50 min. The mixture was stirred at 0 °C for 30 min, and a solution of 10% Na$_2$SO$_3$ of water (100 mL) was added. The mixture was stirred for 30 min at room temperature and diluted with water (100 mL) before separating the organic fraction. The aqueous layer was extracted with DCM (6 x 100 mL). The combined organic layers were

dried (MgSO$_4$), filtered and concentrated under reduced pressure. The residue was purified by chromatography on silica gel (hexane-ethyl acetate, 5%, R$_f$ 0.40) to afford limonene oxide (**248**) as colourless oil which was a 60: 40 mixture of two isomers (20.5 g, 61%); IR (thin film) cm^{-1} 3070 (m) (C-H, stretch), 2918 (m) (C-H, stretch), 1655 (m) (C=C, stretch); ^{1}H-NMR (500 MHz, CDCl$_3$) δ$_H$ 1.23 and 1.25 (3H, s, C*H*$_3$CO), 1.60 and 1.64 (3H, s, C*H*$_3$C=C), 1.43-2.18 (7H, m, 3 x C*H*$_2$, C*H*), 3.00 and 3.02 (1H, dd, *J* = 6.5 Hz, C*H*O), 4.68 (1H, s, C*H*$_a$H=C), 4.74 (1H, s, CH*H*$_b$=C); ^{13}C-NMR (125 MHz, CDCl$_3$) δ$_C$ 17.1 (*C*H$_3$CO), 21.3 (*C*H$_3$C=C), 23.8 (*C*H$_2$CHO), 27.9 (*C*H$_2$CCH$_3$), 28.6 (*C*H$_2$CH), 39.3 (*C*H), 60.3 (CH$_3$*C*O), 63.7 (*C*HO), 110.4 (*C*H$_2$=C), 147.8 (CH$_2$=*C*); HRMS(EI$^+$) found 152.2303, C$_{10}$H$_{16}$O requires 152.2301.

(4*R*)-1-Methyl-4-(prop-1-en-2-yl)-cyclohexane-1,2-diol (249)
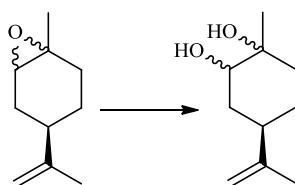
A mixture of (+)-limonene oxide (**248**) (50 g, 0.33 mol), KOH (109 g, 1.96 mol), DMSO (165 mL) and water (150 mL) was heated at 110 ˚C for 24 h. The mixture was cooled to room temperature and placed into an ice-bath to precipitate the diol as white crystals. Crystals were collected by filtration under reduced pressure. The filtrate was extracted with Et$_2$O (6 × 100 mL) and the combined organic layers were dried over Na$_2$SO$_4$, filtered and concentrated under reduced pressure. The extracte diol, in addition to the crystals gave the diol **249** in a combined yield of 42 g (hexane-ethyl acetate, 20%, R$_f$ 0.25, 74%); mp 70-74 ˚C; IR (thin film) cm^{-1} 3396 (s) (br), (OH, stretch), 3080 (m) (CH, stretch), 2924 (m) (CH, stretch), 1653 (m) (C=C, stretch), 1375 (m) and 1265 (m) (CN, stretch); ^{1}H-NMR (400 MHz, CDCl$_3$) δ$_H$ 1.25 [3H, s, C(OH)C*H*$_3$], 1.72 [3H, s, C*H*$_3$C=C], 1.42-2.85 [9H, m, 3 x C*H*$_2$, C*H*, 2 x O*H*], 3.62 [1H, s, C*H*(OH)] and 4.74 (2H, br s, C*H*$_2$=C); ^{13}C-NMR (100 MHz, CDCl$_3$) δ$_C$ 21.1 [C(OH)*C*H$_3$], 26.2 (*C*H$_3$C=CH$_2$), 26.7 (CH*C*H$_2$CH$_2$), 33.6 (*C*H$_2$CHCH$_2$), 34.0 [C(OH)*C*H$_2$CH], 37.4 [C(OH)CH$_3$*C*H$_2$], 71.3 [*C*(OH)CH$_3$], 73.9 [*C*(OH)], 109.0 (*C*H$_2$=C) and 149.3 (CH$_2$=*C*); HRMS(EI$^+$) found 170.1308, C$_{10}$H$_{18}$O$_2$ requires 170.1307.

(5*R*)-2-Hydroxy-2-methyl-5-(prop-1-en-2-yl)-cyclohexanone (250)
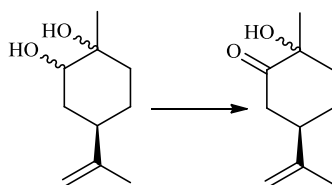
To a stirred suspension of PCC (25 g, 0.14 mol) in DCM (250 mL) was added drop wise at room temperature a solution of freshly prepared diol **249** (10 g, 0.06 mol) in DCM (250 mL). After stirring for 2 h, the reaction mixture was filtered through a short silica- gel column with DCM. The filtrate was concentrated under reduced pressure. Purification of the residue by flash-column chromatography on silica gel (hexane-ethyl acetate, 20%, R_f 0.30) gave the hydroxy ketone **250** as colourless oil (8 g, 83%); IR (thin film) cm^{-1} 3423 (s) (OH, stretch), 3083 (m) (CH, stretch), 2973 (m) (CH, stretch), 1717 (s) (C=O, stretch), 1645 (m) (C=C, stretch) and 1375 (m); ^{1}H-NMR (400 MHz, CDCl$_3$) δ_H 1.37 [3H, s, C(OH)CH_3], 1.75 (3H, s, CH_3C=C), 1.65-2.95 [7H, m, 3 x CH_2, CH], 3.62 (1H, s, OH), 4.70 (1H, s, CH_aH=C), 4.86 (1H, s, CHH_b=C); ^{13}C-NMR (100 MHz, CDCl$_3$) δ_C 21.5 (*C*H$_3$C=CH$_2$), 24.9 [C(OH)*C*H$_3$], 25.2 (*C*H$_2$CHCH$_2$), 40.7 (CH$_2$*C*HCH$_2$), 44.1 [C(OH)CH$_3$*C*H$_2$], 46.2 (*C*H$_2$CO), 75.6 [*C*(OH)CH$_3$], 110.6 (*C*H$_2$=C), 146.13 (CH$_2$=*C*) and 209.64 (C=O); HRMS(EI$^+$) found 168.1152, C$_{10}$H$_{16}$O$_2$ requires 168.1150.

(*R*)-Methyl-6-oxo-3-(prop-1-en-2-yl)-heptanoate (251)
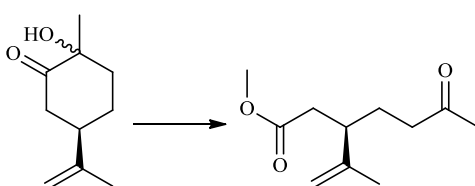
To stirred solution of hydroxy ketone **250** (8 g, 50 mmol) in methanol (40 mL) was slowly added lead tetraacetate (30 g, 68 mmol) at -5 °C over 30 min. The reaction mixture was stirred at 0 °C for an additional 1 h and then diluted with water (40 mL) and brine solution (20 mL). The product was extracted with Et$_2$O (4 × 20 ml) and the combined ethereal extracts were dried with Na$_2$SO$_4$, filtered, and concentrated under reduced pressure. The resulting residue was purified by silica gel column chromatography (hexane- ethyl acetate; 10%, R_f 0.26) to give methyl ester **251** as colourless oil (8.08 g, 81%); IR (thin film) cm^{-1}

3067 (m) (CH stretch), 1738 (s) (ester C=O, stretch), 1716 (s) (ketone C=O, stretch), 1646 (m) (C=C, stretch); ^{1}H-NMR (400 MHz, CDCl$_3$) δ_H 1.66 (3H, s, CH_3C=C), 2.15 (3H, s, CH_3CO), 1.85-2.75 [7H, m, 3 x CH_2, CH], 3.65 (3H, s, OCH_3) and 4.74 (1H, s, CH_aH=C), 4.80 (1H, s, CHH_b=C); ^{13}C-NMR (100 MHz, CDCl$_3$) δ_C 18.7 (CH$_3$C=CH$_2$), 26.6 (CH$_3$CO), 30.4 (CH$_2$CHCH$_2$), 39.3 (CH$_2$$CHCH_2$), 41.5 ($CH_2$COO), 43.4 ($CH_2$CO), 51.9 (O$CH_3$), 113.3 (C=$CH_2$), 145.7 (CH$_2$=$C$), 173.1(CO ester) and 208.8 (CO ketone); HRMS(EI$^+$) found 199.1328, C$_{11}$H$_{18}$O$_3$requires 199.1334.

(*R*)-Methyl-6-(hydroxyimino)-3-(prop-1-en-2-yl)-heptanoate (252)

Hydroxylamine hydrochloride (3.16 g, 49 mmol) was added in one portion to a stirred solution of methyl ester **251** (8.08 g, 40.8 mmol) in pyridine (30 mL) and ethanol (20 mL). The resulting mixture was stirred for 6 h and then diluted with water (100 mL) and extracted with ethyl acetate (6 × 20 mL). The combined organic extracts were washed with aqueous hydrochloric acid (10%, 20 mL), saturated sodium hydrogen carbonate (30 mL) and brine (20 mL). The organic layer was dried (Na$_2$SO$_4$), filtered and concentrated under reduced pressure. The residue was purified by silica-gel column chromatography (hexane-ethyl acetate; 10%, Rf 0.30) to give a mixture of *E/Z* oximes **252** as a colourless oil (7.98 g, 91%); IR (thin film) cm^{-1} 3377 (s) (OH, stretch), 3086 (m) (CH, stretch), 2931 (m) (CH, stretch), 1716 (s) (ester C=O, stretch), 1645 (s) (C=N, stretch), 1656 (m) (C=C, stretch); ^{1}H-NMR (400 MHz, CDCl$_3$) δ_H 1.56 and 1.57 (3H minor and major isomers, 2 x s, CH_3C=C), 1.75 and 1.76 (3H, minor and major isomers, 2 x s, N=CCH_3), 1.80-2.72 (7H, minor and major isomers, m, 3 x CH_2, CH), 3.64 and 3.65 (3H, minor and major isomers, 2 x s, OCH_3), 4.70, 4.74 and 4.75 (2H, br s, minor and major isomers, CH_2=C); ^{13}C-NMR (100 MHz, CDCl$_3$) δ_C 14.0 (CH$_3$C), 18.9 and 18.8 (major and minor isomer, CH$_3$CN), 29.4 and 28.6 (major and minor isomer, CHCH$_2$CH$_2$), 33.9 (CHCH$_2$CH$_2$), 39.9 and 39.4 (CH$_2$$CHCH_2$), 43.6 and 44.2 (major and minor isomer, CH$_2$COOCH$_3$), 51.2 (OCH$_3$), 113.2 and 113.1 (C=CH$_2$), 145.7 (C=CH$_2$), 158.9 and 158.5 (major and minor isomer, C=N) and 173.3 (CO ester); HRMS(EI$^+$) found 213.1360, C$_{11}$H$_{19}$NO$_3$ requires 213.1365.

(R)-Methyl 3-(2-acetamidoethyl)-4-methylpent-4-enoate (253)
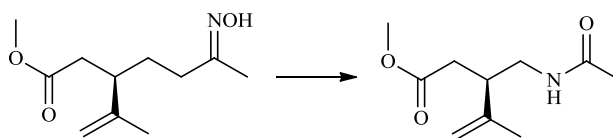
p-Toluene sulfonyl chloride (12.8 g, 67.3 mmol) was added in one portion to a stirred solution of freshly prepared oxime **252** (7.9 g, 37.4 mmol) in dry benzene (20 mL) and pyridine (15 mL). The mixture was stirred at room temperature in the dark for 7 days under nitrogen. The solvent was removed under reduced pressure and the residue was dissolved in ethyl acetate (50 mL) and washed with 10% hydrochloric acid (100 mL). The organic layer was dried over Na_2SO_4, filtered, and the solvent was removed under reduced pressure. The residue was purified by chromatography on silica gel (ethyl acetate, R_f 0.18) to give acetamide **253** as a colourless oil (5.10 g, 64%); IR (thin film) cm^{-1} 3296 (s) (NH, stretch), 3078 (m) (CH, stretch), 2950 (m) (CH, stretch), 1739 (s) (ester C=O, stretch), 1647 (s) (amide, C=O, stretch), 1658 (m) (C=C, stretch); ^{1}H-NMR (400 MHz, $CDCl_3$) δ_H 1.65 (3H, s, CC*H$_3$*), 1.99 (3H, s, COC*H$_3$*), 2.35-2.65 (3H, m, C*H$_2$*, C*H*), 3.01-3.25 (2H, m, C*H$_2$*NH), 3.65 (3H, s, OC*H$_3$*), 4.74 (1H, s, C*H*$_a$H=C), 4.80 (1H, s, CH*H$_b$*=C) and 5.56 (1H, br s, N*H*); ^{13}C-NMR (100 MHz, $CDCl_3$) δ_C 18.6 (*C*H$_3$C), 23.4 (CO*C*H$_3$), 38.4 (*C*H), 39.2 (*C*H$_2$COO), 41.8 (*C*H$_2$NH), 52.1 (O*C*H$_3$), 113.3 (C=*C*H$_2$), 145.7 (*C*=CH$_2$), 170.7 (C=O amide) and 173.7 (CO ester); HRMS(EI$^+$) found 214.1446, $C_{10}H_{20}NO_3$ requires 214.1443; $[\alpha]^{22}_D$ = + 6.6 (*c* 2.07, $CHCl_3$).

(4*R)*-(Prop-1-ene-2yl) -2-piperidone (254)
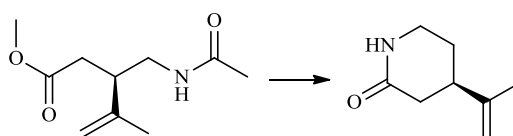
A stirred mixture of acetamide **253** (5.10 g, 23 mmol) and 3 M sodium hydroxide solution (30 mL, 90 mmol) was heated under reflux for 3 h. The solution was cooled, and neutralized to pH 6 with 1M HCl. The resulting mixture was evaporated under reduced pressure to dryness, and the residue was heated at 130 °C for 3 h. The solid was extracted with petroleum ether (12 × 25 ml). The combined ethereal extracts were evaporated under reduced pressure. The residue was purified by chromatography on silica gel (diethyl ether,

R_f 0.35) to give the lactam **254** as white crystals (3.17 g, 95%); mp 53-55˚C; IR (NaCl) cm^{-1} 3212 (s) (NH, stretch), 3083 (m) (CH, stretch), 2923 (m) (CH, stretch), 1668 (s) (lactam C=O, stretch), 1646 (s) (C=C, stretch); ^{1}H-NMR (400 MHz, CDCl$_3$) δ_H 1.69 (3H, s, CCH_3), 1.18-1.88 (1H, m, CH$_2$CHCH$_2$), 2.15-2.23 (2H, q, J = 6.0, 5.5 Hz, CHCH_2CH$_2$), 2.37-2.46 (2H, m, CHCH_2CO), 3.27-3.28 (2H, m, CH_2N), 4.68 (1H, s, CH_aH=C), 4.76 (1H, s, CHH_b=C) and 6.38 (1H, br s, NH); ^{13}C-NMR (100 MHz, CDCl$_3$) δ_C 21.0 (CH$_3$C), 27.2 (CH$_2$CHCH$_2$), 36.8 (CH$_2$CHCH$_2$), 39.6 (CH$_2$CO), 41.5 (CH$_2$NH), 110.6 (C=CH$_2$), 146.8 (C=CH$_2$) and 173.0 (C=O lactam); HRMS(EI$^+$) found 139.0996, C$_8$H$_{13}$NO requires 139.0997; $[\alpha]^{22}_D$ = + 5.8 (c 3.22, CHCl$_3$).

(4R)-(Prop-1-ene-2yl) piperidine-2-thione (255)
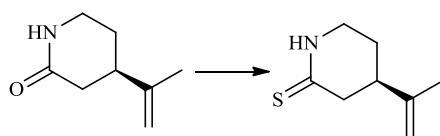
A mixture of lactam **254** (3.17 g, 22.8 mmol) and Lawesson's reagent (4.16 g, 11.4 mmol) was suspended in anhydrous toluene (30 mL), and heated under reflux for 1 h under nitrogen. The resulting mixture was cooled to room temperature, and then the solvent was removed under reduced pressure. The residue was purified by slica-gel column chromatography (DCM: petroleum ether, 2:1, R_f 0.33) to give a yellow powder. Recrystallisation from *i*-PrOH produced analytically pure white needles of thiolactam **255** (2.80 g, 78%); mp 93-95 ˚C; IR (NaCl) cm^{-1} 3169 (s) (NH, stretch), 3086 (m) (CH, stretch), 2952 (m) (CH, stretch), 1645 (s) (C=C, stretch), 1258 (m) and 1119 (s) (C=S); ^{1}H-NMR (400 MHz, CDCl$_3$) δ_H 1.65 (3H, s, CH_3C=C), 1.70-1.89 (1H, m, CH$_2$CHCH$_2$), 2.32 (2H, m, CHCH_2CH$_2$), 2.69 (1H, dd, J = 4.0, 8.0 Hz, HCHC=S), 3.06 (1H, dd, J = 4.0, 8.0 Hz, HCHC=S), 3.27-3.40 (2H, m, CH_2N), 4.85 (1H, s, CH_aH=C), 4.94 (1H, s, CHH_b=C) and 8.85 (1H, br s, NH); ^{13}C-NMR (100 MHz, CDCl$_3$) δ_C 20.2 (CH$_3$C), 26.3 (CH$_2$CHCH$_2$), 38.7 (CHCH$_2$CH$_2$), 41.2 (CH$_2$NH), 45.7 (CH$_2$C=S), 112.8 (C=CH$_2$), 145.7 (C=CH$_2$) and 206.9 (C=S); HRMS(EI$^+$) found, 156.0847 C$_8$H$_{13}$NS requires 156.0847 $[\alpha]^{22}_D$ = + 3.4 (c 0.62, CHCl$_3$).

(4*R*)-(Prop-1-ene-2yl)-(3-oxopentyl) piperidine-2-thione (256)
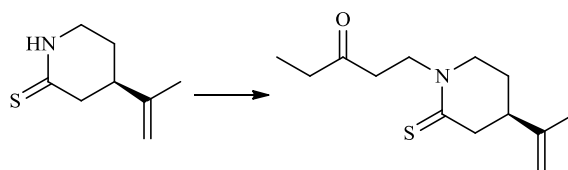
Piperidine-2-thione **255** (1.4 g, 9.02 mmol), anhydrous K_2CO_3 (2.75 g, 19.85 mmol) (kept at 140 °C for 12 h before use), and 18-crown-6 (0.30g, 1.13 mmol) were suspended in anhydrous THF (20 mL). After cooling to 0 °C, a first portion of ethyl vinyl ketone (1.2 mL, 12.09 mmol) was added dropwise with stirring under nitrogen. After the addition was complete, the solution was left at 0 °C for 5 min and then at room temperature for 1 h. The solution was cooled again to 0 °C, and a second portion of ethyl vinyl ketone (1.2 mL, 12.09 mmol) was added. Stirring was continued for 1 h at room temperature, monitoring the reaction by TLC. Sodium sulfate was then added, and the solution filtered and concentrated under reduced pressure. The resulting crude material was purified by silica column chromatography (eluent DCM, R_f 0.25) to give pure oxo-piperidine-2-thione **256** as a light yellow oil (1.82 g, 84.3%): IR (thin film) cm^{-1} 3085 (m) (CH, stretch), 1712 (s) (ketone C=O, stretch), 1645 (s (C=C, stretch), 1348 (s) and 1161 (m)(C=S); ^{1}H-NMR (400 MHz, CDCl$_3$) δ_H 1.03 (3H, t, *J* = 5.0 Hz, COCH$_2$C*H$_3$), 1.65 (3H, s, C*H$_3$C=C), 2.01 (1H, m, CH$_2$C*H*CH$_2$), 2.44 (2H, q, *J* = 7.5, 6.0 Hz, COC*H$_2$CH$_3$), 2.65 (2H, t, *J* = 6.5 Hz, C*H$_2$CH$_2$N), 2.97 (2H, dt, *J* = 6.5, 4.0 Hz, CH$_2$C*H$_2$CO), 3.10 (2H, ddd, *J* = 2.0, 3.5, 6.0 Hz, C*H$_2$CS), 3.59 (1H, app ddd, *J* = 4.0, 5.5, 13.0 Hz, C*H*N), 3.44 (1H, app ddd, *J* = 5.0, 10.0, 13.0 Hz, C*H*N), 4.10- 4.20 (2H, dt, *J* = 6.5, 13.0 Hz, NC*H$_2$CH$_2$CO) and 4.74 (1H, s, C*H$_a$H=C), 4.80 (1H, s, CH*H$_b$=C); ^{13}C-NMR (100 MHz, CDCl$_3$) δ_C 7.7 (COCH$_2$*C*H$_3$), 20.6 (*C*H$_2$CH$_2$CN), 27.5 (*C*H$_3$CH=CH$_2$), 36.1 (CH$_2$*C*HCH$_2$), 38.4 (*C*H$_2$CH$_2$CO), 38.6 (CO*C*H$_2$CH$_3$), 46.7 (*C*H$_2$CS), 49.9 (CN*C*H$_2$CH$_2$), 51.8 (*C*H$_2$CN), 110.5 (*C*H$_2$=CH), 145.8 (*C*=CH$_2$), 198.9 (C=O) and 209.8 (C=S); HRMS(EI$^+$) found 239.1352, C$_{13}$H$_{21}$NOS requires 239.1344;. [α]$^{22}_D$ = + 7.8 (*c* 2.27, CHCl$_3$).

(*R*)-9-methyl-2-(prop-1-en-2-yl)-3,4,6,7-tetrahydro-1H-quinolizin-8(2H)-one (257)
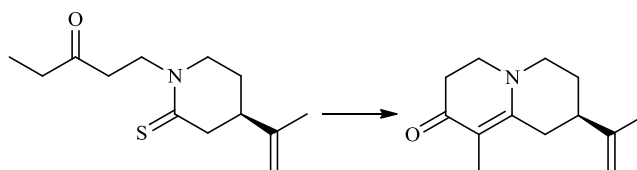
To a stirred suspension of oxo-piperidine-2-thione **256** (750 mg, 3.13 mmol) in anhydrous benzene (10 mL) under nitrogen was added freshly distilled Me_2SO_4 (0.49 mL, 5.33 mmol) drop wise by a syringe. The mixture was heated under reflux. After 1 h, 1, 8-diazabicyclo [5.4.0] undec-7-ene (DBU) (0.80 mL, 5.33 mmol) was added drop wise by a syringe; the resulting solution was heated under reflux for further 1 h. After cooling to room temperature, the solution was diluted with DCM (100 mL), and washed with water (100 mL). The combined organic extracts were dried over Na_2SO_4 then filtered and concentrated under reduced pressure. The residue was adjusted to pH 2 with 10% HCl (10 mL) and extracted with Et_2O (3× 10 mL). The aqueous phase was adjusted to pH 12 with NaOH (pellets) and extracted with Et_2O (5 x 10 mL). The combined ethereal layers were dried (K_2CO_3) and filtered, and the solvent was removed under reduced pressure. The crude was purified by chromatography on alumina (hexane: diethyl ether, 10%, R_f 0.35). The by-product eluted first and was isolated as a yellow oil (185 mg, 41%). Further elution with (hexane: diethyl ether, 30%, R_f 0.27) to give bicyclic enone **257** as colourless oil (360 mg, 40%); IR (thin film) cm^{-1} 3080 (m) (CH, stretch), 2925 (m) (CH, stretch), 1660 (m) (C=C, stretch), 1643 (m) (ketone C=O, stretch), 1656 (m) (C=C, stretch), 1346 (m) and 1241 (m) (CN, stretch); ^{1}H-NMR (400 MHz, CDCl$_3$) δ_H 1.52 [3H, s, C=C(C*H$_3$*)CO], 1.55 (3H, s, C=CC*H$_3$*), 1.81 (1H, m, C*H*), 2.08 (2H, d, *J* = 3.5 Hz, CHC*H$_2$*C), 2.252 (2H, q, *J* = 6.0, 5.5 Hz, CHC*H$_2$*CH$_2$), 2.52 (2H, m, C*H$_2$*CO), 3.02-3.14 (4H, m, CH$_2$C*H$_2$*NC*H$_2$*), 4.63 (1H, s, C*H$_a$*H=C), 4.73 (1H, s, CH*H$_b$*=C); ^{13}C-NMR (100MHz, CDCl$_3$) δ_C 9.6 (CH$_2$=C*C*H$_3$), 20.6 [C=C(*C*H$_3$)CO], 27.4 (CH$_2$*C*HCH$_2$), 32.2 (CH*C*H$_2$CH$_2$N), 35.1 (CH*C*H$_2$C), 38.1 (CO*C*H$_2$CH$_2$), 50.2 (CO*C*H$_2$CH$_2$N), 50.6 (CH$_2$*C*H$_2$N), 103.0 (*C*H$_2$=CCH$_3$), 110.5 [C=*C*(CH$_3$)CO], 146.9 (*C*=CCH$_3$), 160.3 [*C*=C(CH$_3$)CO] and 189.0 (*C*O ketone); HRMS(EI$^+$) found, 206.1540. C$_{13}$H$_{19}$NO requires 206.1545; $[\alpha]^{22}_D$ = + 9.1 (*c* 4.6, CHCl$_3$).

**(R)-8-hydroxy-9-methyl-2-(prop-1-en-2-yl)-1,2,3,4,6,7-hexahydroquinolizin-5-ium (258)**
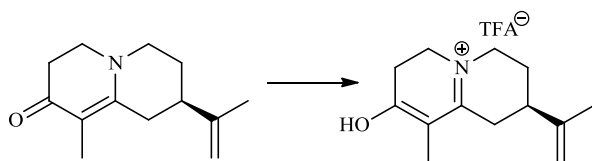
To a stirred solution of bicyclic enone **257** (250 mg, 1.21 mmol) in dry DCM (3 mL) was added TFA (0.1 mL, 1.21 mmol). After stirring for 5 min, the excess of TFA and solvent were removed under reduced pressure and the residue was placed under high vacuum to give the TFA salt **258** as yellow-orange oil (350 mg, 91%); IR (thin film) cm^{-1} 3340 (m) (OH, stretch) 3085 (m) (CH stretch), 2822 (m) (CH, stretch), 1640 (m) (C=C, stretch), 1346 (m) and 1241 (m) (C-N stretch); ^{1}H-NMR (400 MHz, CDCl$_3$) δ$_H$ 1.82 [3H, s, C=C(CH$_3$)CO], 1.85 (3H, s, C=CCH$_3$), 2.11 (1H, m, CH), 2.48 (2H, d, J = 3.5 Hz, CHCH$_2$C), 2.61 (2H, q, J = 6.0, 5.0 Hz, CHCH$_2$CH$_2$), 2.92 (2H, m, CH$_2$CO), 3.62-3.84 (4H, m, CH$_2$CH$_2$NCH$_2$), 4.75 (1H, s, CH$_a$H=C), 5.13 (1H, s, CHH$_b$=C); ^{13}C-NMR (100 MHz, CDCl$_3$) δ$_C$ 8.4 (CH$_3$C=COH), 22.5 (CH$_3$C=C), 31.3 (CH$_2$C=N), 32.1 (CH$_2$CH$_2$N), 33.8 (CH$_2$CH$_2$N), 38.5 (CH), 44.6 (CH$_2$N), 45.9 (CH$_2$N), 105.7 (C=COH), 105.1 (CH$_2$=CCH$_3$), 111.1-115.9 (q, J = 285 Hz, CF$_3$), 147.9 (C=CCH$_3$), 158.9-159.9 (q, J = 38 Hz, COO), 172.1 (C=N), 174.2 (COH=C). This salt was used in the next step without purification.

(1S,8R,9aS)-1,9a-Dimethyl-8-(prop-1-en-2-yl)hexahydro-1H-quinolizin-2(6H)-one (259)
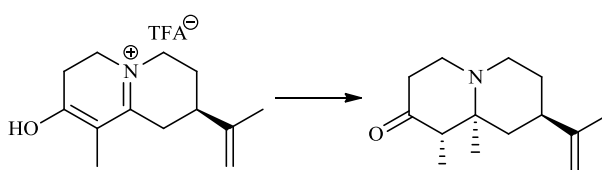
To a stirred solution of freshly prepared TFA salt **258** in dry THF (5 mL) was added methylmagnesium bromide (3 M in diethyl ether, 2.1 mL, 4.8 mmol) at room temperatur under argon. The mixture was heated under reflux for 24 h and then, after cooling to room temperature, a solution of saturated NH$_4$Cl (10 mL) and 10% NH$_4$OH (10 mL) were added and the resulting mixture was extracted with Et$_2$O (3 × 10 mL). The resulting residue was adjusted to pH 2 with 10% HCl (5 mL) and extracted with Et$_2$O (3 × 10 mL). The aqueous phase was adjusted to pH 12 with NaOH (pellets) and extracted with Et$_2$O (5 x 10 mL). The

combined ethereal layers were dried (K$_2$CO$_3$) then filtered and the solvent was removed under reduced pressure. The crude product was purified by chromatography on alumina (hexane-ethyl acetate; 20%, R$_f$ 0.26) to give amino ketone **259** as pale yellow oil (145 mg, 63%); IR (thin film) cm^{-1} 3050 (m) (CH, stretch), 2790-2966 (s) (CH, stretch), 1718 (s) (C=O, stretch), 1670 (m) (C=C, stretch), 1326 (m) and 1252 (s) (CN, stretch); ^{1}H-NMR (500 MHz, CDCl$_3$) δ$_H$ 0.71 (3H, s, CC*H$_3$*), 0.90 (3H, d, *J* = 7.0 Hz, C*H$_3$*CH), 1.12-1.15 [2H, m, C(CH$_3$)C*H$_2$*CH], 1.17-1.25 (2H, m, C*H$_2$*CH), 1.50-1.55 (2H, ddd, *J* = 7.0, 6.5, 5.0 Hz, C*H$_2$*CO), 1.63 (3H, s, C*H$_3$*C=C), 1.95-2.01 (1H, m, CH$_2$C*H*CH$_2$), 2.41-2.50 (1H, dddd, *J* = 8.0, 7.5, 6.0 Hz, C*H*CH$_3$), 2.62-2.69 (2H, m, C*H$_2$*N), 2.80-2.86 (2H, m, C*H$_2$*N), 4.65 (1H, s, C*H$_a$*H=C), 4.69 (1H, s, CH*H$_b$*=C); ^{13}C-NMR (125 MHz, CDCl$_3$) δ$_C$ 14.0 (*C*H$_3$C), 15.2 (*C*H$_3$CH), 20.6 (*C*H$_3$C=C), 31.9 (*C*H$_2$CH$_2$N), 37.6 (*C*H$_2$CCH$_3$), 41.2 (*C*H$_2$CO), 43.3 (*C*H$_2$CHCH$_2$), 49.7 (*C*H$_2$N), 50.0 (*C*H$_2$N), 56.5 (*C*HCH$_3$), 60.0 (*C*CH$_3$), 109.1 (*C*H$_2$=C), 149.1 (CH$_2$=*C*), 210.6 (*C*=O); HRMS(EI$^+$) found 221.1783, C$_{14}$H$_{23}$NO requires 221.1781.

(1*R*,8*R*,9aS)-1,9a-Dimethyl-8-(prop-1-en-2-yl)decahydroquinolizin-5-ium2,4,6-trinitrophenolate (260)
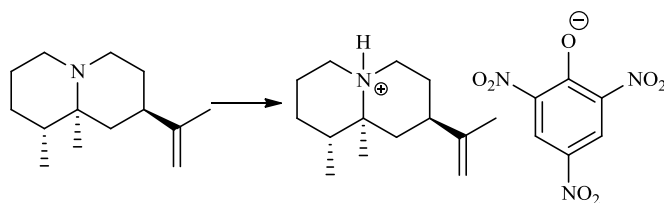
This salt was prepared by Dr. Juan. A. Faraldos: To a solution of the free amine **107** (20 mg, 0.09 mmol) in ethanol (4 mL) was added picric acid (20.6 mg, 0.09 mmol). After stirring for 1 h, the crystals were filtered and washed with ethanol (10 mL) to give picrate salt **260** (28 mg, 90%) as yellow crystals; IR (thin film) cm^{-1} 3070 (m) (CH, stretch), 2825 (m) (CH, stretch), 1660 (m) (C=C, stretch), 1619 (m), 1346 (m) and 1241 (m) (CN, stretch); ^{1}H-NMR δ$_H$ (500 MHz, CDCl$_3$) 0.76 (1H, m, *H*CHCHCH$_3$), 0.80 (3H, d, *J* = 6.5, C*H$_3$*CH), 1.24 (3H, s, C*H$_3$*C), 1.41 (1H, m, HC*H*CHCH$_3$), 1.72 (3H, s, C*H$_3$*C=C), 1.74-1.87 (3H, m, C*H$_2$*CCH$_3$, C*H*CH$_3$), 1.87-1.91 (2H, m, C*H$_2$*CH$_2$N), 2.12-2.16 (1H, t, *J* = 12.0 Hz, C*H*), 2.33-2.38 (2H, m, C*H$_2$*CH$_2$N), 2.95-3.00 (2H, m, C*H$_2$*N), 3.30-3.37 (2H, m, C*H$_2$*N), 4.74 (1H, s, C*H$_a$*H=C), 4.80 (1H, s, CH*H$_b$*=C), 8.86 (2H, s, ArH), 9.69 (1H, br s, NH); ^{13}C-NMR (125 MHz, CDCl$_3$) δ$_C$ 9.35 (*C*H$_3$CH), 15.72 (*C*H$_3$C), 20.50 (*C*H$_3$C=C), 22.78 (*C*H$_2$CHCH$_3$), 23.91 (*C*H$_2$CCH$_3$), 26.93 (*C*H$_2$CH$_2$N), 33.76

(CH$_2$CH$_2$N), 37.80 (CH), 38.95 (CHCH$_3$), 50.36 (CH$_2$N), 50.41 (CH$_2$N), 65.49 (CH$_3$C), 110.16 (CH$_2$=C), 126.61 (ArCH, ArCH), 127.89 (ArCNO$_2$), 141.80 (ArCNO2, ArCNO$_2$), 146.92 (CH$_2$=C), 161.65 (ArCO$^-$); HRMS(EI$^+$) found 208.2066. C$_{14}$H$_{26}$N requires 208.2065.

(1R,8R,9aS)-1,9a-Dimethyl-8-(prop-1-en-2-yl)decahydroquinolizin-5-iumperchlorate (261)
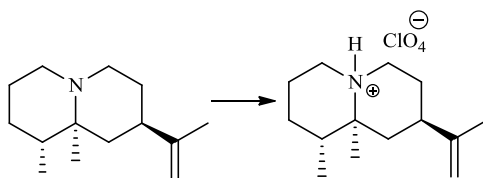
This salt was prepared by Dr. Juan. A. Faraldos: To a solution of the free amine **107** (20 mg, 0.09 mmol) in dry Et$_2$O (4 mL) was added perchloric acid (9.0 mL, 0.09 mmol) under a nitrogen. After stirring for 15 min, the crystals were filtered and washed with dry ether (10 mL) to give perchlorate salt **261** (35 mg, 88%) as white crystals ; IR (thin film) cm^{-1} 3068 (m) (CH, stretch), 2825 (m) (CH, stretch), 1665 (m) (C=C, stretch), 1619 (m), 1346 (m) and 1241 (m) (CN, stretch); ^{1}H-NMR (500 MHz, D$_2$O) δ_H 0.80-0.81 (3H, d, J = 6.5 Hz, CH$_3$CH), 1.18 (3H, s, CH$_3$C), 1.36-1.41 (1H, m, CHCH$_3$), 1.45-1.59 (4H, 2 x CH$_2$), 1.60 (3H, s, CH$_3$C=C), 1.73-2.05 (4H, m, CH$_2$CH$_2$N, CH$_2$CH$_2$N), 2.35 (1H, m, CH), 2.92-3.02 (3H, m, CH$_2$N, CHN), 3.11-3.19 (1H, ddd, J = 3.5, 3.0, 2.0 Hz, CHN), 4.66 (1H, s, CH$_a$H=C), 4.71 (1H, s, CHH$_b$=C); ^{13}C-NMR (125 MHz, D$_2$O) δ_C 9.8 (CH$_3$CH), 15.4 (CH$_3$C), 20.7 (CH$_3$C=C), 24.1 (CH$_2$CHCH$_3$), 27.5 (CH$_2$CCH$_3$), 29.2 (CH$_2$CH$_2$N), 37.7 (CH$_2$CH$_2$N), 41.5 (CH), 42.3 (CHCH$_3$), 50.8 (CH$_2$N), 50.9 (CH$_2$N), 66.8 (CCH$_3$), 110.4 (CH$_2$=C), 148.4 (CH$_2$=C); HRMS(EI$^+$) found 208.2058, C$_{14}$H$_{26}$N requires 208.2065.

(3R)-6-Methyl-3-(prop-1-en-2-yl)-1,2,3,4,6,7,8,9-octahydroquinolizin-5-ium bromide (262)
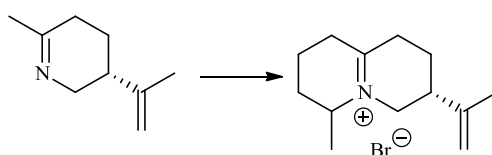
To a stirred solution of LDA (2 M in THF, 2 mL, 4.01 mmol) in dry THF (8 mL) at -35 °C under argon was added 3S-(prop-1-en-2-yl)-6-methyl-2,3,4,5-tetrahydropyridine (**182**) (500 mg, 3.6 mmol) in dry THF (5 mL) and the resulting mixture was stirred at this temperature for 45 min. After cooling to -78° C, a solution of 1,3-dibromo butane (0.46 mL, 4.01 mmol) in

dry THF (3 mL) was added, then the reaction mixture was stirred overnight at room temperature. The solvent was evaporated under reduced pressure and residual solvent was removed under high vacuum to yield a yellow-orange oil of dehydroquinolizinium bromide **262** (512 mg, 74%) that was used for the next step without purification;. IR (NaCl) cm-^{1} 3060 (m) (CH, stretch), 2850 (m) (CH, stretch), 1665 (m) (C=C, stretch), 1672 (m) (stretch, C=N); ^{1}H-NMR (400 MHz, CDCl$_3$) δ_H 1.64 (3H, d, J = 7.0 Hz, CH_3), 1.69 (3H, s, CH_3), 1.80-1.95 (6H, m, 3CH_2), 2.09 (1H, m, CHN), 2.40-2.92 (4H, m, 2CH_2C=N$^+$), 3.55-3.77 (1H, m, HCHN$^+$), 4.11-4.20 (1H, m, HCHN$^+$), 4.30-4.42 (1H, CHN$^+$), 4.67 (1H, s, CH_aH=C), 4.78 (1H, s, CHH_b=C); HRMS(EI$^+$) found, 192.1283 C$_{13}$H$_{22}$N requires 192.1280.

(3R,6S,9aS)-6,9a-Dimethyl-3-(prop-1-en-2-yl)decahydroquinolizine 5-oxide (282)
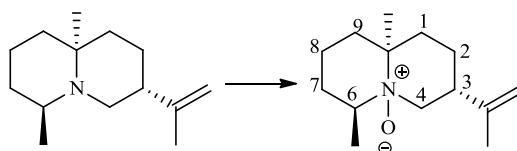
To a stirred solution of free amine **108** (15 mg, 0.07 mmol) in DCM (2 mL) were added K$_2$CO$_3$ (28 mg, 0.20 mmol) and *m*CPBA (77% in H$_2$O, 8.06 mg, 0.105 mmol) at 0 °C. After stirring for 2h at the same temperature, the mixture was filtered through a short pad of silica gel. The filtrate was concentrated under reduced pressure and the residue was purified by basic alumina-column (diethyl ether-methanol, 50%, R$_f$ 0.20) to afford N-oxide **282** as a yellow oil (12.1 mg, 76%); IR (NaCl) cm^{-1} 3376 (N-O, stretch), 2735-2822 (CH, stretch), 1658 (m) (C=C, stretch); ^{1}H-NMR (400 MHz, CDCl$_3$) δ_H 1.07-1.09 (2H, m, H9eq + H1eq), 1.17-1.19 (3H, d, J = 6.0 Hz, CH_3CH), 1.30-1.38 (1H, m, H7eq), 1.42 (3H, s, CH_3C), 1.45-1.68 (4H, m, H8 +H2), 1.71 (3H, s, CH_3C=CH), 2.25 (1H, ddd, J = 6.0, 5.5, 4.0 Hz, H7ax), 2.45-2.48 (1H, ddd, J = 5.5, 4.5, 4.0 Hz, H9ax), 2.55-2.62 (1H, ddd, J = 6.0, 4.5, 4.0 Hz, H1ax), 2.82 (1H, t, J = 6.5 Hz, H4), 3.18 (2H, m, H3+H4), 3.39 (1H, m, H6), 4.69 (1H, s, CH_aH=C), 4.78 (1H, s, CHH_b=C); ^{13}C-NMR (100MHz, CDCl$_3$) δ_C 15.0 (*C*H$_3$CH), 18.2 (*C*H$_2$), 18.9 (*C*H$_3$C), 21.4 (*C*H$_3$C=C), 23.6 (*C*H$_2$), 28.6 (*C*H$_2$), 32.4 (*C*H$_2$), 33.5 (*C*H$_2$), 37.7 (*C*H), 60.1 (*C*H$_2$N), 63.4 (*C*HN), 69.5 (CH$_3$*C*), 110.4 (*C*H$_2$=C), 146.4 (CH$_2$=*C*) HRMS(EI$^+$) found 224.2005, C$_{14}$H$_{25}$NO requires 224.2014.

(3S,6R,9aR)-6,9a-Dimethyl-3-(prop-1-en-2-yl)decahydroquinolizin-5-iumtrifluoroacetate (292)
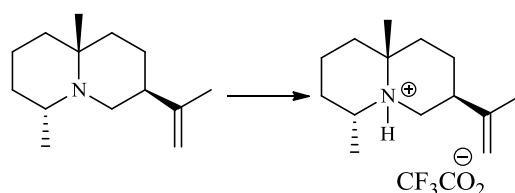
To a stirred solution of free amine **110** (20 mg, 0.096 mmol) in dry DCM (2 mL) was added TFA (8 μL, 0.096 mmol). After 15 min the solvent was evaporated under reduced pressure, and the residue was purified by column chromatography on alumina (ethyl acetate-methanol, 15%, R_f 0.16) to afford pure TFA salt **292** as yellow-orange oil (25 mg, 82%); IR (thin film) cm^{-1} 3060 (m) (CH, stretch), 2750-2876 (m) (CH, stretch), 1672 (m) (C=N, stretch), 1650 (m) (C=C, stretch); ^{1}H-NMR (400 MHz, CDCl$_3$) δ_H 1.27-1.28 (3H, d, J = 6.0 Hz, CH$_3$CH), 1.30 (3H, s, CH_3C), 1.70 (3H, s, CH_3C=C), 1.73-1.85 (10H, m, 5 x CH_2), 2.43 (1H, m, CH), 2.57 (1H, m, HCHN), 3.15 (1H, m, HCHN), 3.42 (1H, m, CHN), 4.68 (1H, s, CH_aH=C), 4.81 (1H, s, CHH_b=C), 7.25 (1H, br s, NH); ^{13}C-NMR (100 MHz, CDCl$_3$) δ_C 13.6 (CH$_3$CH), 16.7 (CH$_3$C=C), 19.4 (CH$_3$C), 22.2 (CH$_2$CH$_2$CCH$_3$), 28.7 (CH$_2$CHCH$_3$), 31.3 (CH$_2$CH$_2$CCH$_3$), 36.1 (CH$_2$CCH$_3$), 36.5 (CH$_2$CCH$_3$), 40.5 (CH), 47.6 (CH$_2$N), 55.7 (CH$_3$CHN), 61.9 (CN$^+$), 110.6 (CH$_2$=C), 111.3-117.5 (q, J = 286.0 Hz, CF$_3$), 142.4 (CH$_2$=C), 158.6-159.6 (q, J = 40.0 Hz, COO); HRMS(EI$^+$) found 208.2066. C$_{14}$H$_{26}$N requires 208.2065.

Jones oxidation of diol 249 to (R)-6-oxo-3-(prop-1-en-2-yl)-heptanoic acid (294)
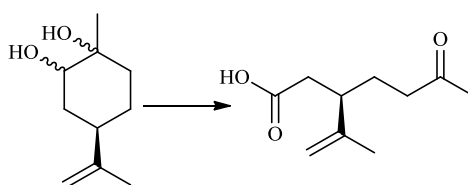
To a stirred solution of diol **249** (16.2 g, 0.09 mol) in acetone (200 mL) was added Jones reagent (~50 mL) slowly with stirring at 0 °C for 20 min. The addition was continued until the characteristic orange colour of the reagent persisted for about 20 min. A solution of NaHCO$_3$ (100 mL) was added, and the suspension was stirred vigorously until the pH of reaction mixture was neutral. The suspension was filtered and the residue was washed

with acetone (100 mL). H_2O (150 mL) was added to filtrate solution which was then extracted with DCM (5 x 100 mL). The organic layers were dried over $MgSO_4$, filtered and concentrated under reduced pressure. The residue was purified by silica-gel column chromatography (hexane-ethyl acetate; 15%, R_f 0.21) to give pure keto acid **294** as colourless oil (12.1 g, 69%); IR (thin film) cm^{-1} 3300 (vs) (OH, stretch), 2845 (m) (C-H, stretch), 1738 (s) (acid C=O, stretch), 1715 (s) (ketone C=O, stretch), 1660 (m) (C=C, stretch); ^{1}H-NMR (400 MHz, $CDCl_3$) δ_H 1.56 (3H, s, CCH_3), 1.8-2.7 (7H, m, 3 x CH_2, CH), 2.15 (3H, s, COCH_3) and 4.74 (1H, s, CH_aH=C), 4.80 (1H, s, CHH_b=C); ^{13}C-NMR (100 MHz, $CDCl_3$) δ_C 18.8 (*C*H$_3$C), 26.6 (*C*H$_3$CO), 30.4 (*C*H$_2$CH$_2$CO), 39.2 (*C*H$_2$CHCH$_2$), 41.5 (*C*H$_2$COO), 43.1 (*C*H$_2$CO), 113.5 (C=*C*H$_2$), 145.4 (CH$_2$=*C*), 178.5 (*C*O acid), 209.3 (*C*O ketone); HRMS(EI$^+$) found 185.1178, $C_{10}H_{16}O_3$ requires 185.1178.

(*S*)-4-Methoxybenzyl (5-oxo-2-(prop-1-en-2-yl)hexyl)carbamate (297)
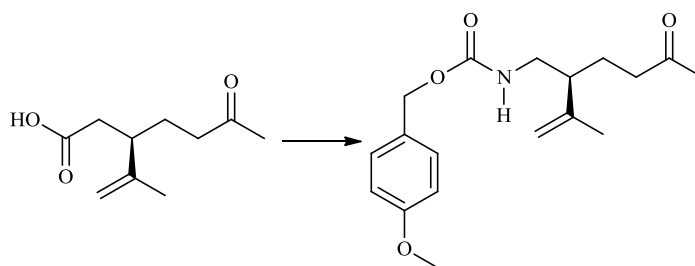
To stirred solution of keto acid **294** (12.1 g, 0.06 mol) in dry toluene (30 mL) was added Et_3N (25 mL, 0.143 mol) followed by diphenylphosphoryl azide (21 mL, 0.143 mol). After 15 min at room temperature the solution was heated at reflux for 2.5 h, after which time the starting material was converted completely to the isocyanate as judged by TLC (eluent hexane-ethyl acetate, 25%, R_f 0.37). *p*-Methoxybenzyl alcohol (15.1 mL, 0.143 mol) was then added and heated under reflux for 24 h. The solvent was evaporated under reduced pressure to give a black oil that was purified by chromatography on silica gel (hexane-ethyl acetate, 25%, R_f 0.28) to give the urethane **297** as pale yellow oil (10.5 g, 60%); IR (NaCl) cm^{-1} 3120 (m) (NH urethane, stretch), 2975 (m) (CH, stretch), 1716 (C=O, stretch), 1660 (m) (C=C, stretch); ^{1}H-NMR (400 MHz, $CDCl_3$) δ_H 1.52 (3H, s, CH_3C=C), 2.14 (3H, s, CH_3C=O), 1.80-2.72 [5H, m, (CH_2)$_2$CH], 2.91-3.10 (1H, m, CHNH), 3.20-3.31 (1H, m, HCNH), 3.75 (3H, s, OCH_3), 4.74 (1H, s, CH_aH=C), 4.80 (1H, s, CHH_b=C), 5.25 (2H, s, OCH_2), 6.85 (2H, d, *J* = 8.5 Hz), 7.27 (2H, d, *J* = 8.5 Hz); ^{13}C-NMR (100 MHz, $CDCl_3$) δ_C 18.2 (*C*H$_3$C=C), 23.9 (*C*H$_3$CO), 30.0

(CH_2CH), 40.9 (CH_2CO), 43.1 (CH), 46.6 (CH_2N), 55.2 (OCH_3), 66.4 (OCH_2), 113.9 ($CH_2=C$), 114.2 (ArCH, ArCH), 128.7 (ArCCH$_2$O), 129.9 (ArCH, ArCH), 144.3 ($CH_2=C$), 156.3 (COO), 159.6 (ArCOCH$_3$), 208.3 (C=O); HRMS(EI$^+$) found 319.1812, $C_{18}H_{25}NO_4$ requires 319.1811.

(*S*)-6-Methyl-3-(prop-1-en-2-yl)-2,3,4,5-tetrahydropyridine (298)
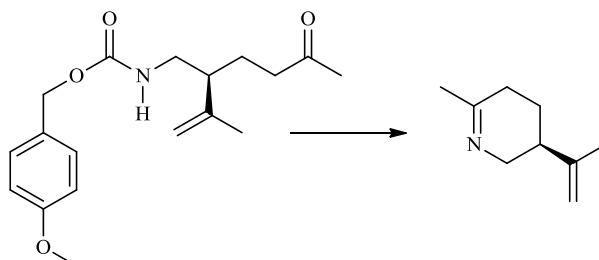
To a stirred solution of urethane **297** (10.5 g, 0.03 mol) in DCM (50 mL) was added, dropwise, a solution of TFA (20 mL) in DCM (50 mL) to give a bright orange solution. After 10 min, triisopropylsilane (3.2 mL) was added and stirring was continued for 5 min before ice-water (100 mL) was added. The aqueous phase was washed with DCM (2 x 20 mL) and then adjusted with KOH (pellets) until the pH reached 12. The equeous layer was extracted with DCM (4 x 20 mL). The combined DCM extracts were dried over K_2CO_3 and concentrated under redued pressure. The crude was purified by chromatography on basic alumina (hexane-diethyl ether, 50%, R$_f$ 0.35) to give cyclic imine **298** as yellow oil (3 g, 72%); IR (NaCl) cm^{-1} 3035 (m) (CH, stretch), 2975 (s) (CH, stretch), 1667 (m) (C=C, stretch), 1612 (m) (C-N, stretch); ^{1}H-NMR (400 MHz, CDCl$_3$) δ_H 1.42-1.60 (1H, m, HCHCH$_2$C=N), 1.65 (3H, s, CH_3C=C), 1.70-1.81 (1H, m, HCHCH$_2$C=N), 1.87 (3H, s, CH_3C=N), 2.01-2.11 (1H, m, CH), 2.15-2.25 (2H, m, CH_2C=N), 3.10-3.25 (1H, m, HCHN), 3.65-3.78 (1H, m, HCHN), 4.67 (1H, s, CH_aH=C), 4.78 (1H, s, CHH_b=C); ^{13}C-NMR (100MHz, CDCl$_3$) δ_C 20.0 (CH_3C=C), 24.4 (CH_3C=N), 27.0 (CH_2CH$_2$C=N), 30.3 (CH_2C=N), 39.7 (CHCH$_2$), 54.1 (CH_2N), 110.0 (CH_2=C), 147.2 (CH_2=C), 167.5 (C=N); HRMS(EI$^+$) found 138.1283, $C_9H_{16}N$ requires 138.1280.

(3*S*)-6-Methyl-3-(prop-1-en-2-yl)-1,2,3,4,6,7,8,9-octahydroquinolizin-5-ium bromide (299)
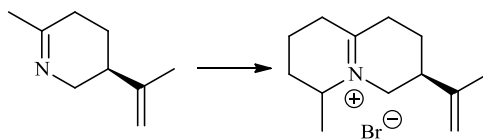
To a stirred solution of LDA (2 M in THF, 5 mL, 10.4 mmol) in dry THF (10 mL) at -35 °C under argon was added 3*R*-(prop-1-en-2-yl)-6-methyl-2,3,4,5-tetrahydropyridine (**298**) (1.3 g, 9.4 mmol) in dry THF (5 mL) and the resulting mixture stirred at this temperature for 45 min. After cooling to -78° C, a solution of 1,3-dibromo butane (0.50 mL, 10.4 mmol) in dry THF (3 mL) was added, then, the reaction mixture was stirred for 24 h at room temperature. The solvent was evaporated under reduced pressure, and residual solvent was removed under high vacuum to yield **299** as an orange solid (900 mg, 57%) that was used for the next step without purification;. IR (NaCl) cm^{-1} 3030 (m) (CH, stretch), 2850 (m) (CH, stretch), 1672 (m) (stretch, C=N), 1665 (m) (C=C, stretch); ^{1}H-NMR (400 MHz, CDCl$_3$) δ_H 1.64 (3H, d, *J* = 7.0 Hz, C*H$_3$*), 1.69 (3H, s, C*H$_3$*), 1.80-1.95 (6H, m, 3C*H$_2$*), 2.09 (1H, m, C*H*N), 2.40-2.92 (4H, m, 2C*H$_2$*C=N$^+$), 3.55-3.77 (1H, m, HC*H*N$^+$), 4.11-4.20 (1H, m, *H*CHN$^+$), 4.30-4.42 (1H, C*H*N$^+$), 4.67 (1H, s, C*H$_a$*H=C), 4.78 (1H, s, CH*H$_b$*=C); HRMS(EI$^+$) found, 192.1283. C$_{13}$H$_{22}$N requires 192.1280.

(3*S*,6*S*,9a*S*)-6,9a-Dimethyl-3-(prop-1-en-2-yl)decahydroquinolizin-5-iumtrifluoroacetate (300)
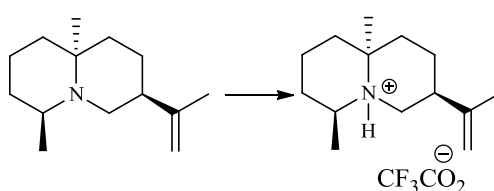
To a stirred solution of free amine **111** (12 mg, 0.057 mmol) in dry DCM (2 mL) was added TFA (5 µL, 0.057 mmol). After 15 min the solvent was evaporated under reduced pressure, and the residue was purified by column chromatography on alumina using (ethyl acetate-methanol, 15%, R$_f$ 0.150) to afford pure TFA salt **300** as yellow-orange oil (15 mg, 82%); IR (NaCl) cm^{-1} 3040 (m) (CH, stretch), 2830-2740 (m) (CH, stretch), 1672 (m) (C=N, stretch), 1665 (m) (C=C, stretch); ^{1}H-NMR (400 MHz, CDCl$_3$) δ_H 1.27-1.29 (3H, d, *J* = 6.5 Hz, CH$_3$C*H*), 1.53 (3H, s, C*H$_3$*C), 1.70 (3H, s, C*H$_3$*C=C), 1.29-1.1.79 (10H, m, 5 x C*H$_2$*), 2.09 (1H, m, C*H*),

2.72 (1H, m, *H*CHN), 3.20 (1H, m, HC*H*N), 3.87 (1H, m, C*H*N), 4.70 (1H, s, C*H*aH=C), 4.81 (1H, s, CH*H*b=C), 6.50 (1H, br s, NH); ^{13}C-NMR (100 MHz, CDCl$_3$) δ_C 17.6 (*C*H$_3$CH), 18.5 (*C*H$_3$C=C), 21.2 (*C*H$_3$C), 23.3 (*C*H$_2$CH$_2$CCH$_3$), 23.6 (CH$_2$*C*H$_2$CCH$_3$), 25.4 (*C*H$_2$CCH$_3$), 25.8 (*C*H$_2$CCH$_3$), 37.3 (*C*H$_2$CHN), 40.0 (*C*H), 34.2 (*C*H$_2$N), 53.2 (CH$_3$*C*HN), 60.6 (*C*N$^+$), 111.5 (*C*H$_2$=C), 112.2-117.3 (q, J = 287.0 Hz, *C*F$_3$), 144.8 (CH$_2$=*C*), 160.2-160.9 (q, J = 40.0 Hz, *C*OO); HRMS(EI$^+$) found 208.2066. C$_{14}$H$_{26}$N requires 208.2065.

(*R*)-6-(3-(2-Methyl-1,3-dioxolan-2-yl)propyl)-3-(prop-1-en-2-yl)-2,3,4,5-tetrahydropyridine (302)
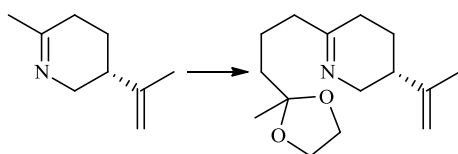
A stirred solution of LDA (0.8 mL, 2 M in THF, 1.59 mmol) in dry THF (5 mL) under argon was cooled to -78 °C and a solution of 3*S*-(prop-1-en-2-yl)-2, 3, 4, 5-6-methyl-tetrahydropyridine (**182**) (200 mg, 1.45 mmol) in dry THF (3 mL) was added. The solution was allowed to warm slowly to -35 °C and was stirred at this temperature for 30 min. The bright orange solution was then cooled to -78°C and a solution of 1-bromo-3-butane ethylene acetal (**301**) (0.20 mL, 1.59 mmol) in dry THF (3 mL) was added dropwise. After the addition, the reaction was allowed to warm to room temperature over 2 h. As the temperature reached to -15 °C the orange colour disappeared. The reaction was then stirred for 24 h at room temperature, before quenching with water (10 mL). The aqueous phase was extracted with ether (3 x 5 mL) and the combined organic layers dried over K$_2$CO$_3$ and filtered. The filtrate was evaporated under reduced pressure affording crude of product as a yellow oil. This was purified by chromatography on basic alumina (hexane-diethyl ether, 50%, R$_f$ 0.37) to give pure imine acetall (**302**) as pale yellow oil (175 mg, 70% yield); IR (NaCl) cm^{-1} 3060 (m) (CH, stretch), 1660 (m) (C=C, stretch), 1672 (m) (C=N, stretch); ^{1}H-NMR (400 MHz, CDCl$_3$) δ_H 1.33 [3H, s, C*H*$_3$C(OCH$_2$)$_2$], 1.60-1.64 (6H, m, 3 x C*H*$_2$), 1.73 (3H, s, C*H*$_3$C=C), 2.17 (4H, m, 2C*H*$_2$C=N), 2.19 (1H, m, C*H*), 3.19 (1H, m, *H*CHN), 3.73 (1H, m, HC*H*N), 3.96 (4H, m, OC*H*$_2$C*H*$_2$O), 4.71 (1H, s, C*H*aH=C), 4.78 (1H, s, CH*H*b=C); ^{13}C-NMR (100MHz, CDCl$_3$) δ_C 20.9 (*C*H$_3$C=C), 23.8 [*C*H$_3$(CH$_2$O)$_2$], 26.4 (*C*H$_2$), 35.4 (*C*H$_2$), 37.1 (*C*H$_2$), 39.5 (*C*H$_2$), 40.5 [*C*H$_2$C(CH$_2$O)$_2$], 41.1 (*C*H), 54.0 (*C*H$_2$N), 64.6 (*C*H$_2$O), 64.7 (*C*H$_2$O),

109.7 (*CH*$_2$=C), 109.8 [CH$_2$*C*(CH$_2$O)$_2$], 147.1 (CH$_2$=*C*), 171.2 (*C*=N); HRMS(EI$^+$) found 251.1283,. C$_{15}$H$_{25}$NO$_2$ requires 251.1280.

REFERENCES

1. Buckingham, J. (ed), (1998) Dictionary of natural product on CD-ROM. 6.1. Chapman Hall, London.

2. Kliebenstein, D. J., Lambrix, V. M., Reichelt, M. and Mitchell-Olds, T. (2001) Gene duplication in the diversification of secondary metabolism: tandem 2-oxoglutarate-dependent dioxygenases control glucosinolate biosynthesis in arabidopsis. *Plant Cell*. **13**, 681-693.

3. Bick, J. A. and Lange, B. M. (2003) Metabolic cross talk between. cytosolic and plastidial pathways of isoprenoid biosynthesis: unidirectional transport of intermediates across the chloroplast envelope membrane. *Arch. Biochem. Biophys.415*, 146-154.

4. Sacchettini, J.C. and Poulter, C.D. (1997) Creating isoprenoid diversity. *Science. 277*, 1788-1789.

5. Christianson, D.W. (2007) Roots of biosynthetic diversity. *Science 316*, 60-61.

6. Davis, E. and Croteau, R. (2000) Cyclization enzymes in the biosynthesis of monoterpenes, sesquiterpenes, and diterpenes. Eds. F. Leeper, and J. Vederas, Springer Berlin Heidelberg. 53-95.

7. Cane, D. (1999) Comprehensive Natural Products Chemistry: Isoprenoids Including Carotenoids and Steroids; Barton, D., Nakanishi, and K., Meth-Cohn, Eds. Cane, D. E., Vol. Ed., UK, Vol. 2. pp. 155-200. Elsevier Science, Oxford.

8. Poulter, C.D. and Rilling, H.C. (1976) Prenyl transferase: the mechanism of the reaction. *Biochemistry 15*, 1079-1083.

9. Ogura, K. and Koyama, T. (1998) Enzymatic aspects of isoprenoid chain elongation. *Chem. Rev. 98*, 1263-1276.

10. Paul, M.D. (1997) Medicinal Natural Products: A Biosynthetic Approach. UK. Chap. 5, pp. 186. John Wiley & Sons.

11. Chappell, J. (1995) The biochemistry and molecular biology of isoprenoid metabolism. *Plant Physiol. 107*, 1-6.

12. McGarvey, D. J. and Croteau, R. (1995) Terpenoid metabolism. *Plant Cell. 7,*1015-1026.

13. Crowell, P. L. (1999) Prevention and therapy of cancer by direct monoterpenes. *J. Nutr. 129,* 775S-778S.

14. Santoyo, S., Cavero, S., Jaime, L., Ibanez, E., Senorans, J. and Reglero, G. (2005) Chemical composition and antimicrobial activity of *Rosmarinus officinalis* L. essential oil obtained via supercritical fluid extraction. *J. Food Protect. 68*, 790-795.

15. Glasby, J. S. (1982) Encyclopedia of Terpenoids, Wiley, Chichester.

16. Cane, D. E. (1985) Isoprenoid biosynthesis. Stereochemistry of the cyclization of allylic pyrophosphate. *Acc. Chem. Res.18*, 220-226.

17. Christianson, D. W. (2006) Structural biology and chemistry of the terpenoidcyclases. *Chem. Rev. 106*, 3412-3442.

18. Cane, D. E. (1990) Enzymic formation of sesquiterpenes. *Chem. Rev. 90,*1089-1103.

19. Newman, D. J., Cragg, G. M. and Sander, K. M. (2000) The influence of natural product upon drug discovery. *Nat. Prod. Rep*. 17. 215-234.

20. Hien, T. T., White, N. J. and White, B. C. (1993) Qinghaosu. *The Lancet. 341*, 603-608.

21. Bouwmeester, H. J., Wallaart, T. E., Janssen, M. H., Loo, B. V., Jansen, B. J., Posthumus, M. A., Schmidt, C. O., De Kraker J. W., Konig, W. A. and Franssen, M. C. R. (1999) Amorpha-4, 11-diene synthase catalyses the first probable step in artemisinin biosynthesis. *Phytochem.52,* 843-854.

22. Faraldos, J. A., Gonzalez, V., Li, A., Yu, F., Köksai, M., Christianson, D. W. and Allemann, R. K. (2012) Probing the mechanism of 1, 4-conjugate elimination reactions catalyzed by terpene synthases. *J. Am. Chem. Soc. 134*, 20844-20848.

23. Pickett, J. A. and Griffiths, D. C. (1980) Composition of aphid pheromones. *J. Chem. Ecol.6,* 349-360.

24. Essenberg, M., Grover, P. B. and Cover, E. C. (1990) Accumulation of antibacterial sesquiterpenoids in bacterially inoculated *Gossypium* leaves and cotyledons. *Phytochemistry 29*, 3107-3113.

25. Felicetti, B. and Cane, D. E. (2004) Aristolochene synthase: mechanistic analysis of active site residues by site-directed mutagenesis. *J. Am. Chem. Soc.126*, 7212-7221.

26. Sitton, D. and West, C. A. (1975) Casbene: An anti-fungal diterpene produced in cell-free extracts of *Ricinus communis* seedling. *Phytochem.14*, 1921-1925.

27. Jennewein, S. and Croteau, R. (2001) Taxol: biosynthesis, molecular genetics, and biotechnological applications. *Appl. Microbiol. Biot. 57*, 13-19.

28. Pandit, J., Danley, D. E., Schulte, G. K., Mazzalupo, S., Pauly, T. A., Hayward, C. M., Hamanaka, E. S., Thompson, J. F. and Harwood, H. J. (2000) Crystal structure of human squalene synthase A key enzyme in cholesterol biosynthesis. *J. Biol. Chem. 275*, 30610-30617.

29. Chichester, C. O. and Nakayama, T. O. M. (1963) The Biosynthesis of Carotenoids and Vitamin A in Biogenesis of Natural Compounds, Peter Bernfield. Pergamon Press Ltd., Norwich.

30. Fishkin, N., Berova, N. and Nakanishi, K. (2004) Primary events in dim light vision: A chemical and spectroscopic approach toward understanding protein/ chromophore interactions in rhodopsin. *Chem. Rec. 4*, 120-135.

31. Cemek, M., Dede, S., Bayiroglu, F., Caksen, H., Cemek, F. and Yuca, K. (2005) Oxidant and antioxidant levels in children with acute otitis media and tonsillitis: A comparative study. *Int. J. Pediatr. Otorhi. 69*, 823-827.

32. Wallach, O. (1887) Zur Kenntnis der Terpene und Ätherischen Oele. *Justus Lieb. Ann. Chem. 238*, 78-89.

33. Ruzicka, L. (1953) The isoprene rule and the biogenesis of terpenic compounds. *Experientia 9*, 357-367.

34. Eschenmoser, A., Ruzicka, L., Jeger, O. and Arigoni, D. (1955) Zur kenntnis der Triterpene. 190. Mitteilung. Eine stereochemische Interpretation der Biogenetischen Isoprenregel bei den Triterpenen. *Helv. Chim. Acta. 38*, 1890-1904.

35. Eisenreich, W., Bcher, A., Arigoni, D. and Rohdich, F. (2004) Biosynthesis of isoprenoids via non-mevalonate pathway. *Cell. Mol. Life. Sci. 61*, 1401-1426.

36. Poulter, C. D. and Rilling, H. C. (1981) Prenyl transferases and Isomerases, John Wiley & Sons. New York.

37. Bach, T. J., Rogers, D. H. and Rudney, H. (1986) Detergent-solubilization, purification, and characterization of membrane-bound 3-hydroxy-3-methylglutaryl-coenzyme. A reductase from radish seedlings. *Eur. J. Biochem. 154*, 103-111.

38. Qureshi, N. and Porter, J. W. (1981) Conversion of Acetyl-CoA to Isopentenyl Pyrophosphate in Biosynthesis of Isoprenoid Compounds, John Wiley & Sons. New York.

39. Rohmer, M., Knani, M., Simonin, P., Sutter, B. and Sahm, H. (1993) Isoprenoid biosynthesis in bacteria: a novel pathway for the early steps leading to isopentenyl diphosphate. *Biochem. J. 295*, 517-524.

40. Rohmer, M. (1999) The discovery of a mevalonate-independent pathway for isoprenoid biosynthesis in bacteria, algae and higher plants. *Nat. Prod. Rep. 16*, 565-574.

41. Chappell, J. and Coates, R. M. (2010) Comprehensive Natural Products II: Chemistry and Biology. Chap. 16, pp.609-637. Elsevier, Amsterdam.

42. Munck, S. L. and Croteau, R. (1990) Purification and characterization of the sesquiterpene cyclase patchoulol synthase from *Pogostemon cablin*. *Arch. Biochem. Biophys. 282*, 58-64.

43. Vogeli, U., Freeman, J. W. and Chappell, J. (1990) Purification and characterization of an inducible sesquiterpene cyclase from Elicitor-treated tobacco cell suspension cultures. *Plant Physiol. 93*, 182-187.

44. Cane, D. E. and Kang, I. (2000) Aristolochene synthase: purification, molecular cloning, high-level expression in *Escherichia* coli, and characterization of the *Aspergillus terreus* cyclase. *Arch. Biochem.Biophys. 376,* 354-364.

45. Holloway, P. W. and Popjak, G. (1967) The purification of 3, 3-dimethylallyl- and geranyl-transferase and of isopentenyl pyrophosphate isomerase from pig liver. *Biochem. J. 104*, 57-70.

46. Tarshis, L. C., Yan, M., Poulter, C. D. and Sacchettini, J. C. (1994) Crystal structure of recombinant farnesyl diphosphate synthase at 2.6-Å. resolution. *Biochemistry 33*, 10871-10877.

47. Sander, C. and Schneider, R. (1991) Database of homology-derived protein structure and the structural meaning of sequence alignment. *Protein. 9*, 56-68.

48. Caruthers, J. M., Kang, I., Rynkiewicz, M. J., Cane, D. E. and Christianson, D. W. (2000) Crystal structure determination of aristolochene synthase from the blue cheese mold, *Penicillium roqueforti*. *J. Biol. Chem. 275*, 25533-25539.

49. Shishova, E. Y., Costanzo, L., Cane, D. E. and Christianson, D. W. (2007) X-ray crystal structure of aristolochene synthase from *Aspergillus terreus* and evolution of templates for the cyclization of farnesyl diphosphate. *Biochemistry 46,* 1941-1951.

50. Wendt, K. U. and Schulz, G. E. (1998) Isoprenoid biosynthesis: manifold chemistry catalyzed by similar enzymes. *Structure 6*, 127-133.

51. Lesburg, C. A., Caruthers, J. M., Pascall, C. M. and Christianson, D. W. (1998) Managing and manipulating carbocations in biology: terpenoid cyclase structure and mechanism. *Curr. Opin. Struct. Biol. 8*, 695-703.

52. Sun, T. P. and Kamiya, Y. (1994) The *Arabidopsis* GA1 locus encodes the cyclase *ent*-kaurene synthetase A of gibberellins biosynthesis. *Plant Cell. Online. 6*, 1509-1518.

53. Chen, X. Y., Chen, Y., Heinstein, P. and Davisson, V. J. (1995) Cloning, expression, and characterization of (+)-delta-cadinene synthase: a catalyst for cotton phytoalexin biosynthesis. *Arch. Biochem. Biophys. 324*, 255-266.

54. Starks, C. M., Back, K., Chappell, J. and Noel, J. P. (1997) Structural basis for cyclic terpene biosynthesis by tobacco 5-*epi*-aristolochene synthase. *Science 277*, 1815-1820.

55. Cane, D. E., Prabhakaran, P. C., Salaski, E. J., Harrison, P. H., Noguchi, H. and Rawlings, B. J. (1989) Aristolochene biosynthesis and enzymatic cyclization of farnesyl pyrophosphate. *J. Am. Chem. Soc.* *111*, 8914-8916.

56. Govindachari, T. R., Mohamed, P. A. and Parthasarathy, P. C. (1970) Ishwarane and aristolochene, two new sesquiterpene hydrocarbons from *Aristolochia indica. Tetrahedron 26*, 615-619.

57. Cane, D. E., Rawlings, B. J. and Yang, C. C. (1987) Isolation of (-)-gamma-cadinene and aristolochene from *Aspergillus terreus*. *J. Antibiot. 40*, 1331-1334.

58. Proctor, R. H. and Hohn, T. M. (1993) Aristolochene synthase. Isolation, characterization, and bacterial expression of a sesquiterpenoid biosynthetic gene (*Ari1*) from *Penicillium roqueforti. J. Biol. Chem. 268*, 4543-4548.

59. Hohn, T. M. and Plattner, R. D. (1989) Purification of the sesquiterpene cyclase aristolochene synthase from *Penicillium roqueforti. Arch. Biochem. Biophys. 272*, 137-143.

60. Deligeorgopoulou, A., Taylor, S. E., Forcat, S. and Allemann, R. K. (2003) Stabilisation of eudesmane cation by tryptophan 334 during aristolochene synthase catalysis. *Chem. Commun.,* 2162-2163.

61. Forcat, S. and Allemann, R. K. (2004) Dual role for phenylalanine 178 during catalysis by aristolochene synthase. *Chem. Commun.*, 2094-2095.

62. Forcat, S. and Allemann, R. K. (2006) Stabilisation of transition states prior to and following eudesmane cation in aristolochene synthase. *Org. Biomol. Chem. 4*, 2563-2567.

63. Cavert, M. J., Taylor, S. E. and Allemann, R. K. (2002) Tyrosine 92 of aristolochene synthase directs cyclisation of farnesyl pyrophosphate. *Chem. Commun.,* 2384-2385.

64. Yu, F., Miller, D. J. and Allemann, R. K. (2007) Probing the mechanism of aristolochene synthase with 12,13-difluorofarnesyl diphosphate. *Chem. Commun.*, 4155-4157.

65. Cane, D. E., Prabhakaran, P. C., Oliver, J.S. and McIlwaine, D. B. (1990) Aristolochene biosynthesis. Stereochemistry of the deprotonation steps in the enzymatic cyclization of farnesyl pyrophosphate. *J. Am. Chem. Soc. 112,* 3209-3210.

66. Miller, D. J., Gao, J., Truhlar, D. G., Young, N. J., Gonzalez, V. and Allemann, R. (2008) Stereochemistry of eudesmanecation formation during catalysis by aristolochene synthase from *Penicillium roqueforti. Org. Biomol. Chem. 6*, 2346-2354.

67. Calvert, M. J., Ashton, P. R. and Allemann, R. k. (2002) Germacrene A is a product of the aristolochene synthase-mediated conversion of farnesyl pyrophosphate to aristolochene. *J. Am. Chem. Soc. 124*, 11636-11641.

68. Miller, D. J., Knight, D. W. and Allemann, R. K. (2009) 6- and 14-Fluorofarnesyl diphosphate: mechanistic probes for the reaction catalysed by aristolochene synthase. *Org. Biomol. Chem. 7*, 962-975.

69. Köksai, M., Zimmer, I., Schnitzler, J. P. and Christianson D. W. (2010) Structure of isoprene synthase illuminates the chemical mechanism of teragram atmospheric carbon emission. *J. Mol. Biol. 402*, 363-373.

70. Dougherty, D. A. (1996) Cation-π interactions in chemistry and biology: a new view of benzene, Phe, Tyr, and Trp. *Science 271,* 163-168.

71. Miller, D. J. and Allemann, R. K. (2012) Sesquiterpene synthases: passive catalysts or active players? *Nat. Prod. Rep. 29*, 60-71.

72. Cane, D. E. and Tsantrizos, Y. S. (1996) Aristolochene synthase. Elucidation of the cryptic germacreneA synthase activity using the anomalous substrate dihydrofarnesyl diphosphate. *J. Am. Chem. Soc. 118*, 10037-10040.

73. Miller, D. J., Yu, F. and Allemann, R. K. (2007) Aristolochene synthase- catalyzed cyclization of 2-fluorofarnesyl-diphosphate to 2-fluorogermacrene A. *Chem. Bio. Chem. 8*, 1819-1825.

74. Faraldos, J. A., Antonczak, A. K., Gonzalez, V., Fullerton, R., Tippmann, E. M. and Allemann, R. K. (2011) Probing eudesmane cation- π interactions in catalysis by aristolochene synthase with non-canonical amino acids. *J. Am. Chem. Soc. 133*, 13906-13909.

75. McGeady, P., Pyun, H. J., Coates, R. M. and Croteau, R. (1992) Biosynthesis of monoterpenes: inhibition of (+)-pinene and (-)- pinene cyclases by thia and aza analogs of the 4R- and 4S- alpha-terpinyl carbocation. *Arch. Biochem. Biophys. 299*, 63-72.

76. Whittington, D. A., Wise, M. L., Urbansky, M., Coates, R. M., Croteau, R. B. and Christianson, D. W. (2002) Bornyl diphosphate synthase: structure and strategy for carbocation manipulation by a terpenoid cyclase. *Proc. Natl. Acad. Sci.USA. 99*, 15375-15380.

77. Cane, D. E., Yang, G., Coates, R. M., Pyun, H. J. and Hohn, T.M. (1992) Trichodiene synthase. Synergistic inhibition by inorganic pyrophosphate and aza analogs of the bisabolyl cation. *J. Org. Chem. 57*, 3454-3462.

78. Peters, R. J., Ravan, M. M., Coates, R. M. and Croteau, R. B. (2001) Bifunctional abietadiene synthase: free diffusive transfer of the (+)-copalyl diphosphate intermediate between two distinct active sites. *J. Am. Chem. Soc. 123*, 8974-8978.

79. Ravan, M. M., Peters, R. J., Coates, R. M. and Croteau R. (2002) Mechanism of abietadiene synthase catalysis: stereochemistry and stabilization of the cryptic pimarenyl carbocation intermediates. *J. Am. Chem. Soc. 124*, 6998-7006.

80. Sandifer, R. M., Thompson, M. D., Gaughan, R. G. and Poulter, C. D. (1982) Squalene synthase. Inhibition by an ammonium analogue of a carbocationic intermediate in the conversion of presqualene pyrophosphate to squalene. *J. Am. Chem. Soc. 104*, 7376-7378.

81. Ruhl, K. K., Anzalone, L., Arquropoulos, E. D., Gayen, A. K. and Spencer, T. A. (1989) Aza decalin analogs of 4, 4, 10β-trimethyl-trans-decal-3β-ol: synthesis and assay as inhibitors of oxidosqualene cyclase. *Bioorg. Chem. 17*, 108-120.

82. Steiger, A., Pyun, H. J. and Coates R. M. (1992) Synthesis and characterization of aza analog inhibitors of squalene and geranygeranyl diphosphate synthases. *J. Org. Chem. 57*, 3444-3449.

83. Koohang, A. and Coates R. M. (1999) Synthesis and evaluation of aziridine analogues of presqualene diphosphate as squalene synthase inhibitors. *J. Org. Chem. 64,* 6-7.

84. Narula, A. S., Rahier, A., Benveniste, P. and Schuber, F. (1981) 24-Methyl-25-aza cycloartanol, an analog of a carbonium ion high-energy intermediate, is a potent inhibitor of (s)-adenosyl-l-methionine: sterol c-24-methyl transferase in higher plant cells. *J. Am. Chem. Soc. 103*, 2408- 2409.

85. Rahier, A., Taton, M. and Benveniste, P. (1990) Inhibition of sterol biosynthesis enzymes *in vitro* by analogues of high-energy carbocationic intermediates. *Biochem. Soc. Trans. 18*, 48-52.

86. Poulter, C. D. (1990) Biosynthesis of non-head-to-tail terpenes. Formation of 1'-1 and 1'-3 linkages. *Acc. Chem. Res. 23*, 70-77.

87. Abe, I., Rohmer, M. and Prestwich, G. D. (1993) Enzymatic cyclization of squalene and oxidosqualene to sterols and triterpenes. *Chem. Rev. 93*, 2189-2206.

88. Rahier, A., Genot, J. C., Schuber, F. and Narula, A. S. (1984) Inhibition of S-adenosyl-l-methionine sterol-c-24-methyltransferase by analogues of a carbocationic ion high-energy intermediate. Structure activity relationship for C-25 heteroatoms (N, As, S) substituted triterpenoid derivatives. *J. Biol. Chem. 259*, 15215-15223.

89. Faraldos, J. A., Kariuki, B. and Allemann, R. K. (2010) Intermediacy of eudesmane cation during catalysis by aristolochene synthase. *J. Org. Chem. 75*, 1119-1125.

90. Koohang, A., Bailey, J. L., Coates, R. M., Erickson, H. K., Owen, D. and Poulter, C. D. (2010) Enantioselective inhibition of squalene synthase by aziridine analogues of presqualene diphosphate. *J. Org. Chem. 75*, 4769- 4777.

91   Roy, A., Robert, F. G., Wilderman, P. R., Zhou, K., Peters, R. J. and Coates, R. M. (2007) 16-Aza-*ent*-trachylobane: potent mechanism-based inhibitors of recombinant ent-kaurene synthase from *Arabidopsis thaliana*. *J. Am. Chem. Soc. 129*, 12453-12460.

92   Nishikawa, Y., Kitajima, M., Kogure, N. and Takayama, H. (2009) A divergent approach for the total syntheses of cernuane-type and quinolizidine-type Lycopodium alkaloids. *Tetrahedron 65*, 1608-1617.

93   Moynehan, T. M., Schofield, K., Jones, R. and Katritzky, A. R. (1962) The synthesis and stereochemistry of quinolizidine and the monomethylquinolizidines, and of their salts and quaternary salts. *J. Chem. Soc.,* 2637-2658.

94.   Bohlmann, F. (1958) Lupinen-alkaloide, VIII. Zur Konfigurationsbest-immung von Chinolizidin- derivaten. *Chem. Ber. 91*, 2157-2167.

95.   Boekelheide, V. and Rothchild, S. (1949) Curariform activity and chemical structure. 5. Syntheses in the quinolizidine series. *J. Am. Chem. Soc. 71*, 879-886.

96.   Bohlmann, F., Ottawa, N. and Keller, R. (1954) Aufbau des tetrahydro-chinolizons und des "Bispidins" (Beiträge zur synthese des cytisins). Justus Lieb. Ann. Chem. *587*, 162-176.

97.   Rodd, H. and Coffey, S. (1978) Rodd's Chemistry of Carbon Compounds: A Modern Comprehensive Treatise, Vol. 4, Heterocyclic Compounds. Isoquinoline, Lupinane and QuinolizidineAlkalids. 2nd Ed., Elsevier. Amsterdam.

98.   Goldberg, S. I. and Ragade, I. (1967) A total synthesis of optically active lupinine without benefit of resolution. *J. Org. Chem. 32*, 1046-1050.

99.   Leonard, N. J. and Hay, A. S. (1956) Unsaturated amines. V. The attack of ternary iminium compounds by nucleophilic reagents *J. Am. Chem. Soc. 78*, 1984-1987.

100. Boekelheide, V., Linn, W. J., O'Grady, P. and Lamborg, M. (1953) Quinolizidine derivatives. A study of the reductive cyclization of some γ-(2-pyridyl)-butyronitriles. *J. Am. Chem. Soc. 75*, 3243-3248.

101. Gerrans, G. C., Howard, A. S. and Orlek, B. S. (1975) General methods of alkaloid synthesis. Ambident nucleophilicitiy of vinylogous urethanes. Synthesis of (±) lupinine and a functionalised hydrojulolidine derivative. *Tetrahedron Lett. 16*, 4171-4172.

102. Takahata, H., Yamabe, K., Suzuki, T. and Yamazaki, T. (1986) Reaction of cyclic thioimidates with methyl 3-oxo-4-pentenoate (Nazarov's reagent). Total synthesis of (±)-*epi*-lupinine. *Heterocycles. 24*, 37-39.

103. Takahata, H., Yamabe, K., Suzuki, T. and Yamazaki, T. (1986) An efficient total synthesis of (±)-epilupinine and (±)-lupinine from a common quinolizidine intermediate. *Chem. Pharm. Bull. 34*, 4523-4526.

104. Mozingo, R., Harris, S. A., Wolf, D. E., Hoffhine, C. E., Easton, N. R. and Folkers, K. (1945) Hydrogenation of compounds containing divalent sulfur. *J. Am. Chem. Soc. 67*, 2092-2095.

105. Leonard, N. J., Hay, A. S., Fulmer, R. W. and Gash V. W. (1955) Unsaturated amines. III. Introduction of α,β-unsaturation by means of the mercuric acetate :$\Delta^{1(10)}$-dehydroquinolizidine. *J. Am.Chem. Soc. 77*, 439-444.

106. Taber, D. F., Guo, P. and Pirnot, M. T. (2010) Conjugate addition of lithiated methyl pyridines to enones. *J. Org. Chem. 75*, 5737-5739.

107. Shvekhgeimer, A. M.-G. (1998) 2,3,4,5-Tetrahydropyridine (Δ^{1}-piperideine) and its derivatives. Synthesis and chemical properties. *Russ. Chem. Rev. 67*, 1031-1060.

108. Evans, D. A. (1970) New endocyclic enamine synthesis. *J. Am. Chem. Soc. 92*, 7593-7595.

109. Gaidarova, E. L., Borisenko, A. A., Chumakov, T. I., Melnikov, A. V., Orlov, I. S. and Grishina, G. V. (1998) A simple and convenient route to 1,2,3,4,5,6,7,8-octahydro-1,6-naphthyridines. *Tetrahedron Lett. 39*, 7767- 7770.

110. Filimonov, D. A. and Poroikov, V. V. (1996) PASS: computerized prediction of biological activity spectra for chemical substances. Bioactive compound design: possibilities for industrial use. pp. 47-56. BIS Scientific Publishers, Oxford.

111. Simonsen, J. and Barton, D. H. R. (1952) The sesquiterpenes, diterpenes and their derivatives 2nd Ed. pp. 592. University Press. Cambridge.

112. Corey, E. J. andXue-Ming C. (1995) The logic of Chemical Synthesis: General Approaches to the Analysis of Complex Synthesis Problems. pp. 436. John Wiley & Sons.

113. Jie, J. L. and Corey, E. J. (2000) Name Reactions for Carbocyclic Ring Formations. pp. 774. John Wiley & Sons. London.

114. Kido, F, Yamaji, K., Sinha, S. S., Abiko, T. and Kato, M. (1995) Carbocyclic construction by the [2,3] sigmatropic rearrangement of cyclic sulfoniumylides. A new entry for the stereoselective synthesis of substituted cyclohexanones. *Tetrahedron 51*, 7697-7714.

115. Wolinsky, J. and Chan, D. (1966) Carbonyl-olefin reactions. The cyclization of 3-isopropenyl-6-oxoheptanoic acid. *J. Org. Chem. 31*, 2471-2474.

116. Mori, K. and Fukamatsu, K. (1992) Pheromone Synthesis, CXXXVII. A new synthesis of (±)-grandisol. *Lieb. Ann. Chem. 1992,* 489-493.

117. Mehta, G., Karmakar, S. and Chattopadhyay, S. K. (2004) Grob-type fragmentation of a carvone derived β-hydroxymesylate: application to the synthesis of chiral lavandulol derivatives. *Tetrahedron. 60*, 5013-5017.

118. Bruckner, R. (2002) Advanced Organic Chemistry: Reaction Mechanisms. pp. 642. Harcourt Academic Press.

119. Krow, G. R. and Szczepanski, S. (1980) Unusual regiochemistry in a Beckmann-like rearrangement of camphor. α- Camphidone via methylene migration. *Tetrahedron Lett. 21*, 4593-4596.

120. Paquette, L. A., Varadarajan, A. and Bay, E. (1984) Triplet-sensitized photoisomerization of 1,4-disubstituted benzonorbornadienes. Intramolecular competition by electronically diverse bridgehead functionality. *J. Am. Chem. Soc. 106*, 6702-6708.

121. (a) Jackman, L. M., Webb, R. L. and Yick, H. C. (1982). Synthesis and chiroptical properties of some piperidin-2-ones. *J. Org. Chem. 47*, 1824- 1831. (b) Gavagan, J. E., Fager, S. K., Fallon, R. D., Folsom, P. W., Herkes, F. E., Eisenberg, A., Hann, E. C. and DiCosimo, R. (1998). Chemoenzymic Production of Lactams from Aliphatic α, ω-Dinitriles. *J. Org. Chem. 63,* 4792- 4801.

122. Kim, G., Margaret, Chu-Moyer, M. Y., Danishefsky, S. J. and, Schulte, G. K. (1993) The total synthesis of indolizomycin. *J. Am. Chem. Soc. 115*, 30-39.

123. Guarna, A., Lombardi, E., Machetti, F., Occhiato, E. G. andScarpi, D. (2000) Modification of the aza-Robinson annulations for the synthesis of 4-methyl-benzo[c] quinolizine-3-ones potent inhibitors of steroid 5-alpha- reductase 1. *J. Org. Chem. 65*, 8093-8095.

124. Heathcock, C. H., Davidsen, S. K., Mills, S. G., and Sanner, M. A. (1992) Daphniphyllum alkaloids. 10. Classical total synthesis of methyl homodaphniphyllate. *J. Org. Chem. 57*, 2531-2544.

125. Mook, J. R., Lackey, K. and Bennett, C. (1995) Synthesis of phenanthridin-3-one derivatives: non-steroidal inhibitors of steroid 5-α-reductase. *Tetrahedron Lett. 36,* 3969-3972.

126. Lacroix, S., Rixhon, V. and Marchand-B., J. (2006) Synthesis of ω-aminodithioesters. *Synthesis 2006,* 2327-2334.

127. Occhiato, E. G., Ferrali, A., Menchi, G., Guarna, A., Danza, G., Comerci, A.,Mancina, R., Serio, M., Garotta, G., Cavali, A., De Vivo, M. and Recanatini, M. (2004) Synthesis, biological activity, and three-dimensional quantitative structure-activity relationship model for a series of benzo[c] quinolizin-3-ones, nonsteroidal inhibitors of human steroid 5a-reductase 1. *J. Med. Chem. 47*, 3546-3560.

128. Piers, E. and Keziere, R. J. (1969) Stereoselective synthesis of (±)-eremophil-3,11-diene and related compounds. Concerning the structure of eremophilene. *Can. J. Chem. 47*, 137-144.

129. Corey, E. J. and Boaz, N. W. (1985) The reactions of combined organocuprate-chlorotrimethylsilane reagents with conjugated carbonyl compounds. *Tetrahedron Lett. 26*, 6019-6022.

130. Brown, J. D. Foley, M. A., and Comins, D. L. (1988) A highly stereocontrolled, four-step synthesis of (±)-lasubine II. *J. Am. Chem. Soc. 110,* 7445-7447.

131. Greenhill, J. V. (1977) Enaminones. *Chem. Soc. Rev. 6*, 277-294.

132. Meyers, A. I. and Singh, S. (1967) The chemistry of cyclic enaminoketones. II. 1,2-and 1,4-addition of nucleophiles leading to substituted heterocycles. *Tetrahedron. Lett. 8*, 5319-5322.

133. Tubery, F., Grierson, D. S. and Husson, H.-P. (1987) Simple 4-acetoxy-5,6-dihydropyridinium salts: new synthons for the preparation of functionalized piperidine systems. *Tetrahedron Lett. 28*, 6457-6460.

134. Cui, L., Peng, Y. and Zhang, L. (2009) A two-step, formal [4+2] approach toward piperidin-4-ones via Au catalysis. *J. Am. Chem. Soc. 131*, 8394- 8395.

135. Caglioti, L. and Magi, M. (1963) The reaction of tosylhydrazones with lithium aluminium hydride. *Tetrahedron. 19*, 1127-1131.

136. Takatsu, N., Noguchi, M., Ohmiya, S. and Otomasu, H. (1987) The synthesis of lupin alkaloids. II. A formal synthesis of (±)-sparteine. *Chem. Pharm. Bull. 35*, 4990-4992.

137. Maria, F. F. and Monica, M. S. (1987) Synthesis of 5,6,9,10,11,11a-hexahydro-8h-naphtho [2,1-a] quinolizine. *Heterocycles*. 26. 3059-3063.

138. Huang, M. (1946) A simple modification of the Wolff-Kishner reduction. *J. Am. Chem. Soc. 68*, 2487-2488.

139. Lineweaver, H. and Burk, D. (1934) The determination of enzyme dissociation constants. *J. Am. Chem. Soc. 56*, 658-666.

140. Chen, M., Al-lami, N., Janvier, M., D'Antonio, E., Faraldos, J. A., Cane, D. E., Allemann, R. K. and Christianson, D. W. (2013) Mechanistic insights from the binding of substrate and carbocation intermediate analogues to aristolochene synthase. *Biochemistry. 52*, 5441-5453.

141. Coxon, J. M., Dansted, E. and Hartshorn, M. P. (1988) *Org. Synth. Collect. Vol.* VI, pp. 949. Wiley. New York.

142. Cardillo, G., Gentilucci, L. and De Matteis, V. (2002) Lewis acid-promoted synthesis and reactivity of *β*-o-benzylhydroxylamino imide derived from D-glyceraldehyde. *J. Org. Chem. 67*, 5957-5962.

143. Kedrowski, B. L. (2003) Synthesis of orthogonally protected (R)-and (*S*)- 2-methylcysteine via an enzymatic desymmeterization and Curtius rearrangement. *J. Org. Chem. 68*, 5403-5406.

144. Harrison, T. J. and Dake, G. R. (2005) An expeditious, high-yielding construction of the food aroma compounds 6-acetyl-1,2,3,4-tetrahydropyridine and 2-acetyl-1-pyrroline. *J. Org. Chem. 70*, 10872-10874.

145. Alsina, J., Giralt, E. and Albericio, F. (1996) Use of n-tritylamino acids and PyAOP1 for the suppression of diketopiperazine formation in Fmoc/tBu solid-phase peptide synthesis using alkoxybenzyl ester anchoring linkages. *Tetrahedron Lett. 37,* 4195-4198.

146. Hua, D. H., Miao, S. W., Bharathi, S. N., Katsuhira, T. and Bravo, A. A. (1990) Selective nucleophilic addition reactions of alkyllithium reagents with n-(trimethylsilyl) lactams. Synthesis of cyclic ketimines. *J. Org. Chem. 55,* 3682-3684.

147. Paquette, L. A. and Freeman, J. P. (1970) Mechanism of thietane formation from the reaction of 1,3-dioxan-2-ones with thiocyanate ion. Stereochemical investigation. *J. Org. Chem. 35*, 2249-2253.

148. Corey, E. J. and Balanson, R. R. (1976) Studies directed toward the total synthesis of prehydrohistrionicotoxin. *Heterocycles. 5*, 445-470.

149. Tehrani, K. A., D'Hooghe, M. and de Kimpe, N. (2003) Novel synthesis of indolizidines and quinolizidines. *Tetrahedron. 59*, 3099-3108.

150. Johnson, C. D., Jones, R. A. Y., Katritzky, A. R., Palmer, C. R., Schofield, K. and Wells, R. J. (1965) A re-examination of the stereochemistry of quinolizidine and the methylquinolizidines through measurement of their rates of quaternisation and those of the hexahydrojulolidines. *J. Chem. Soc.* 6797-6806.

151. Crab, T. A., Newton, R. F. and Jackson, D. (1971) Stereochemical studies of nitrogen bridgehead compounds by spectral means. *Chem. Rev. 71*, 109-126.

152. Jie, J. L. (2009) A Collection of Detailed Reaction Mechanism and Synthetic Applications. Third Expanded Edition. pp. 652. Springer.

153. Thomas, O. P., Zaparucha, A. and Husson, H. P. (2001) A new rearrangement of n-trifluoroacetoxyammonium salt under Polonovski-Potier reaction conditions: aziridinium versus iminium formation. *Tetrahedron Lett. 42*, 3291-3293.

154. Suau, R., Najera, F. and Rico, R. (2000) The Polonovski-potier reaction of n-oxides. Synthesis of 8-hydroxymethyl and 8-methylberbines. *Tetrahedron. 56*, 9713-9723.

155. Snider, B. B. and Grabowski, J. F. (2007) Total synthesis of (-)-senepodine G and (-)-cemizine C. *J. Org. Chem. 73*, 1039-1042.

156. Nizamkhodzhaeva, A. N., Ishbaev, A. I., Aslanov, K. A. and Mukhamedzhanov, S. Z. (1978) Formation of nitrogen oxides of quinloizidine alkaloids under the effect of atmospheric oxygen. *Chem. Abstr. 88*,121499v.

157. Starks, C. M., Back, K., Chappell, J. and Noel, J. P. (1997) Structural basis for cyclic terpene biosynthesis by tobacco 5-*epi*-aristolochene synthase. *Science. 277*, 1815-1820.

158. Soldaini, G., Gardona, F. and Goti, A. (2007) Catalytic oxidation of imines based on metheyltrioxorhenium/urea hydrogen peroxide: a mild and easy chemo- and regioselective entry to nitrones. *Org. Lett. 9*, 473-476.

APPENDIX

Mechanistic Insights from the Binding of Substrate and Carbocation Intermediate Analogues to Aristolochene Synthase

Mengbin Chen,[†] Naeemah Al-lami,[‡] Marine Janvier,[‡] Edward L. D'Antonio,[†] Juan A. Faraldos,[‡] David E. Cane,[§] Rudolf K. Allemann,[‡] and David W. Christianson*[†]

[†]Roy and Diana Vagelos Laboratories, Department of Chemistry, University of Pennsylvania, Philadelphia, Pennsylvania, 19104-6323, United States

[‡]School of Chemistry, Cardiff University, Park Place, Cardiff CF10 3AT, Wales, United Kingdom

[§]Department of Chemistry, Box H, Brown University, Providence, Rhode Island 02912-9108, United States

ABSTRACT: Aristolochene synthase, a metal-dependent sesquiterpene cyclase from *Aspergillus terreus*, catalyzes the ionization-dependent cyclization of farnesyl diphosphate (FPP) to form the bicyclic eremophilane (+)-aristolochene with perfect structural and stereochemical precision. Here, we report the X-ray crystal structure of aristolochene synthase complexed with three Mg^{2+} ions and the unreactive substrate analogue farnesyl-S-thiolodiphosphate (FSPP), showing that the substrate diphosphate group is anchored by metal coordination and hydrogen bond interactions identical to those previously observed in the complex with three Mg^{2+} ions and inorganic pyrophosphate (PP_i). Moreover, the binding conformation of FSPP directly mimics that expected for productively bound FPP, with the exception of the precise alignment of the C–S bond with regard to the C10–C11 π system that would be required for C1–C10 bond formation in the first step of catalysis. We also report crystal structures of aristolochene synthase complexed with Mg^{2+}_3-PP_i and ammonium or iminium analogues of bicyclic carbocation intermediates proposed for the natural cyclization cascade. Various binding orientations are observed for these bicyclic analogues, and these orientations appear to be driven by favorable electrostatic interactions between the positively charged ammonium group of the analogue and the negatively charged PP_i anion. Surprisingly, the active site is sufficiently flexible to accommodate analogues with partially or completely incorrect stereochemistry. Although this permissiveness in binding is unanticipated, based on the stereochemical precision of catalysis that leads exclusively to the (+)-aristolochene stereoisomer, it suggests the ability of the active site to enable controlled reorientation of intermediates during the cyclization cascade. Taken together, these structures illuminate important aspects of the catalytic mechanism.

Terpenoids, including steroids and carotenoids, comprise the largest class of natural products, with more than 70,000 members identified to date (Dictionary of Natural Products: http://dnp.chemnetbase.com). Remarkably, the structural and stereochemical complexity of these organic molecules is rooted in diverse biosynthetic pathways involving simple five-carbon isoprenoid precursors. For example, dimethylallyl diphosphate and two molecules of isopentenyl diphosphate can be coupled together in head-to-tail fashion to generate the C_{15}-isoprenoid farnesyl diphosphate,[1,2] which can then be converted into myriad cyclic hydrocarbon products through multistep reactions catalyzed by sesquiterpene synthases.[3–11]

Class I terpenoid cyclases share a common α-helical fold and utilize a trinuclear metal ion cluster (usually Mg^{2+}, sometimes Mn^{2+} or Co^{2+}) to trigger the departure of the pyrophosphate (PP_i) leaving group. This generates a highly reactive allylic cation that reacts with one of the remaining π bonds of the substrate, thereby initiating a cyclization sequence typically proceeding through multiple carbocation intermediates. The binding of three Mg^{2+} ions and substrate induces protein conformational changes that enclose the active site, as first observed in the structure of trichodiene synthase complexed with Mg^{2+}_3-PP_i,[12] which establishes a cyclization-competent substrate conformation and protects carbocation intermediates from premature quenching by solvent. The specific sequence of carbon–carbon bond forming reactions is governed by the conformational control that the enzyme exerts over the substrate and the stabilization of carbocation intermediates. Ultimately, the cyclization cascade is terminated by deprotonation or addition of water to the final carbocation intermediate. Intriguingly, while many cyclases are high-fidelity enzymes that precisely chaperone successive carbocation intermediates to form a single product, others are more promiscuous in that they generate a mixture of products.

Aspergillus terreus aristolochene synthase (ATAS) catalyzes the cyclization of farnesyl diphosphate (FPP) to form the bicyclic eremophilane (+)-aristolochene (Figure 1), which is the hydrocarbon parent of several fungal toxins such as gigantenone, bipolaroxin, and PR-toxin.[13] Unlike its counter-

5441
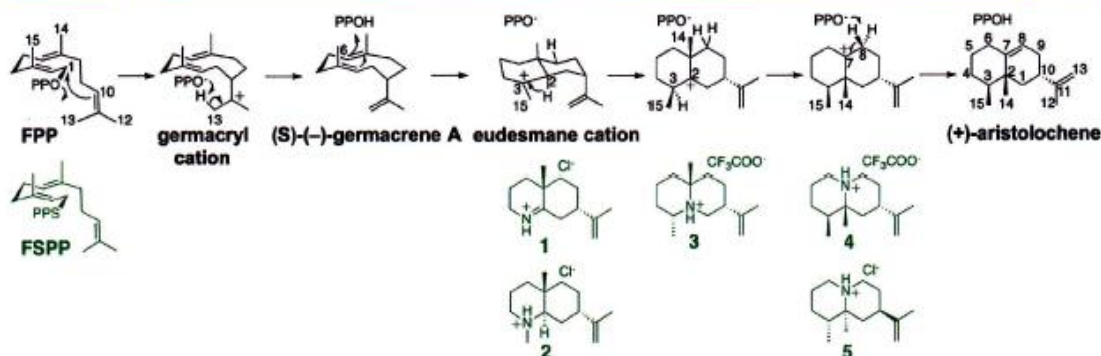
Figure 1. Proposed mechanism of (+)-aristolochene generation as catalyzed by *A. terreus* aristolochene synthase (PPO = diphosphate; PPO⁻ = inorganic pyrophosphate; PPOH = protonated inorganic pyrophosphate). Note that the germacrene A intermediate must reorient itself relative to protonated inorganic pyrophosphate (which is rigidly positioned by metal coordination and hydrogen bond interactions) to enable subsequent protonation and deprotonation steps in catalysis. Certain sequences might proceed in concerted rather than stepwise fashion, in which case carbon atoms bearing full positive charges would only develop partial positive charges. Carbon atoms are numbered in all structures based on the numbering scheme shown for FPP to better follow relevant carbon atoms during the course of the reaction. Analogues of substrate and possible carbocation intermediates in the cyclization cascade are shown in green.

part in *Penicillium roqueforti* that produces a mixture of products, ATAS is a high-fidelity enzyme that generates (+)-aristolochene exclusively.[14] To date, no crystal structures of *P. roqueforti* aristolochene synthase or ATAS complexed with analogues of substrate or carbocation intermediates have been reported in which the active site is locked in the fully closed, active conformation by three Mg²⁺ ions. Here, we report the structure of the ATAS-Mg²⁺₃ complex with the unreactive substrate analogue farnesyl thiolodiphosphate (FSPP), as well as the first structures of ATAS-Mg²⁺₃ complexes with ammonium and iminium aza-analogues of possible carbocation intermediates in the cyclization cascade (Figure 1). While carbocation intermediates are of course too short-lived to be studied in their enzyme complexes by typical X-ray crystallographic methods, the use of cationic aza-analogues enables the study of molecular strategies for stabilizing and manipulating the transient carbocation intermediates that they mimic.[15–17] Additionally, the binding of aza-analogues with unusual stereochemistries provides insight on the structural basis of fidelity in the cyclization cascade that exclusively yields (+)-aristolochene.

■ MATERIALS AND METHODS

Aza Analogues of Carbocation Intermediates. The syntheses of (4aS,7S)-4a-methyl-7-(prop-1-en-2-yl)-2,3,4,-4a,5,6,7,8-octahydroquinolin-1-ium (**1**) and (4aS,7S)-1,4a-dimethyl-7-(prop-1-en-2-yl)decahydroquinolin-1-ium (**2**) have been previously reported.[18,19] The syntheses of (3R,6R,9aR)-6,9a-dimethyl-3-(prop-1-en-2-yl)decahydroquinolizin-5-ium (**3**) and (1S,8S,9aR)-1,9a-dimethyl-8-(prop-1-en-2-yl)-decahydroquinolizin-5-ium (**4**) were accomplished in six and eight steps, respectively, starting from the known keto ester (S)-methyl-6-oxo-3-(prop-1-en-2-yl)heptanoate, which was obtained by degradation of (−)-limonene.[20–22] The synthesis of **3** features a modified Curtius rearrangement[23] that gives rise to the 3,6-dialkylated cyclic imine (R)-6-methyl-3-(prop-1-en-2-yl)-2,3,4,5-tetrahydropyridine after acid-promoted cyclization.[24] The latter was easily converted to the final (3R,6R,9aR)-trialkyl substituted quinolizidine **3** essentially as described by De Kimpe using MeMgBr.[25] This protocol generates an equal

amount of the (3R,6S,9aS)-diastereomer of **3**. Starting from the same (S)-configured keto ester, amine **4** was prepared via a Beckmann rearrangement[26,27] that provided after cyclization[27] the enantiopure lactam (S)-4-(prop-1-en-2-yl)piperidin-2-one. This lactam was then converted to the final quinolizidine **4** via a tandem aza-Robinson annulation/Michael alkylation/Wolff–Kishner reduction that installed the syn vicinal methyl groups of **4** with excellent stereospecificity.[28–30] An identical synthetic protocol was repeated from (+)-limonene to give (1R,8R,9aS)-1,9a-dimethyl-8-(prop-1-en-2-yl)decahydroquinolizin-5-ium (**5**), the enantiomer of quinolizidine **4**. The absolute configuration of amines **3**, **4**, and **5** was determined using a combination of one- and two-dimensional (1D and 2D) NMR experiments and confirmed by X-ray crystal structure determinations of the perchlorate salts of **3**, **4**, and **5**. Full details of the syntheses of amines **3**–**5** will be published separately.

Preparation of Recombinant ATAS. To minimize molecular disorder and simplify enzyme purification, a new truncation variant of ATAS was prepared in which the first 12 residues at the N-terminus were deleted and replaced by a hexahistidine tag using PCR mutagenesis. This was achieved in two separate steps. First, to prepare the deletion variant, the forward and reverse primers for the deletion were as follows: 5′-GTT TAA CTT TAA GAA GGA GAT ATA CAT ATG CTT GAG CCA CCC CCC TCT ACG TTC-3′, and 5′-GAA CGT AGA GGG GGG TGG CTC AAG CAT ATG TAT ATC TCC TTC TTA AAG TTA AAC-3′. Plasmids were transformed into *Escherichia coli* XL1-Blue cells (Novagen) and amplified. They were purified using miniprep kits, and the deletion was confirmed by DNA sequencing. In the second step, the His₆ tag was spliced between M1 and L14 of the deletion variant to generate the new truncation variant designated His₆-Δ12-ATAS. The corresponding primers were 5′-GTT TAA CTT TAA GAA GGA GAT ATA CAT ATG CAT CAT CAC CAT CAC CAT CTT GAG CCA CCC CCC TCT ACG TTC-3′, and 5′-CAA ATT GAA ATT CTT CCT CTA TAT GTA TAC GTA GTA GTG GTA GTG GTA GAA CTC GGT GGG GGG AGA TGC AAG-3′. Plasmids of His₆-Δ12-ATAS were prepared and purified as described above.

201

Table 1. Data Collection and Refinement Statistics

complex	ATAS–FSPP	ATAS-1	ATAS-2	ATAS-3	ATAS-4	ATAS-5
			A. Data Collection			
resolution limits (Å)	50.0–1.90	50.0–2.15	50.0–2.40	50.0–2.10	50.0–1.95	50.0–1.86
total/unique reflections measured	1605556/142524	537459/96119	783788/69718	1104453/105878	965747/130854	1034908/151303
space group	$P3_121$	$P3_121$	$P3_121$	$P3_121$	$P3_121$	$P3_121$
unit cell: a, c (Å)	124.0, 203.5	123.4, 201.6	122.8, 202.5	124.4, 202.9	124.3, 203.0	123.8, 202.1
$R_{merge}{}^{a,b}$	0.102 (e)	0.106 (0.569)	0.094 (0.277)	0.127 (0.702)	0.132 (0.681)	0.102 (0.763)
$I/\sigma(I)^a$	30.4 (1.5)	16.3 (3.2)	30.0 (9.3)	19.3 (3.4)	14.1 (3.3)	17.5 (2.8)
redundancy^a	11.3 (10.9)	5.6 (5.6)	11.2 (9.4)	10.4 (9.9)	7.4 (7.3)	6.8 (6.6)
completeness (%)^a	100.0 (100.0)	99.1 (99.9)	100 (100)	100.0 (100.0)	99.4 (98.8)	100 (100)
			B. Refinement			
reflections used in refinement/test set	142431/7147	96109/4811	69619/3517	105808/5287	130821/6591	150235/7536
$R_{work}{}^c$	0.189	0.208	0.174	0.194	0.191	0.193
$R_{free}{}^c$	0.226	0.240	0.212	0.229	0.238	0.226
protein atoms^d	9831	9816	9816	9839	9831	9831
ligand atoms^d	96	92	96	96	96	96
Mg^{2+} ions^d	12	12	13	12	12	12
solvent atoms^d	978	892	980	980	1077	1024
glycerol atoms^d	12	0	24	12	6	12
avg B factors (Å²)						
main chain	32	19	26	29	26	24
side chain	37	22	28	32	30	28
ligand	33	13	35	31	29	26
Mg^{2+} ions	27	16	23	23	22	18
solvent	37	27	30	35	31	29
r.m.s. deviations						
bonds (Å)	0.014	0.005	0.005	0.005	0.007	0.016
angles (deg)	1.4	0.8	0.8	0.8	1.0	1.5
Ramachandran Plot (%)						
allowed	95.1	95.3	94.8	95.0	95.5	95.2
additionally allowed	4.9	4.7	5.2	5.0	4.5	4.8
generously allowed	0.0	0.0	0.0	0.0	0.0	0.0
disallowed	0.0	0.0	0.0	0.0	0.0	0.0
PDB accession code	4KUX	4KVI	4KVD	4KVW	4KVY	4KWD

^{a}Numbers in parentheses refer to the highest resolution shell of data. $^b R_{merge}$ for replicate reflections, $R = \sum |I_h - \langle I_h \rangle| / \sum \langle I_h \rangle$; I_h = intensity measure for reflection h; and $\langle I_h \rangle$ = average intensity for reflection h calculated from replicate data. $^c R_{work} = \sum ||F_o| - |F_c|| / \sum |F_o|$ for reflections contained in the working set. $R_{free} = \sum ||F_o| - |F_c|| / \sum |F_o|$ for reflections contained in the test set held aside during refinement (5% of total). $|F_o|$ and $|F_c|$ are the observed and calculated structure factor amplitudes, respectively. ^{d}Per asymmetric unit. $^e R_{merge}$ value higher than 1.000 are reported as 0.000 by HKL2000. Given the exceptionally high redundancy of 10.9 for the outer shell of this data set, R_{pim} is a more appropriate measure of data quality than R_{merge}. For this data set, R_{pim} = 0.037 (0.572).

E. coli BL21(DE3)-pLysS cells (Stratagene, Agilent) carrying the cDNA for His_6-Δ12-ATAS (henceforth designated simply ATAS) were inoculated in 6 × 5 mL Luria–Bertani (LB) medium containing 100 µg/mL ampicillin and grown for 6 h at 37 °C with shaking (250 rpm). Each 5 mL culture was used to inoculate 6 × 1L LB medium containing 100 µg/mL ampicillin. When OD_{600} reached 1.0, the temperature was adjusted to 22 °C, and 1 mM isopropyl β-D-1-thiogalactopyranoside was added to induce protein synthesis. The expression lasted for 7.5 h before the cells were pelleted and stored at −80 °C for further use.

The cell pellet was thawed and suspended in 50 mL of Talon (QIAGEN) wash buffer [50 mM 3-(N-morpholino)-propanesulfonic acid (MOPS) (pH 7.0), 300 mM NaCl, 2 mM β-mercaptoethanol (BME), 10% glycerol]. After sonication, the cell lysate was centrifuged at 15 000 rpm, and the supernatant was loaded onto a pre-equilibrated Talon column at a flow rate of 2 mL/min. Enzyme was eluted with a 0–150 mM imidazole gradient in Talon wash buffer. The most active fractions were combined and dialyzed against HiTrap Q HP wash buffer [20 mM 2-morpholinoethanesulfonic acid (MES) (pH 6.5), 5 mM

ethylenediaminetetraacetic acid (EDTA), 5 mM BME, 10% glycerol] (GE Healthcare Life Sciences). After being loaded on a HiTrap Q HP column (15 mL), enzyme was eluted with a 0–500 mM sodium chloride gradient in HiTrap Q HP wash buffer. Selected fractions were pooled, concentrated, and further purified in 25 mM MES (pH 6.5), 2 mM $MgCl_2$, 150 mM NaCl, 4 mM BME using a HiLoad 26/60 Superdex column (GE Healthcare Life Sciences). The final ATAS sample was 98% pure as indicated by SDS-PAGE and was concentrated to 10 mg/mL.

Crystal Structure Determinations. Crystals of ATAS–inhibitor complexes were prepared by cocrystallization in hanging drops through the vapor diffusion method at 4 °C. Briefly, a 3 µL drop of protein solution [10 mg/mL ATAS, 20 mM MES (pH 6.5), 1.9 mM $MgCl_2$, 120 mM NaCl, 3 mM BME, 1.6 mM sodium pyrophosphate, 1.5 mM inhibitor] was added to a 3 µL drop of precipitant solution and equilibrated against a 500 µL reservoir of precipitant solution. Different precipitant solutions were used for the crystallization of different ATAS–inhibitor complexes as follows: for FSPP (Echelon Biosciences), the precipitant solution was 200 mM

magnesium acetate, 17% polyethylene glycol (PEG) 3350; for **1**, the precipitant solution was 100 mM 4-(2-hydroxyethyl)-1-piperazineethanesulfonic acid (HEPES) (pH 7.7), 200 mM MgCl₂, 23% (w/v) PEG 3350; for **2**, the precipitant solution was 100 mM Bis-Tris (pH 7.0), 200 mM Li₂SO₄, and 27% (w/v) PEG 3350; for **3**, the precipitant solution was 100 mM magnesium formate, 12% PEG 3350; for **4**, the precipitant solution was 2% Tacsimate (pH 6.0), 100 mM Bis-Tris (pH 7.0), 16% (w/v) PEG 3350; for **5**, the precipitant solution was 200 mM sodium malonate (pH 7.0), 15% (w/v) PEG 3350. Crystals generally appeared within 1 week and grew to maximum size within 3—4 weeks. Crystals were gradually transferred to cryoprotectant solution (20% (v/v) glycerol in mother liquor) and flash-cooled in liquid nitrogen.

X-ray diffraction data were collected at beamlines X25 and X29A of the National Synchrotron Light Source at Brookhaven National Laboratory and were indexed, integrated, and scaled using HKL2000.[31] Criteria for determining the resolution cutoff for each data set included R_{merge} < 0.140 and I/σ > 1.5 for outer shell data. For the ATAS-2 complex at 2.4 Å resolution, we had collected slightly higher resolution data sets in different experiments, but we were not able to index these data sets. In the data set that we were able to index, we were limited to 2.4 Å resolution data due to the geometry of the X-ray diffraction experiment. The R_{pim} value was calculated using phenix.merging_statistics in the PHENIX GUI.[32] Molecular replacement was performed with Phaser for Molecular Replacement in the CCP4i package,[33] using a monomer of the previous determined structure of ATAS[34] as a search probe for rotation function and translation function calculations. All crystals formed in a new space group compared with that of the previously reported crystals of full-length ATAS[34,35] and belonged to space group $P3_121$ with four monomers in the asymmetric unit as a dimer of dimers. The quaternary structure of this dimer of dimers is similar but not identical to that reported for full-length ATAS crystallized in space group $P2_1$: one dimer is rotated relative to the second dimer by approximately 30°. Refinement and manual model adjustment were performed with PHENIX and COOT, respectively.[36,37] The disordered N-terminus M1-H7 and C-terminus V312-D314 were excluded in most final models. Refinement statistics are recorded in Table 1. MolProbity was used to validate all structures.[38]

■ RESULTS

ATAS—FSPP Complex. The ATAS—FSPP complex crystallizes with four monomers (designated A—D) in the asymmetric unit as a dimer of dimers, and this arrangement is observed for all complexes prepared with the new ATAS construct utilized in the current study. Roughly similar quaternary structure is observed in previously determined crystal structures of full-length ATAS in a different space group.[34] Significant conformational changes are triggered by the binding of FSPP and three Mg²⁺ ions in the active site, and the root-mean-square (r.m.s.) deviation is 1.2 Å for 241 Cα atoms between the ATAS—FSPP complex and unliganded ATAS (Figure 2).[34] These structural changes include the ordering of the C-terminal end of helix H and the H-α-1 loop (this helps to "cap" the active site), a short coil—helix transition within the F-G1 loop, and the introduction of a small kink in helix I. These structural changes are essentially identical to those observed in the ATAS—Mg²⁺₃—PP₁ complex[34] and appear
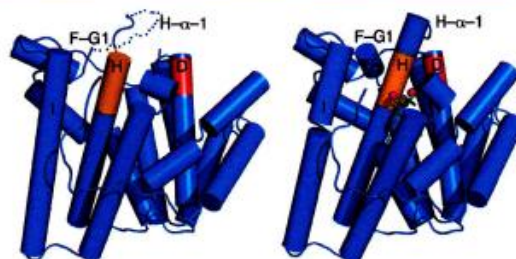
Figure 2. Structural comparison of unliganded ATAS (left) with the ATAS—FSPP complex (right) illustrating conformational changes triggered by the binding of FSPP and three Mg²⁺ ions in the active site. The aspartate-rich DDXXD metal-binding segment on helix D is red and the "NSE" metal-binding segment on helix H is orange. In the ATAS—FSPP complex, Mg²⁺ ions are magenta and FSPP is shown as a stick figure. Selected secondary structure elements are labeled as discussed in the text.

to be driven by protein and substrate coordination interactions with the trinuclear magnesium cluster.

A simulated annealing omit map of the ATAS—FSPP complex is shown in Figure 3a. The α-helices surrounding the active site shift ca. 1.5 Å inward to facilitate van der Waals interactions with the isoprenoid chains of FSPP, and the S225—I234 segment, which was disordered in the unliganded enzyme, becomes ordered and caps the top of the active site. The side chains of E221, N213, and D84 undergo conformational changes to enable Mg²⁺ coordination, and the side chains of R169, N213, K220, R308, and Y309 move to donate hydrogen bonds to the diphosphate group of FSPP. Comparison with the structure of the ATAS—Mg²⁺₃—PP₁ complex[34] shows that the geometry of metal coordination and hydrogen bond interactions with the diphosphate group is maintained regardless of whether or not the diphosphate group is covalently bonded to an isoprenoid (Figure 3b). Deeper in the hydrophobic cavity, it appears that the side chains of V57, L77, and L80 flip to better encase the isoprenoid chain of FSPP (admittedly, these conformational changes could also be the result of refinement with higher resolution diffraction data). The structure of the ATAS—FSPP complex is essentially identical in monomers A—C; slight differences are observed in monomer D, presumably due to the somewhat noisy electron density that characterizes FSPP.

The intermolecular interactions of the diphosphate group of FSPP appear to indirectly influence the isoprenoid chain conformation. The previously determined structure of ATAS complexed with 2-fluorofarnesyl diphosphate revealed the binding of only one Mg²⁺ ion to an incomplete closed active site.[35] Consequently, the isoprenoid conformation and orientation of 2-fluorofarnesyl diphosphate is "flipped" relative to that now observed for FSPP. Therefore, we conclude that a full complement of three Mg²⁺ ions is required to achieve complete active site closure,[10] which in turn is required to achieve a catalytically productive substrate conformation.

In the ATAS—FSPP complex, the distance between C10 and C1 of FSPP is 4.6 Å (monomer A); additionally, the orientation of the C1—S bond with respect to the π system at C10 would not support the C1—C10 bond forming reaction that initiates the cyclization cascade. Since the isoprenoid chain of FSPP is otherwise bound with a productive conformation, however, with the C14 and C15 methyl groups and the terminal
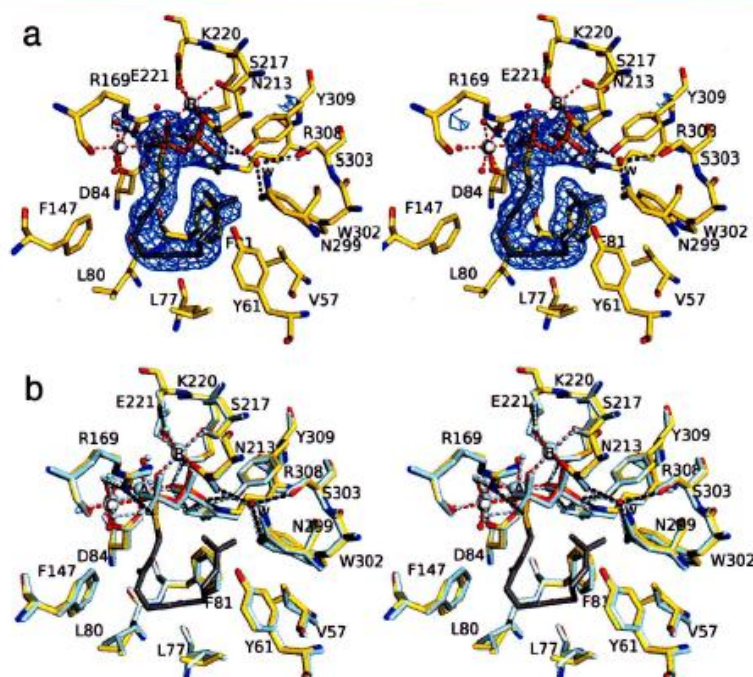
Figure 3. (a) Simulated annealing omit map of FSPP (contoured at 4.0σ) bound to monomer A in the ATAS–Mg^{2+}$_3$–FSPP complex. Atoms are color-coded as follows: C = yellow (protein) or gray (FSPP), O = red, N = blue, P = orange, S = yellow, Mg^{2+} ions = silver spheres, solvent molecules = red spheres. Metal coordination interactions are shown as red dotted lines; hydrogen bond interactions are shown as black dotted lines. Water molecule "w" is trapped in the active site along with FSPP. (b) Superposition of the ATAS–Mg^{2+}$_3$–FSPP complex (color-coded as in (a)) and the ATAS–Mg^{2+}$_3$–PP$_i$ complex (all atoms pale cyan).

isopropylidene group adopting a conformation that would lead to the formation of (S)-(−)-germacrene A as outlined in Figure 1, all that would be necessary for a fully productive conformation would be a ~90° rotation about the C3–C2–C1–S dihedral angle to align the C1–S bond for backside attack by the π system at C10, which would give rise to the observed inversion of configuration at C1.[39]

Studies with isotopically labeled FPP have demonstrated that the initial cyclization reaction forming (S)-(−)-germacrene A requires regiospecific deprotonation of the C13 cis-methyl group of the germacryl cation as shown in Figure 1.[40] Although the phenolic side chain of Y61 is 3.7 Å away from the C13 cis-methyl group of FSPP (monomer A), mutagenesis studies of this residue show that while it is required for optimal catalytic activity,[41] it is not obligatory for the generation of (+)-aristolochene.[14] Thus, Y61 cannot be a catalytically required general base. The C13 cis-methyl group is only 4.0 Å from the thiophosphate sulfur atom of FSPP, however, suggesting the possibility that the corresponding oxygen atom of the diphosphate group of FPP could serve as the general base responsible for the regiospecific proton elimination from the intermediate germacryl cation intermediate shown in Figure 1.

It is interesting to note that a water molecule, labeled "w" in Figure 3, is trapped in the upper active site. This water molecule is fixed in place by hydrogen bonds with N213, N299, and S303. The C13 cis-methyl group of FSPP is 3.9 Å away

from water molecule "w", while the C12 trans-methyl group of FSPP is 3.0 Å away (monomer A). On the basis of the observed binding conformation of FSPP, water molecule "w" is unlikely to mediate the regiospecific deprotonation of the C13 cis-methyl group.

Finally, the steric bulk of aromatic amino acids often defines in large part the active site contour of a terpenoid cyclase, and this is the case for ATAS. Active site aromatic residues thus play an important role in chaperoning the binding conformation of the flexible isoprenoid substrate. The C1–C4 isoprenoid unit of FSPP makes van der Waals contacts with the side chain of F147, while the distal C9–C12 isoprenoid unit is nestled within a shallow crevice formed by the side chains of Y61, F81, and W302. Aromatic residues may also provide electrostatic stabilization of carbocation intermediates and their flanking transition states through cation-π interactions.[42−44]

ATAS-1 Complex. Even though its lacks an N-methyl substituent, iminium cation **1** mimics the eudesmane cation intermediate of the ATAS reaction, presuming that the sp^2-hybridized iminium nitrogen is protonated (pK_a ≈ 7−8) and positively charged (Figure 1).[18,19] The simulated annealing omit map of this complex (Figure 4a) reveals that the Mg^{2+}$_3$ cluster and PP$_i$ group bind with full occupancy and make similar interactions to those observed in the ATAS–FSPP complex, thereby ensuring a fully closed active site conformation. The structure of the ATAS-1 complex is essentially identical in monomers A−C; slight differences are

204
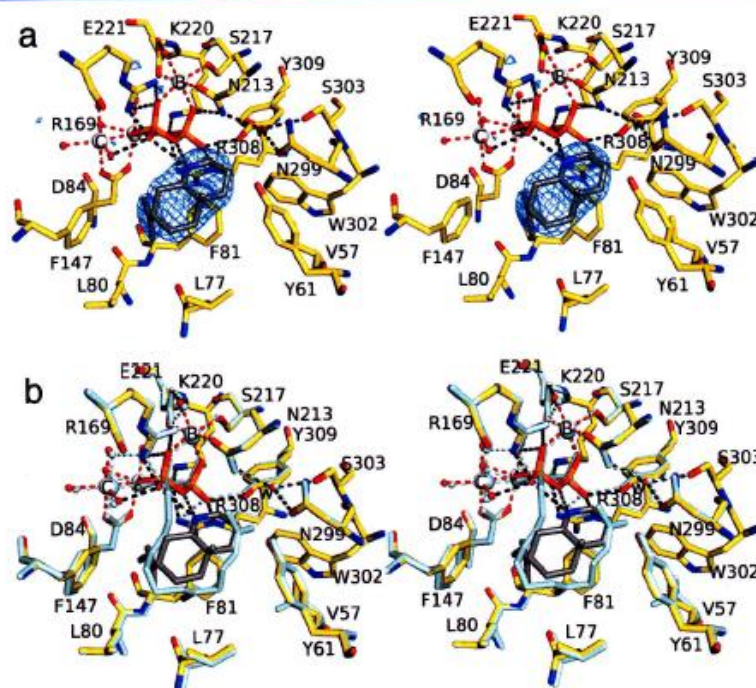
Figure 4. (a) Simulated annealing omit map of iminium cation **1** (contoured at 4.0σ) bound to monomer A in the ATAS-1 complex. Atoms are color-coded as follows: C = yellow (protein) or gray (**1**), O = red, N = blue, P = orange, S = yellow, Mg^{2+} ions = silver spheres, solvent molecules = red spheres. Metal coordination and hydrogen bond interactions are shown as red and black dotted lines, respectively. Water molecule "w" is trapped in the active site along with **1**. (b) Superposition of the ATAS-1 complex (color-coded as in (a)) and the ATAS–FSPP complex (all atoms pale cyan).

observed in monomer D, possibly due to somewhat noisy electron density. In general, active site residues adopt nearly identical conformations in the ATAS-1 and ATAS–FSPP complexes. Intriguingly, however, the orientation of **1** is flipped ~180° relative to that of FSPP, such that the isopropylidene group is sandwiched between F81 and F147 rather than in the shallow crevice formed by the side chains of Y61, F81, and W302 (Figure 4b). Accordingly, the iminium NH group of **1** donates two hydrogen bonds to the PP_i group. Thus, favorable electrostatic and hydrogen bond interactions appear to play a dominant role in governing the binding orientation of **1**.

Trapped water molecule "w" observed in the ATAS–FSPP complex is also present in the ATAS-1 complex, and it makes a similar array of hydrogen bond interactions with N213, N299, and S303. Presuming that water molecule "w" remains bound upon the binding of the actual substrate FPP, hydrogen bond interactions presumably restrain water molecule "w" so that it cannot react with any carbocation intermediates since ATAS does not generate any hydroxylated products.[14] Accordingly, this water molecule appears to be an integral part of the active site contour and inert with regard to the chemistry of catalysis.

ATAS-2 Complex. The simulated annealing omit map of this complex (Figure 5a) reveals that the $Mg^{2+}{}_3$ cluster, the PP_i anion, and tertiary amino cation **2** bind with full occupancy, and the active site adopts a fully closed conformation. Although the resolution of this structure (2.4 Å) is the lowest of the structures described in the current work, the electron density

envelope outlining **2** is reasonably well-defined in all four monomers, and the structure of the ATAS-2 complex is essentially identical in all four monomers.

Tertiary amino cation **2** mimics the eudesmane cation intermediate and binds with an orientation somewhat similar to that of **1**, in that the isopropylidene group lies between F81 and F147. The positively charged amino group of **2** donates a hydrogen bond to the PP_i group, although it is tilted slightly downward and shifted toward F147 and F81 relative to the position of **1** to avoid a steric clash between the N-methyl substituent and the PP_i group. Consequently, the side chain of L77 is flipped to accommodate the isopropylidene group of **2**. The trapped water molecule "w" is present, but it does not make any close contacts with **2**. A superposition of the ATAS-1 and ATAS-2 complexes is shown in Figure 5b.

ATAS-3 Complex. The simulated annealing omit map of this complex (Figure 6a) reveals that the $Mg^{2+}{}_3$ cluster, PP_i anion, and **3** bind with full occupancy in a fully closed active site. The structure of the ATAS-3 complex is essentially identical in all four monomers. Compound **3** partially mimics the possible carbocation intermediate that would be formed in a stepwise mechanism in which the eudesmane cation undergoes a 1,2-hydride transfer to form a tertiary carbocation at the ring-fusion carbon (Figure 1). However, **3** is an imperfect mimic, because the stereochemistry at the C3 atom is R instead of S, the protonated amino nitrogen is sp^3-hybridized rather than sp^2-hybridized, and the analogue adopts a conformation

205
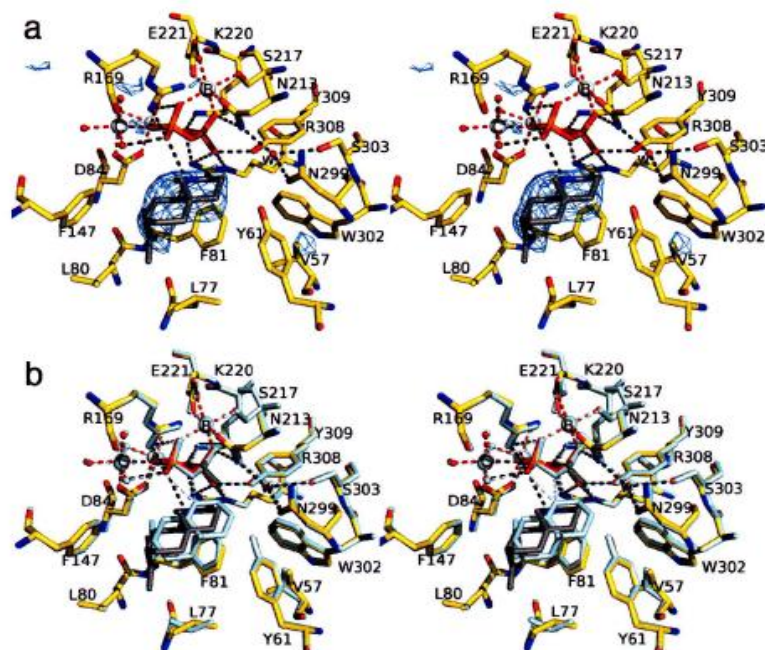
Figure 5. (a) Simulated annealing omit map of tertiary ammonium cation **2** (contoured at 2.6σ) bound to monomer A in the ATAS-2 complex. Atoms are color-coded as follows: C = yellow (protein) or gray (**2**), O = red, N = blue, P = orange, S = yellow, Mg^{2+} ions = silver spheres, solvent molecules = red spheres. Metal coordination and hydrogen bond interactions are shown as red and black dotted lines, respectively. Water molecule "w" is trapped in the active site along with **3**. (b) Superposition of the ATAS-2 complex (color-coded as in (a)) with the ATAS-1 complex (all atoms pale cyan).

comparable to that of a *cis*-decalin. Even so, the binding orientation of **3** is somewhat reminiscent of that of FSPP, in that the isopropylidene group is nestled with the cavity formed by the side chains of Y61, F81, and W302 (Figure 6b). Although the conformations of surrounding residues are identical to those observed in previous structures, F81 moves slightly toward the bottom of the cleft to accommodate **3**. Notably, there is an additional water molecule, labeled "ww", that hydrogen bonds with a $Mg^{2+}{}_C$-bound water molecule, donates a hydrogen bond to the PP_i group, and accepts a hydrogen bond from the protonated amino group of **3**.

Despite the fact that **3** is an imperfect analogue of a possible carbocation intermediate in the ATAS reaction, it is interesting to note that the methylene group corresponding to that which undergoes stereospecific deprotonation of the H-8_{si} atom is oriented toward the PP_i anion. This suggests the possibility that the PP_i anion could serve as a general base that removes the H-8_{si} proton[40] in the cyclization cascade leading to (+)-aristolochene formation as shown in Figure 1.

ATAS-4 Complex. The simulated annealing omit map of this complex (Figure 7a) reveals that the $Mg^{2+}{}_3$ cluster, PP_i anion, and **4** bind with full occupancy, ensuring a fully closed active site conformation. The structure of the ATAS-4 complex is essentially identical in monomers A–C; slight differences are observed in monomer D, presumably due to the relatively poor electron density that characterizes **4**. Tertiary amino cation **4** mimics the final carbocation intermediate proposed in the

stepwise mechanism leading to the formation of (+)-aristolochene. Although the amino nitrogen bears a positive charge and all stereocenters are correctly constructed, the sp^3-hybridization of the cationic tertiary amino group makes it an imperfect mimic of the planar sp^2-hybridized tertiary carbocation shown in Figure 1. The amino nitrogen of **4** faces the PP_i group, and van der Waals interactions occur between the ring carbon atoms of **4** and the PP_i group (Figure 7a). The isopropylidene group of **4** is nestled in the aromatic cleft formed by Y61, F81, and W302. This is the same general location occupied by the terminal isoprenoid unit of FSPP, as shown in the superposition in Figure 7b. If this orientation were adopted by the final carbocation intermediate in catalysis, it is interesting to note that the C8 methylene group is oriented toward the PP_i anion. This further supports the possibility that the PP_i anion could serve as a general base for the stereospecific deprotonation of the H-8_{si} atom in the cyclization of FPP to (+)-aristolochene.

ATAS-5 Complex. In order to probe stereochemical discrimination in the active site of ATAS, we prepared the complex with tertiary ammonium cation **5**. This analogue has opposite stereochemistry at all stereocenters relative to **4**, including the stereochemistry at the protonated tertiary amino group. The stereochemistry of **5** is therefore inconsistent with that of any structure encountered in the natural ATAS mechanism shown in Figure 1. Despite this fact, **5** is readily accommodated in the active site of ATAS, which is stabilized in

206
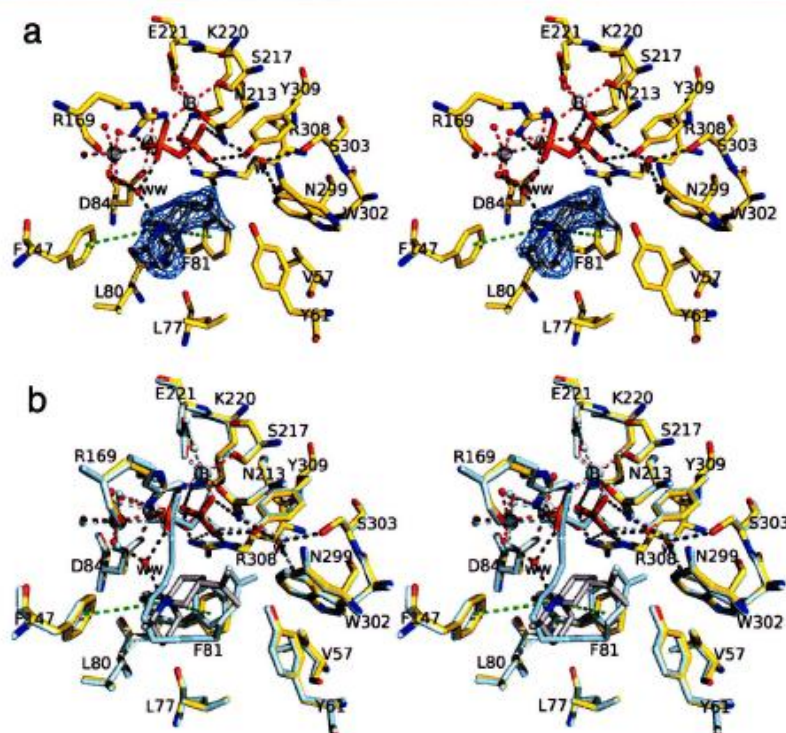
Figure 6. (a) Simulated annealing omit map of tertiary ammonium cation 3 (contoured at 3.5σ) bound to monomer B in the ATAS-3 complex. Atoms are color-coded as follows: C = yellow (protein) or gray (3), O = red, N = blue, P = orange, S = yellow, Mg²⁺ ions = silver spheres, solvent molecules = red spheres. Metal coordination, hydrogen bond, and cation-π interactions are shown as red, black, and green dotted lines, respectively. Water molecules "w" and "ww" are trapped in the active site along with 3. (b) Superposition of the ATAS-3 complex (color-coded as in (a)) with the ATAS–FSPP complex (all atoms pale cyan).

the fully closed conformation by Mg²⁺₃-PPᵢ bound with full occupancy (Figure 8a). The structure of the ATAS-5 complex is essentially identical in monomers A–D, even though the electron density of 5 in monomer D is somewhat noisy. To avoid a steric clash with the isopropylidene group, Y61 rotates ∼90° relative to its observed conformation in the ATAS-4 complex, but the conformations of other active site residues are essentially identical to those observed in the ATAS-4 complex. As in other complexes, trapped water molecule "w" hydrogen bonds with N213, N299, and S303; the additional trapped water molecule, "ww" is also observed and is stabilized by hydrogen bond interactions with the PPᵢ group, a Mg²⁺_C-bound water molecule, and the amino group of 5. A superposition comparing the binding modes of correct stereoisomer 4 and incorrect stereoisomer 5 complexed with ATAS is shown in Figure 8b.

■ DISCUSSION

Aromatic Triad Y61, F81, and F147 Enables Cation-π Stabilization and Contributes to the Template for FPP Cyclization. The structures of several bicyclic aza analogues of carbocation intermediates bound in the active site of ATAS demonstrate the feasibility of cation stabilization through charge-quadrupole or cation-π interactions,[42,43] as originally suggested in the first reported structures of terpenoid cyclases.[45−47] While different positions and orientations are

observed for each, analogues 1−4 bind in a region that is encircled by the faces of three aromatic residues: Y61, F81, and F147 (Figures 4−7). Because of the conformational change of Y61 that accommodates the binding of analogue 5, which has "incorrect" stereocenters, the edge of this residue rather than its face is oriented toward the active site cavity (Figure 8). Nevertheless, the binding of aza analogues 1−4, which better mimic carbocation intermediates in the ATAS reaction, suggests that Y61, F81, and F147 are ideally positioned to stabilize carbocation intermediates and their intervening transition states in the ATAS reaction.

Residues Y61, F81, and F147 are conserved in the closely related aristolochene synthase from *P. roqueforti* (PRAS) as Y92, F112, and F178, consistent with a conserved functional role for these aromatic residues. Interestingly, Y92F PRAS exhibits lower catalytic activity[14,41] but nevertheless retains the ability to generate aristolochene;[14] the Y92V, Y92C, and Y92A mutations similarly exhibit compromised catalytic activity but also generate (E)-β-farnesene, demonstrating that the bulky tyrosine side chain is part of the template that enforces the cyclization of FPP to form aristolochene.[48,49] A template function for the aromatic triad is consistent with the structure of the ATAS−FSPP complex (Figure 3), in which Y61, F81, and F147 make significant van der Waals contacts with the flexible isoprenoid group of the substrate analogue, thereby enforcing its bound conformation.

207
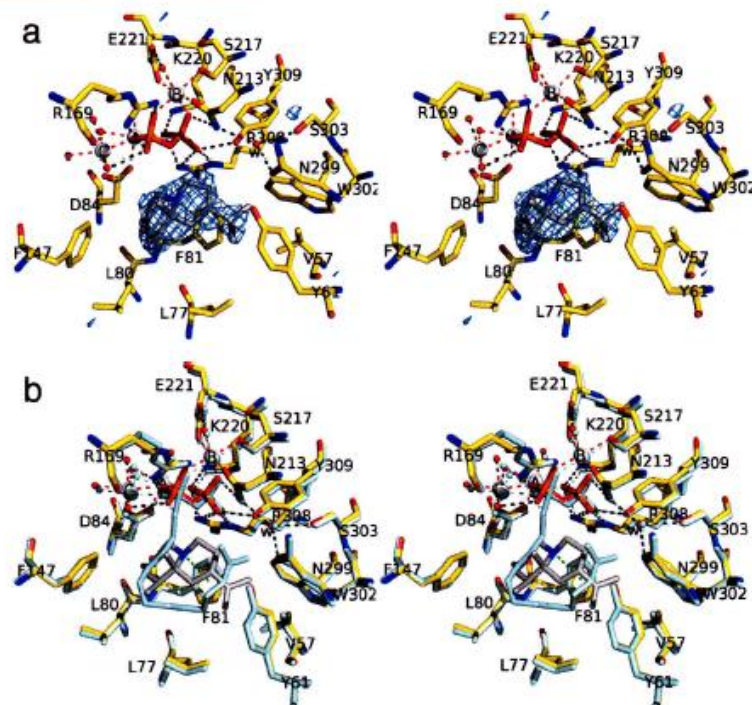
Figure 7. (a) Simulated annealing omit map of tertiary ammonium cation 4 (contoured at 3.0σ) bound to monomer A in the ATAS-4 complex. Atoms are color-coded as follows: C = yellow (protein) or gray (4), O = red, N = blue, P = orange, S = yellow, Mg^{2+} ions = silver spheres, solvent molecules = red spheres. Metal coordination, hydrogen bond, and cation-π interactions are shown as red, black, and green dotted lines, respectively. Water molecule "w" is trapped in the active site along with 4. (b) Superposition of the ATAS-4 complex (color-coded as in (a)) with the ATAS−FSPP complex (all atoms pale cyan).

Structural studies of the unrelated bacterial sesquiterpene cyclase epi-isozizaene synthase have also shown that three aromatic residues (F95, F96, and F198) encircle the active site and make cation-π interactions with the benzyltriethylammonium cation;[16] the bacterial sesquiterpene cyclase pentalenene synthase also contains three aromatic residues (F76, F77, and Y146) oriented so as to enable cation-π interactions in the active site.[45] Alternatively, sesquiterpene cyclase active sites can be defined by the faces of only two aromatic residues capable of engaging in cation-π interactions, such as those of 5-epi-aristolochene synthase (W273 and Y527),[46] trichodiene synthase (Y93 and F157),[12] and δ-cadinene synthase (W279 and Y527).[50] Thus, a working hypothesis is that a sesquiterpene cyclase active site can be encircled by a triad of aromatic residues with general primary structure (F,Y)-$X_{1-20}FX_{70-100}$(F,Y); if not, then it contains two aromatic residues quite distant from one another in the protein primary structure with their ring faces oriented toward the active site.

Charge−Charge Interactions with the PP_i Anion Appear to Govern the Orientation of Cationic Aza Analogues. It is notable that bicyclic aza analogues 1−4 bind with two general orientations. In one orientation, the branched isopropylidene group is nestled between F81 and F147 (analogues 1 and 2); in the other orientation, the isopropylidene group is oriented toward Y61 (analogues 3 and 4). In the ATAS−FSPP complex, the isopropylidene C12

and C13 atoms are similarly oriented toward Y61. Although it is unlikely that the carbocation intermediates in the ATAS reaction exhibit exceptional mobility during catalysis that would facilitate lengthwise flipping of the bicyclic ring system, the ability of ATAS to accommodate multiple conformations of the aza analogues suggests the intriguing possibility that the transiently generated, uncharged germacrene A intermediate may undergo a reorientation within the active site cavity so as to present the 6,7-double bond to the cogenerated pyrophosphoric acid, allowing protonation at C6, followed by transannular cyclization, rearrangement, and final deprotonation of H-8$_{si}$ by the appositely located PP_i anion. In principle, the requisite reorientation of the germacrene A intermediate could take place either by a ~120° rotation about an axis passing through the average plane of the germacrene A ring or by a ~180° rotation about an axis passing through C5 and C10. Since the PP_i ion appears to be firmly anchored by the surrounding network of ion−metal, oxyanion−cation, and hydrogen bond interactions, reorientation of the germacrene A intermediate would allow the pyrophosphate to access both C6 and C8 in order to mediate the key protonation and eventual deprotonation steps at these centers with the observed stereochemistry.

Interestingly, in each enzyme−inhibitor complex, the cationic ammonium or iminium group is oriented toward the PP_i anion, so the binding orientation of each aza analogue appears to be
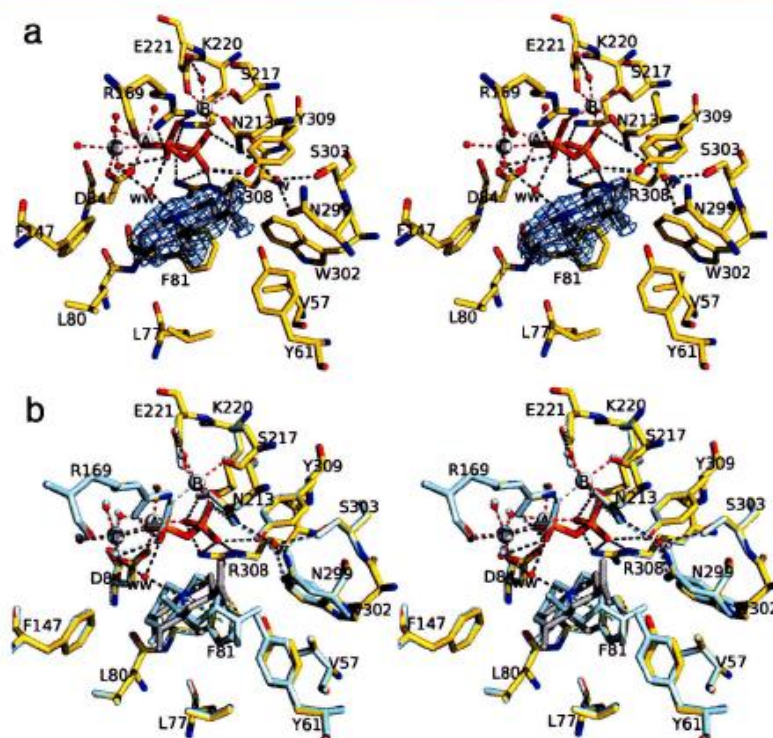
208

Figure 8. (a) Simulated annealing omit map of tertiary ammonium cation 5 (contoured at 3.1σ) bound to monomer A in the ATAS-5 complex. Atoms are color-coded as follows: C = yellow (protein) or gray (5), O = red, N = blue, P = orange, S = yellow, Mg²⁺ ions = silver spheres, solvent molecules = red spheres. Metal coordination, hydrogen bond, and cation-π interactions are shown as red, black, and green dotted lines, respectively. Water molecules "w" and "ww" are trapped in the active site along with 5. (b) Superposition of the ATAS-5 complex (color-coded as in (a)) with the ATAS-4 complex (all atoms pale cyan).

governed largely by favorable charge−charge interactions with the PP$_i$ anion and not just cation-π interactions with aromatic residues. Positively charged ammonium groups of aza analogues 1 and 2 donate hydrogen bonds directly to the PP$_i$ anion, and aza analogues 3 (and 5) donate hydrogen bonds to water molecule "ww", which in turn donates a hydrogen bond to the PP$_i$ anion. Aza analogue 4, while not hydrogen bonding to the PP$_i$ anion, is oriented so that the positively charged amino group is near the PP$_i$ anion. Presumably, the thermodynamically favored binding position and orientation of the aza analogue in the enzyme active site are attained as enzyme and inhibitor equilibrate in the cocrystallization experiment. Thus, the observation of two general binding orientations for these analogues is likely to be an artifact of favorable charge−charge interactions between the aza analogues and the PP$_i$ anion.

Which orientation, then, corresponds to the productive orientation of catalysis? We hypothesize that the catalytically productive orientation is that which orients the isopropylidene group toward Y61, since this orientation better corresponds to that observed for the binding of the substrate analogue FSPP. The binding orientation and conformation of FSPP are not subject to direction by PP$_i$ anion−cation interactions, and FSPP is bound with a nearly productive conformation. Notably, this is the first crystal structure of a terpenoid cyclase in which a bound substrate analogue adopts a conformation similar to that required for the precatalytic enzyme−substrate complex. The

crystal structures of the ATAS-3 and ATAS-4 complexes also provide substantial mechanistic and conformational information. Having previously advanced the idea that aza analogues that are more product-like in structure are more likely to be bound with catalytically productive orientations[51] based on several crystal structures of terpenoid cyclase-aza analogue complexes,[17,51] we suggest that since 4 is the most product-like of all the aza analogues studied, the corresponding ATAS-4 complex represents the most catalytically productive orientation of the bicyclic aza analogue in the ATAS active site. This is consistent with the orientation of the final carbocation intermediate of a terpenoid cyclization being proximal to the PP$_i$ anion, which may play a key role in quenching the final carbocation intermediate (*vide infra*).

Role of Active Site Water in Catalysis. The active site of a terpenoid cyclase is generally quite hydrophobic, more complementary in chemical nature to a nonpolar isoprenoid hydrocarbon than to a polar molecule such as water. However, it is intriguing that substrate binding to ATAS does not displace all of the water molecules presumed to solvate the active site in the unliganded enzyme. Trapped water molecule "w" is held firmly in place by hydrogen bonds with N213, N299, and S303 in all structures (Figures 3−8). Since ATAS is a high-fidelity cyclase and there is no evidence for hydroxylated products, this water molecule cannot be acting as a nucleophile. Moreover, a role for this water molecule as a general base is ruled out based

209

on its intermolecular contacts in the ATAS–FSPP complex. Therefore, trapped water molecule "w" simply comprises part of the active site contour, comparable to the trapped water molecule observed in ligand complexes with bornyl diphosphate synthase.[17]

Also interesting is water molecule "ww", which is observed in the ATAS-3 and ATAS-5 complexes; however, both 3 and 5 possess incorrect stereochemistry with regard to the ATAS reaction, so we cannot make conclusive mechanistic statements about this water molecule. Since water molecule "ww" is not observed in the ATAS–FSPP complex, the initial assumption would be that it could not enter the active site during catalysis — ostensibly, it only binds when the enzyme is allowed to equilibrate with an aza analogue during the cocrystallization experiment. However, water molecule "ww" is hydrogen bonded to the PP_i anion as well as a Mg^{2+}_C-bound water molecule, which in turn is exposed to bulk solvent. If sufficient void volume were created upon formation of the germacrene A intermediate to open up a new water binding site, this would allow a Mg^{2+}_C-bound water molecule to move into the "ww" position and another water molecule from bulk solvent to move into the vacant coordination site on Mg^{2+}_C. If water molecule "ww" is present during catalysis, it is highly controlled, in that it cannot react with any carbocation intermediates.

Role of the PP_i Anion in Catalysis. As previously discussed, the PP_i anion appears poised to accept a proton from the cis-C13 methyl group of FPP based on the structure of the ATAS–FSPP complex, consistent with the regiochemistry previously established for this step of the reaction.[40] Since the PP_i anion is a weak base, especially as coordinated to three Mg^{2+} ions, the protonated PP_i anion could serve as the Brønsted acid that protonates the C=C bond at C6 of the reoriented germacrene A intermediate (Figure 1). Although the proton initially abstracted from C13 of FPP is not added back to the substrate,[40,52] this does not rule out the possible role of the protonated PP_i anion as a general acid, provided that exchange of the proton with water is faster than reprotonation of the newly generated germacrene A.

The PP_i anion hydrogen bonds to the same Mg^{2+}_C-bound water molecule in the ATAS-2, ATAS-4, and ATAS-5 complexes, as well as the ATAS-PP_i complex;[34] this Mg^{2+}_C-bound water molecule is exposed to bulk solvent. Thus, if the PP_i anion regiospecifically deprotonates the germacryl cation intermediate from the carbon derived from the cis-C13 methyl group of FPP, and if proton transfer between the conjugate acid of the PP_i anion, the Mg^{2+}_C-bound water molecule, and bulk solvent is rapid relative to the rate of C=C bond protonation, then the proton (or deuteron) derived from the cis-C13 methyl group of FPP would exchange with solvent before reprotonation of the germacrene A intermediate. This likely accounts for the fact that the proton initially abstracted from C13 of FPP is not added back to the substrate.[40,52]

In the final step of catalysis, the H-8_{si} proton of the C8 methylene group is oriented toward the PP_i anion, suggesting that the PP_i anion also serves as the general base for the stereospecific deprotonation resulting in formation of (+)-aristolochene. Water molecule "ww" is also located on the same side of analogue 3 as the PP_i anion, so it is possible that water molecule "ww" could function in this role as well. Since water molecule "ww" is not observed in the ATAS-4 complex, which mimics the putative bound final carbocation intermediate, this may disfavor the role of water molecule "ww" as a proton acceptor. Regardless of whether it is the PP_i anion or water

molecule "ww" that accepts the proton from the final carbocation intermediate, this proton is presumably released rapidly into bulk solvent through exchange with the hydrogen bonded Mg^{2+}_C-bound water molecule.

An emerging role for the PP_i anion as a general base–general acid–general base in the ATAS mechanism is suggested by the ATAS crystal structures and is consistent with available enzymological measurements. The potential for product-assisted catalysis by the PP_i anion was first suggested by Caruthers and colleagues in the analysis of structure–function relationships in aristolochene synthase from *P. roqueforti*.[53] Subsequently, the structure of FPP synthase from *E. coli* complexed with dimethylallyl-S-thiolodiphosphate (DMASPP) and isopentenyl diphosphate similarly implicated the diphosphate group of DMASPP as the stereospecific general base in the chain elongation reaction.[1,54] Recent studies suggest that active site arginine residues that hydrogen bond with the diphosphate group of FPP play an important role in activating the diphosphate leaving group and modulating the chemistry of the diphosphate/PP_i anion in its potential function as a general acid.[55]

Stereochemical Discrimination in the ATAS Active Site. It is surprising that ATAS is capable of binding carbocation analogue 5, which mimics the incorrect stereoisomer of the product (+)-aristolochene, particularly in view of the fact that ATAS is a high-fidelity cyclase — not only does ATAS generate no other cyclic sesquiterpene with an alternative carbon skeleton, but it generates no stereochemical product other than (+)-aristolochene. Such strict product specificity implies that ATAS has evolved to catalytic perfection — in this case, "perfection" does not refer to catalytic efficiency but instead to the fidelity of the FPP cyclization cascade. A catalytically perfect cyclase has evolved with an active site contour that serves as a template for the generation of one sole product. While the active site contour of ATAS is quite product-like, i.e., it is complementary in shape to that of (+)-aristolochene, it is remarkable that modest flexibility in the active site accommodates an aristolochene analogue with incorrect stereochemistry.

Transition state binding in an enzyme active site is under kinetic control, with the reaction coordinate from one intermediate to the next being governed by the barrier height separating the intermediates and not the relative binding energies of the intermediates. Thus, the orientation, conformation, and stereochemistry of an analogue designed to mimic a carbocation intermediate allowed to achieve the most favorable binding energy and structure will not necessarily reflect the kinetically favored structure encountered in catalysis for the corresponding intermediate or transition state. However, the orientations and conformations of stereochemically correct analogues may become thermodynamically more favorable as the product structure is approached,[51] and this appears to be the case in the ATAS-4 complex. Thus, a terpenoid cyclase active site — even that of a high-fidelity terpenoid cyclase — may be capable of binding terpenoids and terpenoid analogues with "incorrect" structures and stereochemistries, even though these structures and stereochemistries are not ordinarily encountered under kinetic control during the cyclization cascade. Our future studies will continue to probe these aspects of structural and stereochemical discrimination in terpenoid cyclization reactions catalyzed by ATAS.

210

■ ASSOCIATED CONTENT

Accession Codes

The atomic coordinates and crystallographic structure factors of ATAS—FSPP, ATAS-1, ATAS-2, ATAS-3, ATAS-4, and ATAS-5 complexes have been deposited in the Protein Data Bank (www.rcsb.org) with accession codes 4KUX, 4KVI, 4KVD, 4KVW, 4KVY, and 4KWD, respectively.

■ AUTHOR INFORMATION

Corresponding Author

*Address: Department of Chemistry, University of Pennsylvania, 2001 Roy and Diana Vagelos Laboratories, 231 South 34th Street, Philadelphia, PA, 19104-6323 USA. Tel: 215-898-5714; e-mail: chris@sas.upenn.edu.

Notes

The authors declare no competing financial interest.

■ ACKNOWLEDGMENTS

■ ABBREVIATIONS

ATAS, *Aspergillus terreus* aristolochene synthase; BME, β-mercaptoethanol; EDTA, ethylenediaminetetraacetic acid; FPP, farnesyl diphosphate; LB, Luria—Bertani; PP$_i$, inorganic pyrophosphate; FSPP, farnesyl thiolodiphosphate; HEPES, 4-(2-hydroxyethyl)-1-piperazineethanesulfonic acid; MES, 2-morpholinoethanesulfonic acid; MOPS, 3-(N-morpholino)-propanesulfonic acid; PEG, polyethylene glycol; PRAS, *Penicillium roqueforti* aristolochene synthase; r.m.s., root mean-square

■ REFERENCES

(1) Poulter, C. D., and Rilling, H. C. (1978) The prenyl transfer reaction. Enzymic and mechanistic studies of the 1'-4 coupling reaction in the terpene biosynthetic pathway. *Acc. Chem. Res. 11*, 307–313.

(2) Poulter, C. D. (2009) Bioorganic chemistry. A natural reunion of the physical and life sciences. *J. Org. Chem. 74*, 2631–2645.

(3) Cane, D. E. (1985) Isoprenoid biosynthesis. Stereochemistry of the cyclization of allylic pyrophosphates. *Acc. Chem. Res. 18*, 220–226.

(4) Cane, D. E. (1990) Enzymatic formation of sesquiterpenes. *Chem. Rev. 90*, 1089–1103.

(5) Wendt, K. U., and Schulz, G. E. (1998) Isoprenoid biosynthesis: manifold chemistry catalyzed by similar enzymes. *Structure 6*, 127–133.

(6) Christianson, D. W. (2006) Structural biology and chemistry of the terpenoid cyclases. *Chem. Rev. 106*, 3412–3442.

(7) Christianson, D. W. (2008) Unearthing the roots of the terpenome. *Curr. Opin. Chem. Biol. 12*, 141–150.

(8) Allemann, R. K. (2008) Chemical wizardry? The generation of diversity in terpenoid biosynthesis. *Pure Appl. Chem. 80*, 1791–1798.

(9) Degenhardt, J., Köllner, T. G., and Gershenzon, J. (2009) Monoterpene and sesquiterpene synthases and the origin of terpene skeletal diversity in plants. *Phytochemistry 70*, 1621–1637.

(10) Aaron, J. A., and Christianson, D. W. (2010) Trinuclear metal clusters in catalysis by terpenoid synthases. *Pure Appl. Chem. 82*, 1585–1597.

(11) Miller, D. J., and Allemann, R. K. (2012) Sesquiterpene synthases: passive catalysts or active players? *Nat. Prod. Rep. 29*, 60–71.

(12) Rynkiewicz, M. J., Cane, D. E., and Christianson, D. W. (2001) Structure of trichodiene synthase from *Fusarium sporotrichioides* provides mechanistic inferences on the terpene cyclization cascade. *Proc. Natl. Acad. Sci. U. S. A. 98*, 13543–13548.

(13) Proctor, R. H., and Hohn, T. M. (1993) Aristolochene synthase. Isolation, characterization, and bacterial expression of a sesquiterpenoid biosynthetic gene (Ari1) from *Penicillium roqueforti*. *J. Biol. Chem. 268*, 4543–4548.

(14) Felicetti, B., and Cane, D. E. (2004) Aristolochene synthase: mechanistic analysis of active site residues by site-directed mutagenesis. *J. Am. Chem. Soc. 126*, 7212–7221.

(15) Köksal, M., Hu, H., Coates, R. M., Peters, R. J., and Christianson, D. W. (2011) Structure and mechanism of the diterpene cyclase ent-copalyl diphosphate synthase. *Nat. Chem. Biol. 7*, 431–433.

(16) Aaron, J. A., Lin, X., Cane, D. E., and Christianson, D. W. (2010) Structure of epi-isozizaene synthase from *Streptomyces coelicolor* A3(2), a platform for new terpenoid cyclization templates. *Biochemistry 49*, 1787–1797.

(17) Whittington, D. A., Wise, M. L., Urbansky, M., Coates, R. M., Croteau, R. B., and Christianson, D. W. (2002) Bornyl diphosphate synthase: Structure and strategy for carbocation manipulation by a terpenoid cyclase. *Proc. Natl. Acad. Sci. U. S. A. 99*, 15375–15380.

(18) Faraldos, J. A., and Allemann, R. K. (2011) Inhibition of (+)-aristolochene synthase with iminium salts resembling eudesmane cation. *Org. Lett. 13*, 1202–1205.

(19) Faraldos, J. A., Kariuki, B., and Allemann, R. K. (2010) Intermediacy of eudesmane cation during catalysis by aristolochene synthase. *J. Org. Chem. 75*, 1119–1125.

(20) Ishmuratov, G. Y., Legostaeva, Y. V., Botsman, L. P., Nasibullina, G. V., Muslukhov, R. R., Kazakov, D. V., and Tolstikov, G. A. (2012) Ozonolytic transformations of (S)-(−)-limonene. *Russ. J. Org. Chem. 48*, 18–24.

(21) Takikawa, H., Sano, S., and Mori, K. (1997) Pheromone synthesis, CLXXXVI. Synthesis of (1S,2R,5R)-bicolorin, the aggregation pheromone of male beech bark beetles (*Taphrorychus bicolor*), and its (1R,2R,5S) isomer. *Eur. J. Org. Chem. 12*, 2495–2498.

(22) Kido, F., Yamaji, K., Sinha, S. C., Abiko, T., and Kato, M. (1995) Carbocyclic construction by the [2,3]sigmatropic rearrangement of cyclic sulfonium ylides — a new entry for the stereoselective synthesis of substituted cyclohexanones. *Tetrahedron 51*, 7697–7714.

(23) Kedrowski, B. L. (2003) Synthesis of orthogonally protected (R)- and (S)-2-methylcysteine via an enzymatic desymmeterization and Curtius rearrangement. *J. Org. Chem. 68*, 5403–5406.

(24) Alsina, J., Giralt, E., and Albericio, F. (1996) Use of N-tritylamino acids and PyAOP(1) for the suppression of diketopiperazine formation in Fmoc/(t)Bu solid-phase peptide synthesis using alkoxybenzyl ester anchoring linkages. *Tetrahedron Lett. 37*, 4195–4198.

(25) Tehrani, K. A., D'hooghe, M., and De Kimpe, N. (2003) Novel synthesis of indolizidines and quinolizidines. *Tetrahedron 59*, 3099–3108.

(26) Mehta, G., Karmakar, S., and Chattopadhyay, S. K. (2004) Grob-type fragmentation of a carvone derived β-hydroxymesylate: application to the synthesis of chiral lavandulol derivatives. *Tetrahedron 60*, 5013–5017.

(27) Jackman, L. M., Webb, R. L., and Yick, H. C. (1982) Synthesis and chiroptical properties of some piperidin-2-ones. *J. Org. Chem. 47*, 1824–1831.

(28) Lacroix, S., Rixhon, V., and Marchand-Brynaert, J. (2006) Synthesis of omega-aminodithioesters. *Synthesis*, 2327–2334.

211

(29) Guarna, A., Lombardi, E., Machetti, F., Occhiato, E. G., and Scarpi, D. (2000) Modification of the aza-Robinson annulation for the synthesis of 4-methyl-benzo[c]quinolizin-3-ones, potent inhibitors of steroid 5α-reductase 1. *J. Org. Chem.* 65, 8093−8095.

(30) Fernández, M. F., and Söllhuber, M. M. (1987) Synthesis of 5,6,9,10,11,11a-hexahydro-8H-naphtho[2,1-a]quinolizine. *Heterocycles* 26, 3059−3063.

(31) Otwinowski, Z., and Minor, W. (1997) Processing of X-ray diffraction data collected in oscillation mode. *Methods in Enzymology. Macromolecular Crystallography (Part A)* (Carter, C. W., Jr., and Sweet, R. M., Eds.) Vol. 276, pp 307−326, Academic Press, New York.

(32) Karplus, P. A., and Diederichs, K. (2012) Linking crystallographic model and data quality. *Science* 336, 1030−1033.

(33) McCoy, A. J., Grosse-Kunstleve, R. W., Adams, P. D., Winn, M. D., Storoni, L. C., and Read, R. J. (2007) Phaser crystallographic software. *J. Appl. Crystallogr.* 40, 658−674.

(34) Shishova, E. Y., Di Costanzo, L., Cane, D. E., and Christianson, D. W. (2007) X-ray crystal structure of aristolochene synthase from *Aspergillus terreus* and evolution of templates for the cyclization of farnesyl diphosphate. *Biochemistry* 46, 1941−1951.

(35) Shishova, E. Y., Yu, F., Miller, D. J., Faraldos, J. A., Zhao, Y., Coates, R. M., Allemann, R. K., Cane, D. E., and Christianson, D. W. (2008) X-ray crystallographic studies of substrate binding to aristolochene synthase suggest a metal ion binding sequence for catalysis. *J. Biol. Chem.* 283, 15431−15439.

(36) Adams, P. D., Afonine, P. V., Bunkoczi, G., Chen, V. B., Davis, I. W., Echols, N., Headd, J. J., Hung, L.-W., Kapral, G. J., Grosse-Kunstleve, R. W., McCoy, A. J., Moriarty, N. W., Oeffner, R., Read, R. J., Richardson, D. C., Richardson, J. S., Terwilliger, T. C., and Zwart, P. H. (2010) PHENIX: a comprehensive Python-based system for macromolecular structure solution. *Acta Crystallogr., Sect. D* 66, 213−221.

(37) Emsley, P., and Cowtan, K. (2004) Coot: model-building tools for molecular graphics. *Acta Crystallogr., Sect. D* 60, 2126−2132.

(38) Chen, V. B., Arendall, W. B., III, Headd, J. J., Keedy, D. A., Immormino, R. M., Kapral, G. J., Murray, L. W., Richardson, J. S., and Richardson, D. C. (2010) MolProbity: all-atom structure validation for macromolecular crystallography. *Acta Crystallogr., Sect. D* 66, 12−21.

(39) Cane, D. E., Prabhakaran, P. C., Salaski, E. J., Harrison, P. H. M., Noguchi, H., and Rawlings, B. J. (1989) Aristolochene biosynthesis and enzymatic cyclization of farnesyl pyrophosphate. *J. Am. Chem. Soc.* 111, 8914−8916.

(40) Cane, D, E., Prabhakaran, P. C., Oliver, J. S., and McIlwaine, D. B. (1990) Aristolochene biosynthesis. Stereochemistry of the deprotonation steps in the enzymatic cyclization of farnesyl pyrophosphate. *J. Am. Chem. Soc.* 112, 3209−3210.

(41) Calvert, M. J., Ashton, P. R., and Allemann, R. K. (2002) Germacrene A is a product of the aristolochene synthase-mediated conversion of farnesylpyrophosphate to aristolochene. *J. Am. Chem. Soc.* 124, 11636−11641.

(42) Dougherty, D. A. (1996) Cation-π interactions in chemistry and biology: a new view of benzene, Phe, Tyr, and Trp. *Science* 271, 163−168.

(43) Dougherty, D. A. (2013) The cation-π interaction. *Acc. Chem. Res.* 46, 885−893.

(44) Faraldos, J. A., Antonczak, A. K., González, V., Fullerton, R., Tippmann, E. M., and Allemann, R. K. (2011) Probing eudesmane cation-π interactions in catalysis by aristolochene synthase with non-canonical amino acids. *J. Am. Chem. Soc.* 133, 13906−13909.

(45) Lesburg, C. A., Zhai, G., Cane, D. E., and Christianson, D. W. (1997) Crystal structure of pentalenene synthase: mechanistic insights on terpenoid cyclization reactions in biology. *Science* 277, 1820−1824.

(46) Starks, C. M., Back, K., Chappell, J., and Noel, J. P. (1997) Structural basis for cyclic terpene biosynthesis by tobacco 5-epi-aristolochene synthase. *Science* 277, 1815−1820.

(47) Wendt, K. U., Poralla, K., and Schulz, G. E. (1997) Structure and function of a squalene cyclase. *Science* 277, 1811−1815.

(48) Deligeorgopoulou, A., and Allemann, R. K. (2003) Evidence for differential folding of farnesyl pyrophosphate in the active site of aristolochene synthase: a single-point mutation converts aristolochene synthase into an (E)-β-farnesene synthase. *Biochemistry* 42, 7741−7747.

(49) Calvert, M. J., Taylor, S. E., and Allemann, R. K. (2002) Tyrosine 92 of aristolochene synthase directs cyclisation of farnesyl pyrophosphate. *Chem. Commun.*, 2384−2385.

(50) Gennadios, H. A., González, V., Di Costanzo, L., Li, A., Yu, F., Miller, D. J., Allemann, R. K., and Christianson, D. W. (2009) Crystal structure of (+)-δ-cadinene synthase from *Gossypium arboreum* and evolutionary divergence of metal binding motifs for catalysis. *Biochemistry* 48, 6175−6183.

(51) Vedula, L. S., Rynkiewicz, M. J., Pyun, H.-J., Coates, R. M., Cane, D. E., and Christianson, D. W. (2005) Molecular recognition of the substrate diphosphate group governs product diversity in trichodiene synthase mutants. *Biochemistry* 44, 6153−6163.

(52) Miller, D. J., Gao, J., Truhlar, D. G., Young, N. J., González, V., and Allemann, R. K. (2008) Stereochemistry of eudesmane cation formation during catalysis by aristolochene synthase from *Penicillium roqueforti*. *Org. Biomol. Chem.* 6, 2346−2354.

(53) Caruthers, J. M., Kang, I., Rynkiewicz, M. J., Cane, D. E., and Christianson, D. W. (2000) Crystal structure determination of aristolochene synthase from the blue cheese mold *Penicillium roqueforti*. *J. Biol. Chem.* 275, 25533−25539.

(54) Hosfield, D. J., Zhang, Y., Dougan, D. R., Broun, A., Tari, L. W., Swanson, R. V., and Finn, J. (2004) Structural basis for bi-sphosphonate-mediated inhibition of isoprenoid biosynthesis. *J. Biol. Chem.* 279, 8526−8529.

(55) Faraldos, J. A., González, V., and Allemann, R. K. (2012) The role of aristolochene synthase in diphosphate activation. *Chem. Commun.* 48, 3230−3232.